Intergenerational effects of high fat diet: exploring mechanisms in germ cells

Thomas James Gray Chambers

MRes (Medical Science), University of Manchester

MB ChB, University of Manchester

BSc (Medical Science), University of St. Andrews

Medical Research Council Centre for Reproductive Health

The Queen's Medical Research Institute

47 Little France Crescent

EDINBURGH

EH16 4TJ

Thesis submitted to the University of Edinburgh for the

Degree of Doctor of Philosophy

June 2015

Declaration

The experimental work in this thesis is the sole work of the author except where acknowledgement has been made. These studies have not been submitted in support of another degree or qualification at the University of Edinburgh, or any other institute.

Thomas Chambers

June 2015

Acknowledgements

I would never have embarked on this project were it not for the suggestion, motivation and encouragement of my two supervisors, Mandy Drake and Richard Sharpe. Thank you both for all your help and support over the past three years, for bringing me to Edinburgh, for grounding me when a have crazy ideas and for nudging me on when it looked like nothing was going to work. I could have neither started nor completed this thesis without you.

I have taken advantage of lots of technical expertise from people here at the QMRI along my PhD journey. Special thanks goes to Will Mungal for help with animal husbandry and keeping me company during the Glucose tolerance tests. To Sheila MacPherson and Chris McKinnell for their amazing skills at getting any antibody to work (well almost). Will Ramsay, Shonna Johnston and Fiona Rossi for helping to get the FACS working, and for sitting patiently by the machine to unblock it when the sperm went through 'sideways'. Mike Morgan for great help with the bioinformatics, for taking the time to explain things to me, and for his responses to my questions, no matter how ridiculous. Also Forbes Howie for his quick wit and quicker production of ELISA results.

I would also have been stuck without the other members of the Sharpe group, old and new, in particular Karen Kilcoyne for some motivating chats, Sander van den Driesche for skilled dissection of embryonic tissue, and Pablo Hurtado González for not shouting when I steal stuff from his bench. Also members of team Drake for their help and advice; Khulan Batbayer, Jessy Cartier, Catherine Rose, and Marcus Lyall. I would also like to thank other members of the CRH for technical advice and support over the past three years, especially Diane Rebourcet and Laura O'Hara who let me know that my lab skills weren't "too bad for a medic"!

I would not have managed to get through without some distraction outside the lab; special thanks go to my friend and neighbour Angie Murphy for Westy chat, cooking, and even stocking my fridge when I'm away. Also to the members of The Captain's Biscuit and the Chapter House Singers for providing me with musical diversion.

Finally I would like to thank my family; Mum, Dad, Lettie, Richard and wee Euan for support and encouragement, and especially to Mum for some diligent proof-reading,

Abstract

The prevalence of obesity is increasing each year, likely due to altered diet and a sedentary lifestyle. However, some epidemiological data suggests that parental and grandparental environments may also impact upon weight gain, metabolic health and mortality. This non-genetic inheritance has been reproduced in some experimental animal studies. The mechanisms are, however, unknown. One hypothesis has been that environmental exposures perturb germ cell development. Changes to the germ cell epigenome are an example of one such alteration.

In this thesis, epigenetic mechanisms are explored in rodent and primate male germ cells throughout development. The conservation of global methylation patterns, expression of DNA methyltransferases and of key histone modifications is demonstrated in rat, marmoset and human tissue demonstrating mechanisms are in place that might be disrupted by environmental exposures either *in utero* or during post-natal development.

A rat model of parental high fat diet (HFD) exposure is established and phenotype explored in two generations of offspring. Maternal HFD results in weight gain in male and female offspring and paternal HFD in weight gain in just female offspring. Grand-paternal exposure to HFD via the maternal line has the greatest impact on the second generation where, in males, increased weight, adiposity, reduced insulin sensitivity and an increased luteinising hormone to testosterone ratio were found.

Given that postnatal exposure in males resulted in adverse metabolic health in grand offspring, the exposed germ cells were interrogated by RNA and smallRNA-sequencing. HFD exposure did not alter the germline transcriptome suggesting an alternative mechanism to be responsible for the intergenerational effects observed.

Thus, HFD perturbs metabolic health in two generations of rats in a grand-parent and sex specific manner but does not affect the germ cell transcriptome.

Presentations relating to this thesis

Chambers T, Dean A, MacPherson S, van Den Driesche S, Anderson A, Drake A, Sharpe R Expression of DNMT3a and DNMT3b in fetal germ cells. Meeting of the British Endocrine Society, Harrogate, March 2013. (Poster)

Chambers T, Drake A, Rose C, van den Driesche S, Sharpe R Influence of parental high fat diet on growth and development of the next two generations DoHAD, Singapore November 2013. (Poster)

Rose C, van den Driesche S, Boyle A, Chambers T, Sharpe R, Meehan R, Drake A, Fetal glucocorticoid overexposure impacts on germline epigenetic reprogramming in the rat, BES, Liverpool March 2014. (Poster)

Chambers T, Rebourcet D, Smith L, Drake A, Sharpe R, Sertoli Cell maturation is associated with changes to cytosine 5-methylation and hydroxymethylation. European Testis Workshop, Copenhagen, May 2014 (Oral communication)

Chambers T, Drake A, Sharpe R, Does grandparental diet affect your weight and risk of hypogonadism? British Andrology Society meeting, Edinburgh, 2014. (Oral communication)

Chambers T, Drake A, Sharpe RM, Does grandparents' diet affect weight and risk of hypogonadism in subsequent generations? Academy of Medical Sciences Spring Meeting 2015, (Poster) *Lancet* 2015(385)S29

Prizes

European Society for Endocrinology Basic Endocrinology Course in Reproductive Endocrinology, Poster Prize, Feb 2015

Abbreviations

3βHSD	3-beta hydroxy-steroid dehydrogenase
5caC	5-carboxylcytosine
5fC	5-formylcytosine
5hmC	5-hydroxymethylcytosine
5mC	5-methylcytosine
A	Adenine
ac	Acetylated
ADD	ATRX -DNMT3-DNMT3L domain
ADP	Adenine di-phosphate
AGO	Argonaut
AIC	Akaike information criteria
AID	Activation induced deaminase
AML	Acute myeloid Leukaemia
ANOVA	Analysis of variance
APOBEC1	Apolipoprotein B mRNA-editing enzyme catalytic polypeptide 1
AR	Androgen receptor
ATP	Adenine triphosphate
ATRX	Alpha thalassaemia and X-linked mental retardation
BER	Base excision repair
BMI	Body mass index
BMP	Bone morphogenic protein
bp	base pairs
BRDT	Bromodomain-testis specific
BSA	Bovine serum albumin
BSS	Bisulphite sequencing
CBX	Chromo box
CD	Control diet
CDKN1B	Cyclin dependent kinase 1b
CGI	CpG island
CI	Confidence interval
Col3a1	Collagen 3A1
COUP-TFII	Chicken ovalbumin upstream promoter transcription factor II
CpG	Cytosine-phosphate-Guanine dinucleotide
CST	Cystatin
d	Post-natal day
DAPI	4',6-diamidino-2-phenylindole
DGCR8	Di George Syndrome critical region 8
DDX4	Dead/H box 4 =VASA
DES	Diethylstilbestrol
DKO	Double knockout
DMRT	Doublesex and MAB3 related transcription factor
DNA	Deoxyribonucleic acid
DNMT	DNA methyltransferase
DPPA3	Developmental pluripotency associated gene 3
dsRNA	Double stranded RNA

e	embryonic day
EDTA	Ethylene-diamino-tetra-acetic acid
EED	Embryonic ectoderm developmental protein
EGFP	Enhanced green fluorescent protein
ELISA	Enzyme-linked immunosorbant assay
eRNA	enhancer RNA
EZH2	Enhancer of zeste homolog 2
F0	Founding generation
F1-3	Subsequent generations 1-3
FACS	Fluorescence Assisted Cell Sorting
FAD	Flavin Adenine Dinucleotide
FAM	Carboxyfluorescein
FCS	Fetal calf serum
FRET	Förster Resonance Energy Transfer
G0- G1-G2	Growth phases of cell cycle 0-2
GCeGFP	Germ cell enhanced green fluorescent protein
gDNA	Genomic DNA
GLP	G9a like protein
GNRHR	Gonadotrophin releasing hormone receptor
GTT	Glucose tolerance test
GV	Germinal vesicle
GWAS	Genome wide association study
H1	Histone 1
H2	Histone 2
H2A.Z	Histone 2A Z variant
H3	Histone 3
H3K27	Histone 3 Lysine 27
H3K9	Histone 3 Lysine 9
H3R3	Histone 3 Arginine 3
H4K20	Histone 4 Lysine 20
HDAC	Histone deacetylase
HEK293	Human Embryonic Kidney cell line 293
HEN1	Nascent helix-loop-helix1
HFD	High Fat Diet
hme-DIP	Hydroxymethyl DNA immuno-precipitation
HMT	Histone methyl transferase
HP1	Heterochromatin Protein 1
HRP	Horseradish Peroxidase
IAP	Intracisternal A Particle
IF	Immunofluorescence
IGF1r	Insulin like receptor 1 receptor
IGF2	Insulin like growth factor 2
IGFR2	Insulin like growth factor receptor 2
IUGR	Intrauterine growth restriction
JBP	Thymine dioxygenase
kb	Kilobase (1000bp)

KDM	Lysine demethylase
KO	Knockout
LDHA	Lactose dehydrogenase alpha
LH	Luteinising hormone
LHCGR	Luteinising hormone receptor
LINEs	Long Interspersed Nucleotide Elements
lncRNA	long non-coding RNA
LTR	Long terminal repeat
me	Methylated
me3	Trimethylated
Me-DIP	Methylated DNA immuno-precipitation
mESCs	Murine embryonic stem cells
miRNA	MicroRNA
mitoPLD	Phospholipase D family member 6
MIWI	Murine homolog of PIWI
MLL	Mixed lineage Leukaemia
MMD2	Monocyte to macrophage differentiation associated 2
mRNA	Memory Ribonucleic Acid
ncRNA	Non-coding RNA
NP95	Nuclear Phosphoprotein, 95-KD= UHRF1
nt	Nucleotide
OGTT	Oral glucose tolerance test
PBS	Phosphate buffered Saline
PCA	Principal component analysis
PCGF	Polycomb group ring finger protein
PCR	Polymerase chain reaction
PGC	Primordial germ cell
PI	Propridium iodide
piRNA	PIWI interacting RNA
PIWI	P element induced Wimpey in testis
PIWIL	PIWI like
pnd	Post-natal day
polII	Polymerase II
PRC	Polycomb Repressor Complex
PRDM1	PR domain containing protein 1
qPCR	Quantitative polymerase chain reaction
RA	Retinoic acid
RASGRF1	Ras specific Guanine-nucleotide-releasing factor 1
REML	Restricted maximum likelihood
RIA	Radio immuno-assay
RING1	Ring finger protein 1
RISC	RNA induced silencing complex
RMST	Rhabodomyosarcoma-2 associated transcript
RNA	Ribonucleic acid
ROPN1L	ROPN1 like protein
rpm	Rotations per min

rRNA	Ribosomal RNA
RSPO	R-Spondin
RT	Reverse transcription
SETDB1	SET domain protein, bifurcated 1
SUZ12	Suppressor of zeste 12
SH3GLB1	SH3 domain GRB2-like endophillin B1
SINEs	Short Interspersed Nuclear Element
siRNA	Short inhibiting RNA
smRNA	SmallRNA
snoRNA	Small nucleolar RNA
SNP	Single nucleotide polymorphism
SNRPN	Small nuclear ribonucleoprotein polypeptide N
SOX	SRY-box
SRY	Sex determining region Y
STRA	Stimulated by retinoic acid
SURF	Small university research facility
T	Thymine
TAMRA	6-carboxy-tetramethyl-rhodamine
TAR	Thrombocytopenia-absent radius
TBE	Tris- Borate- EDTA
TBS	Tris-Buffered Saline
TCF	T cell factor
TDG	Thymine DNA glycosylase
TET	Ten- eleven translocation
TMB	Tetramethylbenzidene
TRBP	TAR RNA binding Proteins
tRNA	Transfer RNA
TSA	Tyramide signal amplification
TUNEL	Terminal deoxynucleotidyl transferase dUTP nick end labelling
UHRF1	Ubiquitin-like protein containing PHD and ring finger domains 1
UK	United Kingdom
VC	Variance components
VST	Variance stabilising transformed
w	Week of gestation
WB	Western blot
WG-Bs-seq	Whole genome bisulphite sequencing
WHO	World Health Organisation
WT	Wild type
ZFP57	Zinc finger protein 57

Contents

List of figures

List of tables

1 Literature review

1.1 Introduction

Obesity is a major concern for global health. Worldwide, obesity has doubled since 1980, and 65% of the world's population now lives in countries where overweight and obesity results in more morbidity than undernourishment (WHO, 2014).

Obesity is defined as a body mass index of over 30kg/m^2 (WHO, 2014). A high BMI is associated with an increase in the prevalence of hypertension (Roka et al., 2015), coronary heart disease and stroke (Hägg et al., 2015), type 2 diabetes (Martin-Rodriguez et al., 2015), cancer (Guh et al., 2009) and subfertility in males (Palmer et al., 2012; Stokes et al., 2015) and females (Talmor and Dunphy, 2014). Obesity was estimated to cost the UK tax payer £4.2 billion in 2007, a cost that is rising each year (National Obesity Observatory, 2010; Wang et al., 2011).

The change in the prevalence of obesity is likely influenced by changes in lifestyle over the latter part of the last century, for example, increased snacking and consumption of processed food (Cutler et al., 2003) and reduced levels of physical activity (Bowen et al., 2015). Although twin studies suggest that 40-70% of bodyweight can be explained by genetic factors (Locke et al., 2015), with a few exceptions, specific gene targets have remained elusive and genome wide association studies (GWAS) have only been able to account for 2-4% of heritability (Locke et al., 2015). One possible explanation for this is non-genetic inheritance; there is also accumulating evidence, from both epidemiological and experimental studies, that the environment around our immediate ancestors can influence the risk of obesity (Aiken and Ozanne, 2014; Desai et al., 2015).

In human studies, obesity in parents is strongly predictive of obesity in offspring. These studies are however heavily confounded by the environment in which the offspring are

raised, which is presumably more 'obesogenic' (reviewed in (Patro et al., 2013)). There is also an association between maternal under-nutrition and later risk of obesity and cardiovascular disease in offspring (Painter et al., 2006; de Rooij et al., 2006), and increased BMI in adolescent grand-offspring (Veenendaal et al., 2013) although no change to mortality in those exposed *in utero* to date (Ekamper et al., 2015). Furthermore, multiple experimental models of over- or under-nutrition find altered metabolic, reproductive and behavioural phenotypes in offspring (reviewed in Aiken and Ozanne, 2014; Desai et al., 2015). Thus, there is building evidence for the non-genetic 'intergenerational' transmission of phenotype.

The mechanisms resulting in such intergenerational transmission of phenotype however remain elusive. Hypotheses include transgenerational epigenetic inheritance (DNA methylation or chromatin structure), somatic inheritance, where components of the parental soma alter development, behavioural inheritance, and environmental inheritance, where, for example, parents influence on the environment (e.g. nutrition) around offspring, or the potential of environments to induce mutations in DNA (Bonduriansky and Day, 2013).

Epigenetics refers to a heritable modification within a cell that does not alter the Watson-Crick genetic code (Goldberg et al., 2007). If an environmental exposure could alter the epigenetic make up of a germ cell, it would act as a potential means of passing information from one generation to the next without altering the genetic code. Thus, environmental perturbation of the epigenome has been suggested as a potential mechanism for intergenerational inheritance of phenotype.

The first part of this chapter reviews experimental evidence for the intergenerational programming of phenotype as a result of environmental exposures but with a focus on high fat diet (HFD), following this the mechanisms by which the epigenome of a cell is

regulated and maintained are explored before examining how the epigenome is regulated during germ cell development.

1.2 Intergenerational inheritance of phenotype

1.2.1 Epidemiological studies

In human populations, dietary 'interventions' are one of the most straightforward means to investigate whether environmental exposures might affect future generations. For example, the Dutch famine in 1944-1945 resulted in a finite window of perinatal malnutrition, and the exposed offspring had low birth weight. In adulthood, such females were more obese, male and female offspring had premature cardiovascular disease (Desai et al., 2015; Painter et al., 2006; Ravelli et al., 1999) (summarised in Figure 1.1) and grandchildren had increased BMI and weight according to the paternal *in utero* nutritional exposure (Veenendaal et al., 2013). A less direct effect is seen in the epidemiological studies of a small Swedish town, Överkalix, where data regarding the relative nutrition of grandparents was correlated with the longevity and health of grandchildren. The largest effects were seen when correlating the paternal grandfather to the proband (Kaati et al., 2007; Pembrey et al., 2014, 2006).

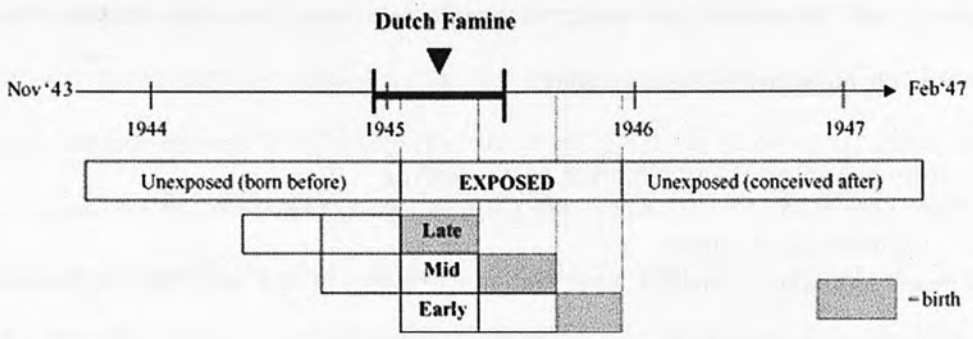

Exposure	Outcome	Ref.
Conception during famine	Coronary artery disease Female obesity	Painter, 2006
Famine in late gestation	Increased glucose during OGTT Increased insulin during OGTT Lower birthweight	Ravelli, 1998 Roseboom, 2006
Famine in early gestation	Increased LDL/HDL cholesterol Coronary artery disease (age and prevalence) Perceived poor health	Roseboom, 2000 Painter, 2006 Roseboom, 2003

Figure 1.1 summary of outcomes following maternal exposure to famine during the Dutch hunger winter Figure adapted from (Painter et al., 2005). Females exposed to famine during each trimester of pregnancy are referred to as late, mid or early exposed. Offspring were compared to those born prior to the famine.

Offspring of obese parents are more likely to be obese, and suffer from adverse metabolic health, with some studies showing the strongest effect for paternal obesity (Jääskeläinen et al., 2011; Patro et al., 2013). However, comparison of multiple studies does not provide conclusive evidence that there is a clear maternal or paternal effect of obesity that can be differentiated, rather the conclusion is that it is difficult to control for the presence of environmental and genetic confounding, which thus makes interpretation complex (Patro et al., 2013).

1.2.2 Experimental studies

1.2.2.1 Paternal nutrition

Observations in human populations are difficult to interpret due to a reliance on self-reporting and the fact that it is impossible to control for environmental changes and confounding factors. For this reason, experimental studies have been useful to identify if effects can be transmitted and then to try and determine the potential mechanisms. Evidence showing the transmission of environmentally-induced phenotypes through the male line is supportive of the concept that transmission may be mediated by changes in the epigenome since this avoids potential complications of 'intra-uterine effects' (Anderson et al., 2006; Carone et al., 2010; Fullston et al., 2013; Ng et al., 2010; Öst et al., 2014). These studies are summarised in Table 1.1. It should be borne in mind however, that paternal behaviour and the constituents of semen may also influence maternal behaviour and or pre-implantation development and thus might also have a part to play (Binder et al., 2015; Bromfield et al., 2014; Crean et al., 2014; Curley et al., 2011).

Table 1.1 Experimental studies of paternal dietary interventions ND not reported, p significance vs. offspring of control diet (CD) fed males.

Study	Species	Exposure	Exposure time	Exposure age	Exposure sex	Outcome	Effect in			
							F1 male	F1 female	F2 male	F2 female
Ost 2014	Dropsophila	High sugar	2 days	4-5 day	Male	Serum triglycerides	p<0.05	ND	NS	ND
Anderson 2006	Mouse: Outbred swiss	24 hour fast	6x over 3 weeks	8 week old	Male	Serum glucose at 6 weeks	p=0.0065	p=0.037	ND	ND
Ng 2010	Rat: Sprague Dawley	40.7-43% fat	13 weeks	from 4 weeks	Male	Increased glucose AUC (12 wk)	ND	p=0.015	ND	ND
Carone 2010	Mouse: C57BL/6	11% vs. 20% protein	6-9 weeks	from 21 days	Male	Lower cholesterol	p=0.01	p=0.01	ND	ND
Fullston 2010	Mouse: C57BL/6	21% vs. 40% fat	10 weeks	from 5 weeks	Male	Bodyweight	p=0.02	p=0.003	P=0.005 (via Fem)	NS
						Glucose tolerance	p<0.05	p<0.05	P=0.05 (via fem)	NS

1.2.2.2 Maternal nutrition

Experimental models investigating the effects of maternal nutrition on offspring (and grand-offspring) have more confounding factors than those where the male is exposed. These include, the length of time the dam was exposed to the diet pre-pregnancy (and thus how obese she is), whether the embryo is exposed to the diet during pregnancy and whether the offspring are exposed during lactation. There is reasonable consistency in the literature that maternal diet programs increased weight gain in offspring (Bellisario et al., 2014; Benatti et al., 2014; Cannon et al., 2014; Cheong et al., 2014; Marco et al., 2014; Melo et al., 2014; Page et al., 2014; Sanders et al., 2014; Song et al., 2015). This phenotype is often exaggerated where the offspring are re-challenged with an obesogenic diet (Vogt et al., 2014). However, there are also examples of models in which maternal diet does not program this effect (King et al., 2013b; Platt et al., 2014). It is not clear why some models do not find changes in offspring. Review of methods from models published over the last year shows that the effect of diet is strongest during lactation and during pregnancy as opposed to pre-pregnancy and also that HFD interventions that are less extreme (for example 30-45% energy from fat) were more effective at programming weight gain in offspring than diets where 60% of energy came from fat. This might suggest that it is the diet itself rather than obesity, which is the main factor in determining a programmed effect (Table 1.2).

Table 1.2 Maternal over-nutrition models published 2014-2015. SC-standard chow (not matched control). ND Not reported,

Study	Species	Control (% fat)	Intervention (% fat)	Exposure from age	Exposure time pre-pregnancy	Exposure in pregnancy	Exposure in lactation	Effect in	
								F1 son	F1 daughter
(Bellisario et al., 2014)	p66KO mice (WT)	17	58	5 weeks	10 weeks	Yes	No	<0.05	<0.05
(Ma et al., 2014)	Macaca fuscata	13	36	ND	3 years	Yes	Yes	<0.05	<0.05
(Sanders et al., 2014)	C57BL/6	10	45	6 weeks	2-3 weeks	yes	?	<0.05	<0.05
(Cheong et al., 2014)	C57BL/6	7	45	10 weeks	6 weeks	Yes	Yes	<0.05	ND
(Mendes-da-Silva et al., 2015)	Swiss mouse	4.5	23	adult	3 weeks	Yes	Yes	<0.05	ND
(Benatti et al., 2014)	Swiss mice	SC	24	7 weeks	2 weeks	Yes	Yes	<0.05	ND
(Melo et al., 2014)	Swiss mice	SC	24	7 weeks	2 weeks	Yes	Yes	<0.05	ND
(Cannon et al., 2014)	C57BL/6	10.5	58	3 weeks	8 weeks	Yes	Yes	<0.05	ND
(Rodríguez-González et al., 2014)	Wistar rat		20% lard	2 weeks	120 days	Yes	Yes	<0.05	ND
(Song et al., 2015)	SD rat	10	45	3 weeks	9 weeks	Yes	Yes	<0.05	ND
(del Bas et al., 2015)	Rat			11 weeks	0 weeks	Yes	Yes	<0.05	ND
(Page et al., 2014)	SD rat	10	45		4 weeks	Yes	Yes	<0.05	ND
(Cordero et al., 2014)	Wistar rat	SC	45	12 weeks	0 weeks	Yes	Yes	<0.05	NS
(Marco et al., 2014)	Wistar rat	6	60	Day 22	58 days	Yes	Yes	ND	<0.05
(Brenseke et al., 2015)	C57BL/6	6.2	60	5 weeks	5 weeks	Yes	Yes and 7 weeks then CD	ND	NS
(Wang et al., 2014a)	NOD mice	10	60	4 weeks	8 weeks	Yes	Yes	ND	NS
(Laker et al., 2014)	C57BL/6	BC	60	8 weeks	6 weeks	yes	yes	ND	NS
(Sasson et al., 2015)	Mouse	25	60	>4 weeks	10-12 weeks	Yes/No	Yes/No	NS	<0.05
(Platt et al., 2014)	ICR mice	10,11	45,60,32,60	14 weeks	4 weeks a	Yes	Yes	NS	<0.05
(Martin et al., 2014)	3xtgAD mice	12	60	8 weeks	0 weeks	Yes	Yes	NS	ND
(King et al., 2014)	C57BL/6	10.5	58	5 weeks	12 weeks	Yes	Yes	NS	NS
(Dearden and Balthasar, 2014)	CD1	SC	58	8 weeks	0 weeks	Yes	Yes/no	NS	NS
(Vogt et al., 2014)	C57BL/6	12.5	55	adult	8 weeks	Yes/no	Yes/no	NS	NS
(Thorn et al., 2014)	Macaca fuscata	15	37	adult	1-5 years	yes	yes	NS	NS
(Desai et al., 2014)	SD rat	10	60	3 weeks	8 weeks	Yes	Yes/no	NS	NS

In order to examine whether there are true intergenerational effects, the grand-offspring of the exposed mothers must be examined. In mice, grand-maternal HFD reduced birthweight weight and insulin response to glucose (despite no clear effect in F1) (King et al., 2013a) and increased body length and reduced insulin sensitivity, even in the 3rd generation (Dunn and Bale, 2009, 2011).

Another murine model demonstrating an intergenerational response to dietary intervention is that of protein restriction/undernourishment where, following maternal exposure, offspring have low birth weight and develop obesity and impaired glucose tolerance, with the reduced insulin sensitivity being passed down to a further generation via the paternal line (Jimenez-Chillaron et al., 2009). Furthermore, sperm from males undernourished *in utero* exhibited reduced cytosine methylation, particularly at intergenic loci and enrichment in areas with greater heterochromatin, suggesting a possible chromatin-regulated mechanism for retention of methylation (Radford et al., 2014). This highlights differences between adult and *in utero* exposures to germ cells, which appear to elicit different epigenetic modifications (Carone et al., 2010; Öst et al., 2014), suggesting that different mechanisms of intergenerational inheritance may be active prenatally compared with postnatally.

1.2.2.3 Reproductive function

A high fat diet results in lower sperm counts and reduced sperm motility in mice, an effect that has also been demonstrated in some human studies (Eskandar et al., 2012; Håkonsen et al., 2011; Hammiche et al., 2012; Hammoud et al., 2008; Jensen et al., 2004). In rats, this was associated with testicular germ cell apoptosis (Li et al., 2013), and in mice with reduction in global spermatozoa methylation (Fullston et al., 2013), increased sperm DNA damage as detected by TUNEL (Fullston et al., 2012) and an increase in H3K9 acetylation (Palmer et al., 2011). The reduction in sperm motility was also noted to occur in the F2 generation grandsons (Fullston et al., 2012). Many of the

changes in the sperm of the F0 males due to HFD were reversed when they lost weight by exercise or diet (McPherson et al., 2014), along with reversal of the programmed paternal effect in the F1 offspring (McPherson et al., 2015). It may thus be that DNA damage or perturbed metabolism in the sperm is responsible for transmission of the phenotypes observed.

1.2.2.4 Exposure to endocrine disruptors

Exposure to chemicals, which can mimic steroid hormones, can program responses in offspring, for example, *in utero* exposure to the chemical dibutylphthalate (DBP) leads to a lower testosterone or compensated Leydig cell failure in adults, a finding associated with reduced testicular Steroid acute regulatory protein (StAR) expression and an increase in the repressive histone mark H3K27me3 at the proximal promoter of StAR (Kilcoyne et al., 2014). This direct exposure does not however suggest maintenance of an epigenetic change down the germ line.

In contrast, exposure *in utero* to Vinclozolin, a fungicide used by vintners, which is metabolised into compounds with high affinity for the androgen receptor (AR), can result in increased rates of germ cell apoptosis, disrupted testis morphology, reduced sperm count and impaired fertility in three generations of offspring, a finding transmitted down the male germ-line (Anway et al., 2005, 2006). Findings were consistent in both inbred Fischer and outbred Sprague Dawley rats (Anway et al., 2006) and associated with altered promoter methylation in the sperm from F3 offspring of exposed animals (Guerrero-Bosagna et al., 2010).

There is also evidence for transgenerational programming following *in utero* exposure to the synthetic oestrogen, diethylstilbestrol (DES). Human *in utero* DES exposure results in increased rates of birth defects in F2 grand-offspring (Titus-Ernstoff et al., 2010) and in mice, increased carcinogenesis (Newbold et al., 1998, 2006), findings

associated with altered methylation of the promoter of the proto-oncogene *c-fos* (Li et al., 2003).

1.2.2.5 Exposure to stress

A separate paradigm for investigating transgenerational effects has been stress exposure. Here (in a rodent model) restraint stress of mothers during pregnancy or postnatal stress (maternal separation) results in increased stress sensitivity and corticosterone response to stress in male offspring and their male grandsons (Franklin et al., 2010; Morgan and Bale, 2011), an effect that could be the result of a perturbed sperm miRNA milieu (Gapp et al., 2014). This paradigm highlights a difficulty in determining mechanisms: are the differences found in F2 offspring the result of the altered phenotype in the F1, or a result of the initial insult to the germline?

An alternative means of modelling *in utero* stress exposure is exposure to glucocorticoids. Dexamethasone is used as it passes into the fetus without degradation by placental enzymes. Here studies in rodents find exposure to dexamethasone *in utero* resulted in reduced birth weight and impaired adult glucose metabolism in the F2 generation (Drake et al., 2005, 2011) and in marmoset, altered lipid profiles in F2 and F3 females (Buchwald et al., 2012).

1.2.3 Summary

The mechanism by which these exposures result in intergenerational changes to phenotype are not clear. The genotype of the animals should not be altered by environmental exposures (although they may exert a selection pressure in non-experimental situations). This suggests that a non-genetic mechanism may be responsible.

1.3 Epigenetic mechanisms

Epigenetics refers to heritable changes in gene expression that does not involve changes to underlying DNA sequence. The term was proposed by Waddington in 1942 to suggest how a cell might interact with its environment to produce a phenotype (Goldberg et al., 2007). The epigenome has since been shown to be essential for regulating transcription factors during cellular differentiation during development (Spivakov and Fisher, 2007). The epigenome is also disrupted in pathological processes, for example, carcinogenesis (Shukla and Meeran, 2014), type 2 diabetes (Gillberg and Ling, 2015), and autoimmune disease (Gupta and Hawkins, 2015). Although, to the present date (with exception of carcinogenesis) the altered epigenome is an association with the pathology and the direction of causality is not clear.

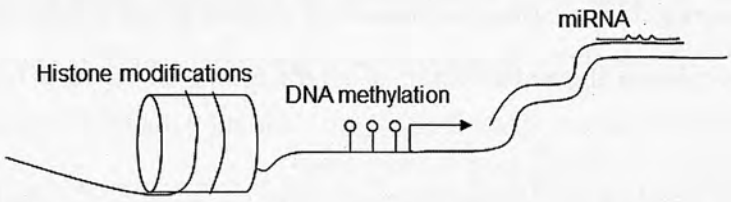

Figure 1.2 Three epigenetic modifications Histones may be modified to alter chromatin structure, cytosines may be methylated and miRNAs can interfere with translation of mRNA. Circles on sticks indicate methylated cytosines.

Three principal mechanisms of epigenetic regulation have been discovered: Cytosine methylation, histone modifications and non-coding RNA regulation of transcription and translation (Figure 1.2). There is strong evidence for the fact that methylation can be copied from a parent to daughter cell, despite the fact that histone modifications appear maintained at loci following mitosis, the mechanisms regulating this are less clearly

defined in mammalian systems. Each of these 'epigenetic modifications' and the mechanisms regulating them are discussed in the following section.

1.3.1 DNA methylation

Nucleotide methylation provides a mechanism for reversibly marking genomic DNA. Prokaryotes can methylate adenosine and cytosine, where in eukaryotes, only methylated cytosine has been discovered (Hotchkiss, 1948; Johnson and Coghill, 1925; Schübeler, 2015). A role for DNA methylation in transcriptional regulation was first demonstrated by injecting *in vitro* methylated DNA into *Xenopus* oocytes or mammalian cells and showing repression of gene expression (Stein et al., 1982; Vardimon et al., 1982). By injecting viral DNA into zygotes, in the same year, it was shown that *de novo* methylation was also able to regulate gene expression (Jähner et al., 1982).

As methylation is able to alter the functional state of DNA without changing the Watson-Crick base pairing it is an example of a classical 'epigenetic' mark. Methylation is implicated in the regulation of gene expression of several functional classes of DNA.

1.3.1.1 Functional classes of DNA regulated by methylation

Although non Cytosine-phosphate-Guanine (CpG) dinucleotides can be methylated, the majority (>75%) of methylation detected in the genome occurs at CpGs. The role of CpA/C/T methylation to date is still not clear, however, it is associated with reduced gene expression, reduced protein-DNA interaction and is enriched in areas of low CpG density (Guo et al., 2014c; Lister et al., 2013).

1.3.1.1.1 CpG Islands (CGIs)

CGIs are loci with the expected frequency of CG dinucleotides, the rest of the genome being relatively CG deplete There are several definitions for what a CGI is, perhaps the clearest being that proposed by Gardiner-Garden and Frommer: a region of at least 200bp and an observed/expected ratio of CG nucleotides of >0.6 (Gardiner-Garden and Frommer, 1987). Many genes have CGIs associated with their promoters (Antequera

and Bird, 1993; Gardiner-Garden and Frommer, 1987), however the majority of CGIs remain unmethylated. An exception to this are long-term mono-allelically silenced genes, for example X inactivation and imprinted genes (Li et al., 1993). Whilst methylation of a CGI within a promoter is highly likely to be associated with reduced transcription, unmethylated CpGs might not necessarily be associated with active genes (in fact very few genes rely solely on methylation for regulation of their transcription), and CGIs in the promoters of inactive genes do not tend to acquire methylation, although they do gain repressive histone marks, thus very few genes are solely reliant on methylation to control their expression (Schübeler, 2015; Tanay et al., 2007).

1.3.1.1.2 Imprinted genes

Imprinted genes are monoallelically expressed, depending on their parental origin. Most imprinted genes are clusters of 1Mbp and include both maternally and paternally expressed genes. Regulation of expression of these genes is coordinated by short sequences of DNA (imprinting control regions), which are differentially methylated depending on whether the allele originates from the mother or father. DNA methylation thus represses expression of part of the imprinted locus and mediates expression of the cluster of genes (Kalish et al., 2014). Thus some genes are only expressed from the paternal allelle and others from the maternal allele. The earliest described imprinted genes were the paternally expressed imprinted gene *Igf2* and the maternally expressed *Igfr2* (Ferguson-Smith et al., 1991). It has been proposed that the antagonistic coevolution between parental genomes could have driven the evolution of imprinted genes. For example, fetal expression of a growth factor not only influences the growth of a fetus, but also the indirectly affects the growth of and potentially fitness of siblings by altering demand for shared maternal resources. Altering fetal expression may thus have different fitness effects, allowing natural selection, especially if the two siblings are paternally unrelated (Moore et al., 2015; Patten et al., 2014).

Deletions or mutations within imprinted genes result in human imprinting disorders, for example, failure to express the maternal or paternal allele of the *SNRPN* locus results in Angelman and Prader-Willi syndromes respectively (Kalish et al., 2014).

1.3.1.1.3 Repetitive DNA

Up to half of the human genome is made up of mobile or transposable repeat sequences; these are thought to have arisen from viral integration. The sequences can be classified both by their ability to integrate into a new site of the genome of their cell of origin, and based on their size and location (Kazazian, 2004) See Figure 1.3.

Telomeric DNA sequences ([TTAGGG]n in vertebrates) are repetitive sequences capping chromosomes, which shorten with age (Eisenberg, 2011; Eisenberg et al., 2012), in order to maintain or extend telomere length, telomerase is expressed. Telomerase is a reverse transcriptase enzyme thought to have evolved from retrotransposons (Eickbush, 1997). Telomerase is expressed in prenatal tissue and cancerous cells but expressed in only low levels in the soma (Eisenberg, 2011). Telomerase is expressed in the germline, with strongest expression in males in the spermatogonia, and length of spermatozoal telomere is thought to correlate positively with age (Eisenberg et al., 2012; Ozturk, 2015) .

1.3.1.1.3.1 DNA transposons (Class II)

These elements are moved from one genomic site to another by a cut and paste mechanism. They are around 1-5kb in length. They have limited specificity of the sequence for integration and thus can insert themselves at a large number of genomic sites; however, most occur close to the parental site. The transposon codes for a transposase enzyme between inverted repeat termini (Kazazian, 2004; Smit and Riggs, 1996). The transposase recognises its origins by the repeat termini and excises itself. The DNA is then integrated into the genome at another location in which the repeat can be found. As the excision site is nicked, the host will 'fill in the gaps' leading to

elongation of the repeated section of DNA (Muñoz-López and García-Pérez, 2010). Transposition of the transposon is potentially unhelpful for the host, as well as the transposon, thus limiting the impact of transposition on host fitness is beneficial both to the host and transposon (Kazazian, 2004).

1.3.1.1.3.2 Retrotransposons (Class I)

Retrotransposons are transcribed into RNA and then reverse transcribed prior to reintegration into the genome, thus there is a duplication of the element. They are classified based on the presence or absence of long terminal repeats (LTR) at both ends. The mechanisms by which retrotransposons re-integrate are less thoroughly understood (Kazazian, 2004).

LTR-retrotransposons, around 5-10kb in length, comprise genes coding for a viral coat, a reverse transcriptase, ribonuclease and an integrase. Unlike retroviruses, they do not code for an envelope protein and thus are confined to remaining intracellular. They often target their reinsertion for fairly specific genomic locations. They include Intracisternal A particles (IAPs)(Crichton et al., 2014; Kazazian, 2004).

Non-LTR retrotransposons are usually 4-6kb in length and have two open reading frames, one coding a nucleic acid binding protein, and the other an endonuclease and an RT. They include the long interspersed nucleotide elements (LINEs), which encode about 20% of the human genome. Short interspersed sequences (SINEs) have shorter repeats of 100s of bps and constitute about 10% of the human genome, the majority being the *Alu* sequence (Crichton et al., 2014; Kazazian, 2004).

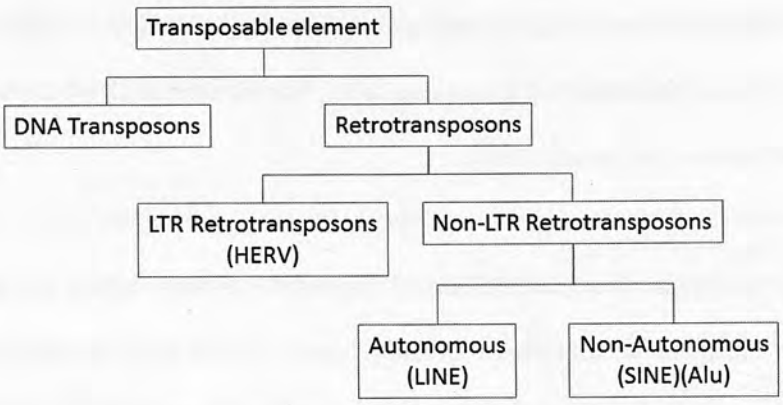

Figure 1.3. Taxonomy of transposable elements. Repeat elements within DNA can be classified based on their structure, size and composition. For example DNA transposons, which do not reverse transcribe themselves, but cut and paste the DNA. Or the retrotransposons, which do reverse transcribe themselves, and thus insert a *copy* into the genome. Retrotransposons can be further classified as to wherether they contain LTRs and, as to if they encode the proteins required for their reveerrse trasnciption (autonomous) or if they rely on the host for these (non-autonomous). Examples of common elements of each class are shown in parentheses.

1.3.1.1.4 X chromosome

Mammals carry the same sex chromosome system with common evolutionary origin at ~180 million years ago. Most humans carry either two X chromosomes or an X and a Y. The Y chromosome carries Sry, the 'sex determining gene', along with an abundance of genes important for sex-determination and spermatogenesis. This results in an imbalance in the dosage of genes on the X chromosome, two doses (XX) or one dose (XY). Expression of genes on the X chromosome is thus regulated to ensure balanced gene expression between the X chromosome and the autosomes, and similar expression between the sexes. X chromosome inactivation was proposed by Lyon in 1961 based on observations of chromatin morphology in male and female cells, and the mottling of female mice heterozygous for coat colour genes (Lyon, 1961). Imbalance of

expression of the X chromosome could be deleterious and mechanisms have evolved to compensate. Following fertilisation, one of the X chromosomes is inactivated, ensuring the correct dosage of genes are transcribed. X inactivation occurs via several mechanisms, which result in the acquisition of silencing histone modifications and methylation of CGIs. It should be noted that around 15% of human X-linked genes fail to become inactivated (Deng et al., 2014; Veitia et al., 2015). These 'duplicated' genes are thought to contribute to sexual dimorphism, and may explain differences in risk of metabolic disease (Chen et al., 2012; Li et al., 2014).

1.3.1.2 Conservation of methylation

Higher eukaryotes contain more abundant methylated cytosine than lower species, for example the mosquito *Aedes albopictus* carries just 0.03% whereas it is 2-8% in mammals (Doerfler, 1983). Recent advances in sequencing technology have meant it is possible to compare methylation of the whole genome in higher primates. Surprisingly, this demonstrated strong heterogeneity between humans and chimpanzees both in terms of abundance of methylation and its location, with more abundant methylation being found at human promoters and Chimpanzee gene bodies (Zeng et al., 2012). Thus, although methylation is widely observed in the natural kingdom, its prevalence and genomic distribution is variable. Care should thus be taken when extrapolating results from methylation studies between species.

Cytosine modification is a dynamic process, it occurs by DNA methyltransferases methylating cytosine to 5-methylcytosine (5mC), and is thought to be reversed by the oxidation of 5mC to 5-hydroxymethylcytosine (5hmC) (Penn et al., 1972), 5-formylcytosine (5fC) (Ito et al., 2011; Pfaffeneder et al., 2011) and 5-carboxylcytosine (5caC) (He et al., 2011) by the ten-eleven-translocation (Tet) enzymes.

DNA methylation is dependent on methyltransferase enzymes, which are introduced below.

1.3.1.3 DNA methyltransferases (DNMTS)

Cytosine methylation is catalysed by DNA methyltransferases (DNMTs). To date, 3 classes of DNMTs have been identified.

1.3.1.3.1 DNMT1

Maintenance methylation occurs each time a cell undergoes mitosis in order that the methylation is copied to each nascent strand of DNA. It is catalysed by DNMT1, which is recruited by NP95 (UHRF1) to hemimethylated CpGs at replication foci (Bostick et al., 2007). Knock out of DNMT1 causes embryonic lethality and extensive demethylation of the genome (Bestor, 1988; Gruenbaum et al., 1982; Lei et al., 1996). Two murine isoforms of DNMT1 have been identified, an oocyte specific (DNMT1o) and a somatic form (DNMT1s), a further splice variant, truncated at the 5' end and expressed, but not thought to be translated, has also been detected in pachytene spermatocytes (Mertineit et al., 1998). DNMT1o shows greater stability than DNMT1s, and it is thought that this aids prolonged activity in the early blastocyst, where methylation needs to occur rapidly (Ding and Chaillet, 2002). DNMT1o mutant mice have altered expression of imprinted genes in the placenta and 8-cell blastocyst. This results in lipid accumulation within the placenta, and altered fetal growth and impaired X-chromosome activation, implying a role beyond that simply of copying methylation from parent to daughter cells (Himes et al., 2015; McGraw et al., 2013).

1.3.1.3.2 DNMT2

Initially, DNMT2 was not found to have any *de novo* activity (Okano et al., 1998), however, it has since been shown to methylate tRNA and H4K20 (Goll et al., 2006; Phalke et al., 2009). Methylation by DNMT2 of tRNAs, which are abundant in sperm has also been suggested to be a mechanism by which paramutation might occur.

Paramutation is an epigenetic change caused by the mutation in one allele for a gene, which alters the expression of the complementary allele (Rassoulzadegan et al., 2006). Knockout of DNMT2 results in the loss of a paramutating mechanism (Kiani et al., 2013).

1.3.1.3.3 DNMT3

De novo methylation at unmethylated CpGs is conducted by DNMT3A and B (Okano et al., 1998a, 1999). *Dnmt3a* knockout mice survive to term but grow poorly and die at around 4 weeks of age (Okano et al., 1999). *Dnmt3b* knock-outs develop normally until e9.5 but then are non-viable; double knockouts were also non-viable, smaller and die before e11.5 (Okano et al., 1999). DNMT3A and 3B target different loci although there is some compensation of activity with respect to catalysing *de novo* methylation, especially at retrotransposons (Kato et al., 2007).

DNMT3L has a conserved structure to DNMT3a and 3b but lacks the catalytic domain (Aapola et al., 2000). Despite this, it remains essential for reproductive function, with disruption resulting in progressive azoospermia, failure of spermatocytes passing into the pachytene stage, and failure of imprinting at some maternally imprinted loci (Bourc'his and Bestor, 2004; Bourc'his et al., 2001). DNMT3L knockout results in reactivation of LINE1 and IAP elements, which leads to a checkpoint failure during spermatogenesis, and induction of apoptosis. Maternal null-derived embryos are also not viable, likely as a result of failure of imprinting in the oocyte (Bourc'his and Bestor, 2004; Bourc'his et al., 2001). DNMT3L knockouts are however viable, the early methylation in the zygote occurs, albeit at a reduced rate as a result of compensation by DNMT3a and 3b (Guenatri et al., 2013). The main functionality of DNMT3L appears to be through its ATP dependent helicase (ATRX)-DNMT3-DNMT3L (ADD) domain, which allows it to bind to histone 3 (H3)(Argentaro et al., 2007). Ablation of this domain results in a phenotype similar to the DNMT3L knockout (Vlachogiannis et al., 2015).

Methylation of H3 at lysine 4 (H3K4) results in failure of DNMT3L and histone binding and suggests why inactive promoters decorated with non-methylated H3K4 are able to become methylated (Hu et al., 2009; Tomizawa et al., 2012).

Given their essential role in *de novo* methylation, the DNMT3s play a role in the establishment of a new epigenetic code in the germline and could perturb methylation patterns in offspring. DNMT3a expression appears to increase during spermatogonial remethylation, from e14.5 onwards (Sakai et al., 2004; La Salle et al., 2004). DNMT3b expression appears to commence earlier, protein being detected at e12.5 (Hajkova et al., 2002; Kato et al., 2007; Niles et al., 2011; Sakai et al., 2001; La Salle et al., 2004). A summary of this is shown in Figure 1.4.

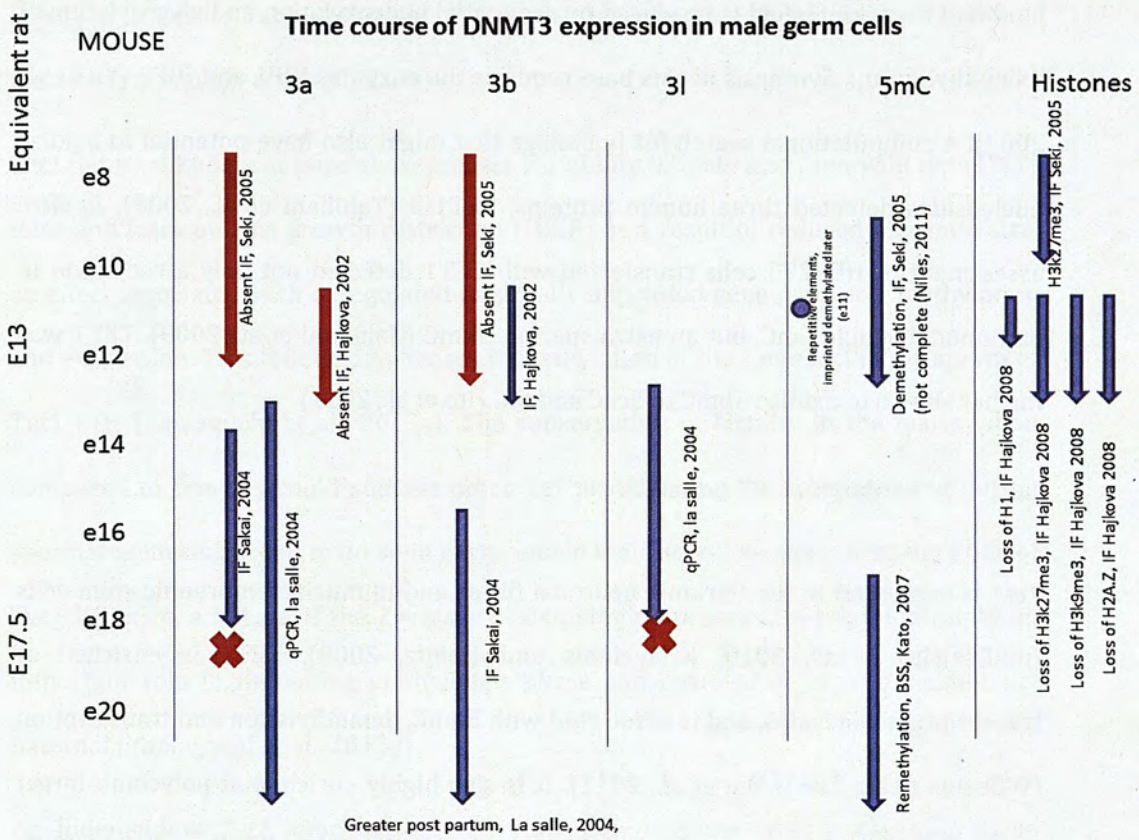

Figure 1.4 Expression of DNMT3 enzymes during germ cell development in the murine model . IF immunofluorescence, qPCR, quantitative polymerase chain reaction, BSS bisulphite sequencing, blue arrow indicates expression, red arrow indicates no expression, red-cross indicates that expression stops.

1.3.1.4 Ten-eleven-translocase enzymes

The ten-eleven translocase1 gene (*TET1*) was first detected as an oncogene commonly seen in acute myeloid leukaemia (AML)(Lorsbach et al., 2003; Ono et al., 2002). The translocation t(10;11)(q22;q23) was noted in several patients with AML and cloning of the breakpoint identified a well conserved protein family of (at the time) unknown biologic function next to the *mixed lineage leukaemia gene (MLL)* at *11q23* (Lorsbach et al., 2003; Ono et al., 2002). Two further human proteins with significant homology to TET1 were designated TET2 and TET3 (Lorsbach et al., 2003). It was a further five years before the function of the enzyme was determined; trypanosomes contain a

modified thymine (called J) produced by sequential hydroxylation and glycosylation of its methyl group. Synthesis of this base requires the enzymes JBP1 and JBP2 (Yu et al., 2007). A computational search for homologs that might also have potential to oxidise nucleosides detected three human proteins, TET1-3 (Tahiliani et al., 2009). *In vitro* assessment of HEK293 cells transfected with TET1 detected not only a reduction in immunodetectable 5mC, but an extra species, 5hmC (Tahiliani et al., 2009). TET1 was further shown to oxidise 5hmC to 5caC and 5fC (Ito et al., 2011)

1.3.1.4.1 Functions of TET proteins

1.3.1.4.1.1 Tet1

Tet1 is expressed in the Purkinje neuronal fibres and in murine embryonic stem cells (mESCs)(Ito et al., 2010; Kriaucionis and Heintz, 2009). TET1 is enriched at transcription start sites, and is associated with 5hmC, demethylation and transcription (Williams et al., 2011; Wu et al., 2011). It is also highly enriched at polycomb target gene promoters that are involved in transcriptional repression (Williams et al., 2011; Wu et al., 2011).

In e9.5 to e13.5 murine embryos, *Tet1* expression is greatest in the primordial germ cells (PGCs) (Hajkova et al., 2010). Using a gene trap derived mutant of *Tet1*, resulting in around 5% expression, *Tet1* homozygous mutants show reduced viability with 1/3 the frequency of expected viable animals. They also show reduced litter size when breeding heterozygotes together, an effect exacerbated when crossing homozygotes. The male gonad was morphologically normal, however there was a 30% reduction in ovary to weight ratio in homozygous females (Yamaguchi et al., 2012). Despite the loss in *Tet1* function, there was no significant reduction in global demethylation although there was a reduction in demethylation at gene bodies, IAPs, and other LTR-retrotransposons (Yamaguchi et al., 2012). The ovarian phenotype could be a result of

failure of meiosis; Tet1 is thought to act as a transcription factor for mediators of meiosis (Yamaguchi et al., 2012).

Tet1 paternal knockout pups show greater variability in body size than wild type (WT) mice and intra uterine growth restriction (IUGR) as a result of reduced placental size, an effect associated with deregulated paternally imprinted gene promoter methylation and expression. This followed increases in methylation at the same loci in the sperm of Tet1 KOs (Yamaguchi et al., 2013a). The conservation of fertility in the males when compared to females could suggest other Tet proteins may be compensating during spermatogenesis but fail to do so in early female meiosis. When examining the PGCs of Tet1 KO mice, a failure of the 2nd wave of demethylation was observed, indicating an important role in the active methylation phase and removal of imprints, especially paternal (Yamaguchi et al., 2013a).

An independent *Tet1* knockout was developed by excising exon 4, resulting in an unstable protein without the catalytic domain. These mutants did not show changes in fetal viability although did demonstrate increased size variability. Males and females were still fertile although litter sizes were reduced (Dawlaty et al., 2011)

1.3.1.4.1.2 Tet2

Tet2 is also expressed in mESCs but at lower levels than *Tet1* (Koh et al., 2011). Tet2 mutants are viable but demonstrate perturbed haematopoiesis as 5hmC is essential for the regulation of stemness in haematopoietic stem cells (Ko et al., 2011; Moran-Crusio et al., 2011). Knockdown of Tet1 or Tet2 results in reduced abundance of 5hmC (Dawlaty et al., 2011; Koh et al., 2011).

Combined knockdown of *Tet1* and *Tet2* confirms this with a greater loss of 5hmC in mESCs. Double knockouts (DKOs) are viable but suffer perinatal mortality with variable penetrance. Of the 40% surviving to adulthood, females had reduced ovary size and

males, variable testis size and, when crossed with WT mice, litter size is reduced. The apparent subtlety of the phenotype here may be due to the compensation by Tet3, expression of which was increased (Dawlaty et al., 2013).

1.3.1.4.1.3 Tet3

Tet3 is expressed in the zygote and oocyte. Its principal role appears to be the demethylation of paternal imprints following fertilisation and knock down results in embryonic lethality and failure to express pluripotency genes from the paternal genome resulting in impaired embryonic growth (Gu et al., 2011; Wossidlo et al., 2011).

1.3.2 Non-coding RNA

Known protein coding genes are estimated to account for about 10% of the mammalian genome. Transcriptomic studies however suggest that the majority of the genome is transcribed and a large number of transcripts do not encode proteins. The transcripts are known as non-coding RNA (ncRNA)(Luk et al., 2014).

ncRNAs are classified according to their length, which is thought to impact on their function. Short RNA refers to transcripts of fewer than 200bp; those longer are referred to as long non-coding RNAs (lncRNA). Short RNAs are divided further by their function and mechanism of action and include rRNA, microRNA (miRNA), short inhibiting RNA(siRNA), and Piwi-interacting RNA (piRNA)(Luk et al., 2014).

1.3.2.1 miRNA

First described in *C. elegans*, miRNAs are RNAs of between 19 and 25nt in length, which regulate mRNA abundance by affecting stability or translation (Kotaja, 2014; Lee et al., 1993; Wang and Xu, 2015). Mammalian genomes comprise around 1000 miRNA species, the majority of which are transcribed by RNA polII (Lee et al., 2004).

Following transcription, miRNA precursors, pri-miRNAs, which are often 5' 7-methylguanosine capped and 3' polyadenylated, form hairpin loops and are truncated

by Drosha, an RNAse and DGCR8, which targets the RNA substrate (Gregory et al., 2004; Lee et al., 2003) to form pre-miRNAs. pre-miRNAs can also be generated from short intronic hairpins that are excised by splicing and branching to mimic pre-miRNA, skipping the first Drosha/DGCR8 step. These are known as mirtrons (Ruby et al., 2007)

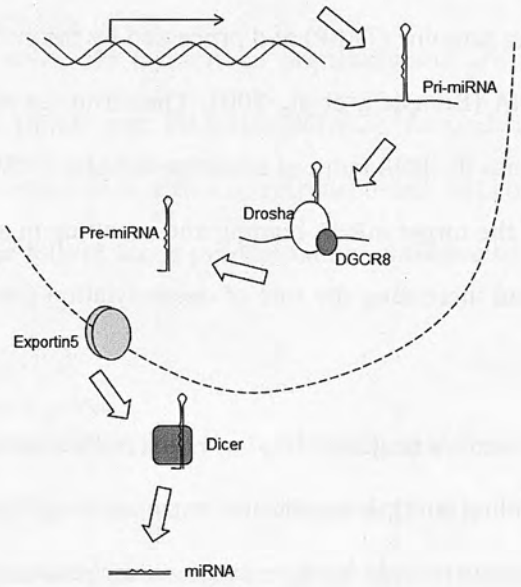

(Figure 1.5).

Figure 1.5 miRNA processing: pri-miRNAs are transcribed from DNA, they are bound by and truncated to pre-miRNA by DROSHA and DGCR8 prior to export from the nucleus by exportin5. Once in the cytoplasm, they are bound and further truncated by dicer forming mature miRNAs, which perturb translation and mRNA degradation.

1.3.2.1.1 siRNA

Endogenous siRNA (endo-siRNA) are transcribed by various means: as short hairpins (with an inverted repeat at each end, and not intronic), or in *cis* where the forward and backward strand of DNA are transcribed and form a dsRNA unit, or by two *trans* 'pseudogene' derived lengths of RNA binding to form a dsRNA unit. Unlike miRNAs, they are not dependent on Drosha and DGCR8 for processing prior to export from the nucleus. They do however require Dicer to enable maturation into mature siRNAs;

Endo-siRNAs are longer than pre-miRNAs but are still processed by the same downstream mechanism (Babiarz et al., 2008).

1.3.2.1.2 pre-miRNA processing

pre-miRNA, of around 55-70nt in length, is transported to the cytoplasm by the exportin-5, Ran-GTP complex (Lund et al., 2004). In the cytoplasm, pre-miRNAs are bound by TAR RNA-binding proteins (TRBP) and processed by the endonuclease Dicer into 22nt lengths of dsRNA (Bernstein et al., 2001; Chendrimada et al., 2005). The mature miRNA is loaded onto the RNA induced silencing complex (RISC) the functional strand, complementary to the target mRNA binding and resulting in a blockage to the ribosomal transcription and increasing the rate of deadenylation (reviewed in (Shen and Hung, 2015)).

Each miRNA can have hundreds of target mRNAs, and each mRNA has many target sites for multiple miRNAs (including multiple sites for the same miRNA). Binding of a miRNA to mRNA in metazoans requires only part sequence complementarity but a 'seed' region of 2-7 nucleotides must match perfectly; this tends to be in the 3' untranslated region. This impairs initiation of translation and also increases the rate of mRNA de-adenylation. miRNA-mRNA interactions are also specific to a cell's status thus, perturbed translation may only be seen at specific developmental stages, or during stress or in response to environmental stimuli (Wilczynska and Bushell, 2015).

1.3.2.2 piRNA

piRNAs are longer than miRNA (25-30nt). There are in the order of 10^5 different sequences within a species and they demonstrate very little conservation between species. The 5' end tends to be a Uridine, and the 3' end 2'-O-methylated (Fu and Wang, 2014; Hawkins et al., 2011). Despite the heterogeneity between species and between piRNAs, they are essential, and knockout of piRNA machinery results in catastrophic

meiotic failure (Bao et al., 2014; Carmell et al., 2007), as a result of derepressed transposon expression.

Two classes of piRNA are generated during mammalian spermatogenesis, pre-pachytene and pachytene.

1.3.2.2.1 Pre-pachytene piRNA

Pre-pachytene piRNAs are transcribed prenatally and are associated with the PIWI proteins PIWIL2 (MILI) and PILWIL4 (MIWI2). Around half of the pre-pachytene piRNAs are transcribed from within retrotransposons. MILI binds to *sense* transposable elements whereas MIWI2 binds predominantly *antisense* to transcripts (Aravin et al., 2008).

1.3.2.2.2 Pachytene piRNA

95% of known piRNAs are transcribed postnatally in the pachytene spermatocytes and round spermatids; they associate with PIWIL1 (MIWI) and MILI. They are mostly transcribed from non-repeat intergenic regions (pachytene piRNA clusters). They show little overlap to pre-pachytene piRNAs and are thought to originate from longer noncoding RNAs targeted by the piRNA pathway (Fu and Wang, 2014; Girard et al., 2006).

1.3.2.2.3 piRNA synthesis

piRNAs are synthesised via two known pathways, primary, via direct transcription of long precursor piRNAs, or via the Ping-Pong secondary synthesis pathway.

1.3.2.2.3.1 Primary synthesis

piRNA precursors can be hundreds of kilobases long and their transcription is initiated by the A-MYB transcription factor. Synthesis of mature piRNAs is independent of DICER but they are trimmed by the endonucleases mitoPLD and ZUCCHUNI. Intermediate length piRNA are further truncated by TRIMMER, the mature piRNA is then 2' o-

methylated by HEN1 and incorporated into a PIWI protein (Fu and Wang, 2014; Hawkins et al., 2011).

1.3.2.2.3.2 Secondary synthesis

During secondary synthesis, piRNA guide the PIWI protein to a complementary RNA target. The PIWI then cleaves the target RNA between the 10th and 11th nucleotide and the final target is methylated at the 3' end by HEN1, allowing the new piRNA to bind to the PAZ domain of PIWI proteins. The generated piRNA is then able to act to repeat the cycle with complementary RNA (Fu and Wang, 2014; Hawkins et al., 2011).

1.3.2.3 lncRNA

lncRNAs are transcribed by RNA polymerase II (PolII) but don't have protein coding ability, as yet there is no known universal protein responsible for processing lncRNA units. lncRNAs have a diverse array of functions (for review see Bonasio and Shiekhattar, 2014).

They can interact with proteins to modify their function for example, the lncRNA RMST interacts with SOX2 to induce neuronal differentiation (Ng et al., 2013) and there are over 22,000 protein–lncRNA interactions, which may play a role in transcriptional regulation (Li et al., 2015a).

lncRNAs also play a role in regulating chromatin structure for example by interacting with components of the PRC2 (Cifuentes-Rojas et al., 2014; Klattenhoff et al., 2013; Ng et al., 2012). However the truncation of these lncRNAs (for example *Airn*) has no effect on the transcriptional silencing, arguing against the specific recruitment of histone modifiers by protein-RNA interactions (Latos et al., 2012). Furthermore, PRC2 has high affinity binding to RNAs even from non-related organisms, casting doubts over whether RNA can specifically guide the PRC2 to sites requiring repression. One theory suggests that this non-specific binding could be a means by which Polycomb target genes, which

have escaped repression, become re-silenced (Davidovich et al., 2013). Another suggests that RNA may bind to the PRC2 in order to de-repress expression (Kaneko et al., 2013). There are certainly differences between binding efficiency and specific RNAs/RNA lengths, which suggest they may have a more specific biological role (Davidovich et al., 2015).

lncRNAs can directly bind DNA, for example *Xist*, which initiates the inactivation of one of the female X chromosomes by recruitment of the PRC2 (Hasegawa et al., 2010; Ohhata et al., 2011) (although high resolution microscopy demonstrates that Xist and PRC2 subunits do not co-localise suggesting an indirect mechanism (Cerase et al., 2014)). lncRNAs can also act as 'decoy' targets for DNA binding proteins for example *TERRA* and inhibition of telomerase (Redon et al., 2010).

lncRNAs reduce accumulation of sense and anti-sense mRNA, in a sequence independent manner, suggesting it may be the transcription of the lncRNA itself that regulates transcriptional rates of local genomic regions in *cis* (Kraus et al., 2013; Martens et al., 2004). lncRNAs can also regulate nuclear export of mRNA (Chen and Carmichael, 2009).

There are also examples of lncRNAs activating transcription. Many distal enhancer elements actually transcribe lncRNAs (eRNAs) that mediate transcription *in cis*, for example, by recruiting chromatin modifying complexes (Bertani et al., 2011). They also can act as miRNA precursors, for example *H19* and miR-675, which supress growth (Keniry et al., 2012).

1.3.3 Chromatin

1.3.3.1 Histones

DNA is packaged in the cell as chromatin. The principal component of chromatin are the nucleosomes that comprise an octomer of histones (H2, H3 and H4) around which

147 base pairs of DNA are wrapped. A linker histone (H1) binds to the nucleosomal and linker DNA resulting in higher-order chromatin structure (Kouzarides, 2007; Rathke et al., 2014).

There are further non-canonical histones, which function to open up the chromatin for transcription. Some of these variants are ubiquitously expressed but many are limited to germ cells where they may play a role in chromatin dynamics associated with meiosis, and with packaging the DNA into a sperm (Rathke et al., 2014).

1.3.3.2 Histone variants

There are three H1 variants present in mammalian testis, H1t, H1t2 and HILS1. Loss of H1t2 results in perturbed chromatin condensation following meiosis and reduced fertility (Martianov et al., 2005; Rathke et al., 2014).

H2A.X and H2A.Y are both expressed in the germ line of male mammals until spermiogenesis and disappear during meiosis. The variants TH2A and TH2B (testis – specific variants of H2A and H2B) are found in post-meiotic spermatids and are lost during condensation. Other testis specific variants (H2AL1/2) are present in condensing spermatids in the peri-centric regions of chromatin, perhaps playing a role in reprogramming. Despite the discovery of many forms of H2, so far, little is understood about its actual function (Govin et al., 2007; Rathke et al., 2014).

H3.3A and B are expressed in post-meiotic and meiotic prophase of spermatids respectively. H4 is the most slowly evolving of the histones and so far no variants have been found (Rathke et al., 2014).

An important feature of histones is the number of modified residues they contain. There are eight known modifications of histones described in Table 1.3. Histone modification is made even more complex by the fact that each residue may have more than one modification; for example Lysines may be mono, di or trimethylated. Each

histone modification may alter a cell's activity and modifications are made in response to signalling conditions within the cell (Kouzarides, 2007).

Table 1.3 Classes of histone modification adapted from (Kouzarides, 2007)

Modification	Residue modified	Functions regulated
Acetylation	K-ac	Transcription, repair, replication, condensation
Lysine methylation	K-me1 K-me2 K-me3	Transcription, repair
Arginine methylation	R-me1 R-me2a R-me2s	Transcription
Phosphorylation	S-ph T-ph	Transcription, repair, condensation
Ubiquitination	K-ub	Transcription, repair
Sumolynation	K-su	Transcription
ADP ribosylation	E-ar	Transcription
Deamination	R>Cit	Transcription
Proline isomerisation	P-cis> P-trans	Transcription
Crotonylation	L-Kcr	Resistance to repressors

1.3.3.3 Histone methylation

Transcriptional repression relies on the reconfiguration of chromatin such that access by transcription factors is reduced. This can be in a permanent manner, for example, in the formation of constitutive heterochromatin, or in a cell differentiation specific manner (facultative heterochromatin) where the chromatin has greater plasticity (Oberdoerffer and Sinclair, 2007). Lysine methylation is a key means by which this is

achieved. Histone acetylation, on the other hand, results in neutralisation of the positive charge of the histone tail thereby loosening histone-DNA interactions and opening up chromatin (Bannister and Kouzarides, 2011).

1.3.3.3.1 Set domain histone methyltransferases (HMT)

These are essential for forming constitutive heterochromatin and thus responsible for gene repression and genomic stability. For example the set domain HMT Suv39h methylates H3K9, which allows HP1 binding, and then recruitment of H4K20 methylation and DNMT3a and b to silence transcription at pericentric repeats (Lehnertz et al., 2003; Schotta et al., 2004)

1.3.3.3.2 Polycomb group proteins

These are repressive chromatin factors. Polycomb repressor complex 1 (PRC1) comprises four proteins, RING1, PCGF, CBX and HPH and inhibits transcription by ubiquitination of H2AK119, binding to H3K27me3 and compacting chromatin. PRC2 consists of EZH2, SUZ12 and EED, which mediate H3K27 methylation (Croce and Helin, 2013; Puschendorf et al., 2008)(Figure 1.6).

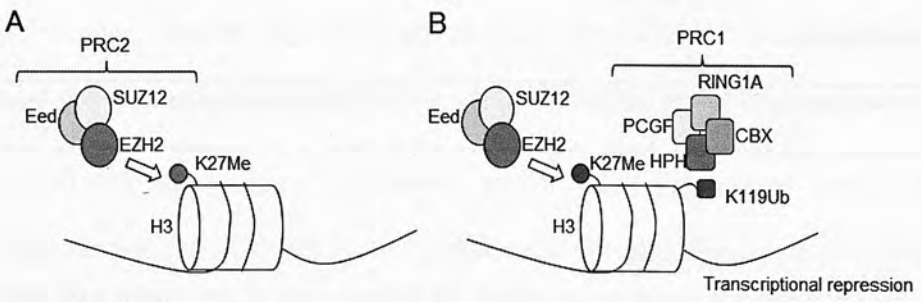

Figure 1.6 Polycomb repressor complex mediated transcriptional repression. (A) Recruitment of PRC2 results in trimethylation at K27 of histone 3. This is thought to result in recruitment of the PRC1 complex, which ubiquitinates K119 resulting in transcriptional repression (B).

1.4 Germ cell development

1.4.1 Introduction

The germ cell lineage is the reservoir of cells with reproductive potential. They are essential for the propagation of a species and the transmission of genetic (and possibly epigenetic) information from one generation to the next. The mammalian germline is responsible for the maintenance of genetic variation within a species, enabled by the unique germ cell process of meiosis, during which genetic material undergoes recombination and diploid cells become haploid. In mammals, PGCs are derived from somatic cells in contrast to flies, nematodes, frogs and fish where they are derived from the germplasm (Messerschmidt et al., 2014; Saitou and Yamaji, 2012). Thus, in mammals, germ cells must undergo a dedifferentiation from the ectodermal lineage; the subsequent differentiation of the germ line occurs early during development and is followed by their proliferation and migration to the developing gonads. Once in the gonads, the behaviour of XX and XY cells diverges and the cells develop into spermatogonia or oogonia. The germline is thus highly specialised and multiple steps during development set these cells apart from their somatic counterparts.

In the following section the development of mature germ cells will be traced from the initial establishment of the germline, paying special attention to the mechanisms in place that preserve integrity of the epigenome and which, might be perturbed by an adverse environment. Developmental biologists have focused on the mouse in order to determine the factors involved in the specification of primordial germ cells. Parallels with other mammalian models have been made but, in general, due to technical and ethical barriers work with early human cells has been limited to induced stem cell lines.

1.4.2 Establishment of primordial germ cells

In the mouse, the germ cell lineage appears to be specified from somatic ectodermal cells in the rapidly dividing, gastrulating embryo stage at e5.5-7.5.

At e5.5, BMP4 expression from the extra-embryonic ectoderm stimulates PGC development in a dosage dependent manner (Lawson et al., 1999). From around e7.5, BMP4 stimulates the expression of *Fragalis*, *Prdm1* and *Stella/Dppa3* in the PGC population of around 40 cells (Ohinata et al., 2005; Saitou et al., 2002).

Prdm1 acts to supress expression of somatic cell differentiation factors, for example the *Hox* genes (Hayashi et al., 2007; Ohinata et al., 2005). Furthermore, *Prdm1* is essential for the maintenance of *Prdm14* expression in PGCs. *Prdm14* is a regulator of GLP, a histone methyltransferase.that interacts with the PRC2 and results in an increase in the presence of H3K27me3 and the repression of somatic cell differentiation factors; mice deficient in *Prdm14* are viable but demonstrate stalled germline epigenetic reprogramming and male and female infertility (Yamaji et al., 2008).

In parallel to the suppression of somatic differentiation genes, pluripotency genes, which are tightly repressed by DNA methylation, become re-expressed or show continued expression in the PGC population. For example *Oct4*, which is expressed at the inner cell mass but expression of which becomes restricted to germ cells by e7.5 (Yeom et al., 1996), and the pluripotency markers *Nanog* and *Sox2*, which become expressed in the PGCs (Campolo et al., 2013; Yamaguchi et al., 2005). Expression of these genes is enabled by global demethylation, which starts to occur in the PGCs from around e8.5 (Hackett et al., 2013; Seisenberger et al., 2012).

1.4.3 PGC migration

Following PGC specification and initiation of replication, the germ cells become mobile and migrate to the genital ridges. In mice, at about e8, most PGCs have migrated posteriorly and laterally from the primitive streak to the endoderm of the invaginating hind-gut (Anderson et al., 2000). Migration continues anteriorly through the hind-gut, the population then splits into two, moving to the left and right before arriving in the

genital ridges at e9.5 to e10.5 (Richardson and Lehmann, 2010). This process is not completely understood but is thought to rely on chemotaxis.

1.4.4 PGC proliferation

During migration, the PGCs undergo proliferation. The e8 pool is roughly 100 PGCs whereas by e9.5 there are around 350 cells and by the time the cells have reached the genital ridge at e10.5 they are around 1000 in number (Tam and Snow, 1981).

During the phase of proliferation and migration, from e9.5 to e13.5, there is a global reduction in cytosine methylation. Evidence points towards two phases of demethylation, firstly, a passive phase where methylation is removed by cell proliferation in the absence of remethylation machinery, secondly, an active phase more heavily reliant on the enzymatic removal of methylation (Seisenberger et al., 2012).

1.4.4.1 Passive DNA demethylation

There is mounting evidence for an initial passive phase of demethylation. By e9.5, expression of the *de novo* DNA methyltransferases *Dnmt3a* and *Dnmt3b* in PGCs is repressed (Kagiwada et al., 2013; Seisenberger et al., 2012; Yabuta et al., 2006). Between e9.5 and e12.5, expression of *DNMT1*, the maintenance methyl transferase, remains abundant, however its essential cofactor *NP95* (*Uhrf1*) exhibits reduced expression and nuclear exclusion. Further evidence for a period of passive demethylation comes from the fact that when looking at strand specific DNA methylation during this period of proliferation, methylated CpGs are almost exclusively found on the same strand, indicating a failure of maintenance methylation mechanisms (Seisenberger et al., 2012).

1.4.4.1.1 Protection from demethylation

Whole genome bisulphite sequencing (WG-BSseq), locus specific BS-seq and Immunofluorescence (IF) all demonstrate a large drop in methylation levels in PGCs

around e6.5 to e9.5 from about 75% to 30% (Guibert et al., 2012; Seisenberger et al., 2012; Seki et al., 2005). This demethylation appears to be global affecting promoters, CGIs, introns, exons, and intergenic regions. However there are a few distinct sequence classes that have their methylation marks persevered in the early phase. These include imprinted genes, in particular the maternally imprinted genes, the promoters of genes required for germ cell development and meiosis, and the CGIs of the inactive X chromosome in females (Seisenberger et al., 2012). Maternally imprinted genes may be relatively protected from demethylation due to the higher CG content of maternal than paternally imprinted genes, and may play a role in regulating expression of paternally imprinted genes (Schulz et al., 2010). ZFP57 is a protein that associates with DNMTs and NP95. Many of the genes, retaining their methylation for longer, are enriched for ZFP57 binding sites, suggesting a mechanism in place to protect demethylation at specific loci (Quenneville et al., 2011; Seisenberger et al., 2012).

DNMT1 may also play a role (independent of NP95) in maintaining methylation at these sites during passive demethylation. There is ongoing expression of DNMT1 in the PGCs although, not of its co-factor *NP95*, perhaps indicating a non-canonical means of maintaining methylation at these sites during PGC proliferation. An argument against this is that tetracycline induced *DNMT1* knock down in ES cells results in continued methylation at key locations including in repeat elements (McGraw et al., 2015). It is postulated that this continued methylation is due to DNMT3A or B activity although, expression of these enzymes is low in the PGCs at this point (McGraw et al., 2015), and no evidence was found by WG-BSseq of PGCs for new methylation marks being laid down (Seisenberger et al., 2012). Thus, the means of maintenance of these methylation marks during PGC proliferation remains unclear. The CpGs escaping demethylation are clearly important as they are a potential means of passing epigenetic information from one generation to another.

There also remains some debate in the literature as to the timing of demethylation. Some studies show erasure of imprints after e11.5 (Hajkova et al., 2002) whereas others show slightly earlier demethylation kinetics (Kagiwada et al., 2013; Seisenberger et al., 2012). This might be explained because experiments are conducted on different strains of mice, or could be the result of differing environmental or experimental conditions.

1.4.4.2 Active DNA demethylation

A mismatch between PGC division and the rate of methylation loss has stimulated investigation into the mechanics behind demethylation. Initial focus was on the cytidine deaminases Activation Induced Deaminase (AID) and apolipoprotein B mRNA-editing enzyme catalytic polypeptide 1 (APOBEC1), deficiencies of which cause a relative increase in methylation compared to WT littermates (Popp et al., 2010). However, mutants of these proteins still undergo global demethylation (Popp et al., 2010) and AID expression appears to be low or absent during PGC demethylation (Kagiwada et al., 2013).

Thymine-DNA glycosylase (*Tdg)* recognises T: G mismatches and removes mismatched bases (for example following deamination or oxidation). It is expressed in PGCs at the message level, and *TDG* mutants exhibit biallelic methylation of the *Igf2r* imprinted region suggesting a role for the enzyme in demethylation (Cortellino et al., 2011). As global remethylation is inhibited in these mutants, this hypermethylation is likely a result of impaired demethylation as opposed to remethylation. Other components of the base excision repair pathways (BER) are also expressed in the PGCs suggesting a possible mechanism is in place for removal of 5mC or its oxidised derivatives (Cortellino et al., 2011). However, the oxidised derivative of 5mC can be removed even in the absence of *TDG*, indicating that although there is a role for *TDG* in demethylation, it is not essential (Guo et al., 2014a).

1.4.4.2.1 Active demethylation by TET enzymes

TET enzymes are also expressed in PGCs (Messerschmidt et al., 2014). Thus, the sequential oxidation of 5mC to 5hmC, 5fC and 5caC, and then removal by BER is another plausible explanation for the mechanism behind active demethylation. So far, efforts to track 5fC and 5caC though germ cell development using IF have showed few changes, and the roles of these derivatives are unclear (Hackett et al., 2013). Evidence for the role of 5hmC as an intermediate during active demethylation is accumulating.

By IF, levels of 5hmC increase in PGCs from e9.5 to e10.5, in parallel with the loss of 5mC. This is followed by a loss of both 5mC and 5hmC at e11.5-e12.5 (Hackett et al., 2013; Yamaguchi et al., 2013b). This was mirrored by 5mC/5hmC DNA immuno-precipitation and sequencing (5mc-dip-seq and 5hmC-dip-seq), which shows enrichment and then loss over intergenic regions (Hackett et al., 2013). Thus it is proposed that in the mouse, following the early 'passive' phase of demethylation of PGCs, there is an active removal of methylation occurring until around e13.5 when the cells are <5% methylated.

Methylation is retained particularly at Intracisternal A particles (IAPs), and other retrotransposons. CGIs in close proximity to IAPs often retain greater methylation, while those more distal show much greater heterogeneity. This might suggest that the genomic context of the IAP or its chromatin configuration can confer resistance to demethylation at adjacent elements (Guibert et al., 2012; Seisenberger et al., 2012). It is biologically important to keep these elements repressed to avoid mutagenesis in the germline.

CGIs more distal from repeat elements show much greater variability in terms of retention of methylation. However, the retention of methylation at some of these regions appears to be conserved in multiple murine datasets, including those

originating from spermatozoa and oocytes, suggesting they may be a potential means of intergenerational epigenetic inheritance (Seisenberger et al., 2012).

1.4.4.3 Methylation and transcription

The global loss of methylation has surprisingly little effect in terms of overall transcriptional activity, suggesting alternative mechanisms are also in place to regulate gene expression during the demethylation phase (Seisenberger et al., 2012). Promoter methylation at e16.5 did not correlate with transcription for the majority of regions however; there was an association between gene body (as opposed to promoter) methylation and mRNA abundance (Seisenberger et al., 2012). These differences may of course relate to differences in mRNA storage and deadenylation, which will impact on the relative quantity along with transcriptional activity.

Although there is a strong reduction in DNA methylation during PGC proliferation, this is not necessarily matched by transcriptional changes. This implies other mechanisms must be in place to protect the PGCs from the increase in transcription (in particular from repeat elements) that might be expected. Key mechanisms are likely to include changes to chromatin and small-RNA mediated mechanisms for example the PIWI/MIWI regulatory system (see 1.3.2.2).

1.4.4.4 miRNAs during PGC development

Using *TNAP-cre Dicer* conditional knockout mice, which results in loss of mature miRNAs in germ cells, a reduced cell number and proliferation are observed from e13.5 onwards in the neonatal testis (Hayashi et al., 2008). The development of the tubules in this model was unaffected suggesting that the miRNA within germ cells plays little role in the development of these structures (Hayashi et al., 2008). miRNAs (and endo-siRNAs, which rely on dicer) thus appear important but not indispensable in germ cell development. However there was poor penetration of the transgene in this model making further evaluation difficult.

1.4.4.4.1 piRNAs

Despite the poor conservation of sequence observed in piRNAs, they have a critical importance in transposon silencing, which is vital following demethylation. piRNAs work by targeting transposons directly for breakdown but also by recruiting methylation machinery during *de novo* methylation (Fu and Wang, 2014). Inactivation of MIWI2 or MILI results in increased LINE-1 and IAP expression, a reduction in the *de novo* methylation of the imprinted region *Rasgrf1*, and is associated later with meiotic arrest in the male germline (Aravin et al., 2008). MIWI2 mutation has a mild effect on reducing piRNA expression in e16.5 testis where MILI deficiency results in a more profound loss in expression (Aravin et al., 2008; Fu and Wang, 2014; Kuramochi-Miyagawa et al., 2008). Even in the absence of methylation and pre-pachytene piRNA, LINE1 expression is still repressed, perhaps by gain of the repressive histone mark H3K9me2 (Di Giacomo et al., 2013).

1.4.4.5 Chromatin changes during PGC proliferation

PGCs undergo a prolonged G2 phase in the cell cycle during migration. It is thought that this enables a restructuring of the epigenome; alongside the genome wide cytosine demethylation there is loss of H3K9me2 and H3K9me1 immunostaining from e7.5 to e10.5, a loss of which continues from its highest point at fertilisation (Seki et al., 2007). H3K9me2 is a mark associated with repressed genes and is associated with cytosine methylation (Seki et al., 2005, 2007). H3K9me3 expression has increased again by e13.5, where it protects against expression of repeat elements (Liu et al., 2014; Seki et al., 2005). H3K9 methylation is conducted in part by Setdb1 (Schultz et al., 2002). Conditional depletion of *Setdb1* in the germ line results in reactivation of a subset of repetitive elements, and reduced cytosine methylation at loci with depleted H3K9me3 suggesting a role for the histone modification in the laying down of methylation patterns (Liu et al., 2014). Furthermore, looking at temporal H3K4me2 and 5mC

sequencing data from male germ cells e13.5-e16.5 shows that peaks of the histone mark corresponded to regions with lower levels of methylation, and at the same loci as observed in mature sperm (Singh et al., 2013), suggesting the H3K4me might protect the genome from *de novo* methylation.

Over this time, in PGCs there is a gain in H3K27me3 (a repressive modification with plasticity), H4R3me2 (a repressive histone mark), H3K4me2 (an activating mark), and H3K9Ac (an activating mark) (Abe et al., 2011, Ancelin et al., 2006; Hajkova et al., 2008; Ikeda et al., 2013; Seki et al., 2005, 2007). H3K4 methylation and H3K9 acetylation become more abundant in the PGCs at e10.5 when they colonise the genital ridges, and expression regresses at e12.5 (Seki et al., 2005). The simultaneous gain of repressive and activating marks at the same loci, many of which are for developmental genes has led to the hypothesis that these genes are 'poised' and ready for transcription (Sachs et al., 2013).

The increase in transcription, which might be expected given the loss of repressive histone markers, is ameliorated by a reduction in RNAPII activity (Seki et al., 2007). Following e11.5, there is loss of H3K27me3, which then reappears at e13.5 despite continuing presence of EZH2. There is also loss of the histone variant H2A.Z (Hajkova et al., 2008).

The H3K64me3 modification is associated with pericentric heterochromatin, especially IAPs, LINE1 and subtelomeric repeats, but not with genic promoters. H3K64me3 is present in PGCs at e10.5 but is lost by e12.5, reappearing from e13.5 to e15.5 (Daujat et al., 2009).

Loss of H1, the linker histone and thus the opening up of chromatin is observed at e11.5 (Hajkova et al., 2008). This may enable transcription of genes regulating germ cell

development and also enable access of the *de novo* DNA methyltransferases to the chromatin.

1.4.4.6 Sex determination

Once they have arrived at the genital ridges, the PGCs become gonocytes reflecting a reduction in their potentiality to form terratomata. The morphology of the cells changes and they become easily identifiable by their large, round nuclei, containing one or two nucleoli, and ring of cytoplasm (Baillie, 1964). It is at this stage that signals from the surrounding somatic tissue initiate sex determination of the gonocytes. In ovaries, XX gonocytes enter the 1st phase of Meiosis I from e13.5. In testes, XY gonocytes stop proliferating and are arrested in the G1/G0 phase of the cell cycle at around e12.5 (Monk and McLaren, 1981).

In the majority of mammals, sex determination is controlled by the *Sry* (or homologs) gene on the Y chromosome. XY mice with no functional SRY develop ovaries (Lovell-Badge and Robertson, 1990) and conversely, addition of SRY to XX mice triggers testis formation (Koopman et al., 1991). *Sry* expression in somatic cells initiates expression of factors such as *Sox9*, and the differentiation of Sertoli cells that are essential for the organisation of the testis into cords and the interstitial spaces in which androgen producing Leydig cells develop (reviewed in Brennan and Capel, 2004).

1.4.4.7 Early male gonad development

Following differentiation, there is continued proliferation of the male gonocytes. Less is known about the factors involved in stimulating proliferation at this stage but there is evidence for importance of Retinoic acid (RA). RA is instrumental in determining fetal germ cell fate, and can induce proliferation of quiescent type A spermatogonia in vitamin A deficient mice and stimulate both proliferation and apoptosis of gonocytes (Trautmann et al., 2008). Proliferation discontinues at about e16.5 until the cells enter

G0/G1 arrest. At this stage, the cells are positioned centrally in the seminiferous tubules surrounded by Sertoli cells (Spiller and Koopman, 2011).

1.4.4.8 Remethylation

It is during this phase of proliferation and quiescence that the DNA within the male gonocyte undergoes remethylation. Genome wide scrutiny of the remethylation process is not yet reported however, although there is clear remethylation of the paternally imprinted genes from e16.5 with almost complete methylation seen at these loci by birth (Davis et al., 2000; Li et al., 2004). The rate of methylation appears to be different for the maternal and paternal alleles, with the paternal allele becoming more fully methylated earlier than the maternal copy (Davis et al., 2000). Methylation of retrotransposons seems to start a little later than that of imprinted genes (Kato et al., 2007), and some of these escape and are thought to require piRNA mediated recruitment of methylation complexes in order to control their expression (Chen et al., 2002a; Davis et al., 2000; Kato et al., 2007; Li et al., 2004; Molaro et al., 2014, Singh et al., 2013).

1.4.4.9 Chromatin changes following sex determination

In males, over the course e11.5-e17.5, there is an increase and then reduction in H3K9ac and H3K9me2, an increase in H3K4me3 and H3K9me3, and stable expression of H3K27me3. In contrast, in females, H3K9ac, H3K4me3, H3K9me2 and 3 showed little change in immunoexpression whilst H3K27me3 showed a reduction (Abe et al., 2011).

Active chromatin marks (for example H3K4me2) appear to protect DNA from remethylation and distinguish between maternally and paternally imprinted DMRs. The histone demethylases *Kdm1a*, *1b* and *5a* show expression in male germ cells during remethylation, indicating a possible mechanism by which histone marks are removed and *de novo* methylation occurs (Singh et al., 2013).

1.4.5 Spermatogenesis

Between p0.5 and p5.0, there is another phase of male germ cell proliferation that follows expansion of their cytoplasmic processes and their migration to the basement membrane of the cords. These cells are then termed spermatogonia, which includes the spermatogonial stem cells that establish and maintain spermatogenesis in adulthood (Clermont and Perey, 1957). There then follows a period of quiescence until pre-puberty. This phase results from the initiation of successive cycles in which the spermatogonial stem cells become committed to differentiate, undergo meiosis and form spermatids (Clermont and Perey, 1957).

Rodent spermatogenesis consists of three principal phases (reviewed in Manku and Culty, 2015)

1. A mitotic phase during which undifferentiated spermatogonia type A (single, pair and aligned) differentiate into type B spermatogonia via intermediate stages (types A1-4 and intermediate) (Figure 1.7).
2. A meiotic phase during which primary spermatocytes become secondary spermatocytes and then haploid spermatids. The meiotic prophase comprises the preleptotene, leptotene, zygotene and pachytene spermatocytes, distinguished by their position within the tubule, the presence of heterochromatin and synaptonomeal complexes in the nuclei
3. Spermiogenesis where spermatids elongate and undergo final maturation in the epididymis.

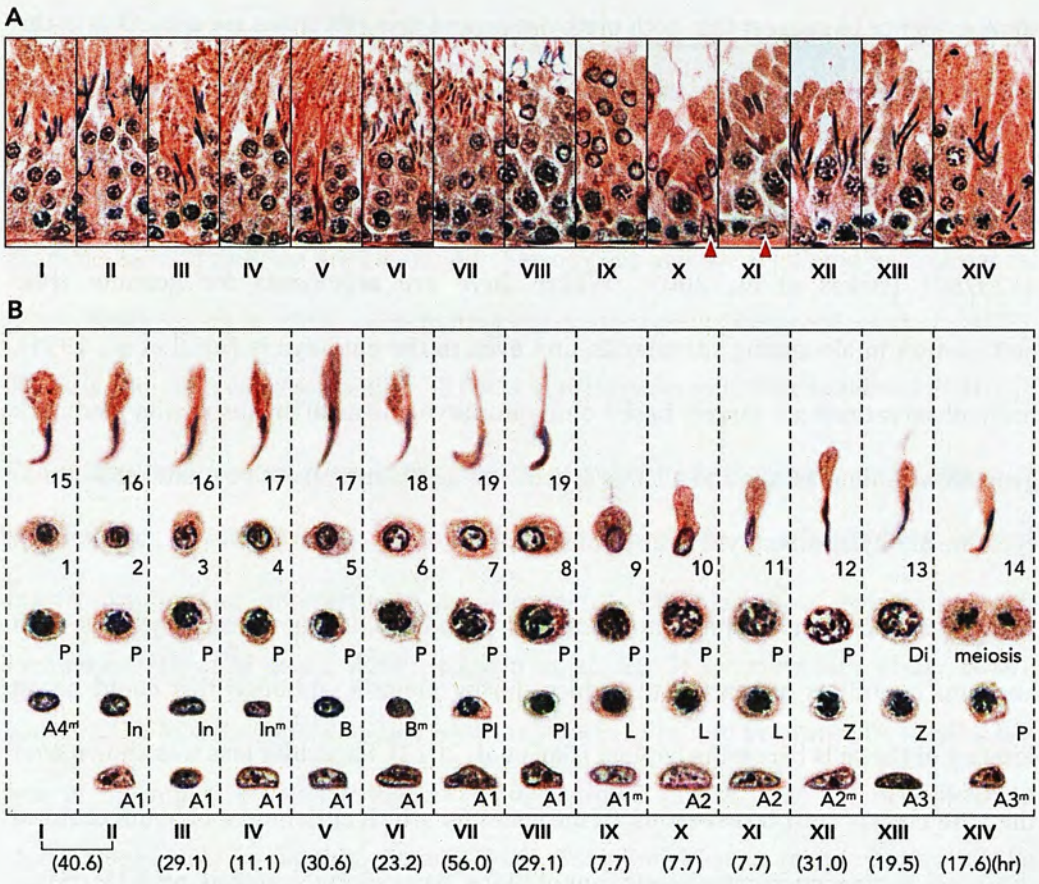

Figure 1.7 The spermatogenic cycle. Each stage of the cycle shown in **A** illustrates a unique association of specific germ cells and the Sertoli cell in the seminiferous epithelium, and the different germ cell types that are found in each stage are shown in **B**. In short, the entire epithelial cycle from I to XIV takes ~12.9 days to complete. However, a type A1 spermatogonium in stage II must pass through the epithelial cycle 4.5 times (58 days in the rat) before it becomes a step 19 spermatid in stage VIII. A1, type A1 spermatogonium; A1m, type A1 spermatogonium undergoes mitosis; In, intermediate spermatogonium; Inm, intermediate spermatogonium undergoes mitosis; B, type B spermatogonium; Bm, type B spermatogonium undergoes mitosis; Pl, preleptotene spermatocyte; L, leptotene spermatocyte; Z, zygotene spermatocyte; P, pachytene spermatocyte; 1–19, step 1 to step 19 spermatids that are formed during Spermiogenesis; ES, ectoplasmic specialization; Red arrowhead, Sertoli cell. (Xiao et al., 2014).

1.4.5.1 Methylation during spermatogenesis

The majority of methylation, particularly at imprinted loci and transposons, has been established by the time the type A spermatogonia are established at the basement membrane (Kato et al., 2007; Lees-Murdock et al., 2003; Li et al., 2004). There is also

some evidence to suggest that both methylation and demethylation are occurring in the adult testis, particularly between type A and pachytene spermatogonia. Whilst most genes remain methylated during spermatogenesis, a minority show increasing methylation (for example *Tcf3*) or even reduced methylation for example the LTR *AK137601* (Oakes et al., 2007). Whilst there are arguments for genome wide methylation in elongating spermatids, and even in the epididymis (Ariel et al., 1994), these observations are largely based on immunocytochemical or Restriction landmark genomic scanning assays and a locus specific, in-depth analysis of postnatal changes to cytosine methylation has yet to be published.

5hmC is also present in spermatogonia and spermatids during spermatogenesis, with absolute quantities appearing to reduce during meiosis, although this could be an artefact of the cells becoming haploid (Gan et al., 2013). Particular loss was shown over the SINE class of retrotransposons. Of the genes for which enrichment of 5hmC changed the most during spermatogenesis, annotations particularly matched protein coding genes related to phosphate metabolism. Furthermore, there was an enrichment for *Prm1, Prm2 and Prm3* in pachytene spermatocytes, just prior to the increase in transcription of protamine seen in the round spermatids in order that DNA can be repackaged (Gan et al., 2013).

In human adult male germ cells, expression of DNMT1, 3A and 3B has been demonstrated using both qPCR and immunofluorescence. Expression of DNMT1 and DNMT3B was shown at all stages during spermatogenesis (Marques et al., 2011). In mice, two isoforms of *Dnmt3a* have been identified, the 2nd truncated isoform showing similar expression to the larger form. In adult murine testis, expression of *DNMT3A* was strongest in type B spermatogonia whilst expression of *DNMT3B* was strongest in type A spermatogonia (La Salle and Trasler, 2006).

1.4.5.2 Non-coding RNA in spermatogenesis

1.4.5.2.1 miRNA

The male germ line contains several classes of miRNA, many of which are highly or exclusively transcribed in the testis, and in specific cell types (Kotaja, 2014). For example, several miRNAs are common in Sertoli cells and are regulated by androgens, so are likely to play a role in coordinating spermatogenesis (Panneerdoss et al., 2012). There is abundant expression of small RNAs in male germ cells (Buchold et al., 2010).

Conditional knockout of *Dicer* in the murine germline results in poor spermatogonial proliferation, reduced testis size as a result of reduced germ cell numbers, altered mRNA profile and, interestingly an unexpected suppression of retrotransposon expression (Hayashi et al., 2008; Romero et al., 2011; Zimmermann et al., 2014). Knockout of *Dgcr8* in the germline, which results in failure to produce pre-miRNA, has less of an impact on spermatogenesis, suggesting a greater role of endo-siRNA in spermatogenesis (Zimmermann et al., 2014). *Dicer* knockout under the control of the vasa homolog *Ddx4* results in severe defects in meiosis and apoptosis in spermatocytes (Romero et al., 2011). *Stra8* and *Ngn3*-cre dicer knockouts have reduced expression in spermatogonia type A and show a less severe phenotype (Korhonen et al., 2011; Liu et al., 2012). Finally, knockout of *dicer* in protamine expressing spermatids results in subfertile males with reduced sperm counts, litter sizes and apoptotic round spermatids (Chang et al., 2012). Thus at all stages of spermatogenesis, miRNAs play a pivotal role in the regulation of meiosis and the earlier in germ cell development that knockout of *dicer* is induced, the greater the accumulation of defects resulting in a more severe phenotype. In contrast to oocytes, in which endo-siRNAs seem more functionally important, both *Drosha* and the downstream *Dicer* small RNA processors are important in postnatal male germ cells (Kotaja, 2014; Wu et al., 2012). However, germ cell conditional knockout of *Ago2* results in no adverse effects on spermatogenesis implying

either compensation by another mechanism or an AGO2-independent means of miRNA regulation must be operational (Hayashi et al., 2008).

Endo-siRNAs are different to miRNAs in that under normal circumstances, dsRNA would mount an immune response via interferon (Song et al., 2011). Due to the immune privileged state of the germ cells in the testis, they are able to produce dsRNAs without mounting an immune response. The siRNAs are also transcribed from multiple positions in the genome, one example is expressed from every chromosome except the Y. They are also much more promiscuous than miRNAs when it comes to target mRNAs (Song et al., 2011).

During male meiosis, there is inactivation of the X and Y chromosomes, likely to reduce gene dosage issues. However, an island on the X chromosome expressing a set of miRNAs remains active, the exact role of these miRNAs is yet to be established (Buchold et al., 2010).

1.4.5.2.2 lncRNA

During the first wave of spermatogenesis in the postnatal murine testis, expression of 947 lncRNAs becomes upregulated, however the function of these has yet to be established (Laiho et al., 2013). In germ cells from adult rat testis, 1419 novel testis specific lncRNAs have been identified (Chalmel et al., 2014). Examples include testis specific X-linked (*Tsx*), which is important for progression through meiosis (and fear conditioning)(Anguera et al., 2011) and *dmrt1 related gene* (*dmr*), which trans-splices with *dmrt1* and regulates DMRT1 at a translational level (Zhang et al., 2010). The presumptive wealth of information regarding lncRNAs in the testis is yet to be explored at a functional level and may reveal insights into the regulation of spermatogenesis and the establishment of the 'sperm epigenome'.

1.4.5.2.3 piRNAs

Murine mutants of piRNA proteins arrest meiosis around the zygotene stage and there is large scale DNA damage, possibly as a result of derepressed retrotransposon activity, or perhaps as part of a cellular response to the deregulation (Fu and Wang, 2014). There is a second wave of piRNA expression during pachytene meiosis, which may be the result of MIWI breaking down retrotransposons or lncRNAs. Expression of MIWI is lost by the time the elongating spermatid stage is reached (Zhao et al., 2013). Thus the role of this second wave of piRNA expression remains unclear.

1.4.5.3 Chromatin changes during spermatogenesis

During spermiation, the chromatin is reconfigured to be tightly packed around protamines. The specific role of this compaction is not known but is likely to help with the generation of a hydrodynamic sperm head, protect the DNA against damage once it is outside the body and may have epigenetic properties (Rathke et al., 2014).

Protamines are high arginine and cysteine proteins likely to have evolved from H1, which has high lysine content (Miller et al., 2010). The abundance of arginine within the protein gives it a strong positive charge meaning they bind strongly to negatively charged DNA (Miller et al., 2010; O'Doherty and McGettigan, 2014). The high cysteine content means that covalent disulphide bridges form, further compacting the structure (O'Doherty and McGettigan, 2014). *Prm1* or *2* haploinsufficiency results in severely impaired sperm morphology and function, preventing transmission of both the WT and mutated alleles (Cho et al., 2001).

Transition proteins, which replace histones in an intermediate step have an equal composition of lysines and arginines. There are two transition proteins known in mammals (TNP1 and TNP2), and they are transcribed at mouse stage VII and stored for three to seven days prior to translation (Meistrich et al., 2003). Knockout of either of the *Tnps* in mice results in partial infertility and incomplete chromatin condensation

with the phenotype being more severe in Tnp1 KOs (Adham et al., 2001; Shirley et al., 2004; Yu et al., 2000).

The chromatin in the elongating spermatid is compacted in a multistep process during which there is an uncoupling of transcription and translation (Sassone-Corsi, 2002). Transcriptional activity may be reduced due to increasing levels of cytosine methylation, although there is no evidence for this yet on a genome wide scale. This is accompanied by increasing histone acetylation (Grimes Jr. and Henderson, 1983; Lahn et al., 2002), and nicks in the DNA made by topoisomerase II that make it more flexible (McPherson and Longo, 1993; Miller et al., 2010; O'Doherty and McGettigan, 2014). This histone removal is facilitated by binding of bromodomain containing proteins, for example BRDT, loss or inhibition of which results in abnormal nuclear architecture and chromatin organisation during spermatogenesis (Gaucher et al., 2012; Matzuk et al., 2012). The DNA is then wrapped around transition proteins, which are then replaced by protamines.

In mice, chromatin to protamine transition occurs around 156 hours after the completion of meiosis when the spermatids are elongating, and histones are no longer present by the time stage XII is reached. By stage XV the transition proteins have disappeared, thus the whole process of histone replacement by protamines is thought to take around 120 hours (Hazzouri et al., 2000; Rathke et al., 2014). The length of time it takes to generate a mature sperm may have relevance when considering environmental exposures, which may be acute or chronic, and thus affect a small subset of sperm at a particular stage in the cycle, or a larger number should the spermatogonia be affected.

Not all histones are removed from the developing spermatids, in particular, 'poised' histone marks have been found in mature spermatozoa, enriched at genes important

for early development and differentiation, thus implying a potential functional role for their retention (Brykczynska et al., 2010; Carone et al., 2014; Puschendorf et al., 2008; Werken et al., 2014). Dietary intervention in a murine model results in altered H3K4me3 retention perhaps suggesting a means of intergenerational inheritance (Carone et al., 2010). In contrast to mice, in which there is ~95% removal of histones during spermatogenesis, in humans, up to 15% of histones are retained (Brykczynska et al., 2010). Furthermore, in humans this retention at regions of constitutive heterochromatin is important for structuring of chromatin in the early embryo, in contrast to mice where PRC1 is essential for its establishment (Werken et al., 2014). Whether this is an indicator of the less efficient process of spermatogenesis in man compared to mice, or if it highlights an increased susceptibility to intergenerational inheritance remains unclear.

A summary of epigenetic changes during male gem cell development in show in Figure 1.8.

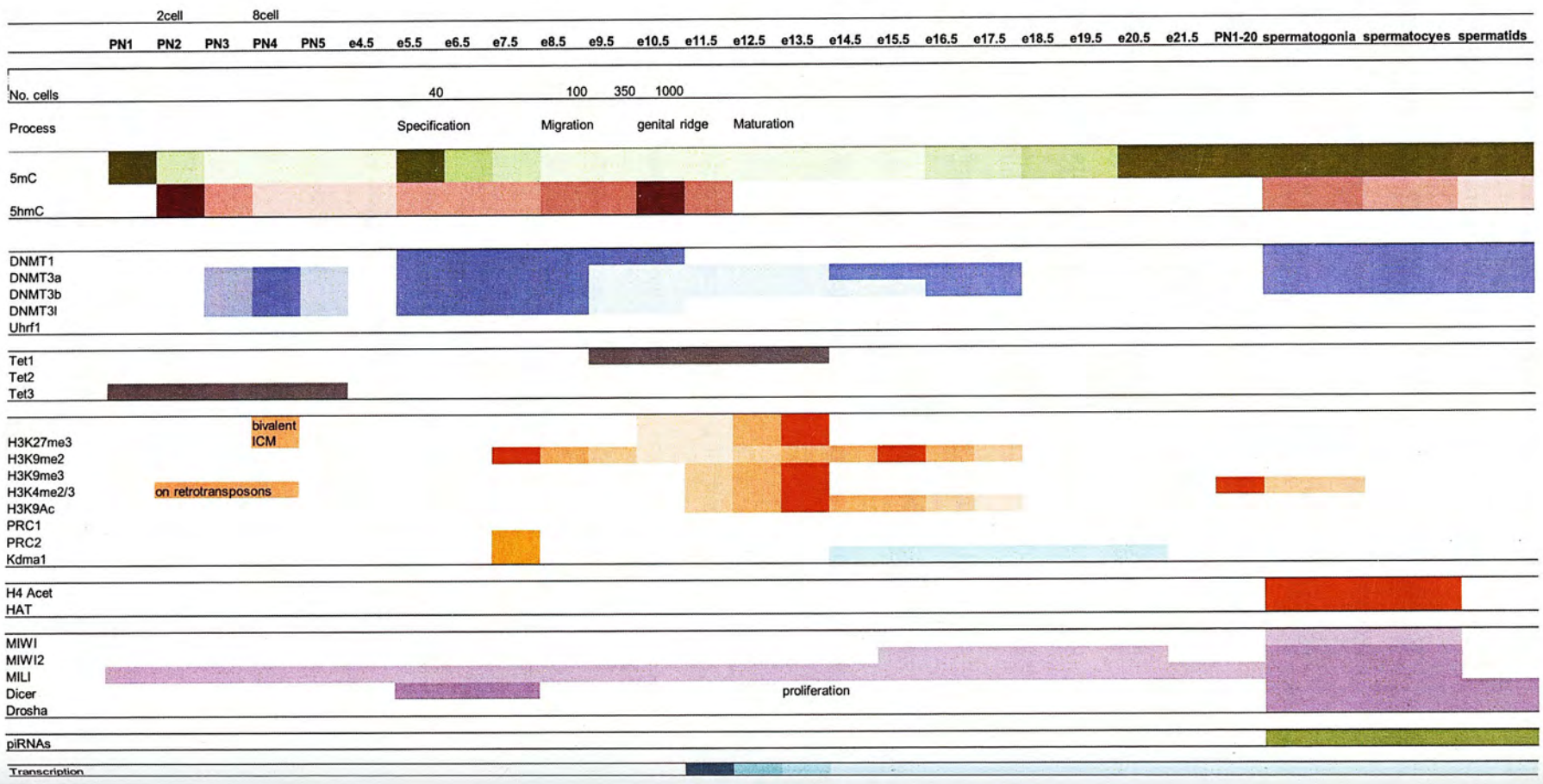
2cell
8cell
PN1
PN2
PN3
PN4
PN5
e4.5
e5.5
e6.5
e7.5
e8.5
e9.5
e10.5
e11.5
e12.5
e13.5
e14.5
e15.5
e16.5
e17.5
e18.5
e19.5
e20.5
e21.5
PN1-20 spermatogonia spermatocyes spermatids
No. cells
40
100
350
1000
Process
Specification
Migration
genital ridge
Maturation
5mC
5hmC
DNMT1
DNMT3a
DNMT3b
DNMT3l
Uhrf1
Tet1
Tet2
Tet3
bivalent
ICM
H3K27me3
H3K9me2
H3K9me3
H3K4me2/3
H3K9Ac
PRC1
PRC2
Kdma1
on retrotransposons
H4 Acet
HAT
MIWI
MIWI2
MILI
Dicer
Drosha
proliferation
piRNAs
Transcription

Figure 1.8 Summary of the epigenetic modifications occurring during male germ cell development

1.4.6 Oogenesis

In XX mammals, in the absence of the *Sry* gene, the bipotential gonad undergoes differentiation into ovaries. There are however, some XX individuals who develop testes in the absence of SRY (McElreavey et al., 1993). Such cases support the hypothesis that there are ovarian determining genes negatively regulated by SRY. Potential candidates include WNT4 (Biason-Lauber et al., 2004) and RSPO1 (Tomizuka et al., 2008). *Wnt4* and *Rspo1* are expressed in somatic tissue but become ovary specific at e11.5. Knockout of *Wnt4* and *Rspo1* and somatic cell ablation of the canonical Wnt signalling pathway result in formation of testis-specific vasculature within XX gonads (Chassot et al., 2008).

The first distinguishable signs of ovarian development appear at e13.5 when the germ cells start to undergo meiosis. The female germ cells pass through the leptotene, zygotene and pachytene stages of meiotic prophase I before arresting in diplotene. During these meiotic stages, the DNA undergoes recombination and chromosome alignment and is extremely vulnerable to damage. This is thought to result in degeneration of many oocytes (around 80% loss of oocytes in rodents, 90% in humans)(Nicol and Yao, 2014). Oocytes arrest at diplotene of prophase I of meiosis as 'primordial follicles'. Following puberty, the oestrus cycle stimulates recruitment of a group of primordial follicles to grow from which one (or several in multi-ovular species) will resume meiosis (for review see van den Hurk and Zhao, 2005; Nicol and Yao, 2014). During the growth phase, the oocytes regain meiotic competence. The surge in gonadotrophin release resumes meiosis in the fully grown oocytes, which mature and arrest at metaphase II until meiotic completion is triggered by fertilisation (van den Hurk and Zhao, 2005).

1.4.6.1 *Methylation of the oocyte genome*

Remethylation of the female gametes follows a later course than that of spermatogonia. Methylation of maternally imprinted genes occurs over pnd1-20, with different loci showing different rates of methylation (Obata and Kono, 2002). Using reduced representative bisulphite sequencing in growing murine ovaries, increasing methylation over the course of growing ovaries up to meiosis II has been observed for all CGIs. Interestingly, the methylated CGIs annotated as intragenic showed increased transcription and, there was no correlation with methylation at promoter CGIs and gene expression during ovarian growth (Smallwood et al., 2011). This provokes the question as to whether it is the transcription of a gene itself that promotes DNA methylation by recruitment of DNMTs. Furthermore, bisulphite sequencing of imprinted loci at different sized follicles showed that increasing follicular size was associated with increasing methylation (Denomme et al., 2012). Over this period there is expression of the *de novo* methyltransferases *Dnmt3a* and *3b*, although, it appears as though *DNMT3B* is excluded from the nucleus between pnd7-21. There is particularly strong expression of *Dnmt3l* over this period, supporting a role for this co-factor in establishing maternal imprints. Additionally, knockout of *Dnmt3a* or *Dnmt3l* results in a large reduction in methylation at CGIs (Lees-Murdock et al., 2008; La Salle et al., 2004; Smallwood et al., 2011). Although *DNMT1o* is expressed in the growing ovary, it is not nuclear at the time points during which the maternal imprints are laid down, and its deficiency does not result in perturbed maternally imprinted loci (Howell et al., 2001; Lees-Murdock et al., 2008). The mature methylated oocyte is then ready for fertilisation.

1.4.6.2 *Small RNAs and oogenesis*

Small RNAs appear essential for normal ovarian development. Conditional knockout of *dicer* in oocytes results in meiotic catastrophe and increased expression of

transposable elements and almost 20% of the transcriptome mis-regulated (Murchison et al., 2007). The fact that *Dgcr8* and *Drosha* null oocytes have a normal transcriptome and undergo meiosis (Suh et al., 2010; Yuan et al., 2014), and that conditional knockout of *Ago2* results in similar failure in oogenesis to that seen in the *dicer* null mice (Stein et al., 2015), suggests that the oocyte is dependent on endo-siRNA to pass safely through meiosis. The precise mechanisms remain to be explored.

The expression of piRNA in oocytes also appears critical and may have a role in intergenerational transfer of epigenetic information. Studies in drosophila deficient in piRNA indicate that introduction of piRNAs into the germline of the next generation (presumably via secondary synthesis) is principally the result of piRNA from the oocyte (Le Thomas et al., 2014).

1.4.6.3 Chromatin changes during oogenesis

The growth of the germinal vesicle (GV) is associated, with an increase in global 5mC and a general reduction in transcriptional activity, similar to the late stages of meiosis in spermatids (Lodde et al., 2008; Luciano et al., 2014). Loss of histone deacetylase 2 (HDAC2) results in infertile or subfertile mice with reduced ovarian weight, failure of some of the oocytes to develop beyond the secondary follicle stage (kinetochore-microtubule instability) and a loss of mitotic potential following insemination. Histone acetylation is associated with permissive chromatin, however, knockdown of HDAC1 and 2 (resulting in increased acetylation) was associated with reduced transcriptional activity, possibly due to associated H3K4 demethylation (Ma and Schultz, 2013; Ma et al., 2012). Immunoexpression studies have shown increasing H3K9, H3K18, H4K5, and H4K12 acetylation, along with increases in H3K4me2, H3K4me3, H3K9me2, and H3K9me3 in the growing GV. However, the role of activating histone modifications in the oocyte during growth remains a puzzle given that there is widespread transcriptional repression (Kageyama et al., 2007).

1.4.7 Reprogramming following fertilisation

Following fertilisation of the oocyte by the spermatozoon, there is a further round of reprogramming, in particular genome wide DNA demethylation. Reprogramming has three potential functions:

1. The resetting of methylation levels such that biallelic expression is possible in potential somatic cells.

2. Demethylation to allow gene expression required for early development.

3. Allowance of the parent-specific expression of imprinted genes. The latter is a function conserved solely in mammals where many of the genes control the growth of the placenta, which for example is not required in zebra fish (Jiang et al., 2013).

As is the case with the development of gametes, the demethylation of the zygote is asymmetrical; the loci that become demethylated depend on the parent of origin and specific location in the genome. This is likely to be as a result of DPPA3 protecting imprinted areas from oxidation by TET3 (Nakamura et al., 2007, 2012). There is ongoing discussion in the literature as to whether demethylation occurs by active or passive mechanisms. Evidence for passive demethylation is becoming increasingly disputed as sequencing technology improves and strand-specific sequencing traces the loss of multiple methylation marks on the same strands of DNA (Hackett et al., 2013; Seisenberger et al., 2012).

5mC-, 5hmC- and 5fC-specific and parent of origin-specific sequencing suggests that the rate of oxidation and removal of 5mC and its oxidised bases is too fast to be accounted for by the rate of cell division, and that active demethylation is occurring on both the paternal and maternal genomes (Guo et al., 2014a). Thus, evidence is mounting (in mouse (Guo et al., 2014a) and human (Smith et al., 2014)) for an active process of

demethylation in mammals during which some genes are protected. There continues to be the missing link in the puzzle and that is the mechanism for converting 5mC or its derivatives back to non-methylated cytosine (which occurs even in the absence of *Tdg*, and cell cycle inhibition)(Gu et al., 2011; Guo et al., 2014a; Smith et al., 2014; Wang et al., 2014b).

Several loci, as in the demethylation of PGCs, escape demethylation, particularly IAPs and imprinted regions (Guo et al., 2013). Likewise there is a stability in CGIs, which remain relatively unmethylated during the remethylation process (Guo et al., 2013; Wang et al., 2014b). Loss of methylation is greatest (perhaps unsurprisingly) on the paternal genome, the maternal genome showing reductions in methylation principally at specification of the inner cell mass (Guo et al., 2013, 2014b; Wang et al., 2014b). Furthermore, comparison between strains of mice shows that SNPs can introduce imprinting control sites, suggesting these regions could have an impact on epigenetic regulation (Wang et al., 2014b)

In the PGCs, methylation has been restored by e6.5. DNMT3a and DNMT3b are expressed in two cell and four cell embryos, thus mechanisms for remethylation are in place, and are presumably essential for correct differentiation (Huntriss et al., 2004; Wang et al., 2014b; Zhang et al., 2015).

1.4.7.1 Non-coding RNA in the fertilised oocyte

Small RNAs but not miRNAs are essential for early embryogenesis: Knockout of *Dgcr8*, essential for pri-miRNA synthesis in the nucleus, has little effect on the development of the preimplantation embryo; knockout of *Dicer* however causes dramatic dysregulation in mRNA, although neither mutant shows changes in retrotransposon expression. This suggests a role for *Dicer* that is independent of miRNAs for example, mirtrons and endo-siRNAs, in regulation of translation during early development and demonstrates

that other mechanisms (likely chromatin and DNA methylation) must regulate transposon activity at this point (Suh et al., 2010).

1.4.7.2 Removal of protamines

The chromatin of the zygote immediately following fertilisation is asymmetrical and remains physically isolated for 24 hours (Burton and Torres-Padilla, 2014). The DNA of the oocyte continues to be wrapped around histones whereas the paternal genome is tightly wrapped around protamines (Burton and Torres-Padilla, 2014; Santos et al., 2005). Chromatin restructuring is crucial to enable proper development, however some information regarding parent of origin for genes must be maintained in order that successful imprinting can occur (Burton and Torres-Padilla, 2014; Werken et al., 2014).

In mice, histones acquired by the paternal genome are derived from the oocyte and are largely devoid of heterochromatin, which must be established from the maternal epigenetic machinery (via the H3K9/HP1 pathway) (Santenard et al., 2010). In contrast, in humans, a greater proportion of histones are retained in the spermatozoa, and there is some evidence to suggest transmission into the embryo and, that the modified histones are maintained through cell divisions, thus paternal constitutive heterochromatin maybe transmitted inter-generationally (Werken et al., 2014).

At the 4-8 cell stage in mice, there is removal of the heterochromatin marks H4K20me3 and H3K64me3 on the maternal genome, potentially allowing reprogramming, this is accompanied by the appearance of the activating histone modifications H2A.Zac and H3K36me3 (but prior to the start of transcription perhaps suggesting an alternative function) (Bošković et al., 2012). At this stage, there is also loss of the active histone mark H3K4me3, which results in silencing of repetitive elements (Fadloun et al., 2013).

Histone methylation occurs in a step-wise manner with mono-methylation relying on different enzymes to di- and tri-methylation. Mono-methylation of H3K4, H3K9, H3k27, and H4K20 can be found in the paternal pronucleus but trimethylation is absent. This mirrors, the delay in accumulation of PRC2 in the paternal pronucleus (Burton and Torres-Padilla, 2014; Santos et al., 2005).

Following this initial phase of reprogramming, the ectodermal cells become specified and will ultimately dedifferentiate into the PGCs and the cycle of gametogenesis continues.

1.4.8 Summary

During germ cell development, the 'epigenome' is reset several times. This enables the packing of DNA into a sperm, unpacking the DNA in the zygote, specification of pluripotent cells, the maintenance of imprinted genes and thus regulation of placental growth in mammals, and the control of repeat elements whilst the DNA is vulnerable during meiosis. These processes are conserved across mammals and to an extent across metazoans. They are intricately linked and show redundancy such that there are 'back-up' mechanisms should there be a failure and, where there is a failure, meiosis is arrested to prevent transmission of the trait across generations.

Reprogramming opens the potential for environmental cues to alter the epigenome of the developing germ cells, and thus modify the development of offspring. Epigenetic regulation of germ cells may thus be a mechanism by which environmental cues may be integrated and a signal regarding the environment can be passed from one generation to the next.

1.5 Summary

The current obesity pandemic is likely the result of altering environments (diet, exercise, toxins) over the past century. However, the epidemiological and experimental

evidence explored above suggests that diet may also have an intergenerational effect, which might be mediated via an epigenetic mechanism transmitted via the germline.

Should this prove to be the case, it could indicate that the health of future generations would be improved by paying attention to the environment around the current generation. However, the potential window of opportunity for intervention is currently unknown, and the time point of gametogenesis at which the germline is susceptible to disruption by environmental factors has not been investigated experimentally. Epidemiological data suggests that puberty is an important time (for example paternal smoking or nutritional exposure) (Northstone et al., 2014; Pembrey et al., 2006).

Much of the evidence examined above comes from murine studies. Whilst an important experimental model, it is prudent to identify if mechanisms are conserved, especially with primates in which germ cell development does differ from rodents (McKinnell et al., 2013). To investigate this, fetal testicular tissue from rats, marmosets and human was examined for epigenetic machinery to identify parallels (Chapter 3).

Mechanisms responsible for intergenerational effects of dietary exposure have so far remained elusive. In order to investigate this further, a HFD exposure was investigated in a transgenic rat expressing eGFP in the germline. The phenotype of two generations of offspring was examined to identify if studies recapitulated findings from other species (Chapter 4).

Taking advantage of the ability to purify germ cells from the testes of exposed eGFP rats, in Chapter 5, the transcriptome of the germline was examined following exposure to HFD to identify if the early steps in spermatogenesis were perturbed by obesity.

1.5.1 Hypotheses

A. Epigenetic machinery in the fetal germline is conserved between rodents and primates.

B. Grandparental high fat diet will impact upon the metabolic and reproductive health of 2 generations of rats.

C. Diet induced obesity perturbs the transcriptome (and epigenome) of male germ cells

1.5.2 Aims

To characterise the epigenetic machinery present in the fetal germline and to identify parallels between primates and rodents in the changes in this machinery.

To establish a model of HFD exposure in *Rattus norvegicus* and characterise the phenotype of two generations of offspring.

To interrogate the transcriptome of germ cells following exposure to HFD.

2 Materials and methods

2.1 Animal work

All animal work was conducted in accordance with the United Kingdom Home Office Animal Experimentation (Scientific Procedures) act 1986. The first cohort of animals was carried out under project licence 60/3962 and the second under 60/4564. William Mungal undertook the daily husbandry. I conducted procedures under my personal licence (60/13651).

2.1.1 Welfare conditions

Animals were housed under standardised conditions with 12 hours of light per day, from 7.00 am until 7.00 pm. The temperature was kept between 20°C and 25°C and the average humidity 55%. Fresh tap water was available *ad libitum*. Animals were kept in clear-sided, solid-bottomed plastic cages. Animals from the first generation in the studies were housed in threes. Thereafter animals were housed with four animals per cage.

2.1.2 Diet studies

2.1.2.1 Derivation of animals

Transgenic rats, expressing enhanced Green Fluorescent Protein (eGFP) in the germline, derived on a Sprague Dawley background (a generous gift from Robert Hammer, University of Texas South Western Medical Centre) (Cronkhite et al., 2005) were imported to the University of Edinburgh. A homozygous male was bred with a wild type Sprague Dawley female. Embryos were transferred to a new Sprague Dawley female to reduce the risk of introducing infections to the unit. Offspring underwent genotyping and those carrying the transgene underwent further brother-sister mating.

Homozygosity was confirmed when all the offspring of a breeding pair carried the transgene. The F0, cohort one of the study was derived from crosses between brother and sister litter mates from the first pair. The F0, cohort two of the study were derived from first generation males with third generation females. Thus, animals were not 'inbred', which requires ten generations of inter-sibling mating. Initially spot genotyping checks were conducted on the F1 animals. In the F2 animals, genotype was confirmed *post mortem* when eGFP was detectable in the testis either on examination under a coaxial fluorescent illuminator (Leica FLUO, UK) or by FACS of dissociated testis.

2.1.2.1.1 Genotyping

Verification of carriage of the eGFP construct was conducted by polymerase chain reaction (PCR) of genomic DNA (gDNA) using primers designed against the eGFP gene. DNA was extracted using the Qiagen DNeasy Blood and tissue Kit (Qiagen, UK, #69504) according to the manufacturer's instructions: Ear notches were placed into lysis buffer supplemented with proteinase K and incubated overnight with shaking at 56°C in an Eppendorf thermomixer comfort (Eppendorf, Germany). Following DNA precipitation with ethanol and buffer AL, the DNA was purified on a column and eluted in 200µl Tris-EDTA (TE) buffer.

PCR was conducted using 10µl of multiplex PCR master mix (a HotStarTaq polymerase) and 2µl of solution Q (Qiagen #206143, UK), 1µl of each forward and reverse primer at 2mM, 5µl of PCR grade water and 1µl of the genomic DNA diluted 1 in 10 (20µl reaction). Genotyping primers were as follows forward: AGA ACG GCA TCA AGG TGA AC and reverse: TGC TCA GGT AGT GGT TGT CG.

Reactions were conducted as follows, 95°C for 10 min to denature DNA, followed by 40 cycles of 20s at 95°C denaturation, 20s at 58°C extension and 20 seconds at 72°C

annealing. PCR products were run on a 2% agarose gel made up with buffer TBE (see Section 2.6). A representative gel is shown in Figure 2.1.

Figure 2.1 Genotyping of eGFP rats. DNA from ear notches was isolated. PCR was conducted with primers against the eGFP insert. The products were run on a 2% agarose gel. The representative gel shown depicts a band from the animals being tested, a band in the positive control and no band in the negative control, gDNA from a wild type Sprague Dawley rat.

2.1.2.2 Breeding

For breeding, the assigned male and female were placed into a grid bottomed cage allowing the tray beneath to be examined for a copulatory plug. Once the copulatory plug was observed, the male was removed and the female housed alone for the remainder of the presumed pregnancy. The number of days between the male and female being co-housed and the observation of the copulatory plug was recorded. Length of gestation was calculated as the number of days between observation of the copulatory plug and delivery of the litter.

Litters were culled to 8 animals following delivery, with 4 males and 4 females kept where possible. To maintain consistency, litters were culled selecting the heaviest animals. At weaning, males and females were separated and ear notches taken to allow identification of individuals within a cage, the tissue was collected and frozen at -20°C for genotyping if required.

The breeding to form the F1 animals was designed such that animals of the same age +/- 2 weeks were selected based upon the experimental or control group required and by starting with the lowest ear notch and by working the way through each litter by ascending ear notch number.

The breeding of the F2 generations was designed such that one animal from each litter in the intervention arm was selected based upon the lowest ear notch number. These were bred to animals from the control arm again selecting animals based upon lowest ear notch. Where there were insufficient animals in the control arm for an animal from a separate litter to be used for each mating, a second and third animal was selected from each litter, working systematically up increasing ear notch numbers and choosing animals of the same age +/- 2 weeks as the animal from the experimental arm with which they were to be bred.

F2 litters were culled to 8 animals following delivery as in the F1. Animals were housed in groups of four at weaning (three weeks). At 6 weeks of age, litters were culled down to 2 animals per litter in order to reduce cage costs. Animals were selected based upon ear notching. 2 animals from each litter were then co-housed in groups of four maintaining experimental groups.

2.1.2.3 Weighing

F0 animals were weighed every two weeks. F1 and F2 animals were weighed every 3 weeks. Animals were placed in a metal bowl on a balance (Mettler, USA) and the weight recorded to the nearest gram.

2.1.2.4 Glucose tolerance testing

Animals underwent oral glucose tolerance testing (OGTT) to determine changes in glucose homeostasis. A three time point protocol was used (Drake et al., 2005). One animal per litter from the F0 and F1 and two animals per litter from F2 underwent OGTT. Animals were weighed and then fasted overnight from around 4pm by removing access to chow. At 9am the following morning a fasting blood sample was obtained by tail nicking: The rat immobilised by wrapping it in a towel and a shallow incision made 6-8cm from the tip of the tail using a disposable scalpel (Swann Morton #0506, UK). A

blob of blood was milked from the incision and drawn into potassium EDTA coated micro tubes (Sarstedt #CB 300 K2E, Germany). 'Milking' of blood continued until around 300µl blood had been collected. The tube was immediately placed on ice to reduce degradation of insulin. 2mg/kg glucose solution (0.5mg/ml w/v) (Sigma, UK) was administered by William Mungal by oral gavage and the time documented. Animals were placed back in their cages. 30 and 120min later, repeat blood sampling was conducted as above using the same incision site. The severity of the procedure was documented according to any distress observed in the rats and their behaviour upon return to the cage. Blood samples were centrifuged at 6000g for 7min at room temperature. The plasma was removed by careful pipetting, avoiding the fibrin plug and placed into a labelled Eppendorf tube. Samples were kept on ice until being stored at -20°C.

2.1.2.5 Necropsy

Animals were killed using a rising concentration of inhaled carbon dioxide and cervical dislocation in accordance with schedule one of the Animal Experimentation (Scientific Procedures) Act 1986. The animal was then weighed to the nearest gram on a balance (Mettler, USA). The length of the animal from the tip of the nose to the base of the tail was measured using a 30cm rule and recorded. The anogenital distance, from the anterior-posterior midpoint to the base of the penis was measured using digital callipers (Faithful, UK). For the F1 animals, there was a technical problem with the callipers thus a 30cm rule was used in place. Measurements were taken to the nearest 0.1mm with callipers and 0.5mm with the rule.

For F0 animals, trunk blood was obtained and for F1 and F2 animals, blood was obtained by cardiac puncture. 2ml aliquots were stored on ice and then centrifuged at 6000g for 7min and the supernatant removed and frozen at -20°C.

A subcutaneous incision was made over the abdomen and subcutaneous fat dissected from the right inguinal fossa and frozen on dry ice. A further incision was then made through the abdominal wall and peritoneum revealing the abdominal viscera.

The penis was dissected, the prepuce removed and the length of the penis from the tip of the glans to the flexure.

For males, the left and right testes, epididymides and epididymal fat were dissected. The fat and testes were further dissected and weighed; the fat discarded, the right testis fixed in modified Bouin's solution and the left prepared for FACS (see section 1.1.2.7). The epididymides were nicked with scissors at the caput and cauda and placed into 5ml of sperm swim buffer at 37°C to allow the sperm to swim out. For females, the fat attached to the endometrium and ovary but inferior to the kidney was dissected and weighed. Ovaries were dissected and weighed and fixed in Bouin's solution.

The pancreas was identified between the spleen and the stomach, dissected, weighed and frozen on dry ice. The left retroperitoneal fat along with the left kidney were dissected, the kidney removed and the fat weighed. The liver was dissected, blotted on tissue paper to remove excess blood and weighed. The caudate process was separated and frozen on dry ice. The small intestine was dissected away from the mesentery. The small intestine was measured using a 30cm rule from the antrum to the caecum, avoiding excess tension. Mesenteric fat was taken and frozen on dry ice.

2.1.2.6 Sperm counting

The epididymides were incubated in sperm swim buffer for 1hour at 37°C. The epididymides were removed, the mixture inverted 5 times and 20µl taken from the top of the sample and diluted 1:3 with sperm swim buffer. 10µl of the suspension was then placed onto a modified haemocytometer and the total and motile sperm were

immediately counted in the four corner and the central large squares of the chamber. Four separate fields were counted per animal equating to at least 200 sperm in accordance with the WHO guidelines (WHO, 2010). Sperm count was calculated by multiplying the average number of sperm per large square by 100 to give a reading of $x10^4$ cells/ml (accounting for the 1 in 4 dilution).

2.1.2.7 Dissociation of germ cells

The tunica albuginea of the testis was removed and the tubules minced with a pair of scalpels in 5ml of ice cold testis dissociation buffer in a petri dish. The suspension was further disaggregated by pipetting up and down before being placed into a 15ml Falcon tube and incubated with gentle rotation for 10min at 37°C in a hybridisation oven. The enzymatic activity was quenched by the addition of Fetal Calf Serum (FCS) (Invitrogen, UK) to a final concentration of 10%. The solution was passed through a 40μm nylon cell strainer (BD, UK) into a 50ml Falcon tube. The cell strainer was further washed with 10ml of FACS buffer. The cells were then pelleted by centrifugation at 500g for 5min at room temperature, the supernatant removed and the cells washed a further 2 times by resuspension in in 10ml of FACS buffer and repeat centrifugation. Finally the cells were suspended in 5ml of FACS buffer ready for cell sorting.

Cells were sorted on a BD FACS Aria II cell sorter. The gating strategy was as follows:

1. Removal of debris
2. Single cells
3. Viability using DAPI (during initial set up)
4. Expression of eGFP

Expression of eGFP was determined during initial set up using a wild type rat testis as a negative control. FACS was conducted by Fiona Rossi and William Ramsay.

EGFP positive cells were sorted and kept on ice until they were centrifuged at 1000g for 5min. The supernatant was removed and the pellet frozen on dry ice and stored at -80°C.

2.1.3 Germ cell studies

2.1.3.1 Rats

2.1.3.1.1 Derivation of animals

Wistar rats obtained from Harlan, UK were utilised and bred 'in-house' at the biological research facility to generate stock.

2.1.3.1.2 Timed mating

Timed mating was used to ascertain the date of conception and thus the age of embryos for study: Grid-bottomed cages were used to allow observation of copulatory plugs. A stud male and female were paired together and monitored for the presence of a plug. Detection of the plug was taken as evidence of mating and was defined as embryonic day 0.5 (e0.5). Stud males were derived from an in-house colony of males of between 6 and 12 months and dams were at least 10 weeks old. Where possible, proven dams were used.

2.1.3.2 Marmoset

Callithrix jacchus, the common marmoset monkey, were captive bred in a closed colony sustained at the University of Edinburgh since 1973. Fetal marmoset testes were obtained from the fetuses of pregnant animals that were being euthanized for colony management purposes. The gestation of marmosets was estimated by systematic palpation and/or ultrasound and has been shown to be accurate +/- 1 week. Mother and fetuses were sacrificed by lethal injection of sodium phenobarbitone (Euthatal, Rhone Merieux, Harlow, Essex, UK). Fetuses were delivered by hysterectomy prior to

dissection. Tissues were fixed in Bouin's solution for 6 hours prior to transfer into 70% ethanol. Tissue was taken at around day 100, 110 and 120 of gestation, which normally lasts about 150 days.

2.1.3.3 Human

Human fetal testes were obtained following termination of pregnancy at 15-18 weeks gestation. Women gave consent for the use of tissue in accordance with National guidelines and following approval by the local research ethics committee. Gestational age was determined by ultrasound examination followed by measurement of foot length (McKinnell et al., 2013). Testes were fixed for 2 hours in Bouin's solution prior to being transferred into 70% ethanol.

2.2 Biochemical assays

2.2.1 Glucose

For F0 animals, glucose was measured using a colorimetric kit (Cayman, USA #100009582), in this assay, glucose is oxidised to form delta-gluconolactone with concomitant reduction of the Flavin adenine dinucleotide (FAD), the reduced FAD (FADH2) is reoxidised by oxygen to produce FAD and hydrogen peroxide. Finally with horseradish peroxidase (HRP) as a catalyst, 3.5-dichloro-2-hydroxybenzenesulfonic acid (yellow) reacts with the hydrogen peroxide and 4-aminoantipyrine to generate the pink dye with absorption at 514nm. Plasma was thawed on ice and diluted 1 in 5 in the dilution buffer from the kit. 100µl of enzyme mix and 85µl assay buffer were added to 15µl of each diluted sample or standards in a colourless 96-well plate and incubated for 1 hour at 37°C before the assay was read at 500nm on a plate reader (Multiscan EX, Labsystems (Thermo Fisher), UK). All samples were assayed in duplicate.

For F1 and F2 glucose assays, samples were assayed kindly by Dr Forbes Howie using a commercial kit (Alpha Laboratories Ltd., Eastleigh, UK) adapted for use on a Cobas Fara centrifugal analyser (Roche Diagnostics Ltd., Welwyn Garden City, UK). Glucose is oxidised by glucose oxidase (GOD) into gluconic acid and hydrogen peroxide, which in the presence of peroxidase reacts with 4-aminoantipyrine and hydroxybenzoic acid, forming a red compound. Colour intensity monitored at 500nm is proportional to the concentration of glucose in the sample (Multiscan EX, Labsystems, UK).

2.2.2 Derivation of standard curve

The standard curve was derived using the 'best fit curve' feature of Masterplex 2010 software (Hitachi solutions, USA) and used for interpolation of concentrations of the analyte in the sample.

2.2.3 Insulin

Insulin was measured in plasma by solid phase two site enzyme-linked immunosorbant assay (ELISA) using a rat insulin ELISA kit (Mercodia #10-1250-10, Sweden). Two monoclonal antibodies directed against separate epitopes of the insulin molecule 'sandwich' insulin in the sample. One of the antibodies is bound to the floor of wells on a 96 well plate, the other conjugated to horse radish peroxidase (HRP). Washing removes unbound conjugated antibody and detection of insulin is determined by reaction with 3,3',5,5'-tetramethylbenzidine (TMB) the reaction stopped by the addition of acid to give a colorimetric endpoint that can be read spectrophotometrically at 450nm using the Multiscan EX plate reader. The standard curve was derived as in 1.2.2. Readings below the sensitivity of the assay (0.15μg/l) were assigned the lowest value of 0.15μg/l. All samples were assayed in duplicate. The assay has a within assay coefficient of variation (CV) of 5.1% and a between assay CV of 10%.

2.2.4 Triglycerides

F0 plasma was assayed using a colorimetric assay kit (Cayman #10010303, USA): triglycerides are hydrolysed to glycerol and fatty acids by lipoprotein lipase. Glycerol was then reacted with ATP to form glycerol-3-phosphate and ADP. Glycerol-3-phosphate and oxygen react to form dihydroxyacetone phosphate and hydrogen peroxide, catalysed by glycerol phosphate oxidase. Hydrogen peroxide then reacts with 4-aminoantipyrine and sodium N-ethyl-N-(3-sulfopropyl) m-anisidine under the activity of peroxidase to form quinoneimine dye and water, which can be assayed spectrophotometrically at an absorbance of 530-550nm.

F1 and F2 plasma triglycerides were kindly assayed by Dr Forbes Howie: Serum triglyceride was determined by a commercial kit (Alpha Laboratories Ltd., Eastleigh, UK) adapted for use on a Cobas Fara centrifugal analyser (Roche Diagnostics Ltd, Welwyn Garden City, UK). Triglycerides are hydrolysed by lipoproteinlipase to glycerol and fatty acids; glycerol is phosphorylated to glycerol-3-phosphate in the presence of glycerol kinase and ATP and then converted by glycerol-3-phosphate oxidase into dihydroxyacetonephosphate and hydrogen peroxide. In the presence of peroxidase, the hydrogen peroxide oxidises the chromogen 4-aminoantipyrine and N-ethyl-N-(2-hydroxy-3sulfopropyl)-3-methylanaline to form a red compound, the colour intensity of which is proportional to the concentration of analyte in the sample. Within run precision was CV < 3% while intra-batch precision was CV < 5%.

2.2.5 Total Cholesterol

F2 cholesterol was kindly assayed by Dr Forbes Howie as follows: Total cholesterol measurements were determined using a commercial kit (Olympus Diagnostics Ltd, Watford, UK) adapted for use on a Cobas Fara centrifugal analyser (Roche Diagnostics

Ltd, Welwyn Garden City, UK). Within run precision was CV < 3% while intra-batch precision was CV < 4%. The sensitivity of the assay was determined at 0.1 mmol/l.

2.2.6 Testosterone

Plasma testosterone was measured kindly by Mr Chris McKinnell by competitive radioimmunoassay (RIA). The method used radiolabelled testosterone (I^{125}, MP Biomedicals, UK) and a rabbit primary antibody 1:600 000, AMS Biotech, Abingdon UK). Residual $I^{125}$was measured with a gamma counter (wizard 1470, Perkin Elmer, Turku, Finland) and testosterone levels were expressed as ng/ml. All samples were analysed in a single assay.

2.3 Protein localisation by immunofluorescence

Immunofluorescence was used to identify if, and in which cell type, proteins were expressed. The technique relies on the principle that antibodies raised against a peptide, which is specifically part of the protein of interest, will bind to that protein on the tissue. A secondary antibody raised against the species of the primary antibody conjugated to HRP then allows indirect detection, in the case of this thesis using tyramide signal amplification.

Tyramide is a phenolic compound that, when activated by HRP, covalently binds to electron rich moieties on the surface of the tissue. This binding only occurs immediately adjacent to where the HRP is bound and multiple depositions can occur quickly allowing a large amplification of signal and increased sensitivity. Conjugation of the tyramide to a fluorophore allows imaging using a confocal microscope. See Figure 2.2.

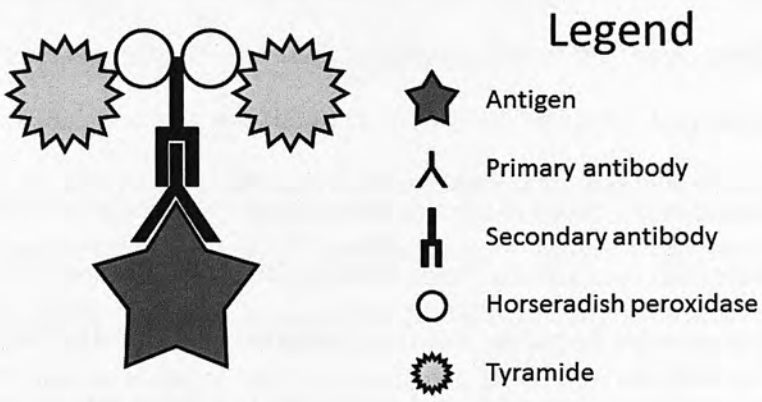

Figure 2.2 Indirect immunofluorescent detection of proteins. Schematic representation of indirect immunofluorescent detection of proteins. The antigen of interest binds the primary antibody. Secondary antibodies conjugated to horseradish peroxidase are then bound to the primary antibody. The HRP catalyses a reaction between the tyramide and the surface of the tissue. The tyramide is conjugated to fluorophores, which allows detection using confocal microscopy.

2.3.1 Fixation

Tissue was fixed in modified Bouin's solution (20:5:1 Picric acid, formalin, acetic acid, Clintech #64-1962, UK). Adult testes were placed in an airtight universal container containing Bouin's fixative for a total of 6 hours. Following 4 hours fixation, the testis was removed and bisected with a razor blade in order to allow penetration of the fixative into the middle of the tissue. The Bouin's solution was then removed and replaced with 70% (v/v) ethanol and samples were stored until ready for paraffin embedding.

2.3.2 Paraffin embedding

Embedding was conducted by the histology team of the small university research facility (SURF) at the University of Edinburgh. Briefly, tissue was processed through a series of concentrations of alcohol for 17.5 hours in an automated Leica ASP300S tissue processor (Leica Microsystems, UK) and embedded manually into molten paraffin wax

using a HistoStar (Thermo Scientific, UK). Tissue blocks were then archived and stored at room temperature.

2.3.3 Sectioning

Paraffin blocks containing the tissue of interest were placed on ice for at least 10min prior to loading them onto a microtome (Leica #RM212 5RT, UK). 5µm sections were cut and ribbons of tissue were floated on 30% (v/v) industrial methylated spirits (IMS; Fischer Scientific) and then onto water heated to 45-50°C in a water bath (Lamb RA #E/65) to allow creases to unfold. Once smooth, tissue sections were separated using fine brushes and mounted onto labelled, electrostatically charged glass slides (Leica 'Apex', UK).

2.3.4 Dewaxing and rehydrating

In order to remove paraffin from the section, slides were incubated twice in xylene (VWR chemicals #28975.325, UK) for 5min. Tissue was then rehydrated by immersion in a series of decreasing concentrations of ethanol (VWR Chemicals #20821.330, UK)(v/v) (100%, 100%, 95%, 80%, 70%) for 20s each, then rinsed in distilled water.

2.3.5 Antigen retrieval

Fixation induces protein cross linking, which improves tissue integrity and preservation but at the cost of masking antigen sites of proteins. In order to un-mask antigens, tissue was treated with heat and pressure in a 'decloaking chamber' (Biocare medical, USA). Antigen retrieval was conducted in different buffers depending on the antibody and following optimisation. The solutions used are indicated in Table 2.1 along with the details of antibodies. The decloaking chamber was programmed to bring slides up to 125°C for 30min; slides were then cooled to 90°C before removal from the chamber and washing sections in dH_2O.

2.3.6 Blocking

To reduce any residual enzymatic activity present in the tissue, slides were incubated in methanol (Fischer, #M/3900/17, UK) with 3% (v/v) hydrogen peroxide (VWR chemicals, #23622.266, UK) on a rocking platform for 30min at room temperature and then washed three times in TBS for five min each (again on a rocking platform at room temperature). To block non-specific protein-antibody interactions, sections were incubated in a blocking solution containing Bovine Serum Albumin (BSA) and sera obtained from a species different from that of the tissue and the primary antibody to be used (see section 2.6). To this end, slides were dried carefully to remove TBS but so as not to disrupt the tissue, and then tissue sections were treated with the appropriate blocking buffer for 30min at room temperature in a humidified chamber.

2.3.7 Primary antibody

Each primary antibody was optimised for use on different species and tissue used in this thesis. Optimisation involved running different titres of antibody, with and without antigen retrieval and use of different antigen retrieval conditions if necessary. The primary antibody was diluted in the appropriate blocking serum. The blocking serum was carefully removed from the tissue and the primary antibody was applied and (unless otherwise stated) was incubated overnight at 4°C in a humidified chamber. As a negative control, one slide was treated with only blocking solution overnight. Conditions and concentrations for primary antibodies are shown in Table 2.1.

2.3.8 Secondary antibodies

Secondary antibodies comprising an immunoglobulin G against the species in which the primary was raised conjugated to HRP were used. The HRP later acts as a catalyst to for the attachment of the fluorophore conjugated tyramide.

Following overnight incubation with the primary antibody, slides were washed twice in TBS on a rocking platform for 5min each. Slides were then incubated with the appropriate secondary antibody diluted in blocking serum at room temperature for 30min in a humidified chamber. Secondary antibodies were raised in the same species as the blocking serum used.

Table 2.1 Antibodies used for immunofluorescence. Their source, species, concentration used and antigen retrieval conditions.

Antibody	Producer	Raised in	Raised to	Cat No	Dilution/ secondary	Retrieval
Leptin receptor (ObR)	SantaCruz	Goat	Mouse	Sc-1834	1:100 (tyramide)	Citrate pH6 PC
3B HSD	SantaCruz	Goat	Human	Sc-308201	1:200 (tyramide)	Citrate pH6 PC
GATA4	SantaCruz	Goat	Mouse	Sc-1237	1:100 (tyramide)	Citrate pH6 PC
DNMT3a	Abcam	Rabbit	Human	Ab14291	1:1200 (tyramide)	Citrate pH6 PC
DNMT3b	Abcam	Rabbit	Human	Ab4922	1:1200 (tyramide)	Citrate pH6 PC
Vasa	Abcam	Rabbit	Human	Ab13840	1:120 (tyramide)	Citrate pH6 PC
Oct4	SantaCruz	Goat	Human	Sc8628	1:100 (tyramide)	Citrate pH6 PC
Dazl	Serotec	Mouse	Human	Mca2336	1:5000 (tyramide)	Citrate pH6 PC
H3K27me3	Active Motif	Rabbit	Human	39155	1:1000 (tyramide)	Citrate pH6 PC
H3K4me3	Active Motif	Rabbit	Human	39159	1:1000 (tyramide)	Citrate pH6 PC
5mC	Eutogentec	Mouse (monoclonal)		BI-MECY-1000	1:1000 (tyramide)	Novocastra pH9 and 4N HCl to denature DNA

5hmC	Active Motif	Rabbit		39769	1:1000 (tyramide)	Novocastra pH9
COUP-TFII	Perseus	Mouse	Human	PP-7147-00		Citrate pH 6
Secondary-peroxidase	Sigma	Rabbit	Goat	A5420	1:200	
Secondary-peroxidase	Dako	Rabbit	Mouse	P0260	1:200	
Secondary-peroxidase	SantaCruz	Chicken	goat	Sc2961	1:200	
Secondary-peroxidase	SantaCruz	Chicken	Rabbit	Sc-2963	1:200	
Secondary-peroxidase	Vector	Goat	Rabbit	BA-1000	1:200	
Secondary-peroxidase	Abcam	Goat	Chicken	Ab97135	1:200	
Secondary-peroxidase	Dako	Goat	Mouse	P0447	1:200	
Secondary-peroxidase	SantaCruz	Chicken	Mouse	Sc2954 and 2962	1:200	

2.3.9 Tyramide

Following incubation with the secondary antibody, slides were again washed twice in TBS at room temperature on a rocking platform. Slides were then incubated for 10min at room temperature, in a dark humidified chamber with Tyramide Signal Amplification (TSA) (Perkin Elmer, UK) conjugated to the appropriate fluorophore and diluted 1:50 in TSA diluent as per the manufacturer's instructions. The reaction was quenched by incubating the slides in TBS twice for five min at room temperature on a rocking platform.

2.3.10 Multiplexed assays

The TSA system allows multiplexing of multiple antibodies on the same tissue section in order to identify if proteins co-localise. In order to layer a second or third antibody onto the section, the activity of the conjugated HRP had to be quenched by incubating the section in 3% hydrogen peroxide (VWR chemicals, UK) in TBS for 30min at room temperature on a rocking platform in the dark. Where use of more than one primary antibody raised in the same species was required, the Fc fragment of the first antibody had to be denatured by microwaving the sections in boiling citrate buffer (pH6) for 4min, allowing the sections to cool for 20min and then washing the slides in TBS twice at room temperature on a rocking platform in the dark. Fixation of endogenous proteins in the tissue prevented damage by this microwaving step, preserving antigens for detection by the next antibody.

2.3.11 Nuclear counterstain

To aid with the visualisation of tissue architecture, a nuclear counterstain was applied. The choice was dependent upon the fluorophores in use on the tissue. Counterstains were used at 1:500 of a 1mM stock solution in TBS and applied to the tissue for 30 min at room temperature in a dark humidified chamber. Counterstains are described in Table 2.2.

Table 2.2 Nuclear counterstains used for immunofluorescent images

Counterstain	Manufacturer	Fluorescence
DAPI 4',6-Diamidino-2-phenylindole dihydrochloride	Sigma #D9542	488nm
TO-PRO	Molecular probes #T3605	647nm
Sytox green	Molecular probes #S7020	523nm
PI Propridium Iodide	Sigma #P4170	535nm

2.3.12 Mounting

Slides were then aqueous mounted using Permafluor (Thermo Fischer, UK) and glass coverslips (Leica, UK). Slides were blotted dry, checked for bubbles and then stored at 4°C wrapped in foil prior to imaging.

2.3.13 Imaging

Slides were imaged using Axiovision LSM 510 or 710 or 780 confocal microscopes (Zeiss, Germany) and using Zen software (Zeiss, Germany).

2.4 RNA analysis

In order to investigate gene expression, mRNA was quantified in the cells/tissue of interest. The principal steps in this procedure include extracting the RNA from fresh or frozen tissue or cells, reverse transcribing the RNA to form cDNA and then quantitative PCR using either SYBR green or Taqman assays to determine relative abundance.

2.4.1 RNA isolation

Two methods were used for RNA isolation. If only RNA was required, RNA was extracted using the Qiagen RNeasy micro kit (Qiagen, UK). If total RNAs were required (for example to include miRNA) then a miRNeasy mini kit (Qiagen, UK) was used.

2.4.1.1 mRNA extraction

Where possible, fresh tissue or cells were used. However, if frozen tissue was used, it had been frozen quickly on dry ice and stored at -80°C in order to reduce degradation by endogenous RNases. Chips of frozen tissue (of roughly 30mg) or aliquots of 1-2 x 10^6 cells were submerged in buffer RLT, supplemented with β-mercaptoethanol 1% (v/v) (in order to denature RNases) in a 2ml Eppendorf tube along with a sterile 5mm stainless steel bead. Tubes were then mounted into a TissueLyser (Qiagen, UK) and homogenised for 2min at 25Hz. The resultant suspension was the centrifuged for 3min at maximum speed. The supernatant was transferred to a clean tube and RNA precipitated by adding an equal volume of 70% (v/v) ethanol. The RNA was then bound to a purification column, washed with buffer RPE, treated with DNase for 15min on the column to remove DNA and then washed again, first with buffer RPE and then with 80% (v/v) ethanol. RNA was eluted from the column into 14µl RNase-free water. RNA samples were then kept on ice for quantification and assessment of purity and degradation.

2.4.1.2 miRNA extraction

Total RNA (including miRNA) was extracted using the Qiagen miRNeasy mini kit (Qiagen #217084, UK) according to the manufacturer's instructions. Briefly, 4-5 x 10^6 cells were homogenised in 700µl QIAzol Lysis reagent by vortexing and passing 5 times through a 22 gauge syringe.

Samples were then incubated at room temperature for 5min. 140µl of chloroform (Sigma, UK) was added to each sample followed by vigorous shaking for 15s and a further incubation at room temperature for 2min. The samples were then centrifuged for 15min at 12,000g at 4°C. The upper aqueous phase containing the RNA was transferred to a new Eppendorf tube avoiding transfer of any of the interphase. RNA was precipitated by adding 1.5 volumes of absolute ethanol. The precipitate was then bound to a purification column, washed once with buffer RWT, treated with DNase for 15min, washed again with buffer RWT, then with buffer RPE, and finally 80% (v/v) ethanol. RNA was eluted in 30µl of RNase-free water.

2.4.2 RNA quantification

2.4.2.1 Spectrophotometry

Where the yield was greater than 100ng/µl, RNA was quantified using a spectrophotometer (Nanodrop-1000, Nanodrop technologies, USA). The ratio of absorbance at 260 and 280nm is useful for assessing for protein contamination (which might affect downstream reactions). A ratio of about 2:1 is considered protein free, a value of >1.9:1 was accepted as sufficient to allow efficient cDNA synthesis. Spectrophotometry was also used to quantitate the RNA

2.4.2.2 Fluorometry

Where RNA yield was lower, more accurate quantification was obtained using fluorometry. The Qubit™ Fluorometer uses fluorescent dyes that bind to RNA or DNA and, which can then be quantified by comparison to standards. As the RNA dyes are specific for RNA, this method gives a more accurate reading and is more sensitive, especially at lower concentrations where the spectrophotometer would give unreliable results.

2.4.2.3 *Non-denaturing 2% agarose gel*

It is also important to check for degradation of RNA. A simple way to check this is by running the RNA on a 2% agarose gel and looking for the bands of 28S and 18S rRNA. A ratio of around 2:1 in the size of the bands and absence of a smear of smaller nucleic acids implies good RNA integrity. This also allows for examination of the samples for gDNA contamination (Figure 2.3).

Figure 2.3 Example electrophoretogram of RNA run on a 2% agarose gel demonstrating the 28S and 18S bands of ribosomal RNA suggesting reasonable RNA integrity.

2.4.2.4 Agilent™ bioanalyser

A more accurate (and more economical in terms of RNA required) means of testing the integrity of RNA is to use the Agilent Bioanalyser™. The Bioanalyser works in a similar way to the agarose gel. The samples, a gel and a fluorescent dye are loaded into small wells on a chip. The chip is inserted into the bioanalyser and electrodes pass a current through each well. RNA molecules of different sizes will flow though the gel in the chip at different speeds, a fluorescent dye intercalates with the RNA so that laser-induced fluorescence can be detected by a sensor. The RNA samples are then compared to a standard ladder. Based upon the expected size of the 28S and 18S rRNAs, their relative abundance and the baseline fluorescence, an 'RNA integrity number' can be calculated of between 1 and 10. Readings of above 7 are suitable for sequencing. An example 'gel' trace from a chip is shown below along with representative example traces (Figure 2.4).

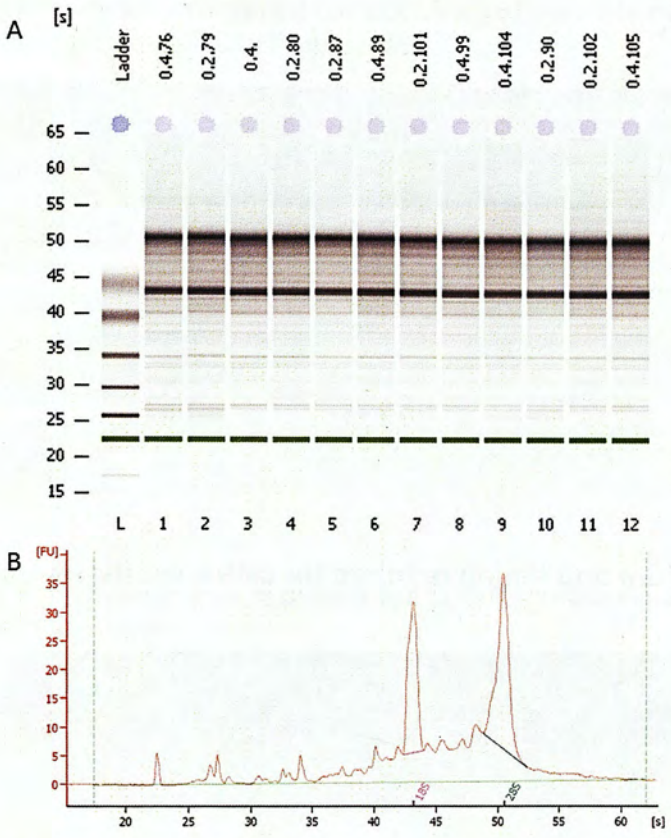

Figure 2.4 A virtual electrophoretogram from RNA run on the Agilent bioanalyser. (**A**) Two strong bands of ribosomal RNA can be seen in all the samples. (**B**) Representative tracing from the bioanalyser showing peaks for the 28S and 18S rRNAs suggesting adequate quality of RNA for downstream processes.

2.4.3 Reverse transcription

2.4.3.1 mRNA

RNA was reverse transcribed to cDNA using the superscript VILO cDNA synthesis kit (Invitrogen, UK). Each tube contained the reagents as per Table 2.3. Reverse transcription negative control samples were run alongside each conversion containing water in place of the RNA. Once all reagents were in the 0.2ml PCR tube, they were placed into a PCR machine and incubated as per Table 2.4. cDNA samples were then stored at -20°C.

Table 2.3 Reagents required for cDNA synthesis using the VILO kit

Reagent	µl per 20µl reaction
5x VILO reaction mix	4
10x Superscript enzyme mix	0.25
RNA (100ng/µl)	1
RNase free water	14.75

Table 2.4 Temperature and timing required for cDNA synthesis using the VILO kit

Temperature (°C)	Time (min)
25	10
42	60
85	5
4	Hold

2.4.3.2 miRNA

The Exiquon miRCURY LNA™ Universal RT mircoRNA PCR kit was used to reverse transcribe miRNAs. Given the small size of the mature miRNAs, it would not be possible to design primers that would amplify them. Thus, the Universal kit combines the RT with the binding of a universal tag, meaning that the cDNA generated is longer than the miRNA and contains an extra sequence at its 5' end that is used to design primers. A spike in non-vertebrate miRNA is included in the RT as a positive control. Water RT negatives are included as negative controls.

Reagents were combined and incubated as follows in Table 2.5 and Table 2.6 respectively. Samples were then stored at -20°C.

Table 2.5 Reagents required for cDNA synthesis for miRNA assays using the Exiqon miRCURY system

Reagent	µl per 20µl reaction
5x Reaction buffer	4
RNase free water	9
Enzyme	2
Spike in control	1
RNA (5ng/µl)	4

Table 2.6 Temperatures required for cDNA synthesis using the Exiquon miRCURY system

Temperature (°C)	Time (min)
42	60
95	5
4	Hold

2.4.4 Quantitative PCR

Quantitative PCR (qPCR) is a technique that determines the relative (or absolute) quantity of DNA of a specific sequence in a sample. During PCR, primers, designed specifically to be complementary to the 3' ends of the sense and antisense strand of the target DNA, and a polymerase amplify the region of DNA of interest. During the reaction, controlled changes in temperature result in:

1. *Denaturation* by disrupting the hydrogen bonds holding two strands of DNA together, resulting in single stranded DNA (ssDNA)
2. *Annealing* to allow primers to bind to the ssDNA

3. *Extension* where the polymerase binds to the primer/template hybrid and begins synthesis.

Providing there are no limiting factors, each cycle will result in a doubling in the amount of DNA amplicon leading to exponential amplification of the target. Thus during a PCR reaction, over the course of 40 cycles, there will be a baseline, where background fluorescence is detected, a linear plateau phase where exponential amplification is occurring and a plateau phase where the amplification has stopped being exponential.

A threshold is set where all the wells are in their exponential phase of amplification and checked by looking at the precision of replicate wells. This allows determination of the threshold cycle (Ct) for each sample (Figure 2.5)

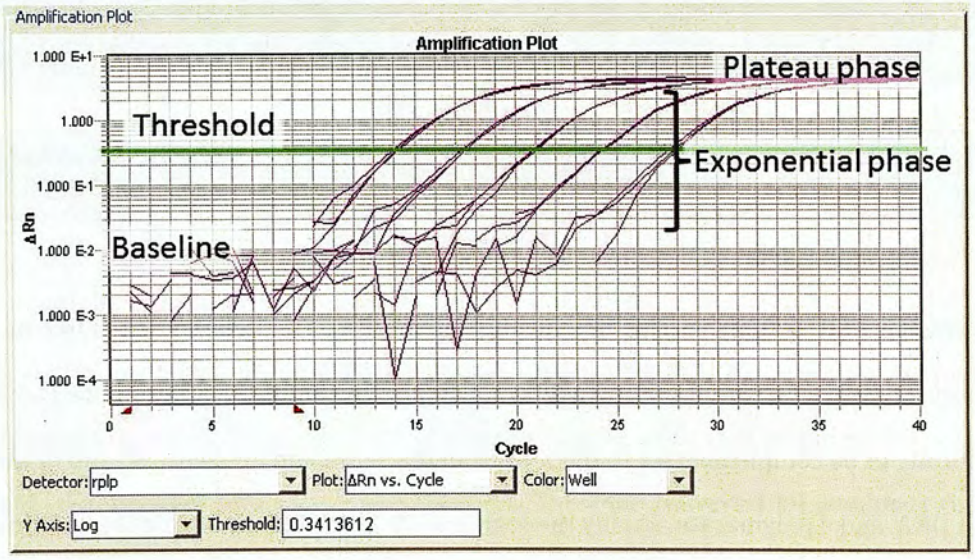

Figure 2.5 Example SYBR green PCR showing determination of the threshold cycle (Ct). The baseline fluorescence, exponential phase of DNA replication and plateau phase can be seen for this example, which shows amplification of a standard curve.

Two methods for (qPCR) have been used in this thesis: SYBR green and Taqman assays.

SYBR green assays are more economical but are reliant on the quality of the primers

and template meaning that more validation is required. Taqman assays have higher specificity and more consistent sensitivity but are more costly.

2.4.4.1 SYBR green qPCR

SYBR green is a fluorescent dye that binds dsDNA by intercalating between base pairs. It fluoresces only when bound to dsDNA. Detection occurs at the end of annealing and during the extension step when the greatest amount of dsDNA is present. Thus, as the number of cycles increases, the fluorescence will increase and can be detected by the PCR machine. As SYBR green detects any dsDNA, the reaction must contain a combination of primers that only generates a sequence-specific amplicon without producing any secondary products.

2.4.4.1.1 Primer design

Primers were designed by selecting the region of interest and pasting the fasta sequence into primer 3 (http://primer3.ut.ee/). This web-based program then designed forward and reverse primers against the target region. Primers are ranked based upon GC content, melting point, and self/pair complementarity. A primer set can then be cross-checked by *in silico* PCR against the genome of interest using this feature available at http://genome.ucsc.edu/cgi-bin/hgPcr. The primers were then synthesised by Eurofins, Germany, and the lyophilised oligomers dissolved into RNase-free water to give stock solutions of 100mM. Aliquots of working stock concentration primers (20mM) were stored at -20°C.

2.4.4.1.2 Validation of primers

Primers were validated by testing a standard curve using a 1 in 10 dilution series of a composite of cDNA (or gDNA if appropriate) from the samples. These were made up in

a reaction mix as shown in Table 2.7. They were run in 96 well plates in a qPCR machine (ABI 7900 HT, ABI, USA).

Table 2.7 Reagents required for a SYBR green qPCR reaction

Reagent	µl per 10µl reaction
2x Agilent Brilliant III SYBR green master mix	5
Forward primer 20mM	0.5
Reverse primer 20mM	0.5
Water	1.85
Reference dye (made up 1 in 50 with water)	0.15
DNA (dilute 1 in 10)or standards	2

Table 2.8 Temperature cycles required for SYBR green PCR

Temperature (°C)	Time (seconds)	
95	180	
95	5	40 cycles
60	15	
Melt curve		

The Ct values from the standard curve were plotted against log transformed relative concentrations. The slope and y-intercept of the curve were obtained using the line of best fit. The efficiency of the PCR was calculated as $E = 10^{-1/slope}$. This was converted to a

percentage by subtracting 1 and multiplying by 100. Efficiency was satisfactory if it was between 90 and 110%. This implies that roughly every cycle the number of amplicons doubled (Figure 2.6D).

The primers were also validated by checking the melt curves, looking for one peak, (Figure 2.6A and B). Finally, PCR products were run on a 2% agarose gel in order to check the size of the amplicon (Figure 2.6C).

If primers met the above criteria, they were used as 2.4.4.1.3. If they failed, either new primers were designed or, if necessary, PCR was optimised by adjusting the concentration of the primers and/or template, and the temperature of the reaction.

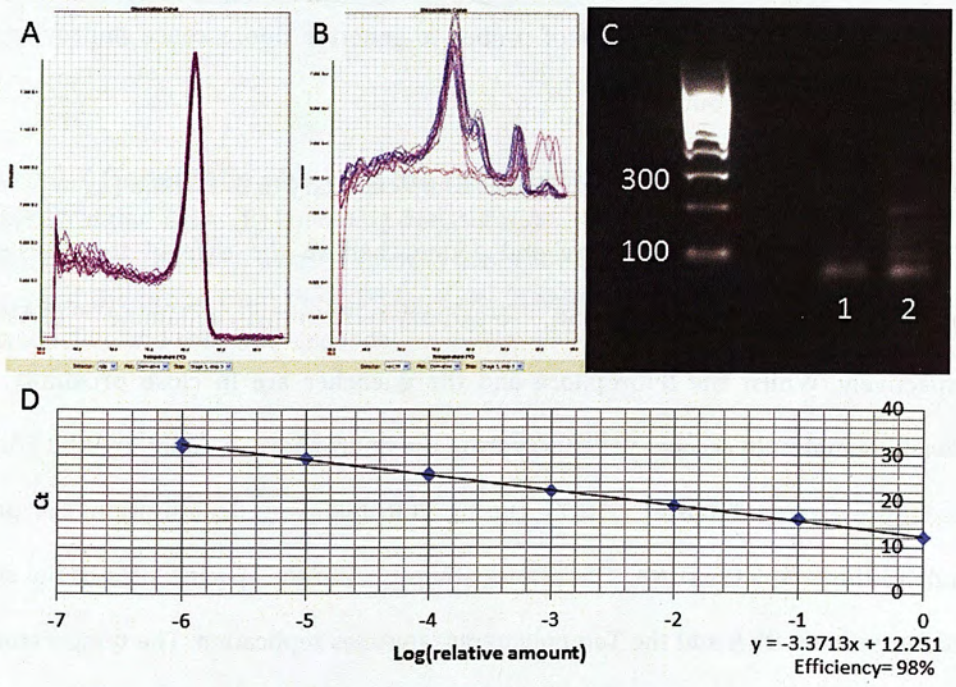

Figure 2.6 Validation of SYBR green primers. A melt curve from successful primers showing one peak. **B** melt curve from primers with secondary products. **C** 2% agarose gel showing products from A and B, 1 shows the clean band of amplicon from A, 2 shows the multiple products generated from form the PCR in B. ladder shows 100 and 300bp. **D** representative standard curve and calculation of PCR efficiency

2.4.4.1.3 qPCR using SYBR

Once primers were validated, samples, cDNA (diluted 1:10-1:20) or gDNA (5ng/µl) were made up as per Table 2.7. Samples were all run in triplicate on an ABI 7900HT PCR machine (Applied Biosystems, UK) with the cycles as Table 2.8 unless stated otherwise.

2.4.4.2 Taqman qPCR

Taqman PCR relies upon the use of probes to generate fluorescence improving the specificity of the read-out.

Probes consist of a sequence of nucleotides complementary to the strand (usually sense) of the DNA target, a fluorophore and a quencher; in the case of this thesis, 6-carboxyfluorexecin (FAM) and 6-carboxy-tetramethyl-rhodamine (TAMRA) respectively. Whilst the fluorophore and the quencher are in close proximity, the quenching molecule accepts the energy from the fluorophore, dissipating it by Förster Resonance Energy Transfer (FRET). During PCR, following denaturation, the probe binds to the template ssDNA. The primers then bind to the specific sites of the sense and antisense ssDNA and the Taq polymerase initiates replication. The temperature is then reduced to allow elongation. During elongation, the probe is degraded, meaning that the fluorophore and the quencher become separated and the FRET signal is lost, resulting in fluorescence. As each cycle of DNA replication occurs, the fluorescence increases (Figure 2.7).

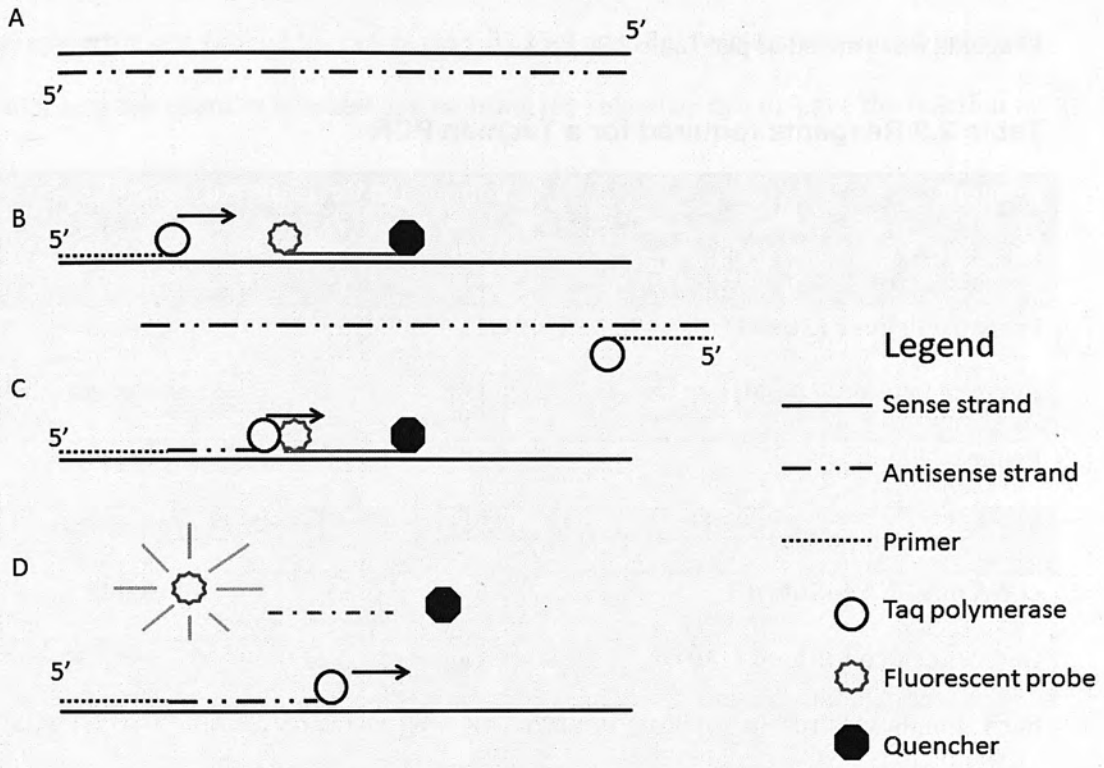

Figure 2.7 Schematic showing the principles behind Taqman qPCR. (**A**) Double stranded DNA. (**B**) Following denaturation, the probe and primers bind to ssDNA. (**C**) The Taq polymerase removes the probe during elongation. (**D**) The removal of the probe from the ssDNA results in separation of the fluorophore and the quencher and thus fluorescence.

2.4.4.2.1 qPCR using Taqman

Reagents were mixed as per Table 2.9.

Table 2.9 Reagents required for a Taqman PCR

Reagent	Volume (µl for 15µl reaction)
Universal master mix	7.5
Forward Primer (20mM)	0.15
Reverse Primer (20mM)	0.15
Probe	0.15
Water	3.9
cDNA or gDNA (~5ng/µl)	1.5
Reference dye (diluted 1:50)	0.15

Each sample was run in triplicate in 96 or 384 well plates on an ABI 7900 HT PCR machine using the cycles as per Table 2.10.

Table 2.10 Temperature cycles required for Taman PCR

Temperature (°C)	Time (seconds)	
95	180	
95	5	40 cycles
60	15	

The threshold was set as in section 2.4.4. The Ct for each sample was exported for analysis.

2.4.4.2.1.1 Duplex Taqman PCR reactions

For selected genes, a duplex assay was run using the rRNA 18S as a reference gene. Where this was the case, a standard master mix comprising primers against 18S, a

fluorescent probe containing the fluorophore VIC for 18S and ROX reference dye was prepared as per Table 2.11. In this case, 0.225µl per 15µl reaction was added per well, adjusting the quantity of water and omitting the reference dye to leave the reaction at the same volume.

Reagent	Volume for 15µl reaction
Nuclease free water	5.325
Taqman Mastermix	7.5
Forward primer (20mmol)	0.15
Reverse primer (20mmol)	0.15
Universal probe	0.15
18S mixture	0.225
cDNA	1.5

Table 2.11 Reagents for multiplex PCR

2.4.4.3 Analysis of results

2.4.4.3.1 Relative quantification using the delta delta Ct method

Where duplex PCR reactions were conducted, results were analysed using the ΔΔCt method (Livak and Schmittgen, 2001). This method makes the assumption that both the gene of interest and the reference gene amplify with the same efficiency. This can be checked by running a standard curve of both genes and checking that there is no variation in the delta Ct (the difference between the Ct for the reference gene and that of the gene of interest). It is also assumed that efficiency is close to 100%, which can be checked using a standard curve as in section 2.4.4.1.2 and Figure 2.6D.

Providing these assumptions are met, the derivation of the ΔΔCt is as follows(Livak and Schmittgen, 2001):

$$X_n = X_0 \times (1+E_x)^n$$

Where X_n is the number of template molecules present at cycle n, X_0 is the number of molecules at the start of the reaction, E_x is the efficiency of amplification and n is the number of cycles. The Ct value indicates the cycle at which the fixed threshold is reached, thus n can be substituted for Ct. The same equation can be drawn for the reference gene(s).

Given that the number of target molecules present at the given threshold will be in a fixed ratio for the target and reference gene (assuming the above caveats):

$$\frac{X_0 \times (1+E_x)^{Ctx}}{R_0 \times (1+E_r)^{Ctr}} = K$$

Where X_0 and R_0 are the number of molecules present pre PCR of the gene and reference gene respectively, E is the efficiency and Ct is the threshold cycle for each.

Assuming efficiencies are equal:

$$E_x = E_r = E$$

Thus:

$$\frac{X_0}{R_0} \times (1+E)^{Ctx-Ctr} = K$$

Or,

$$X_n \times (1+E)^{\Delta Ct} = K$$

$$X_n = K \times (1+E)^{-\Delta Ct}$$

Where X_n is the normalised amount of target and ΔCt the difference in threshold

And then to normalise to a calibrator (cb):

$$\frac{K \times (1+E)^{-\Delta Ctq}}{K \times (1+E)^{-\Delta Ctcb}} = (1+E)^{-(\Delta Ctq - \Delta Ctcb)}$$

And assuming that efficiency is close to 1:

$$Amount\ of\ target = 2^{-(\Delta Ctq - \Delta Ctcb)} = 2^{-\Delta\Delta Ct}$$

2.4.4.3.2 Quantification using a standard curve

An alternative method, which takes into account differences in the efficiencies between different primer sets, is the standard curve method. Here, a standard curve for each gene is run on the same plate as the samples. The log(relative concentration) is plotted against the Ct. The relative amount of starting material can then be interpolated and the ratio of this to the reference gene(s) calculated to give a relative quantification.

2.4.4.3.3 Absolute quantification using oligomers

Absolute cDNA or gDNA quantification can be achieved using oligomers of the PCR product of known concentration. These can be used to set up a standard curve with known concentration and the absolute quantity of cDNA or gDNA in the sample can be interpolated and normalised to a reference gene as above. This allows easier comparison between plates.

2.5 Statistics

2.5.1 Diet studies

Several of the comparisons made in the diet studies would violate the assumption of independence of the standard Analysis of variance (ANOVA). These include where repeated measures are made for the same animal (for example in a growth curve or glucose tolerance test) or for data where animals are clustered within litters. In these situations, multi-level modelling is appealing as it allows comparisons to be made between groups whilst accounting for non-independent (random) factors, and for the fact the variances of the differences between the groups (sphericity) are likely to change with time (Laird and Ware, 1982).

Thus:

$$\square = \square\square + \square\square + \square$$

Where y is the observed dependent variable, β the unknown vector of fixed-effects with design matrix X (the independent variable for example grandparental diet), γ an unknown vector of random effects with design matrix Z (for example the litter) and ε the residual error (how far the measured variable is from the that predicted by the model (the statistical 'noise'). The model can be built up to include multiple fixed and random effects.

Linear mixed modelling was achieved using the MIXED function of SPSS version 19.0 (IBM, USA). For repeated measurement experiments of weight, an autoregressive data structure was used, given that the variation would increase as the animals aged and a fixed intercept was assumed. For other models, a Variance components (VC) covariance matrix was utilised given the variances between the random effects were presumed to be independent and a random intercept was assumed. The covariance structure chosen was confirmed using model testing and finding the lowest Akaike Information Criteria (AIC), which gives an impression of the goodness of fit of data to a model. Given the small sample sizes, restricted maximum likelihood (REML) estimators were utilised. Degrees of freedom are calculated in SPSS using Satterthwaite's method. Thus, for non-repeated measure comparisons, the following syntax was used:

```
MIXED DependentVariable BY Sex Group LitNo
/FIXED=Sex*Group | NOINT SSTYPE(3)
/METHOD=REML
/RANDOM=LitNo(Group) | COVTYPE(VC)
/EMMEANS=TABLES(Sex*Group) COMPARE(Group) ADJ(BONFERRONI).
```

And for repeated comparisons:

```
MIXED Weight BY Time Sex Group LitNo
/FIXED=Time*Sex*Group | SSTYPE(3)
/METHOD=REML
/RANDOM=LitNo(Group) | COVTYPE(VC)
/REPEATED=Time | SUBJECT(ID) COVTYPE(AR1)
```

/EMMEANS=tables(sex*group*time) compare(group) adj(BONFERRONI).

Comparisons between F0 animals were conducted using a general linear mixed model with diet as a fixed factor and cohort as a random factor. Comparisons between F1 and F2 animals were conducted using a general linear mixed model with parent or grandparental diet and sex as a fixed factors and litter as a random factor. Where significant differences were identified between groups, unless otherwise stated, *post hoc* Bonferroni tests were applied to determine between which groups there were differences. Bonferroni testing adjusts for the increased risk of type 1 statistical error where there is an increase in the number of groups between which comparisons are being made.

Normality was assessed using the Shapiro Wilk test. In some of the studies, normality had to be assumed despite failing to meet the Shapiro Wilk criteria, likely due to the limitation of this test with small sample sizes. In these cases, a second test, a Q-Q plot in which the expected values of a normal distribution are plotted against the actual values was constructed and assessed visually to judge 'bestness of fit' to a straight line. Although debated, there is some evidence to suggest that the liner mixed model copes well with some skewness in relatively small groups, especially where clustering overlaps the fixed effects as is the case here (Galbraith et al., 2010).

2.6 Solutions

2.6.1.1 Phosphate Buffered Saline (PBS)

10 PBS tablets (Sigma, UK) were dissolved in 1 litre of dH_2O to form a 10X stock solution, which was autoclaved and stored at 4°C for up to 6 months.

2.6.1.2 10x TBE (1x is 89mM Tris, 89mM Boric acid, 2mM EDTA)

108g Tris (Sigma, UK)

55g Boric acid (Sigma, UK)

40ml EDTA 0.5M pH 8 (Sigma, UK)

Made up to 1litre with dH_20, autoclaved and stored at room temperature for up to 6 months

2.6.1.3 2% (w/v) agarose gel

4g Agarose (Sigma, UK)

200ml 1xTBE

Heat in microwave full power for 50s. Check to ensure dissolved, cool under cold tap then add 20µl Gel red (Biotium. UK) and poor into gel tray, add comb, remove bubbles and allow to set for at least 30min.

2.6.1.4 Sperm swim buffer (2% BSA (w/v) /10% FCS (v/v) in DMEM/F12 (phenol red free))

2g Bovine Serum Albumin (Sigma, UK)

10ml Fetal Calf Serum

Made up to 100ml with DMEM/F12 (Invitrogen# 11039-021, UK). Use fresh.

2.6.1.5 Testis dissociation buffer (1ug/ml (w/v) collagenase IV in Hanks buffered saline solution)

10µl of Collagenase IV (1mg/ml) (Sigma # C5138, UK)

10ml of Hanks Buffered Saline Solution supplemented with Magnesium and Calcium (Invitrogen #14025050, UK)

Use fresh.

2.6.1.6 FACS buffer (2% (v/v) Fetal Calf Serum (FCS) in Dulbecco's Phosphate buffered saline (PBS))

2ml FCS

98ml 1x PBS

Use fresh.

2.6.1.7 Tris Buffered Saline (TBS) (50mM Tris-Cl, 150mM NaCl) for 10l 10x solution:

605g Tris (Sigma, UK)

876g NaCl (Sigma, UK)

Made up to 8l with dH_2O and adjusted to pH 7.4 using concentrated HCl (VWR Chemicals, UK) then made up to 10l. 10x stock solution stored at 4°C.

2.6.1.8 Blocking buffer (20% (v/v) sera, 5% (w/v) BSA in TBS)

20ml Sera (Diagnostic, UK)

5g Bovine Serum Albumin (Sigma, UK)

Made up to 100ml with 1x TBS

Stored in 5ml aliquots at -20°C.

2.6.1.9 0.1M Citrate buffer

42.02g citric acid monohydrate (Sigma, UK)

Made up to 1.8l using dH_2O and pH adjusted to pH 6.0 using conc. NaOH and made up to 2l. Store at 4°C. Use at 0.01M for antigen retrieval.

3 Epigenetic mechanisms in germ cell development

3.1 Introduction

Chapter 1 highlighted the many mechanisms in place to modulate the germ cell epigenome during fetal and postnatal development. Most of the literature has focussed on a murine model, with relatively few examples of data regarding primates. There is also a focus on primordial germ cells during the period of DNA demethylation, but little attention has been paid to the remethylation stages, or indeed the postnatal gonad.

Although there are strong parallels between the development of germ cells in different mammalian species, there are important differences in the timing and synchronicity of germ cell maturation between rodents and primates (Mitchell et al., 2008). Furthermore, the timing and duration of epigenetic remodelling could have implications as to when the epigenome is most vulnerable to perturbation. Epigenetic reprogramming and germ cell maturation occurs asynchronously in primates, and given that environmental insults can perturb the male germline epigenome during adult and fetal life (Carone et al., 2010; Marczylo et al., 2012; Radford et al., 2014), the length, and timing of an exposure could determine if and how any disruption occurs.

Intergenerational programming models have insulted the male germline during various points of development, for example *in utero* (Anway et al., 2006; Radford et al., 2014) or during puberty and adulthood (Fullston et al., 2013; Ng et al., 2010) but no study as yet has tried to identify a 'window of maximal effect' thus we do not know if, when or how the germ line is most susceptible. By correlating the window of exposure, and, literature about germline reprogramming, hypotheses might be made regarding how

an exposure can result in an inter-generationally programmed effect, and thus help to focus research into potential mechanisms.

With this in mind, epigenetic modifications and their regulators were investigated in fetal and postnatal germ cells from a rodent, *Rattus norvegicus*, and two primate species, *Callithrix jacchus* and *Homo sapiens* with the aim of answering the following questions:

- Are the epigenetic dynamics observed during murine germ cell development conserved between rat and primate?
- Do expression patterns of epigenetic factors over time highlight specific windows of potential vulnerability of the germ cell epigenome?

3.2 Methods

Procedures were conducted as indicated in Chapter 2 except for the following cases:

3.2.1 Animals and treatments

3.2.1.1 Human

Adult human testis was from adjacent 'healthy' tissue on a slide from a patient with a Seminoma (LREC10/S1402/33).

3.2.2 Immunofluorescence for 5mC

As the antibody used to detect 5mC was raised against single stranded DNA it was necessary to denature the DNA prior to incubation with the primary antibody. This was achieved by incubating the slides in 4N HCl for 10min at 37° C and neutralising slides in TBS following antigen retrieval and prior to blocking with sera.

3.3 Results

3.3.1 DNMT3A and DNMT3B expression in fetal rat germ cells

Cytosines within germ cell DNA become remethylated in the male rat between e18.5 and e21.5 (Rose et al., 2014). Expression of the *de novo* DNA methyltransferases

DNMT3A and DNMT3B was thus examined in the rat over these time points to establish if they might potentially play a role in remethylation. Germ cells were identified by immunoexpression of cytoplasmic VASA, an RNA-helicase specific to germ cells from e13.5 (Encinas et al., 2012). DNMT3B was expressed in all germ cells at the time points from e15.5 to e21.5. DNMT3A demonstrated clear immunoexpression from e19.5 but less expression than in surrounding somatic cells at the preceding time points (Figure 3.1). Thus, the number of germ cells expressing DNMT3A increased over the time investigated, parallel to the increase in 5mC expression, whereas DNMT3B was expressed across all the time points investigated.

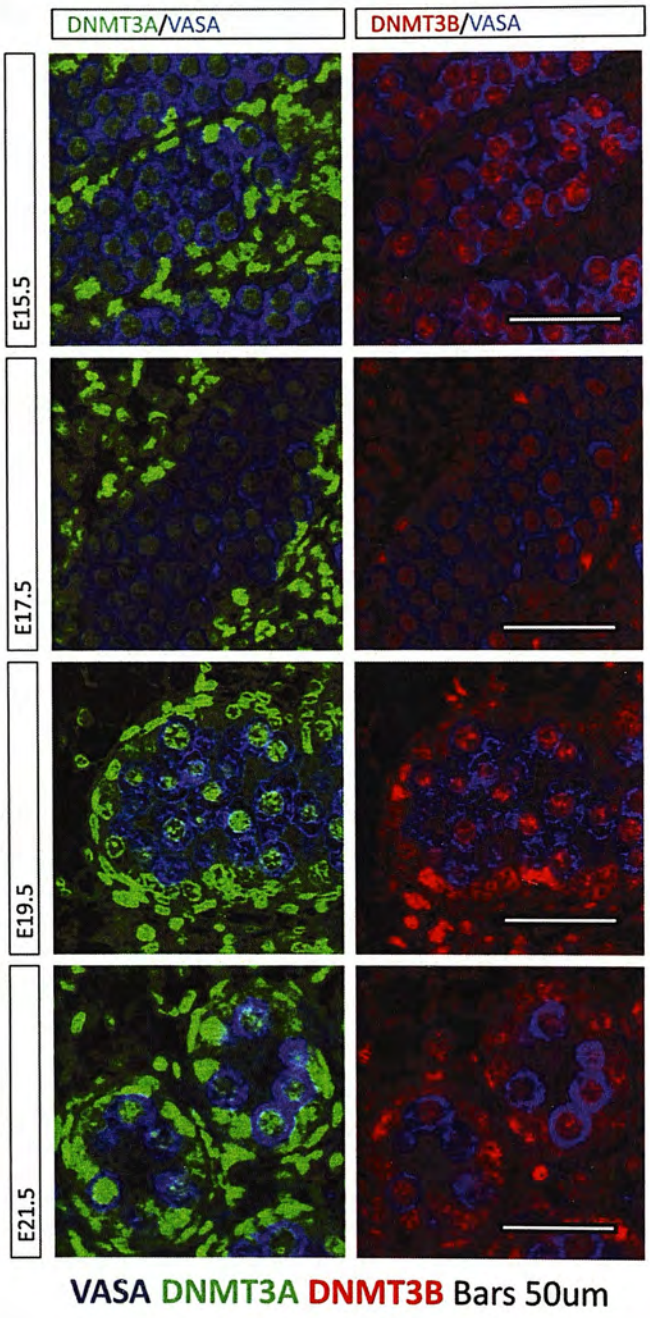

Figure 3.1 Representative immunofluorescent confocal micrographs of DNMT3A (green) and DNMT3B (red) in fetal rat testis. Germ cells are identified by immunostaining with VASA (blue). N>3 for each age. Bar represents 50µm.

3.3.2 DNMT3A and DNMT3B expression in fetal marmoset and human germ cells

Expression of DNMT3A and DNMT3B was examined in fetal marmoset and human germ cells. Germ cell development in primates, unlike in rodents, is asynchronous. As a result there is a gradual loss of immunoexpression of cells positive for OCT4, a transcription factor associated with pluripotency, and gain in the number of VASA positive cells from the second trimester in the human and between 11 and 15 weeks in the marmoset (Mitchell et al., 2008). In order to identify germ cells, tissue was thus immunolabelled using antibodies raised against both OCT4 and VASA.

In marmoset fetal testis, DNMT3A expression was found in the somatic component of the testis (arrowheads) but was absent from the VASA and OCT4 positive germ cells from d98 to d110 (arrow). Likewise, in the human fetal tissue at week 14 and 20 of gestation, there was no co-localisation of DNMT3A with the OCT4 positive cells (arrow) but strong expression in the somatic cells (arrowheads) under these conditions (Figure 3.2). Thus, DNMT3A expression is low or non-detectable in the germ line in rodent and primate germ cells during mid gestation.

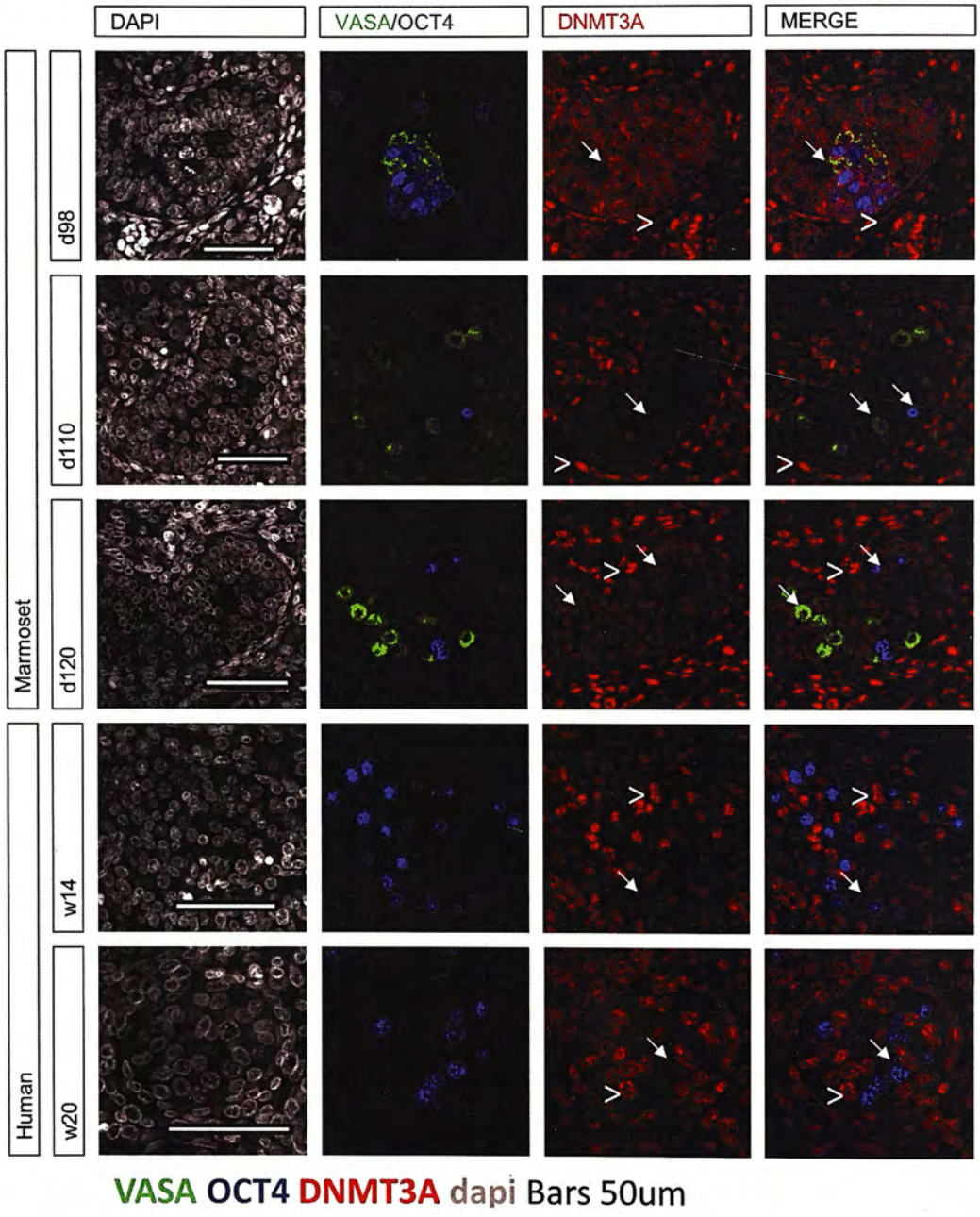

Figure 3.2 Representative immunofluorescent confocal micrographs of DNMT3A (red) in fetal marmoset and human testis. Germ cells are identified by immunostaining with VASA and OCT4 (blue) NB VASA staining not present on fetal human images. Arrows indicate germ cells, arrowheads somatic cells. DAPI counterstain shown in grey. N=2-3 for each age. Bar represents 50µm.

Marmoset and human fetal germ cells expressing OCT4 (arrows), VASA (arrowheads) or both, co-expressed DNMT3B at all of the time points investigated, mirroring the findings in the rat (Figure 3.3).

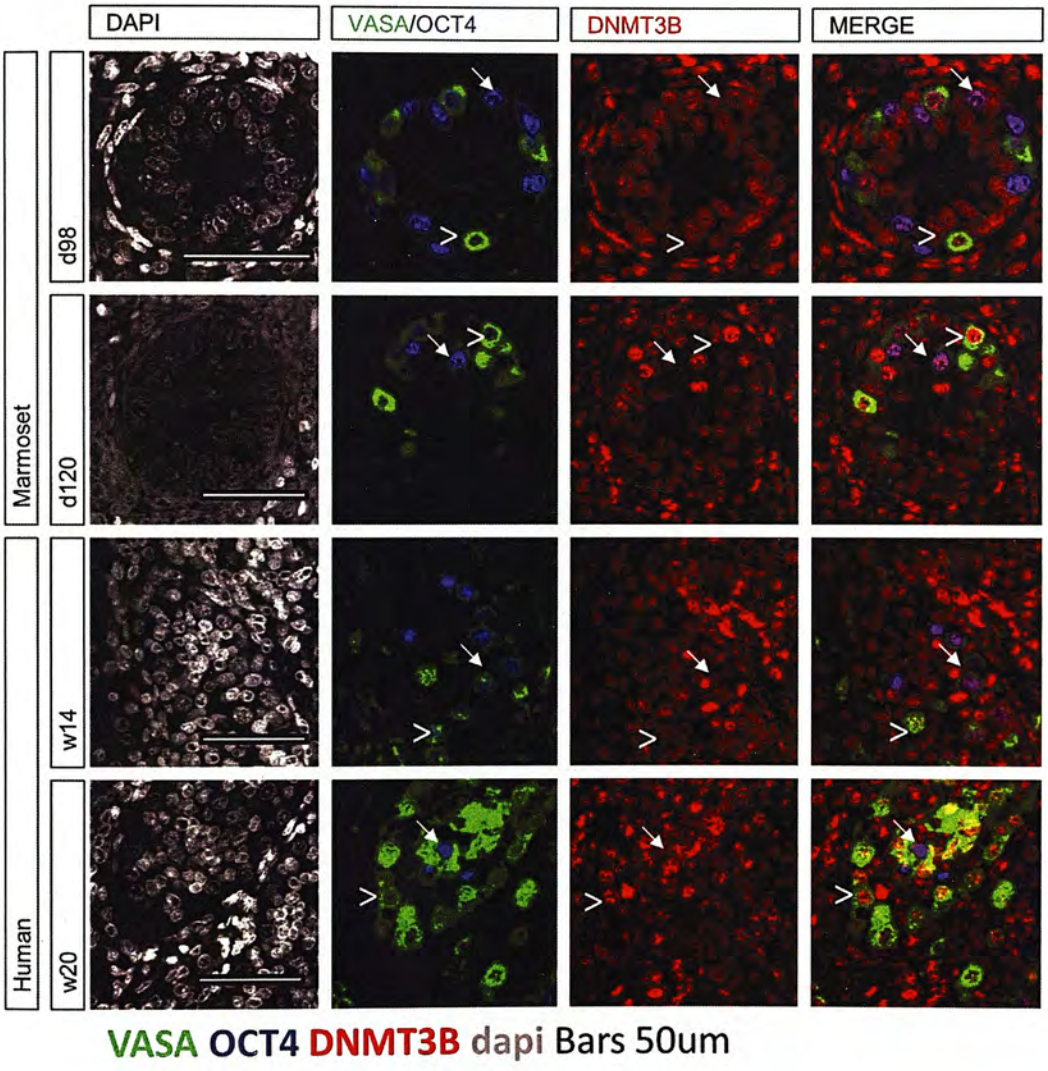

Figure 3.3 Representative immunofluorescent confocal micrographs of DNMT3A (red) in fetal human and marmoset testis. Germ cells are identified by immunostaining with VASA and OCT4 (blue). Arrows indicate OCT4 positive germ cells, arrowheads VASA positive germ cells. DAPI counterstain shown in grey. N=2-3 for each age. Bar represents 50μm.

3.3.3 H3K4me3 and H3K27me3 immunoexpression in fetal germ cells

Fetal rat germ cells expressing VASA all stained positively for the activating histone mark H3K4me3 from e15.5 to e21.5 (Figure 3.4 asterisk). Some tissue sections at e15.5 exhibited germ cells that co-expressed the repressive histone mark H3K27me3. This tended to be orientated along one edge of the testis (Figure 3.4, top right, in white boundary). This could mean that immunoexpression detection is dependent on fixation, which might vary from the outside to the inside of the testis. H3K27me3 immunoexpression was low/not evident at e17.5 and germ cells remained negative for the H3K27me3 mark for the rest of gestation. Sertoli cells can be identified by a peripheral location within the seminiferous tubule and the morphology of their nuclei. Sertoli cells stained strongly for H3K27me3 from e19.5 to e21.5 (Fig. 3.4, lower two right panels, arrowheads).

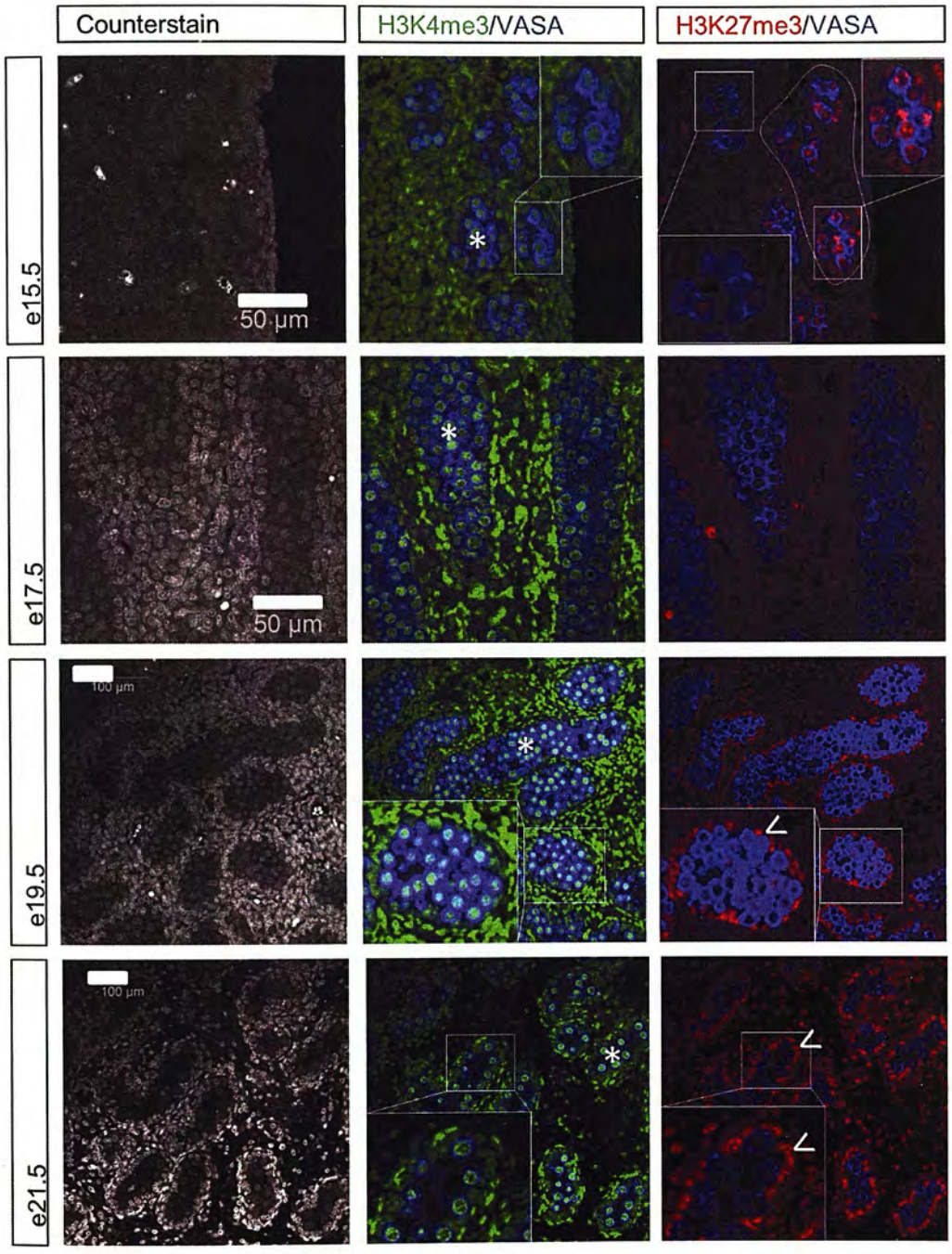

Figure 3.4 Representative immunofluorescent confocal micrographs of H3K4me3 (green) and H3K27me3 (red) in rat testis. Germ cells are identified by immunostaining with VASA (blue). DAPI counterstain shown in grey. * H3K4me3 staining in germ cells, white boundary- H3K27me3 staining in germ cells at e15.5, ^ H3K27me3 staining in Sertoli cells. N=2-3 for each age. Bar represents 50um.

Expression of H3K27me3 was examined in human fetal germ cells at week 20 of gestation. At this age, immunoexpression of H3K27me3 was strongest in the somatic cells with no immunoexpression in the germ cells staining for VASA or OCT4 (Fig. 3.5, arrowheads).

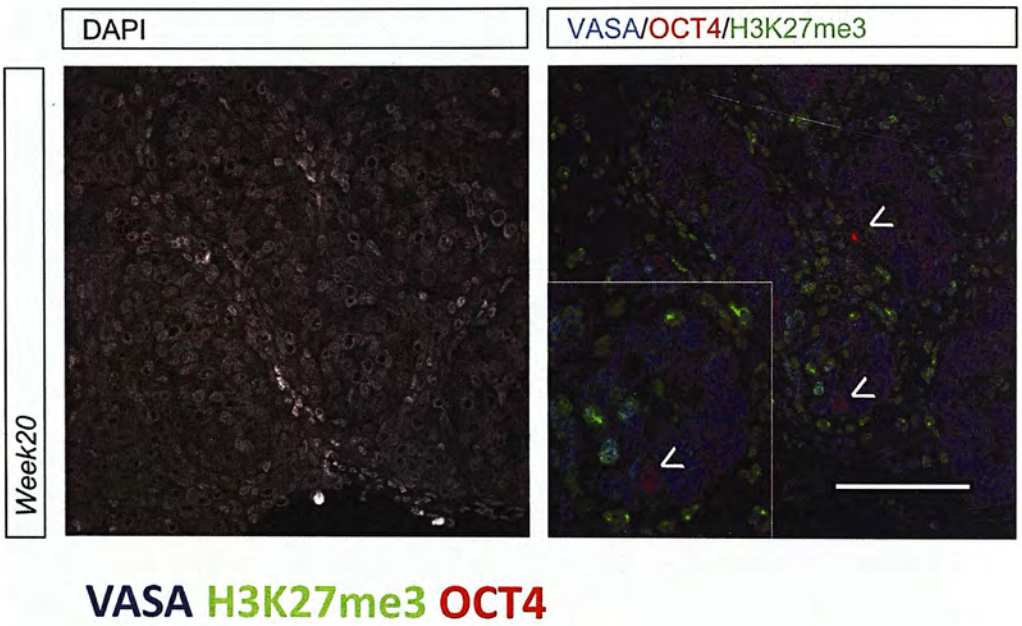

Figure 3.5 Representative immunofluorescent confocal micrograph of H3K27me3 (green) in human fetal testis. Germ cells are identified by staining for VASA (blue) or OCT4 (red, also highlighted by arrowhead). DAPI counterstain shown in grey. Bar represents 50μm.

Thus, H3K4me3 immunoexpression is detectable in germ cells throughout fetal development but H3K27me3 expression appears only early in gestation, with loss of expression between e15.5 and e17.5 in the rat.

3.3.4 Expression of DNMT3A and DNMT3B in the postnatal rat testis

Immunoexpression of DNMT3A and DNMT3B was examined in the postnatal rat testis. DNMT3A and DNMT3B expression was evident in VASA positive germ cells at d6, in the spermatogonia at d15 and d25 and in spermatogonia and spermatids of all stages in the adult testis (arrowheads) (Figure 3.6). There was strong DNMT3B staining in the Sertoli cells (arrows) in the adult testis, although this was less clear in the peripubertal Sertoli cells at day 25.

Thus, postnatal rat germ cells all expressed DNMT3A and DNMT3B. Sertoli cells stained strongly for DNMT3B in the post pubertal rat testis.

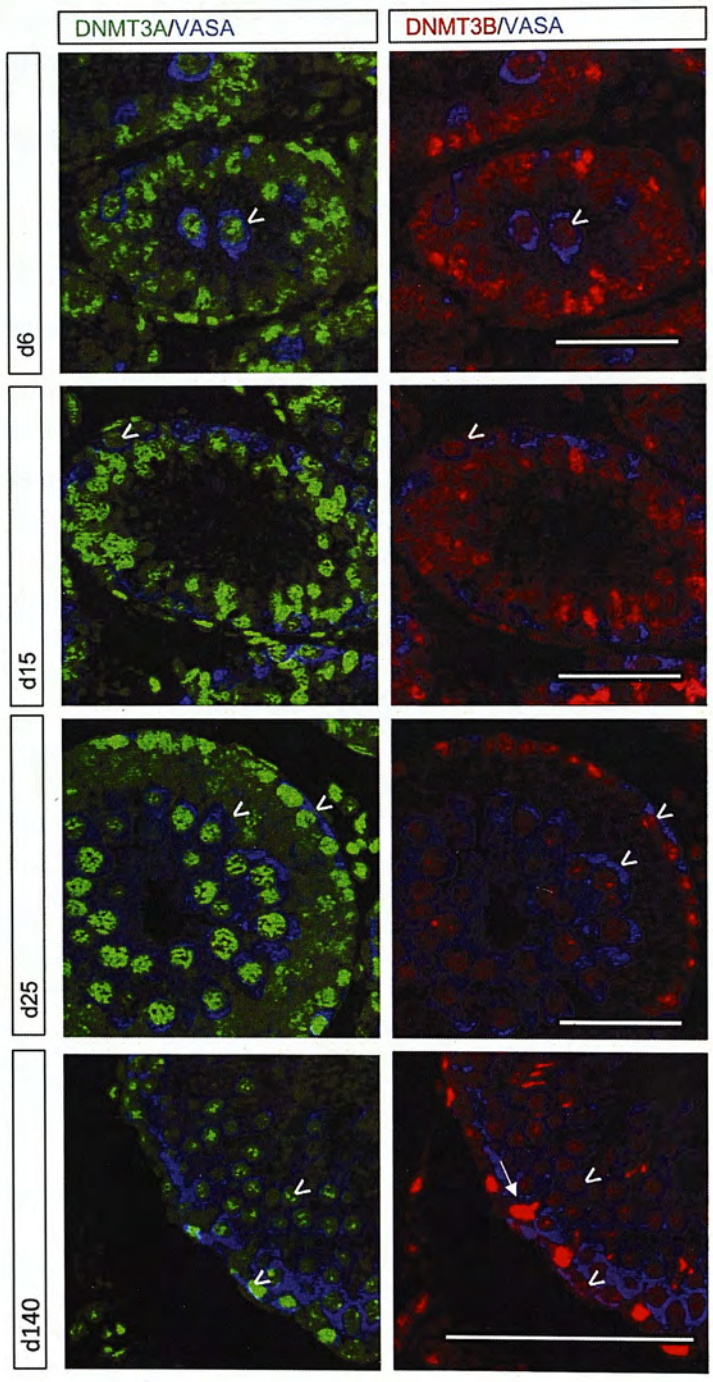

Figure 3.6 Representative immunofluorescent confocal micrographs of DNMT3A (green) and DNMT3B (red) in rat testis. Germ cells are identified by immunostaining with VASA (blue) (arrowheads) Arrows, Sertoli cells). N>3 for each age. Bar represents 50μm.

3.3.5 Expression of H3K4me3 and H3K27me3 in the postnatal rat testis

H3K4me3 expression was abundant in the VASA positive germ cells in the rat testis at postnatal days 6 and 15 (Figure 3.7, top middle panel). At d25, a stage specific pattern was observed with a loss of H3K4me3 expression in germ cells during development (Figure 3.7, middle panel, asterisks) and clear loss of staining in the adult testis at stage VIII of the spermatogenesis cycle in the pachytene spermatocytes but increased staining in the zygotene spermatocytes (middle bottom panel, asterisks).

H3K27me3 on the other hand showed only weak immunoexpression in the germ cells at d6 and d15, with stronger expression in the Sertoli cells (Figure 3.7, right top panel, arrowheads). At d25, there was a stage specific period of immunoexpression of H3K27me3 in germ cells that was lost in the adult testis where immunoexpression was once again confined to Sertoli cells (Figure 3.7, lower right panel and inset, arrow).

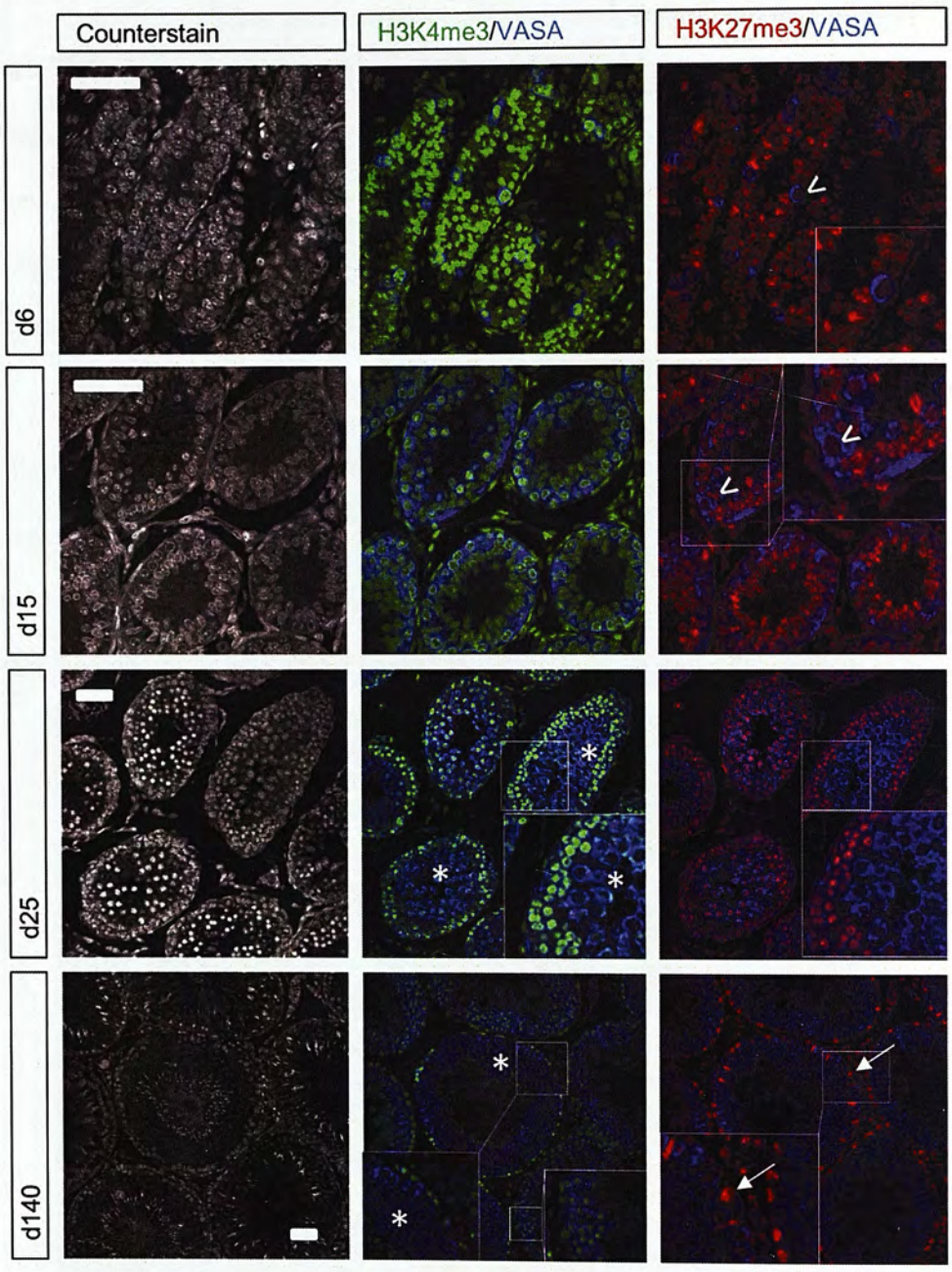

Figure 3.7 Representative immunofluorescent confocal micrographs of H3K4me3 (green) and H3K27me3 (red) in rat testis. Germ cells are identified by immunostaining with VASA (blue). DAPI counterstain shown in grey. *Germ cells negative for H3K4me3, ^ germ cells negative for H3k27me3, arrow Sertoli cells positive for H3K27me3. N=2-4 for each age. Bar represents 50µm.

3.3.6 Expression of 5mC and 5hmC in postnatal rat and marmoset testis

Given that DNMT3A and DNMT3B were expressed in the postnatal rat testis, immunoexpression of 5mC and 5hmC was explored. Germ cells expressed 5mC at each of the time points explored, through to adulthood. It was also observed that during puberty (pnd15-30), there was a loss of 5mC staining and a gain of 5hmC staining in germ cells (red) (Figure 3.8, arrowheads). This was also observed in the developing marmoset testis, in which germ cells stained strongly for 5mC and where during puberty there was loss of 5mC and gain of 5hmC staining in Sertoli cells. (Figure 3.9, arrowheads). A similar pattern was also found in the adult human testis (Figure 3.10).

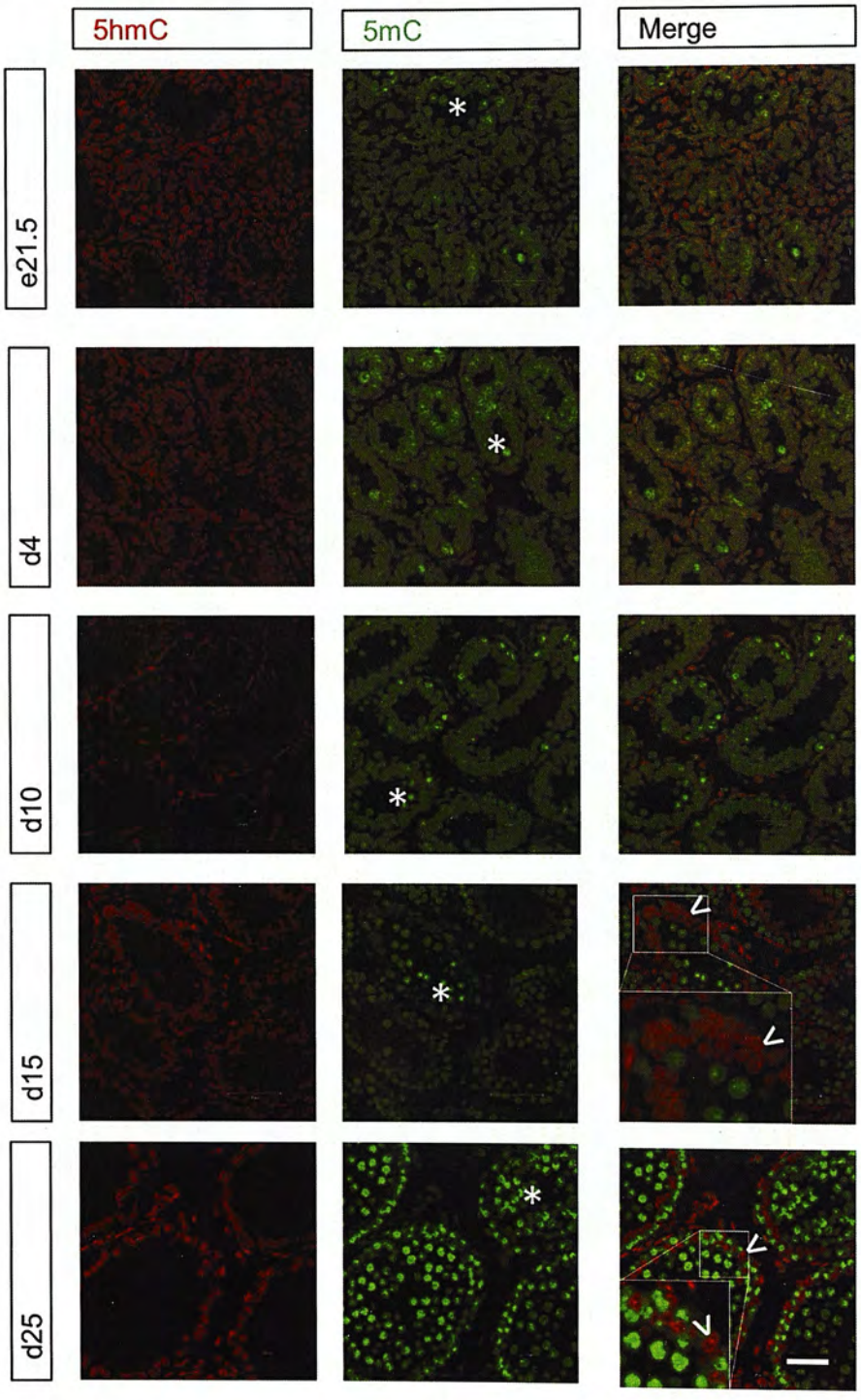

Figure 3.8 Representative immunofluorescent confocal micrographs of 5mC (green) and 5hmC (red) on fetal and neonatal rat testis. Arrowheads point to Sertoli cells,*indicates germ cells within seminiferous tubules. N=2-4 for each age. Bar represents 50μm.

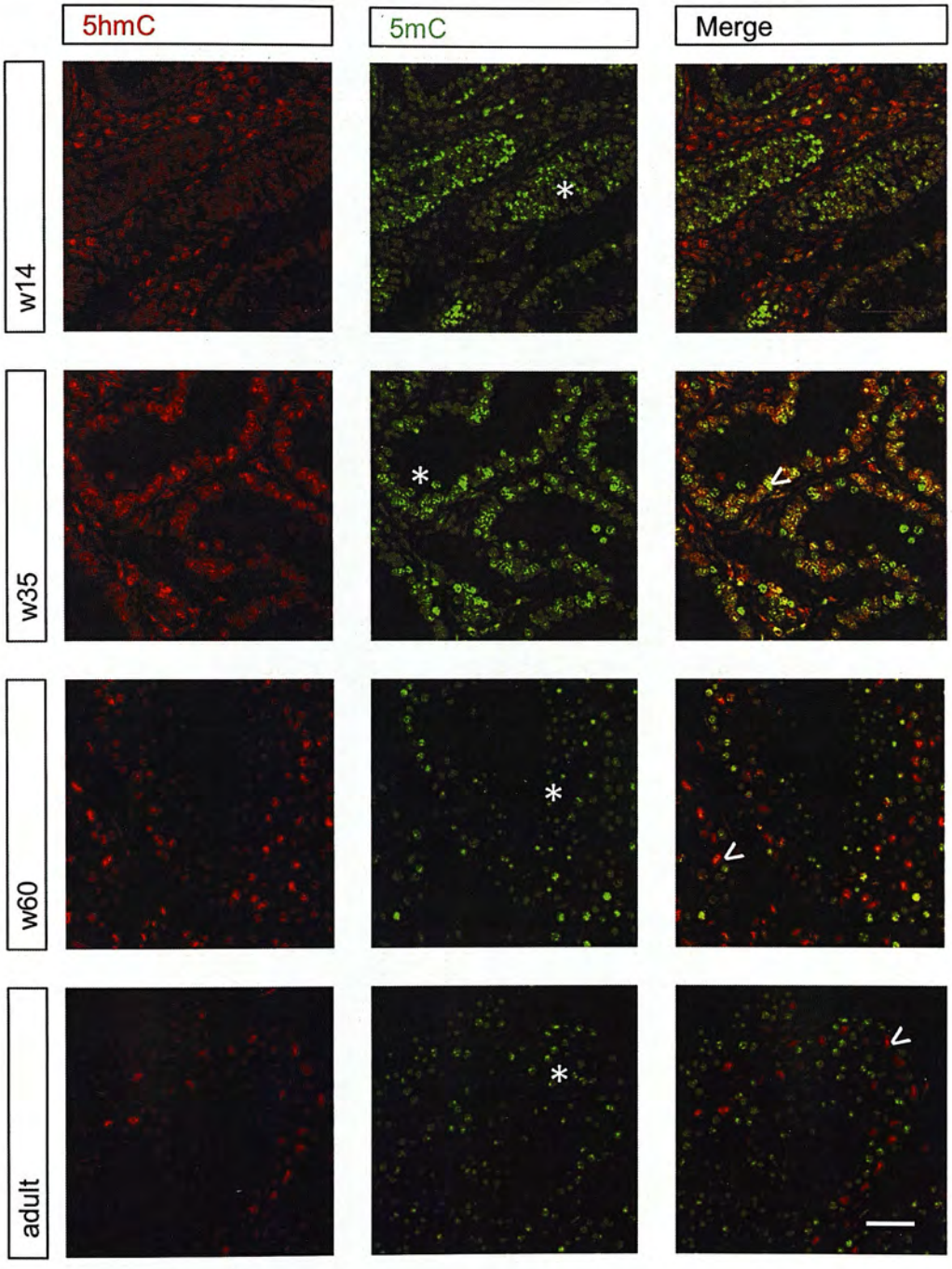

Figure 3.9 Representative immunofluorescent confocal micrographs of 5mC (green) and 5hmC (red) neonatal and adult marmoset testis.
Arrowheads point to Sertoli cells. N=2-3 for each age. * demonstrates germ cells. Bar represents 50μm.

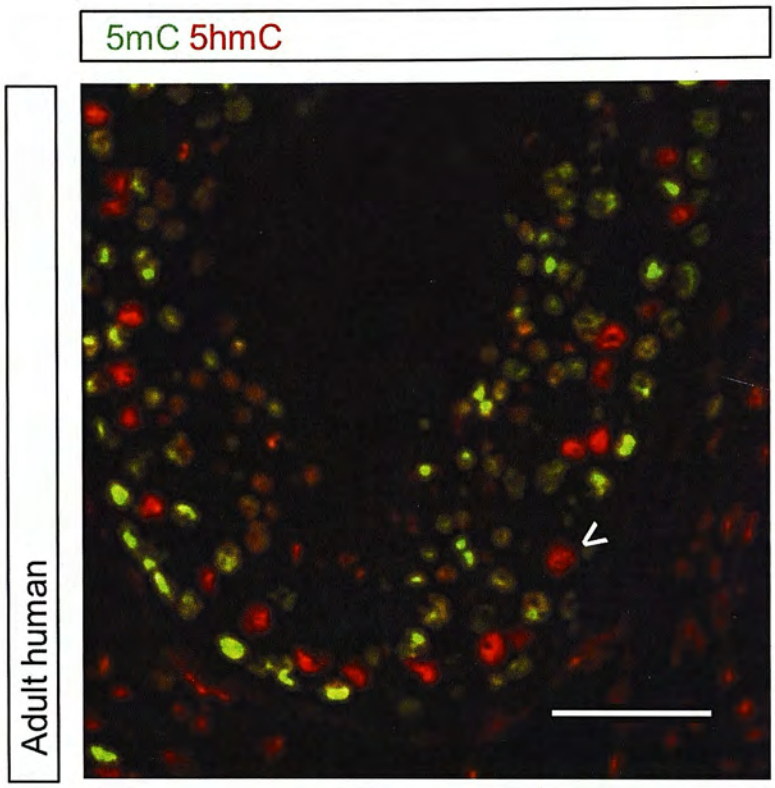

Figure 3.10 Representative immunofluorescent confocal micrograph of 5mC (green) and 5hmC (red) on adult human testis. Arrow heads point to Sertoli cells n=1-2. Bar represents 50um.

3.3.7 Expression of Tet1 in developing rat testis

Given the abundance of 5hmC in the mature Sertoli cells, TET1 expression was examined during postnatal rat testis development. Here expression of TET1 was found in the interstitial cells until postnatal day 10 when expression became greater within the seminiferous tubules, and was found in both germ cells and Sertoli cells (Figure 3.11, arrowhead).

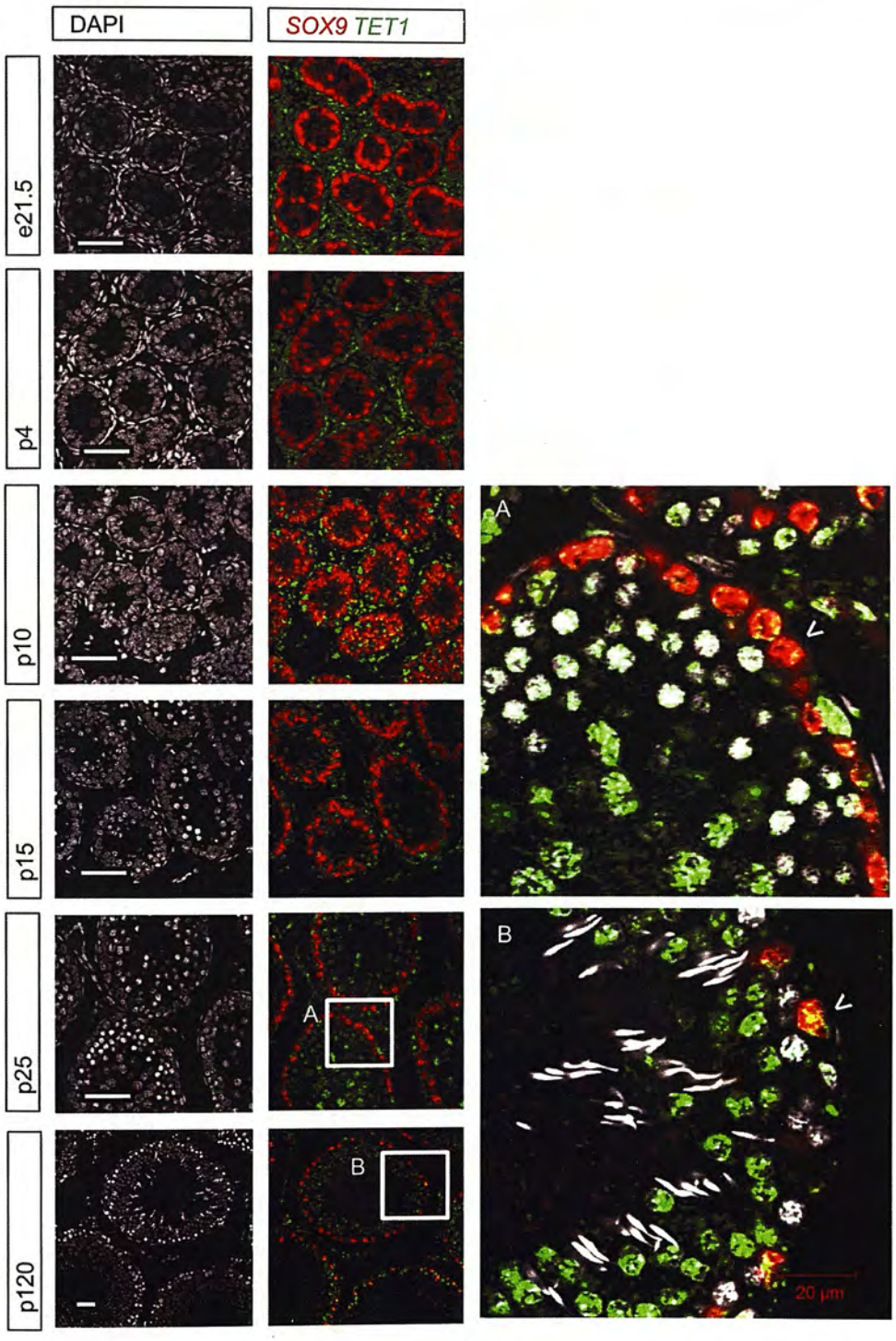

Figure 3.11 Representative immunofluorescent confocal micrographs of SOX9 (red) and TET1 (green) on postnatal rat testis at the ages indicated. Squares indicate insets **A** and **B**. Co-localisation of Tet1 and Sox9 is clear in Sertoli cells (Arrowheads) n=2-3. Bar represents 50µm.

3.4 Discussion

The aim of this chapter was to investigate some epigenetic modifications and their regulators during germ cell development in the rat, marmoset and human. The expression patterns for the different regulators showed consistency between the species and suggests that mechanisms are conserved across mammalian species with respect to regulation of the epigenome during germ cell development. Furthermore, expression of important epigenetic regulators was demonstrated during fetal and postnatal germ cell development, suggesting that at various time points, specific aspects of the epigenome might be vulnerable to environmental perturbation.

3.4.1 A cross- species comparison

3.4.1.1 DNMT3A and DNMT3B

Murine data suggest that DNMT3A is expressed in the germline from around e13.5 (Sakai et al., 2004; La Salle et al., 2004) with loss of expression at e18.5 at the protein level (Sakai et al., 2004) but continued expression at the message level (La Salle et al., 2004). This lines up with the time frame for remethylation in the murine male germline that occurs from e16.5 until birth (Kato et al., 2007; Molaro et al., 2014). In the present studies, expression of DNMT3A in the rat increased during the e17.5 to e19.5 window, which also lines up with remethylation that occurs between e18.5 and birth (at the immunoexpression level)(Rose et al., 2014). Primate fetal testicular tissue was available for the second trimester during which time points DNMT3A was not expressed in the germ cells, either in those that expressed OCT4 or expressed VASA. Tissue was not available for later time points thus it was not possible to show if the levels of DNMT3A increased during the later stages of gestation. A previous study found *DNMT3A* expression increases in the human fetal testis at week 21 at the mRNA level, complementing the findings of the present study (Galetzka et al., 2007).

DNMT3A transcription is controlled by two promoters, each producing a different isoform; *Dnmt3a* and *Dnmt3a2* (Chen et al., 2002b). DNMT3A demonstrates low level ubiquitous expression and localises to heterochromatin, suggesting a house keeping role. DNMT3a2 is expressed specifically in cells undergoing *de novo* methylation and localises to euchromatin (Chen et al., 2002b). The epitope for the antibody used in this study is from the residues 1-300 at the N terminus, which is common to both transcripts, thus it is not possible to say if expression of one isoform altered during development. One might postulate that *Dnmt3a*2 was of most importance during germ cell remethylation.

In keeping with murine data (Hajkova et al., 2002; Sakai et al., 2004), DNMT3B was expressed in germ cells at all of the time points investigated in all species. The ongoing expression of DNMT3B during times at which germ cell remethylation is not thought to be occurring might suggest a redundancy in its activity, despite being expressed. However, *Dnmt3b* knockout results in embryonic lethality at e11.5 (Okano et al., 1999) indicating an important role for this protein, perhaps with respect to remethylation of somatic cells where it was expressed in the fetal and adult rat testis (Figure 3.1 and Figure 3.6). A summary of DNMT3A and 3B expression in fetal germ cells is presented in Figure 3.12.

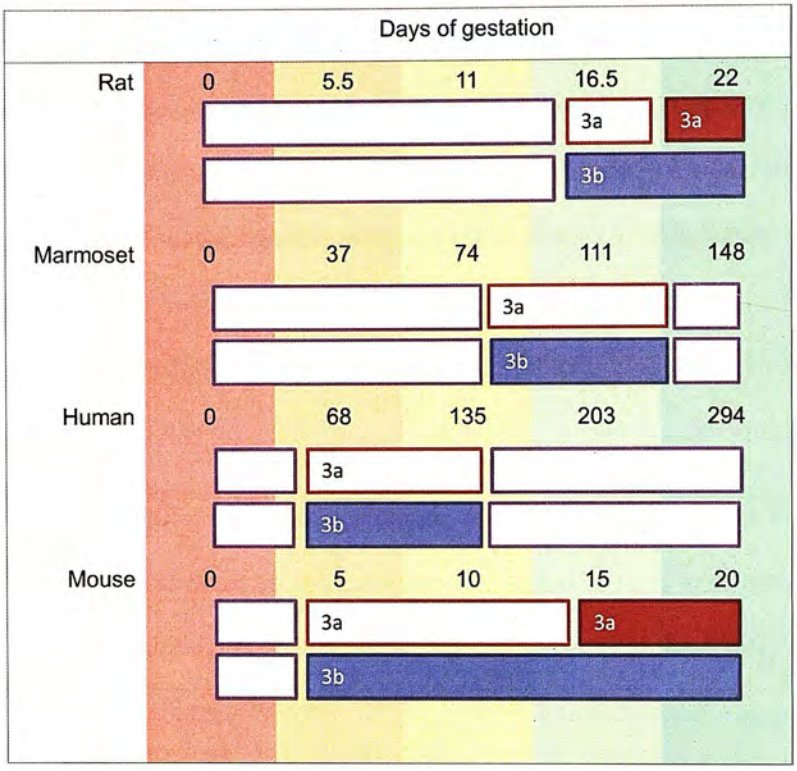

Figure 3.12 Summary of DNMT3A and DNMT3B expression in germ cells during development. Days of gestation indicated giving a rough indication of comparative time points. Blue boxes indicate DNMT3B and red boxes indicate DNMT3A. Filled boxes demonstrate expression in germ cells. Open boxes show expression absent. Purple boxes show studies not done due to availability of tissue. Rat, marmoset, and human data are presented in Chapter 3. Mouse data summarised from literature review (Figure 1.3).

In the adult mouse testis, *Dnmt3a* and *Dnmt3b* expression increased at the leptotene/zygotene stages of development (La Salle and Trasler, 2006). In the rat testis, expression was greatest in the zygotene and pachytene spermatocytes but was less evident in leptotene spermatocytes (Figure 3.6). This could be explained by a delay in translation resulting in immunodetectable protein downstream of initiation of

transcription in the leptotene spermatocytes. No difference in expression between the different stages of spermatogenesis was found in terms of *DNMT3B*, as was found by La Salle and Trassler (2006), perhaps due to differences in either the sensitivity of the technique or translation. Consistent with the rat data, DNMT3A and 3B are expressed in human adult spermatocytes but expression is less in spermatogonia and absent in testicular *carcinoma in situ* cells (Kristensen et al., 2013).

Thus, expression of DNMT3A and 3B can be found in all spermatogonia and spermatocytes in the adult testis, in both rodent and primates.

3.4.1.2 H3K4me3 and H3K27me3

Expression of the activating histone modification H3K4me3 was apparent in the germ cells at all fetal time points examined except during maturation at day 25 (Figure 3.7) and in spermatids beyond stage VIII in the spermatogenic cycle in the adult testis. The loss of canonical histone marks would be expected during spermatogenesis as the histones are acetylated in preparation for replacement by protamines (Rathke et al., 2014). The loss of expression of H3K4me3 during pubertal germ cell maturation has not previously been reported, although may reflect changes in the chromatin in preparation for replacement by protamine. Interestingly, in the hamster, it has been postulated that inadequate chromatin condensation explains the lack of fertility of spermatozoa produced early in puberty (Weissenberg et al., 1995).

H3K27me3 had a more dynamic expression pattern in fetal testes, with expression present along one edge of the testis at e15.5 but then becoming absent from germ cells until day 6 after birth. In the mouse, H3K27me3 expression increases in germ cells during demethylation and has been proposed as a mechanism to prevent aberrant expression of genes otherwise supressed by methylation (for example developmental genes and DNA repeat elements)(Hajkova et al., 2008). It could thus be postulated that

H3K27me3 expression would disappear during germ cell remethylation. The presented data however suggest that expression of this histone mark is lost prior to remethylation, suggesting alternative mechanisms may be in place for regulation of these genes that are otherwise proposed to be regulated by methylation. In FACS sorted mouse germ cells, expression of H3K27me3 appears to continue until at least e17.5 (Abe et al., 2011), whereas the present studies suggest that expression is lost much earlier in the rat. The differences in results could be accounted for by the use of different model species or it could be a sensitivity detection issue, perhaps affected by tissue fixation, or as the cells in the mouse study were *in vitro*, which could have altered behaviour and/or chromatin dynamics. However, the lack of expression of H3K27me3 in germ cells demonstrated in both the rat fetal testis and the human testis during the late 2nd trimester (Figure 3.5 and Figure 3.7) adds weight to the latter argument.

As with the H3K4me3 expression, there was a stage specific re-expression of the H3K27me3 mark germ cell maturation at d25. Again the function of this expression is curious, especially given that this expression is not seen during adult spermatogenesis. Thus, there may be specific genes regulated by chromatin in the germ line during this stage of rat puberty.

3.4.1.3 Epigenetic dynamics and potential perturbation susceptibility time points

Germ cell maturation in primates is asynchronous (Mitchell et al., 2008), as shown in Figure 3.2 and Figure 3.3 in which germ cells are positive for either OCT4 or VASA or both. Expression of DNMT3A and 3B in these cells was ubiquitous, thus no asynchrony in expression of the 'remethylation machinery' was identified. A more direct means of examining remethylation in germ cells would be by direct staining for 5mC, however this was not possible in the present study due to lack of tissue availability from the later stages of gestation (during which methylation would be expected to reappear) in primates.

Thus, expression of the DNA methyltransferases was demonstrated in germ cells through late fetal, neonatal, pubertal and adult spermatogenesis indicating that methylation could be perturbed in these cells by environmental factors across any of these time points. Furthermore, expression appears consistent across mammalian species, indicating conservation of mechanisms and, that animal models may (at least in some part) mimic that which might be seen in humans.

3.4.2 5mC and 5hmC expression in neonatal and mature testis

As would be predicted, the present studies in postnatal testes showed ongoing expression of 5mC in the germ cells through puberty to adulthood (Marques et al., 2011; Soubry et al., 2014). Establishment of methylation at imprinted genes and repeat elements occurs in the fetus (Kato et al., 2007; Molaro et al., 2014). The locus-specific dynamics of 5mC during spermatogenesis postnatally has not yet been reported in the literature. Aging, diet exposure and exercise however have all been shown to affect the global methylation of spermatozoa (Denham et al., 2015; Fullston et al., 2013; Jenkins et al., 2013), and a few studies are starting to identify potential candidate genes that could perturb development, although any causality is still widely debated (Denham et al., 2015). Genome-wide mapping of methylation during adult spermatogenesis and investigation of any retained methylation patterns in offspring, would be a basis for identifying if environment/pathology could impact upon sperm methylation, but has yet to be reported. To date, evidence that aberrant methylation patterns can survive through germ cell development are limited to a study examining the sperm methylome following *in utero* dietary restriction (Radford et al., 2014), a time point at which methylation dynamics are much greater than those seen in adulthood.

The present studies show that in the rat and primate testis, 5mC is globally abundant in germ cells at all stages of spermatogenesis but details regarding the locus-specific dynamics of 5mC location cannot be assessed using immunohistochemical techniques.

5hmC dynamics during spermatogenesis have been reported; interestingly, expression of 5hmC correlates with expression of some key spermatozoal development genes for example *Protamine 1 and 2* (Gan et al., 2013). Furthermore in this paper they show that Sertoli cells also exhibit strong 5hmC expression.

3.4.3 5hmC during Sertoli Cell maturation

The metabolic and physical support of Sertoli cells is essential for spermatogenesis (Sharpe et al., 2003). Examining 5mC and 5hmC staining in the adult rat, marmoset and human testis demonstrated that Sertoli cells stained strongly for 5hmC. During Sertoli cell maturation, the function of the cells changes from proliferation and promoting differentiation of the germ line to supporting spermatogenesis, with cessation of proliferation (Sharpe et al., 2003). Over the postnatal time course in the marmoset and rat testis during which Sertoli cells mature (across puberty), there is a gradual loss of 5mC and gain of 5hmC. Whether changes in DNA methylation result in the changed function and proliferation of Sertoli cells or whether methylation levels change as a result of the altered function is not clear.

It is interesting to compare Sertoli cells with neurones, which show similar developmental trajectories with terminal differentiation associated with reduced proliferation, and in which 5hmC levels are high (Hahn et al., 2013; Li et al., 2015b). TET1 expression was found in maturing Sertoli cells (Figure 3.11), however, loss of *Tet1* does not result in an obvious testicular phenotype (Dawlaty et al., 2011; Yamaguchi et al., 2012) suggesting (if it is functional) an alternative mechanism for the loss of 5mC and gain of 5hmC observed. Expression of *Tet2* and *Tet3* is greater in the testis than *Tet1* (unpublished data from E. Undrell), however, to date, antibodies with sufficient specificity to allow localisation within the testis are not available. Given the importance of *Tet3* for neuronal development (Hahn et al., 2013), it is interesting to speculate that *Tet3* might play a role in Sertoli cell maturation.

Sertoli cells are of key importance for spermatogenesis and their function can be impaired by a high fat diet and impaired glucose homeostasis, which subsequently results in perturbed spermatogenesis (Fan et al., 2015a). However, whether these perturbations might result in an intergenerational effect is unclear.

3.5 Conclusion

DNA methylation and chromatin landscapes are dynamic throughout germ cell development and might be disrupted by environmental stimuli at various time points. Mechanisms appear well conserved between primate and rodent models. Further locus specific interrogation of the 'epigenetic landscape' of developing germ cells in control conditions and following exposure to environmental stimuli may open up clues as to whether changes to the germline epigenome is responsible for intergenerational transmission of phenotype and, during which time windows germ cells are most vulnerable.

4 The effects of grandparental high fat diet in two generations of rats

4.1 Introduction

As discussed in Chapter 1, the prevalence of obesity is rising (WHO, 2014), and, there is accumulating experimental and epidemiological evidence that the ancestral environment might influence health in subsequent generations (Aiken and Ozanne, 2014; Desai et al., 2015). The biological mechanisms resulting in these intergenerational effects remain unknown, but evidence is accumulating for perturbation of the germline epigenome in response to 'adverse' environments. Potential mechanisms include alterations in chromatin dynamics (Carone et al., 2010; Öst et al., 2014), methylation of DNA within spermatozoa (Carone et al., 2010; Fullston et al., 2013; Radford et al., 2014) and miRNA content in mature spermatozoa (Fullston et al., 2013; Gapp et al., 2014). However, the time point at which these changes may occur is unclear and there is evidence to suggest *in utero* (Radford et al., 2014), pre-pubertal (Northstone et al., 2014) or adult exposures (Fullston et al., 2013) could all potentially result in transmission of phenotype. In Chapter 3, expression of epigenetic regulatory factors was demonstrated in germ cells through embryonic development to adulthood, thus, biologically, exposure at any of these time points could result in intergenerational transmission of phenotype.

In order to investigate potential mechanisms for the intergenerational inheritance of a phenotype, a model demonstrating such a transmission has first to be established. In the present chapter, the phenotype of two generations of offspring following exposure to either maternal or paternal HFD is explored. This allowed comparison of the effects of both maternal and paternal increased adiposity. Furthermore, the rodent model used is transgenic and expresses eGFP in the germline, thus allowing for the FACS of germ cells and further investigation of any changes that may have occurred in the germline.

4.2 Materials and methods

Materials and methods are as described in Chapter 2. To exclude the possibility of soya acting as an endocrine disruptor (Napier et al., 2014), a soya free diet was used in the experiment (although it should be noted that the endocrine disrupting effects of soy derived isoflavones are not consistently reported in the literature (Cederroth et al., 2010)). Two diets were used for the study, a control diet (CD) comprising 10% energy from fats, and a HFD comprising 45% energy from fat (with fat obtained from lard). The CD was matched to the HFD in order to try to account for food consumption and micro and macro nutrient intake. In a previous murine study, consumption of a diet with 45% energy from fat for 14 weeks resulted in increased adiposity but no dysregulation of glucose homeostasis (Fullston et al., 2013). Details of the composition of the diet are shown in Table 4.1. Animals were weaned onto the experimental or control diet at 21 days of age. All animals were subsequently maintained on this diet *ad libitum*. Following 12 weeks on the diet, the animals underwent an overnight fast and oral glucose tolerance testing the following morning. Animals were given 2 weeks to recuperate and then bred with animals from the control arm of the study. Mating was conducted as in 2.1.2.2. Subsequent F1 and F2 generations were examined in the same way except all were weaned onto the control diet. OGTT was performed at 12 weeks post weaning and animals were bred at 14 weeks. The number of animals in the study is shown in Figure 4.1.

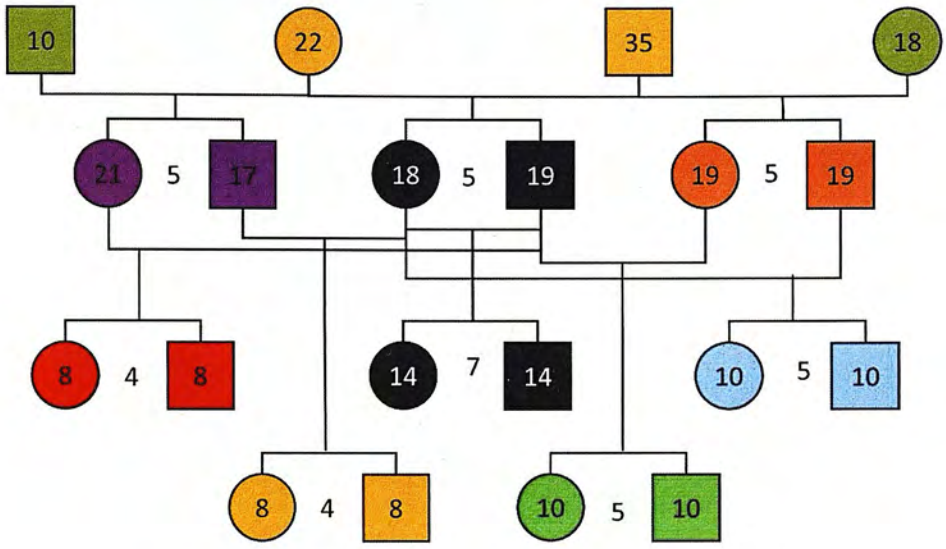

Figure 4.1 Total number so animals. Squares represent males, circles females. In the F0 (top row) green represents HFD and yellow CD. Numbers between siblings indicate number of litters. Total number of animals 298.

	HFD	CD
Research Diets ™ #	D06071701	D06072701
Cysteine (% w/w)	0.35	0.28
Casein (% w/w)	23.31	18.96
corn-starch (% w/w)	8.48	29.86
Maltodextrin (% w/w)	11.65	3.32
Sucrose (% w/w)	20.14	33.17
Cellulose (% w/w)	5.83	4.74
Corn oil (% w/w)	2.91	2.37
Mineral mix (% w/w)	1.17	0.95
Vitamin mix (% w/w)	1.17	0.95
Lard (% w/w)	20.68	1.90
Calories/100g	473	385
% of total energy from carbohydrate	35	70
% of total energy from protein %	20	20
% of total energy from lipid %	45	10

Table 4.1 Composition of the control (CD and high fat (HFD) diets used in the experiments. In the HFD, fat replaces the carbohydrate component of the diet.

4.3 Results

4.3.1 A HFD induces obesity but not altered glucose tolerance in exposed animals (F0)

Following 14 weeks consumption of a HFD, F0 males were on average 9.3% heavier and F0 females 14.7% heavier compared to animals fed a CD, $p<0.001$ for interaction between diet, time and sex, with a significant difference in male bodyweight from 60 days of diet and females from 100 days (Figure 4.2). In the males, the adiposity index (the sum of the fat pads divided by body weight) was increased by 31% ($p<0.001$), plasma leptin was increased around 3-fold although failed to reach statistical significance (Table 4.2). There were no changes plasma lipids or triglycerides between either of the groups (Table 4.2). Insulin secretion in response to a glucose challenge was increased in the HFD fed males ($p<0.001$), however despite this, there was no change in plasma glucose levels. There was no difference in sperm count and motility according to diet (Table 4.2). HFD did not result in altered testicular cell apoptosis as assessed by TUNEL staining (Figure 4.3 and Table 4.2).

	CD	HFD	
N (litters)	7-15(6)	7-15(6)	
	Mean±SEM	Mean±SEM	p
Body size			
Weight (g)	416±14	454±14	0.003
Body length (cm)	24±0.25	24±0.31	0.565
Organ weights			
Pancreas weight/bodyweight (mg/g)	4.7±0.3	6.9±0.4	0.416
Liver/bodyweight (mg/g)	1.9±0.1	**1.8±0.1**	**<0.001**
Adipose weights			
Retroperitoneal Fat/bodyweight (g/g)	0.7±0.04	**0.7±0.03**	**<0.001**
Gonadal fat/bodyweight (mg/g)	6.3±0.3	**8.3±0.3**	**<0.001**
Adiposity Index (mg/g)	12.7±0.6	**16.7±0.7**	**<0.001**
Biochemistry			
Leptin (ng/ml)	1.7±0.8	5.3±1.2	0.054
Insulin AUC µg/l.min	96±11	**145±10**	**0.003**
Glucose AUC mM.min	647±23	672±18	0.400
Triglycerides mg/dl	72±5	65±6	0.719
Cholesterol mg/dl	59±3	61±4	0.414
Reproduction			
AGD (mm)	46.9±1.3	45.9±0.8	0.520
Testis weight (g)	1.8±0.1	1.7±0.1	0.334
Penis length (mm)	11±0.1	12±0.1	0.250
Sperm count (10^{-6})	19±2.6	18±1.4	0.598
Testosterone (ng/ml)	5.1±1.5	7.3±0.7	0.060
% motile sperm	32.3±4.4	26.6±2.5	0.277
TUNEL (pixels)	1110±414	1450±263	0.504

Table 4.2 Phenotyping of Founding F0 males after exposure to HFD.
Data is taken from post-mortem dissection and measurement of organs at 19 weeks of age. Biochemical data is derived from 09.00 fasting plasma obtained during glucose tolerance testing at 17 weeks of age. Data was analysed by a linear mixed model with diet as a fixed factor and cohort as a random factor and using post hoc Bonferroni analysis. Values that are significantly altered by HFD ($p<0.05$) are shown in **bold**.

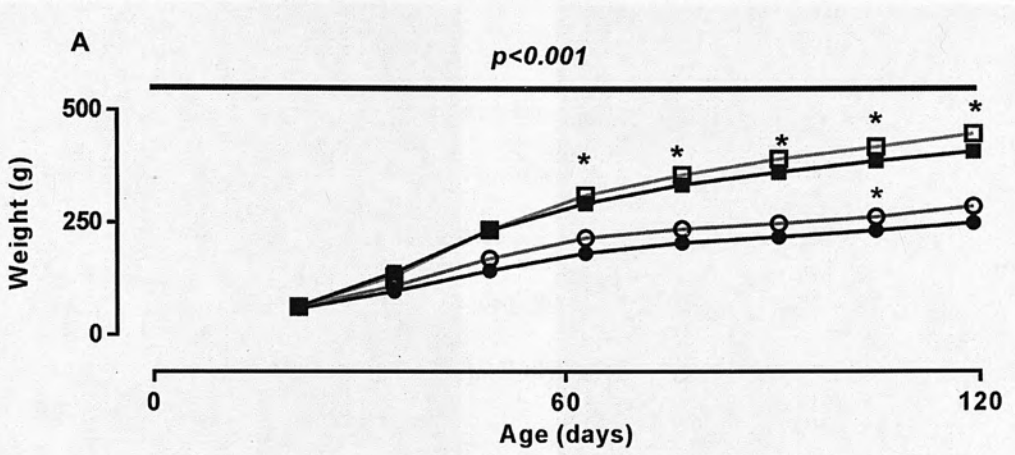

Figure 4.2 Bodyweight of the founding generation from weaning. Legend: Squares males, circles females, Grey line HFD, black line CD. Data were analysed by linear mixed model with diet and sex as fixed factors, time as a repeated factor and cohort as a random factor with Bonferroni post hoc testing for effect of diet within a sex. N= 35 (CD) and 35 (HFD) males and 18 (CD) and 10 (HFD) females from two cohorts. Data are mean ±SEM * p<0.05 HFD vs CD.

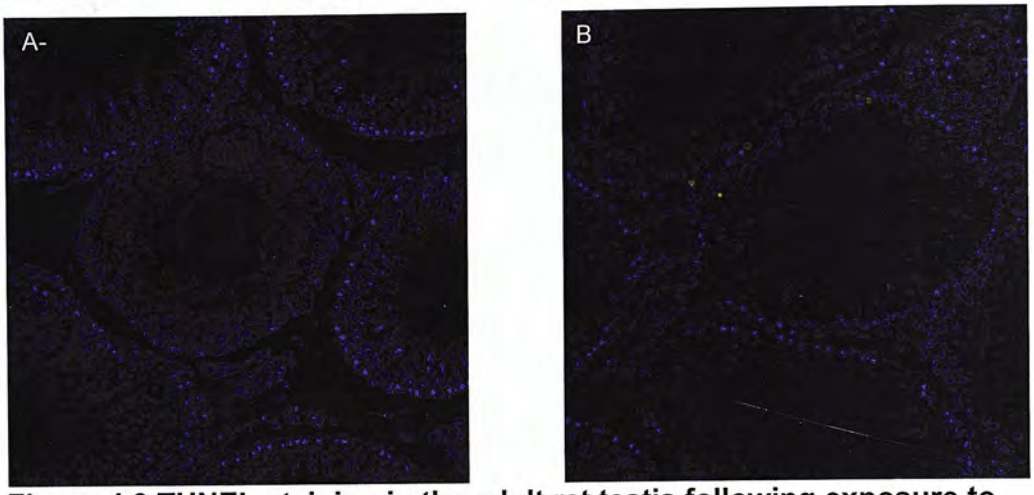

Figure 4.3 TUNEL staining in the adult rat testis following exposure to HFD or CD for 14 weeks. Formalin fixed, paraffin embedded testis was examined for DNA damage, a marker of apoptosis using the Promega deadend™ kit with the modifications as described in materials and methods. A. representative example from CD. B representative example from HFD. N=7, number of TUNEL positive pixels was assessed using imageJ, and the data presented in Table 4.2.

4.3.2 Maternal HFD results in heavier offspring (F1)

There was no difference in litter size, days taken to plug, gestation length, mean birthweight or proportion of males per litter in the F1 animals born to parents who had consumed a HFD or a CD (Table 4.3).

	CD	Mother HFD	Father HFD	
Litters	5	5	5	
	Mean±SEM	Mean±SEM	Mean±SEM	p
Litter size	10.2±1.4	12.6±0.9	12.4±0.8	0.24
Birthweight (g)	6.9±0.1	6.7±0.2	6.6±0.3	0.79
% males per litter	48±11	29±3	49±4	0.11
Days to plug	5.3±1.2	3.2±0.2	3.5±0.7	0.14
Gestation	22.8±0.2	22.5±0.2	22.6±0.2	0.64

Table 4.3 Demographics of F1 litters born to rats exposed to CD or HFD.

There was a significant difference between the growth trajectories of the F1 offspring ($p<0.001$) with the principal differences occurring between male and female offspring of mothers who had consumed the HFD, when compared to F1 animals in the control arm, and, the female offspring of males who had consumed the HFD, with differences significant from 60 days (Figure 4.4). Bodyweight at sacrifice was significantly increased for male (10% heavier) and female (7% heavier) F1 offspring born to mothers consuming a high fat diet ($p<0.001$) (Figure 4.4 and Table 4.4). Despite these differences in bodyweights, there was no significant difference in adiposity, the weight of fat pads, or plasma leptin in these F1 rats (Table 4.4). There was also no difference according to parental diet in plasma glucose or insulin during OGTT (Table 4.4 and Figure 4.4). Plasma testosterone was elevated in the sons of mothers who consumed a HFD ($p=0.02$) (Table 4.4).

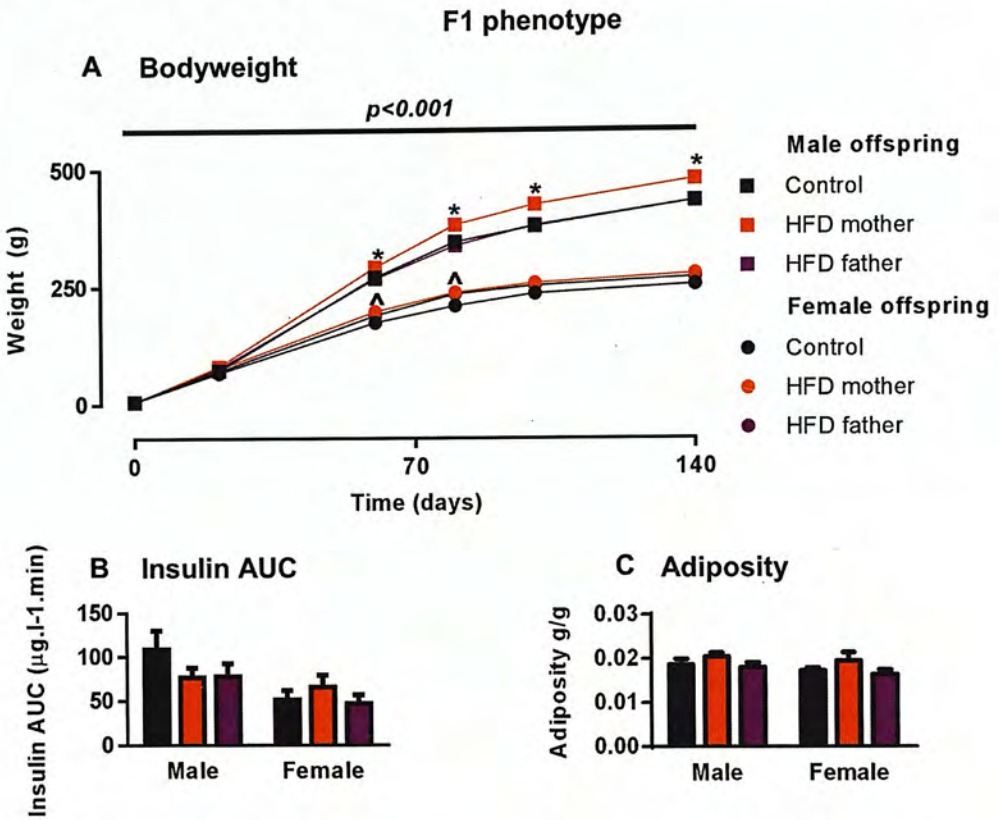

Figure 4.4 Phenotyping of F1 offspring according to parental diet. A: Bodyweight of F1 rats from birth to sacrifice. Squares are males and circles females. Analysis was by linear mixed model with group and sex as fixed factors and litter as a random factor; N= Males: Control (19), maternal HFD (19), paternal HFD (17), from 5-9 litters and females: control (18) Maternal HFD (20) and Paternal HFD (21) from 5-9 litters. **B**: Insulin AUC calculated following an oral glucose tolerance test; N= Male: control (5), Maternal HFD (5), Paternal HFD (6), Females: control (6) maternal HFD (5) paternal HFD (5) from 5-6 litters (Non-significant by mixed linear model with group and sex as fixed factors). **C**: Adiposity calculated as the sum of gonadal and retroperitoneal adipose pads/bodyweight; N= Males: Control (31) maternal HFD (18), paternal HFD (17) 17-31 from 5-6 litters and females: control (15) maternal HFD (14) paternal HFD (17) from 5-6 litters. (Non-significant by linear mixed model with group and sex as fixed factors and litter as random factor). Data are mean ±SEM.

Sex	Male			Female			
Group	Control	Maternal HFD	Paternal HFD	Control	Maternal HFD	Paternal HFD	p
N (litters)	19-32 (9)	13-19 (5)	10-17 (5)	10-17 (9)	14-20 (5)	13-21 (5)	
	Mean± SEM	Mean± SEM	Mean± SEM	Mean± SEM	Mean± SEM	Mean± SEM	group* sex
Body size							
Weight (g)	434±4	**478±10**	432±8	260±5	278±5	270±4	**0.003**
Length (cm)	23.8±0.2	24.1±0.3	23.5±0.3	21.2±0.2	21.1±0.2	21.2±0.2	0.114
AGD (mm)	47±0.5	46±2.2	45±0.8	21±0.3	19±0.8	19±0.8	0.945
Adiposity							
Gonadal fat/bodyweight (mg/g)	7.7±0.3	7.5±0.3	6.7±0.4	6.3±0.3	7.2±0.7	6.3±0.5	0.062
Retroperitoneal fat/ bodyweight (mg/g)	5.2±0.3	5.0±0.4	4.5±0.4	5.1±0.3	4.9±0.6	3.7±0.3	0.177
Adiposity index (mg/g)	12.9±0.6	12.6±0.7	11.2±0.7	11.4±0.5	12.1±1.2	10.0±0.7	0.062
Biochemistry							
Leptin (ng/ml)	1.3±0.3	1.7±0.5	0.9±0.1				0.346^
Insulin AUC µg/l.min	107±22	77±11	78±15	51±10	66±13	47±10	0.249
Glucose AUC mM.min	984±32	931±37	951±39	931±37	938±24	904±73	0.846
Reproduction							
Penis length (mm)	12.1±0.1	**11.8±0.2**	**11.7±0.2**				**0.023^***
Gonad weight (g)	1.9±0.02	2.0±0.07	1.9±0.07	0.08±0.00	0.08±0.00	0.12±0.02	0.148
Testosterone (ng/ml)	4.2±0.6	**7.4±0.9**	2.7±0.5				**0.020^**

Table 4.4 Phenotyping of F1 offspring according to parental diet. Data taken from post-mortem dissection and measurement of organs at 19 weeks of age. Biochemical data derives from 09.00 fasting plasma obtained during glucose tolerance testing at 17 weeks of age. Data was analysed by linear mixed model with group and sex as fixed factors and litter as a random factor, with post hoc Bonferroni analysis comparing groups within each sex. Values shown in **bold indicates** $p<0.05$. * indicates significantly different only with least significant

difference analysis (not taking multiple testing into account). ^ indicates sex not used as a fixed factor as data only available for males.

4.3.3 Grand-paternal diet affects metabolic physiology of F2 offspring in a parent- and sex-specific manner

There was no difference in litter size, percentage of males per litter or birth weights of pups that were the grand-offspring of CD or HFD fed rats (Table 4.5. However, by 9 weeks of age, the male offspring whose maternal grandfather consumed a HFD were significantly heavier, a trend that continued until sacrifice when they were 7.7% heavier than the grand-offspring of rats fed CD ($p<0.001$)(Figure 4.5).

	Control	Maternal Grandfather	Maternal Grandmother	Paternal Grandfather	Paternal Grandmother	
Litters	7	4	4	5	5	
	Mean±SEM	Mean±SEM	Mean±SEM	Mean±SEM	Mean±SEM	p
Birthweight (g)	6.9±0.2	6.9±0.4	6.9±0.3	7.1±0.3	6.9±0.2	0.986
% male pups	46.5±2.8	58.2±4.0	46.0±5.6	55.0±8.4	58.6±7.6	0.384
Litter size	12.6±0.5	12.5±1.7	12.3±1.5	11.8±0.6	11.2±2.1	0.934

Table 4.5 Demographics of F2 litters according to grandparental HFD exposure. All other animals were maintained on CD.

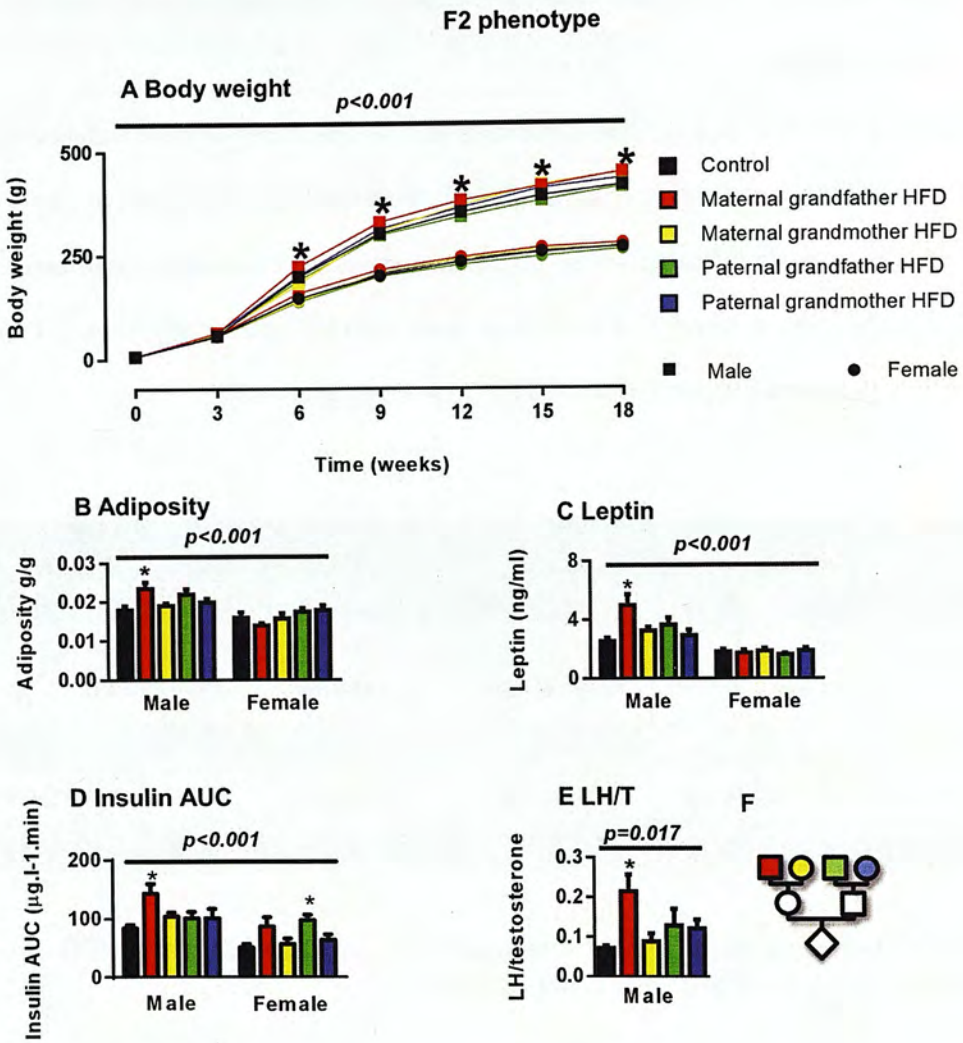

Figure 4.5 Phenotyping of F2 rats according to grandparental HFD exposure. A: Bodyweight of F2 offspring from birth to 18 weeks of age. Squares males, circles females. Colours denote the diet of grandparents as shown in the key in panel A. Analysis was by linear mixed model with sex and group as fixed factors, time as a repeated factor and litter as a random factor, with post hoc Bonferroni analysis. **B**: Adiposity calculated as the sum of adipose pads/bodyweight. **C**: Plasma leptin. **D**: Insulin AUC, calculated following an oral glucose tolerance test. **E**: Plasma LH to testosterone ratio. Analysis was by linear mixed model with sex and group as fixed factors and litter as a random factor with Bonferroni post hoc test (B, C and D) or least significant difference post hoc test (C). **F**: Pedigree of the different F2 offspring, each colour showing which grandparent consumed the HFD. N= Males: Control (14), maternal grandfather (8), maternal grandmother (8), paternal grandfather (10), and paternal grandmother (10). Females: Control (14), maternal

grandfather (8), maternal grandfather (8), paternal grandmother (10) and paternal grandfather (9) from 4-7 litters. Data are mean ±SEM.

	Male					Female					
	Control	Maternal grandfather	Maternal grandmother	Paternal grandfather	Paternal grandmother	Control	Maternal grandfather	Maternal grandmother	Paternal grandfather	Paternal grandmother	p
N (litters)	14 (7)	8 (4)	8 (4)	8 (4)	10 (5)	14 (7)	8 (4)	8 (4)	8 (4)	10 (5)	
	Mean± SEM	Mean± SEM	Mean± SEM	Mean± SEM	Mean± SEM	Mean± SEM	Mean± SEM	Mean± SEM	Mean± SEM	Mean± SEM	group* sex
Body size											
Weight (g)	416±5	448±13	446±9	412±11	433±10	268±8	277±5	269±8	262±6	271±5	0.124
Length (cm)	23.3±0.1	23.5±0.2	23.5±0.2	22.8±0.1	23.4±0.2	21.1±0.2	20.9±0.1	21.0±0.2	20.7±0.2	21.1±0.2	0.613
Organ weights											
Liver/ bw (mg/g)	43.2±0.8	40.8±0.5	42.3±1.4	42.8±1.2	44.4±1.4	38.9±0.9	37.0±1.5	34.3±1.5	38.4±1.4	37.6±1.1	0.240
Pancreas/ bw (mg/g)	2.6±0.1	2.4±0.2	2.1±0.1	2.3±0.1	2.2±0.1	3.5±0.1	3.5±0.2	3.8±0.4	4.0±0.2	3.0±0.2	**0.007**
Adiposity											
Retroperitoneal fat/ bw (mg/g)	4.8±0.4	**6.6±0.5**	5.1±.4	6.3±0.5	6.1±0.4	4.1±0.5	3.6±0.2	3.9±0.7	4.9±0.3	5.2±0.3	**0.003**
Gonadal fat/ bw (mg/g)	6.6±0.3	**8.4±0.6**	7.0±0.2	**7.9±0.5**	6.9±0.4	5.9±0.5	5.2±0.3	5.9±0.4	6.3±0.4	6.3±0.5	**0.017***
Adiposity index (mg/g)	18.0±1.0	**23.4±1.7**	19.0±0.7	22.0±1.3	19.9±1.0	16.0±1.3	14.0±0.6	15.7±1.3	17.4±0.9	17.8±1.2	**0.012**

	Male					Female					
	Control	Maternal grandfather	Maternal grandmother	Paternal grandfather	Paternal grandmother	Control	Maternal grandfather	Maternal grandmother	Paternal grandfather	Paternal grandmother	p
N (litters)	14 (7)	8 (4)	8 (4)	8 (4)	10 (5)	14 (7)	8 (4)	8 (4)	8 (4)	10 (5)	
	Mean± SEM	Mean± SEM	Mean± SEM	Mean± SEM	Mean± SEM	Mean± SEM	Mean± SEM	Mean± SEM	Mean± SEM	Mean± SEM	group* sex
Biochemistry											
Insulin AUC (µg/l.min)	90±11	**149±18**	104±7	119±13	129±19	60±7	86±16	48±3	103±8	72±12	**0.016***
Glucose AUC (mM.min)	964±19	904±7	947±37	954±11	966±6	947±24	931±19	921±28	1146±13	978±9	0.150
Leptin (ng/ml)	2.5±0.3	**5.0±0.8**	3.3±0.2	3.6±0.5	2.9±0.4	1.8±0.2	1.7±0.2	1.9±0.2	1.6±0.1	1.9±0.2	**0.001**
Cholesterol (mM)	1.1±0.03	1.2±0.05	1.0±0.07	1.2±0.05	1.0±0.04	1.0±0.04	1.1±0.08	1.1±0.06	1.3±0.06	1.1±0.07	0.474
Triglycerides (mM)	1.1±0.05	1.3±0.19	1.5±0.13	1.2±0.10	1.3±0.12	0.8±0.05	0.8±0.04	1.2±0.12	0.8±0.07	1.1±0.13	0.106
Reproduction											
LH (ng/ml)	0.6±0.1	1.2±0.2	0.7±0.7	1.0±0.2	1.0±0.2						0.250 ^
Testosterone (ng/ml)	8.5±0.5	6.1±0.8	8.6±1.4	8.7±1.4	7.80±0.6						0.270 ^
LH to T ratio	0.1±0.0	**0.2±0.0**	0.1±0.0	0.1±0.0	0.1±0.0						**0.01^**

	Male					Female					
	Control	Maternal grandfather	Maternal grandmother	Paternal grandfather	Paternal grandmother	Control	Maternal grandfather	Maternal grandmother	Paternal grandfather	Paternal grandmother	p
N (litters)	14 (7)	8 (4)	8 (4)	8 (4)	10 (5)	14 (7)	8 (4)	8 (4)	8 (4)	10 (5)	
	Mean± SEM	Mean± SEM	Mean± SEM	Mean± SEM	Mean± SEM	Mean± SEM	Mean± SEM	Mean± SEM	Mean± SEM	Mean± SEM	group* sex
Penis Length (mm)	12.1±0.1	12.3±0.2	12.5±0.2	12.3±0.2	12.3±0.1						0.61^
Sperm count x10^6	6.0±12	36.3±7.5	22.4±7.3	33.2±8.8	23.3±7.7						0.629
AGD (mm)	48.6±0.7	49.5±0.9	49.9±1.1	47.8±0.8	50.9±0.6	21.3±0.5	23.1±0.2	21.7±0.4	22.4±0.4	22.7±0.4	0.121

Table 4.6 Phenotyping of F2 offspring according to grandparental HFD exposure. (Previous page) Data was taken from post-mortem dissection and measurement of organs at 19 weeks of age. Biochemical data was derived from 09.00 fasting plasma obtained during glucose tolerance testing at 17 weeks of age. Data was analysed by linear mixed model with group and sex as fixed factors and litter as a random factor with post hoc Bonferroni analysis comparing groups within each sex; values that are significantly different ($p<0.05$) are shown in **bold**. * indicates different only with least significant difference analysis (not taking multiple testing into account). ^ indicates sex not used as a fixed factor as data only available for males, bw bodyweight.

At sacrifice, the adiposity index of the F2 male rats whose maternal grandfather consumed a HFD was 31% greater than F2 male animals from the control arm of the study $p=0.01$ (Figure 4.5). This increased adiposity was associated with a 97% increase in plasma leptin $p<0.001$ (Figure 4.5). In the same animals, there was also decreased insulin sensitivity during the glucose tolerance test with insulin area under the curve increasing by ~70% following an oral glucose challenge $p<0.001$ (although significance was lost when taking into account multiple testing) (Figure 4.5).

There was a significant increase ($p=0.017$) in the LH to testosterone ratio in the males whose maternal grandfather consumed the HFD, implying compensated Leydig Cell failure. There was no difference in sperm count, which was highly variable between individuals within each group and litter (Table 4.6).

In female F2 animals no difference was found in terms of weight, adiposity or size of organs in animals whose grandfather or grandmother consumed a HFD, when compared to control animals (Table 4.6). There was however an increase in the insulin AUC ($p<0.001$) following an oral glucose tolerance test in the group whose paternal grandfather had consumed the HFD (Figure 4.5).

4.4 Discussion

In the present study, F0 male and female rats were, respectively, 9·7% and 14·7% heavier after 14 weeks' HFD, with a 33·3% increase in visceral adiposity. F1 male and female offspring off HFD mothers were heavier than controls. F1 daughters of HFD fathers were also heavier than controls. F2 male offspring whose maternal grandfather had consumed the HFD were 7·7% heavier, exhibited a 31% increase in visceral adiposity, a 97% increase in plasma leptin, 70% increased insulin secretion in response to an oral glucose challenge and a 3 fold increase in the luteinising hormone to testosterone ratio. The findings are summarised in Figure 4.6.

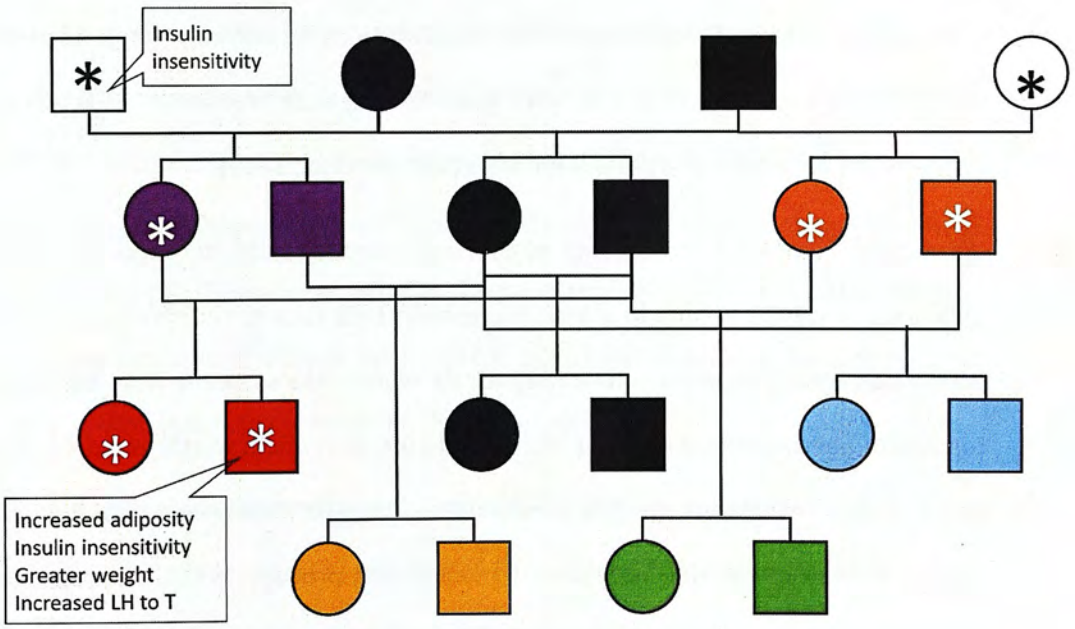

Figure 4.6 Summary of phenotyping findings Squares represent males and circles females. Asterisk refers to significant increases in weight gain compared to control (in black). In the F0 black represent CD and white HFD.

The findings are discussed below in the context of the current literature, and the relevance to humans.

4.4.1 Effects of HFD on the F0 (founding) generation

Exposure from weaning to a 45% HFD for 14 weeks induced modest weight gain in male and female rats, and in the males, there was the development of impaired insulin sensitivity without alteration to glucose levels. Comparison of weight gain between rodent and humans is difficult, especially as rats continue to grow in length following puberty, meaning BMI may not be a useful comparator. Body length itself was not affected by the dietary interventions (Table 4.2), and the adiposity index, independent of length, is a useful means of determining the cause for the increase in bodyweight. Rat 'BMI' has been demonstrated in one study to correlate with increased carcass fat and serum triglyceride concentrations suggesting the measurement may have some comparative value (Novelli et al., 2007). Assessment of adiposity may have more accurate had a technique such as NMR (nuclear magnetic resonance) or DEXA (duel energy x-ray absorptiometry) been employed (Miller et al., 2011).

As show in Figure 4.7, for humans, as BMI and weight are directly proportional, each 10% gain in weight results in a 10% increase in BMI, thus to put this weight gain in proportion with humans, a ~20% weight gain would take someone from being at the top end of normal weight to being 'obese' and 30% increase in weight required to take one from 'overweight' to 'morbid obesity'. Thus the ~10-15% weight gain seen in the rats as a result of the HFD is relatively modest, and probably would not constitute a model of developing 'obesity' in humans. When considering that 25.6% of the Scottish population are obese (Scottish health survey, 2013) (i.e. 30% heavier than would be advised), the potential implications for future generations are potentially concerning.

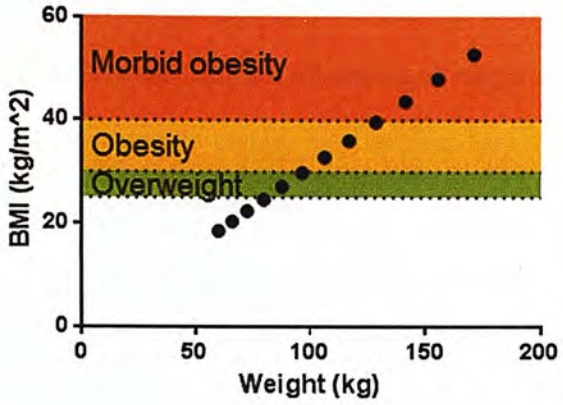

Figure 4.7 Impact of 10% increases in bodyweight on BMI in humans.
Each 10% interval increases. BMI by 10%, thus a 20% increase in bodyweight would take someone from normal weight to obese, and a 30% increase in bodyweight from overweight to morbid obesity.

It is difficult to compare the dietary intervention studies between rodents and humans. There is evidence from studies in humans that covert manipulation of fat content (from 20 to 60%) in a meal does not alter food preference or the quantity of food consumed, (although increased consumption of the fatty food was described in humans with MC4R mutations) (van der Klaauw et al., 2015). Moreover, supplementation of a standardised diet with increasing quantities of fat results in only modest gains in weight over the course of 50 days in healthy individuals (Kasper et al., 1973).

One should also be cautious when extrapolating the studies in rodents to humans, as metabolism is very different between species (Bergen and Mersmann, 2005), and even within rodent models, there is considerable variation between strains. For example, in mice C57BL/6 are generally considered obesity prone whereas the A/J strain are more often obesity resistant (West et al., 1992, 1995). The same can be said for rat strains: Osborne-Mendel rats acquire greater adiposity as a result of HFD than do S 5B/PL rats (Nilsson et al., 2012; Schemmel et al., 1972). Responsiveness to HFD might be a genetic trait, for example affecting appetite signalling (Kappeler et al., 2004). However, in

mouse experiments, despite weight gain in response to HFD, no difference in food consumption was found, suggesting altered metabolism as the cause (West et al., 1992).

Mouse studies in which male C57BL/6 mice were fed a similar 45% fat diet resulted in a 14.9% weight gain in comparison to mice fed on a control diet with 21% of energy available from lipids (Fullston et al., 2012, 2013). In a study in which adult male rats were fed for 12 weeks on a similar 45% HFD as in the present studies, or a matched 10% fat CD, a 23% increase in body weight was noted after HFD exposure (Li et al., 2005a), whilst another study found that 12 weeks HFD resulted in a more overt 28% weight gain, and associated glucose intolerance, although the contents of the intervention diet are not clear (Ng et al., 2010).

Thus, in the presented study, the modest 9.7-14.7% increase in weight following 14 weeks consumption of a 45% diet is consistent with mouse studies (Fullston et al., 2012, 2013), but the weight gain was generally lower than that observed in other rat models (Li et al., 2005a; Ng et al., 2010).

4.4.2 Effects of maternal HFD

As reviewed in Chapter 1, multiple models of maternal HFD exposure pre-pregnancy, during pregnancy and during lactation have been shown to cause reprogramming effects on offspring, although not with absolute consistency. As shown in Table 1.2, some studies, show increased weight gain in offspring following maternal exposure to HFD (Bellisario et al., 2014; Cheong et al., 2014; Sanders et al., 2014) whilst others find no change (Brenseke et al., 2015; Desai et al., 2014; King et al., 2013b; Laker et al., 2014; Vogt et al., 2014). In other studies, significant differences between offspring can often only be teased out when re-challenging offspring with a HFD, to which they seem in general to be more susceptible (Vogt et al., 2014). The inconsistency in the literature makes it difficult to form definite conclusions as to the effect of maternal/*in utero* HFD

exposure. Discrepancies could be said to be strain specific, although many of the reported studies use C57BL/6 mice but remain inconsistent in outcome. It is interesting to note, with respect to dietary intervention, that there is a trend for mid-range HFDs (30-45%) rather than very high fat (~60%) being more likely to result in a programmed weight gain effect in offspring, a trend recapitulated in the study from Platt *et al.* in which six different diets were used, and where it was the 32% rather than 60% (or 10% control) diet that resulted in programming of weight gain in female offspring (Platt et al., 2014).

It may also be that other factors play a role, for example stress around the rodents may impact upon appetite and weight gain (Levine and Morley, 1981; Pecoraro et al., 2004), and the environment around previous generations may potentially mask results as discussed in 1.2.2.

Impaired glucose homeostasis in the offspring of mothers exposed to HFD has also been described extensively in the literature, although again with inconsistency. For example, sons having worse glucose tolerance than daughters (Yokomizo et al., 2014), or daughters more affected than sons (Dearden and Balthasar, 2014) after maternal HFD exposure (see (Williams et al., 2014) for review). In the present study, no difference was found in the glucose tolerance of the offspring whose mothers were exposed to HFD from weaning.

4.4.3 Effects of paternal HFD

The effects of paternal experimental exposure to HFD in mammals has been investigated in both mice and rats by two laboratories. In rats, paternal HFD exposure caused ~28% weight gain and resulted in offspring with impaired β-cell function and impaired glucose tolerance in female offspring but no change in weight gain (Ng et al.,

2010). In mice, paternal HFD resulting in a 14.9% increase in bodyweight resulted in 8% increased bodyweight and 80% increased adiposity in females and a 6% increase in bodyweight in males with no effect on adiposity (Fullston et al., 2013). This matches the results seen in the present studies, in which the only effect of paternal HFD was on weight gain in female offspring. However, in contrast to the cited mouse/rat studies, no change in adiposity or glucose tolerance in offspring was observed in the present studies.

Human studies that have investigated the relative impact of maternal and paternal BMI on offspring find both may play a role (Patro et al., 2013). In studies in which the data presented allows the impact of maternal or paternal obesity on male and female offspring to be assessed separately, the biggest impact on obesity in offspring at age 16 years was between a father and his daughter (odds ratio of 5.58 (CI 3.09-10.07))(Jääskeläinen et al., 2011). However, in this study, offspring were exposed post-natally to a potentially obesogenic environment, which is a strong confounding factor.

4.4.4 Effects of grand-paternal HFD

Two previous studies have investigated the effect of grand-paternal HFD exposure in a mouse model. Both showed increased adiposity and impaired glucose tolerance in grandsons, but only via the maternal grandfather; there were no effects via the paternal grandfather or in females, matching the present data in rats (Fullston et al., 2012, 2013). In contrast, human epidemiological data from Överkalix found that it was replete nutrition around the paternal grandfather during puberty that had the most significant impact on mortality and risk of cardiovascular disease in male grandchildren (Pembrey et al., 2006). The transmission of impaired glucose tolerance via HFD exposure in the paternal grandsire in a mouse model has also been reported,

although the effect of the maternal grandfather was not investigated (Grandjean et al., 2014 (abstract)), thus the mode of transmission is not clear, and there remains evidence for transmission from both grandfathers.

In the F2 males derived from HFD-exposed maternal grandfathers in the present studies, an increased secretion of insulin in response to glucose was observed, although there were no significant changes in plasma glucose from controls. This suggests impaired insulin sensitivity. The optimal way to assess this would be via insulin tolerance testing, or hyperinsulinaemic-euglycaemic clamp (Kim, 2009), although these methods would cause more distress to the subjects. It may be that with a more sensitive technique, clearer differences between the groups would have been found.

An increased LH to testosterone ratio was also found in the F2 grand-offspring whose maternal grandfather was exposed to the HFD. An elevated LH in response to a subtle reduction in plasma testosterone implies compensated Leydig cell failure, a phenomenon that has been reported in ~10% of aging men (Tajar et al., 2010) and in younger men with low sperm counts (Andersson et al., 2004). Hypogonadism is associated with adverse metabolic health, and although some trials show that testosterone replacement in hypogonadal men can improve insulin sensitivity (Jones et al., 2011) they do not show overall improvement in glycaemic control (Basaria, 2014; Jones et al., 2011). Although there is a clear association between metabolic syndrome and hypogonadism, the causality remains unclear (Allen et al., 2000; Jones et al., 2011; Naifar et al., 2015; Tanna et al., 2015). Testosterone production in adult life can be programmed by effects on adult Leydig stem cells *in utero*, suggesting that testosterone production in adulthood could be programmed in the present model and may contribute to the phenotype observed (Kilcoyne et al., 2014). The presented experimental paradigm does not however allow for causality to be interpreted.

4.4.5 Effects of grand-maternal HFD

Grand-maternal exposure to HFD has been investigated previously in mice: Grand-maternal HFD via the father results in reduced insulin sensitivity in male and female mice (Dunn and Bale, 2009). This effect was also noted in the F1 male offspring, potentially indicating direct transmission (Dunn and Bale, 2009). Maternal exposure to HFD *in utero* also results in increased insulin production in response to glucose challenge in male F2 offspring (King et al., 2013b), independent of F1 phenotype. No changes were observed in the F2 female offspring of the present study. Differences between studies and potential explanations are discussed below.

4.4.6 Differences between studies

Whilst there are some consistencies in the literature, not all experiments find the same outcomes in offspring and grand-offspring following exposure to HFD. Some potential explanations include:

- The strain/species used and if inbred or outbred (as discussed in 4.4.1)
- Composition of diet (see 4.4.1)
- Timing of the dietary intervention (see 1.2.2.2)
- The age and condition of the 'control' mates and if they were virgin (Symonds et al., 2004)
- Environmental stress (Levine and Morley, 1981; Pecoraro et al., 2004)
- The sex of the technician, resulting in altered stress levels (Sorge et al., 2014)
- Soya in the diet (Cederroth et al., 2010; Napier et al., 2014)

Every effort was made to control for these potential confounders in the present study, and where comparisons have been made to the literature above, potential differences have been suggested.

4.4.7 Conclusion

The data in this chapter indicate that grandparental HFD exposure can alter the metabolic phenotype of grand-offspring in a sex-specific and grandparent of origin manner. Thus, further evidence that the environment around our ancestors may impact on our health is presented. Some potential mechanisms for the intergenerational inheritance are explored in Chapter 5.

5 Investigation of germ cell transcriptome following HFD exposure

5.1 Introduction

In Chapter 4 increased adiposity and reduced insulin sensitivity were found in the male grand-offspring of males fed a HFD. The mechanism resulting in this transmission of phenotype is investigated in the present chapter.

Several hypotheses have been put forward to suggest how the transmission of phenotype may occur. Evidence from experimental studies is presented in section 1.2.2 and summarised in Table 5.1.

Table 5.1 Studies in which associations with intergenerational programming and a biological factor have been identified.

Proposed Mechanism	Model	Ref
Cytosine methylation	Maternal protein restriction	(Radford et al., 2014)
	Paternal protein restriction	(Carone et al., 2010)
Histone modification	Paternal protein restriction	(Carone et al., 2010)
	Paternal high sugar diet	(Öst et al., 2014)
miRNA	Paternal stress	(Gapp et al., 2014)
	Paternal HFD	(Fullston et al., 2013)
Seminal fluid	Seminal vesectomy	(Bromfield et al., 2014)
	High sugar diet	(Crean et al., 2014)
	Paternal high fat diet	(Binder et al., 2015)
Behaviour	Preferred mate	(Drickamer et al., 2000)

To investigate if the HFD had induced changes in the germline, the transcriptome was evaluated. The following narrative describes the effects of 14 weeks CD or HFD on the germ cell transcriptome.

5.2 Methods

5.2.1 RNA extraction

$6x10^6$ FACS sorted cells were centrifuged for 5min at 500xg and RNA immediately extracted using the Qiagen miRNeasy mini kit (Qiagen, UK) according to the manufacturer's instructions, with lysis carried out by vortexing for 20 seconds and passage through a 22g needle and DNase treatment.

5.2.2 RNA sequencing

Quality and purity of the extracted total RNA was verified using spectrophotometry and the Agilent RNA 6000 nano kit according to manufacturer's instructions before sequencing smRNA and RNA using Illumina HiSeq2500. Intended library size for total RNA was 37.5 million single end reads of 125bp and for small RNA was 20 million single end reads of 50bp. Sequencing was carried out by Edinburgh genomics, University of Edinburgh.

5.2.3 Bioinformatics

Quality of the sequencing was verified using FastQC (Babraham Bioinformatics, UK). Adaptor contamination was removed from the smRNA-seq libraries using trimmomatic (Bolger et al., 2014). SmRNA-seq reads were aligned to the *Rattus norvegicus* genome version rn5 using Butter with default parameters (Axtell, 2014). Differential expression was determined using DESeq2 (Love et al., 2014). RNA-seq libraries were aligned to Rn5 using Star v2.3.0 (Dobin et al., 2013), on a custom-built splice junctions database based on Rn5 ensembl73 protein-coding annotations, with the maximum proportion of mismatches over the read length of 0.05 and minimum mapping read length of 125nts. Bioinformatic analysis was conducted by Dr. Michael Morgan (Computational Genomics and Training, University of Oxford).

5.2.4 Sample clustering and principal components analysis

Variance stabilising transformed (VST) read counts for protein-coding genes, miRNAs, repeats and piRNAs were calculated using DESeq2 (Love et al., 2014). Between-sample Pearson correlations (r) were calculated using VST counts and used to hierarchically cluster samples using average linkage clustering, with distances defined as 1 - | r |. Principal components analysis (PCA) was performed on scaled and centred VST counts using the R *prcomp* function. Sample clustering was visualised using the R *gplots* package function *heatmap.2*, and PCA results were plotted using the R grammar of graphics package, *ggplot2*.

5.2.5 Differential expression testing

Uniquely aligned reads were counted over rn5 genomic annotations for protein-coding genes (ensemble v73), miRBase- miRNAs (Kozomara and Griffiths-Jones, 2014), piRNAQuest- piRNAs (Sarkar et al., 2014) and repBase repeat classes (Jurka et al., 2005)) using featureCounts (Liao et al., 2013). Genomic annotations with a mean read count <1 across all samples were excluded from analysis. This resulted in the differential expression testing of 18,025 protein-coding genes, 285 miRNAs, 7390 piRNA annotations and 522 repeat classes. Statistical testing was carried out separately for protein-coding genes, miRNAs, piRNAs and repeat elements. Differential expression testing was performed using a negative binomial general linear model, regressing genomic annotations read counts on diet, adjusted for library size, and implemented in the Bioconductor package DESeq2 (Love et al., 2014). P-values were calculated based on the Bayesian shrinkage moderated $\log_2$ fold changes by a Wald test with H_0: $\log_2$ fold change = 0, H_A: log2 fold change $\neq$ 0. P-values were then adjusted for multiple testing using the procedure of Benjamini & Hochberg (Benjamini and Hochberg, 1995). Genomic annotations with an adjusted p-value <0.05 were considered to be significantly differentially expressed.

5.2.6 *In silico* spike-in analysis

Evaluation of statistical power was determined using an *in silico* spike-in experiment. Read counts across genomic annotations were randomly shuffled to generate a pseudo-data set of read counts, preserving the experimental design, i.e. counts were shuffled between different genes, but not different treatment groups. Shuffled annotations were retained if $|\log_2 \text{fold change}| \leq 0.6$, to reflect the observations in the experimental data. This spike-in counts table was then used as input into the same differential expression testing procedure described above.

5.2.7 Comparison with Rat body map data

5.2.8 qPCR

qPCR was conducted using the Taqman method (section 2.4.4.2). Three of the most stably expressed genes were assessed across both treatments and 2 cohorts to select appropriate housekeeping genes. The best house keepers were assessed using normfinder (Andersen et al., 2004). Primers used are shown in Table 5.1.

Gene	Forward	Reverse	UPL probe
Ldha	gatctcgcgcacgctact	cacaatcagctggtccttgag	121
Ropn1L	catcctcaagcagttcacca	tacgggaagtgggtctcct	121
Sh3glb1	cgccctgaaggagataacatt	aattcctgttcagattttgtcactt	113
Col3a1	tcccctggaatctgtgaatc	tgagtcgaattggggagaat	49
Decorin	ctccgagtggtgcagtgtt	gcaatgttgtgtcaggtgga	73
Gelsolin	ctggccaagctctacaaggt	agccacgagggagactgac	16

Vasa	cattcagaagaggtgggagaga	tgctggtttcctagaaccaaa	77
Cdkn1b	agacagtccggctgggtta	ttctgttctgttggcccttt	130
Sox9	atcttcaaggcgctgcaa	cggtggaccctgagattg	63
3bHSD	gaccagaaaccaaggaggaa	ctggcacgctctcctcag	105

Table 5.2 Primers for validation of purity of germ cells and sequencing.

5.2.8.1 miRNA qPCR

miRNA quantification was conducted using the miRCURY system (Applied Biosystems, UK). RNA was reverse transcribed with the custom reverse transcription kit according to the manufacturers' instructions with 10ng RNA per each 15µl reaction. This step applies 'barcode' cDNA to the reverse transcript in order that it is sufficiently long to allow for primer design. The resultant RT product then underwent PCR with the appropriate primers as per manufacturers' instructions. PCR was conducted as per section 2.4.2.2 snoRNA was used as a reference control smallRNA.

5.3 Results

5.3.1 Validation of the purity of FACS-sorted germ cells

In order to assess the purity of sorted germ cells, qPCR was conducted for germ cell (Vasa), Sertoli cell (Cdkn1b, Sox9), and Leydig cell (3βHSD) specific genes. Cells were enriched for those expressing *Vasa*, but had reduced relative expression of *Cdkn1b*, *Sox9* and *3βHSD*, confirming a strong enrichment for germ cells (Figure 5.1).

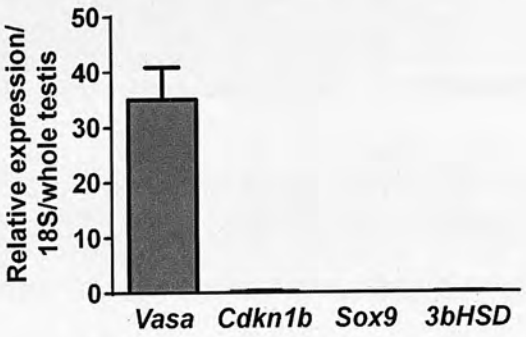

Figure 5.1 Assessment of the purity of FACS purified germ cells by qPCR. qPCR for germ cell (*Vasa*), Sertoli cell (*Cdkn1b and Sox9*) and Leydig cell (*3ϐHSD*) specific genes on RNA extracted from FACS purified germ cells. Data is expressed relative to RNA from whole testis. Data are mean ± SEM, n=4.

5.3.2 Expression of protein coding RNA

5.0-9.0x10^7 reads per animal were obtained for total RNA sequencing. Following alignment, clustering (Figure 5.2A) and PCA (Figure 5.2B) analysis demonstrated remarkable homogeneity between samples. Differential expression analysis found only three genes with significantly reduced expression (Figure 5.2C and Table 5.3). Validation of these findings was conducted by PCR on an independent set of samples collected from similarly exposed animals. Although all of the genes followed the trend for reduced expression when validated across two cohorts of animals, none of the expression changes reached statistical significance (Figure 5.2D).

5.3.2.1 Protein coding genes with differential expression

Expression of *Gelsolin*, *Collagen 3a1* and *Decorin* was reduced in the germ cells from animals consuming HFD when assessed by RNA-seq. Although these genes failed to validate by qPCR, they are discussed briefly below.

Gelsolin binds to the end of actin filaments to prevent monomer exchange, thus plays a role in the assembly and disassembly of the structures (Yin and Stossel, 1979), has a neuroprotective effect against oxygen and glucose deprivation (Meisel et al., 2006) and

is regulated epigenetically (by both cytosine methylation and heterochromatin marks) in neurones (Meisel et al., 2006) and breast cancer cells (Mielnicki et al., 1999).

Mutation of collagen3a1 is associated with vascular Ehlers-Danlos Syndrome (Frank et al., 2015). Sprague Dawley rats fed a high fat diet had reduced expression of *Col3a1* in heart but increased expression in kidney where it is hypothesised to play a role in diabetic nephropathy (Gaikwad et al., 2010). Nephropathy was also associated with increased COL3A1 expression in glomeruli, findings associated with a switch in the ratio of H3K27me and H3K4me3 at the promoter and, increased expression of both Suv39h1 and Ezh2 expression, perhaps suggesting altered balance of transcription of a 'poised' gene (Abrass et al., 2011).

Decorin is an imprinted gene which is maternally expressed in the placenta in the mouse (Mizuno et al., 2002) but appears to be biallelically expressed in humans (Monk et al., 2006). Mouse mutants of *decorin* have an Ehlers-Danlos type phenotype although no human mutations associated with the syndrome have been identified to date (Malfait and De Paepe, 2005). Reduced *DECORIN* expression is associated with inflammation related premature rupture of membranes and pre-term birth (Horgan et al., 2014).

Despite the identified changes in the RNA-seq data these genes did not show altered expression in the qPCR validation and thus interpretation of the results should be cautious. Altered expression may indicate a change to the epigenetic landscape of the germ cells, which could impact upon subsequent generations. It seems unlikely that altered expression of these genes in the germ line directly affects outcomes in offspring or grand-offspring.

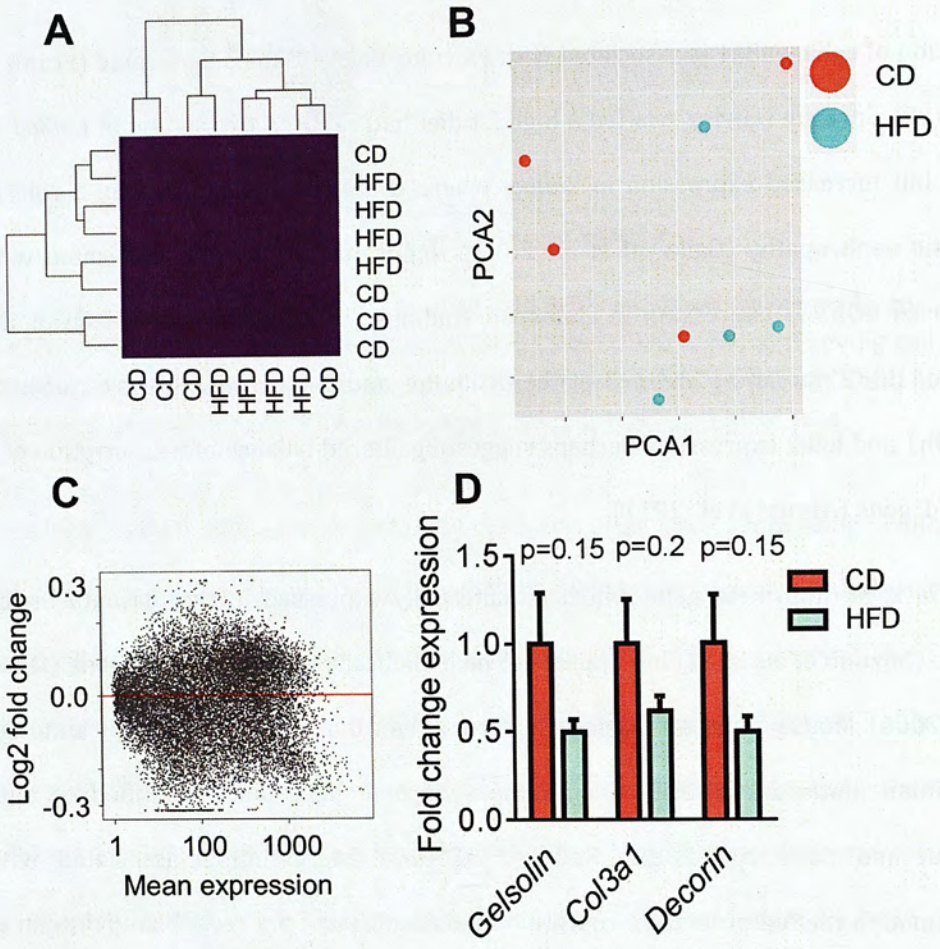

Figure 5.2 Analysis of protein coding genes following RNA-seq of RNA extracted from germ cells exposed to CD or HFD for 14 weeks. A. Clustering analysis of protein coding genes. **B.** PCA analysis comparing protein coding genes from animals consuming CD or HFD. **C.** Differential expression analysis from germ cells extracted from n=4 animals following consumption of CD or HFD for 14 weeks. **D.** qPCR analysis of the top three differentially expressed genes. Data expressed relative to Ropn1L and LDHA and are from n=9-11 animals from 2 cohorts.

Gene	Log_2 fold change	Log_2 fold change SE	p	p adj
Col3a1	-0.706	0.127	2.76×10^{-8}	0.0004
Gelsolin	-0.588	0.125	2.70×10^{-6}	0.0201
Decorin	-0.575	0.128	7.26×10^{-6}	0.0370
AnnexinA1	-0.493	0.115	1.83×10^{-5}	0.0559

Table 5.3 The top 4 differentially expressed protein coding genes following RNA-seq of RNA extracted from germ cells exposed to CD or HFD for 14 weeks. Log_2 fold change expression between the HFD and CD groups is shown with the standard error. The P value and corrected p value following Benjamini and Hochberg's correction (p adj.) is shown. Only three genes showed significantly different expression.

5.3.3 Expression of miRNA

1.2-1.7 $x10^7$ small RNA fragments were sequenced per animal. Again, clustering and PCA did not find any significant correlations between the animals in each treatment group (Figure 5.3A and B). Differential expression analysis identified one miRNA, miRNA-10b, with reduced expression in germ cells from HFD-exposed animals (Table 5.4). However, although there was a reduction in the expression of mir-10b in the qPCR validation, this failed to reach statistical significance (Figure 5.3D), a finding in keeping with the protein coding gene expression described above.

miRNA10b has potential target sites against a number of mRNAs including KDM5B (JARID1b), a histone lysine demethylase, knockdown of which results in impaired preimplantation embryonic development by altering the balance of bivalent histone modifications (Huang et al., 2015), glial cell derived neurotrophic factor (GDNF) produced by Sertoli cells, and essential for spermatogonial stem cell self-renewal

(Meng et al., 2000) and, Tet3, a 5mC oxidase expressed in high levels in oocytes and zygotes (Iqbal et al., 2011). However, expression of none of these genes was altered in the germ cells of HFD-exposed rats in the transcriptome analysis.

miRNA	Log_2 Fold change	Log_2 Fold change SE	p	p adj
Rno-miRNA-10b	-0.260	0.044	$5.04x10^{-9}$	$2.17x10^{-7}$
Rno-miRNA-871	0.274	0.094	0.003	0.077
Rno-miRNA-103-2	0.170	0.090	0.055	0.595

Table 5.4 The top 3 differentially expressed miRNAs following smallRNA-seq of RNA extracted from germ cells exposed to CD or HFD for 14 weeks. Log_2 fold change expression between HFD and CD is shown with the standard error. The p value and corrected p value following Benjamini and Hochberg's correction (p adj.) is shown. Only one miRNA has significantly different expression.

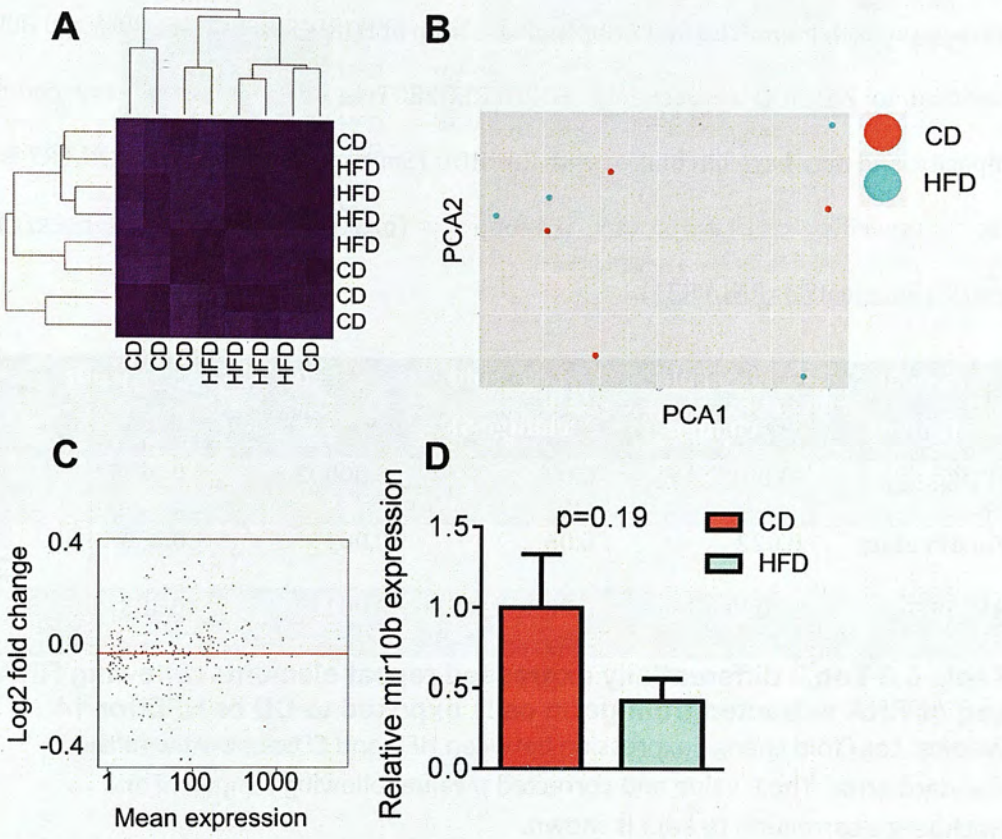

Figure 5.3 Analysis of smallRNA-seq of RNA extracted from germ cells exposed to CD or HFD for 14 weeks. A. clustering analysis of miRNAs. **B**. PCA of miRNAs. **C**. Differential expression analysis of miRNAs. smallRNA was extracted from germ cells following 14 weeks consumption of CD or HFD. N=4 **D**. qPCR or miRNA10b, n= 8 from 2 cohorts. Data are mean ±SEM.

5.3.4 Expression of repeats and piRNA

The expression of transcribed repeat elements and piRNAs was also explored in the sequencing data. Again, no clustering could be identified between the two treatment groups (Table 5.4A and B). There were no significantly differentially expressed piRNAs or repeat elements between the treatment groups (Figure 5.4, Table 5.5 and Table 5.6) but the top three differentially expressed repeat elements are considered briefly here.

5.3.4.1 Repeat elements with non-significant changes in expression

MTE2 is a long transposable repeat element (see 1.3.1.1.3). FORDPREFECT is a class II transposable element. The first 66bp and last 36bp of FORDPREFECT are 90% and 80% identical to ZAPHOD respectively. FORDPREDFECT is not thought to have coding capacity, and may have hitchhiked with ZAPHOD (Smit and Hubley, 2001). RNLTR7 is a rat specific LTR of 476bp (http://www.repeatmasker.org/cgi-bin/ViewRepeat?id=RNLTR21).

Repeat element	Log_2 Fold change	Log_2 Fold change SE	p	p adj
MTE2	-0.092	0.02	0.00002	0.0817
FordPrefect	0.022	0.06	0.001	0.295
RNLTR7	-0.099	0.032	0.001	0.323

Table 5.5 Top 3 differentially expressed repeat elements following RNA-seq of RNA extracted from germ cells exposed to CD or HFD for 14 weeks. Log_2 fold change expression between HFD and CD is shown with the standard error. The P value and corrected p value following Benjamini and Hochberg's correction (p adj.) is shown.

piRNA	Log_2 Fold change	Log_2 Fold change SE	p	p adj
64742	-0.421	0.1	$5x10^{-5}$	0.09
64508	-0.414	0.104	$7x10^{-5}$	0.09
179334	0.053	0.103	0.606	0.995

Table 5.6 Differential expression of piRNAs following RNA-seq of RNA extracted from germ cells exposed to CD or HFD for 14 weeks. Log_2 fold change expression between HFD and CD is shown with the standard error. The P value and corrected p value following Benjamini and Hochberg's correction (p adj.) is shown.

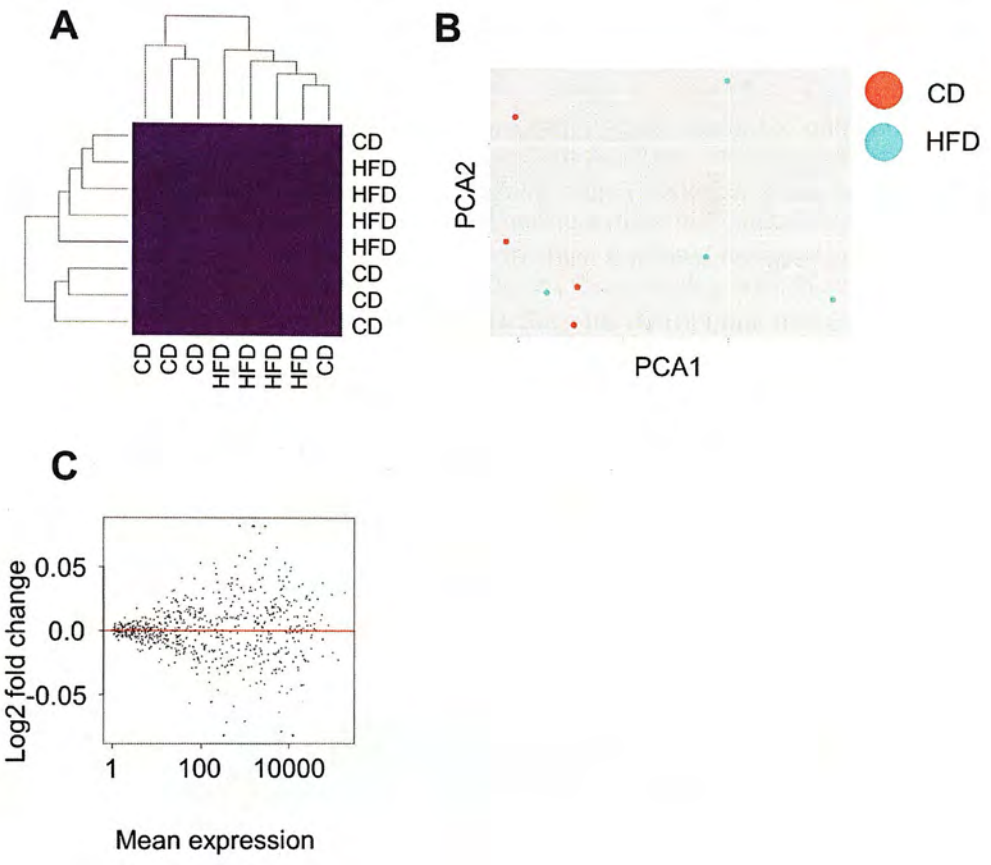

Figure 5.4 Analysis of transcribed repeat elements following RNA-seq of RNA extracted from germ cells exposed to CD or HFD for 14 weeks. **A**. analysis of clustering between treatment groups. **B**. PCA of repeat elements in HFD and CD groups. **C**. differential expression analysis of repeat elements.

5.3.5 Positive control of analysis pathway using rat bodymap data

As a positive control to identify if the bioinformatic process was successful, data from the rat bodymap database (http://pgx.fudan.edu.cn/ratbodymap/index.html) was subjected to the same pipeline. Figure 5.5A shows the large number of differentially expressed genes between liver and testis from the rat (in red). The top 5 differentially expressed genes are shown in Table 5.7. Gnrhr, (gonadotrophin releasing hormone receptor)(Ciaramella et al., 2015), testin (Grima and Cheng, 2000), lhcgr (LH receptor, expressed on Leydig cells) and cst12 (cystatin 12)(Li et al., 2005b) are all expressed in the testis and showed increased expression compared to liver as would be expected. The role of mmd2 (monocyte to macrophage differentiation-associated 2) in the testis is not clear.

Gene	Log_2 Fold change	Log_2 Fold change SE	p adj
Gnrhr	11.36	0.81	$4.95x10^{-43}$
Testin	10.79	0.85	$2.19x10^{-35}$
Lhcgr	9.87	1.13	$1.36x10^{-19}$
Cst12	9.77	0.58	$1.8x10^{-13}$
Mmd2	9.71	0.79	$3.94x10^{-62}$

Table 5.7 Comparison of rat bodymap liver and testis data from the rat bodymap data set http://pgx.fudan.edu.cn/ratbodymap/index.html as a positive control for the analysis. The top five differentially expressed genes between testis and liver from published RNA-seq data are shown.

5.3.6 Spike-in experiment to determine the power of the present study

The absence of effect on gene expression following exposure to the HFD could be due to a technical problem with the study, for example a false negative, or it may be a true finding. In an attempt to rule out type II statistical error, and to assess the power of the data to identify changes, a 'spike in' experiment was devised.

To do this, an artificial data set was synthesised such that the HFD dataset was shuffled to generate pseudogenes with <0.6 $\log_2$ fold change in expression. The 'spike in' data set was then subjected to differential expression analysis. The new data set clustered well by treatment (Figure 5.5B). The generated data set had 2781 differentially expressed genes, shown in Figure 5.5C by the blue circles with black centres, and shown against the 'standard' dataset in red. Thus, the data should have had enough power to determine if there was a difference in the expression profiles of the germ cells following exposure to HFD.

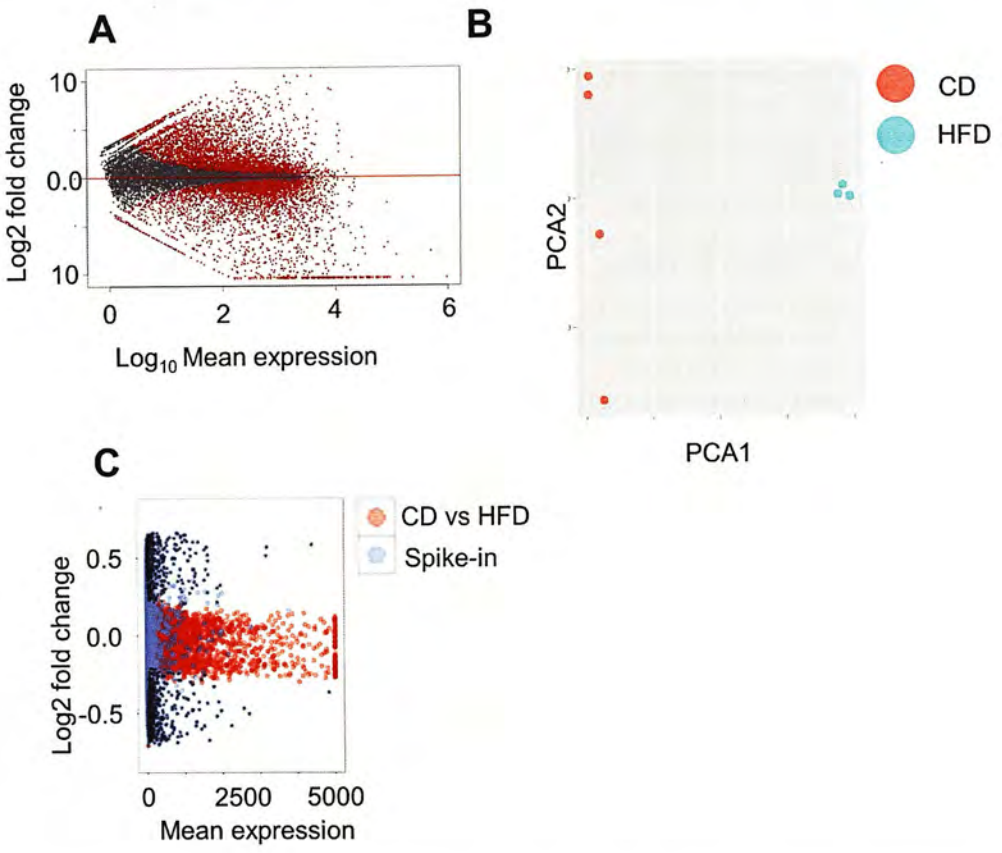

Figure 5.5 Validation of sequencing analysis and power of experiment. **A**. Comparison of existing data from the rat bodymap. Liver and testis RNA-seq data were compared. Red dots indicate differentially expressed genes. **B**. PCA of 'spike-in' data set showing clustering of HFD animals (green) in the pseudo dataset. **C**. Differential expression analysis comparison between spike-in data set (blue) and true data set (red), black dots represent genes with significant difference in expression.

5.4 Discussion

The experiments described in this chapter were designed to see if exposure to HFD might perturb the germline transcriptome and thus give an indication of any changes in the regulation of transcription of the epigenome.

The presented data show that a pure population of germ cells can be obtained from the GC-eGFP transgenic rat, that expression of RNA, miRNA, repeat elements and piRNA was not perturbed by exposure to 14 weeks high fat diet, and that the study should have been statistically powered to identify changes should they be present.

5.4.1 Potential explanations

The data suggest that the intergenerational transmission of the phenotype is not caused by changes to the germ cell transcriptome in this model. Epigenetic changes can regulate expression, however, as was discussed in Chapter 1, methylation patterns and changes to histones do not always correlate with changes in gene expression (1.3.1.1.1). For example, methylation of CpGs within 1500bp of the TSS correlates negatively with expression of only ~30% of genes (Wagner et al., 2014). Histone modifications more robustly predict gene expression although this is less clear at 'poised genes' carrying both activating and inactivating motifs (Dong and Weng, 2013). Thus, there could have been changes to the epigenome that were not identified at a transcriptional level. It is important to note that the assessment of the germline transcriptome would not find any changes to genes not expressed during spermatogenesis but which could play a role in early development, such changes would not have been identified using this study design but could be established by interrogating the germline epigenome, or the transcriptome of early blastocysts to see if transcription had been altered at this stage.

A further complication are the dynamic changes to the epigenome over the course of spermatogenesis (section 1.4.5). Over the later steps of spermatogenesis, when histones are replaced by protamines, transcription has generally stopped due to the changes in chromatin structure (Rathke et al., 2014). Thus if there were perturbations to the removal of histones as a result of HFD exposure, this could affect histone retention in sperm and thus alter the chromatin structure of the paternal DNA following fertilisation. The RNA-seq would have failed to detect any such differences.

In a study in which *drosophila melanogaster* were exposed to a high sugar diet, and in which offspring were metabolically reprogrammed as a consequence, the 'sperm' transcriptome was assessed. This showed that there was increased expression of genes in general, which was suggested to be due to a more relaxed chromatin structure (Öst et al., 2014). These genes were enriched for ion-binding proteins, and genes related to the stress response. However, validation of the gene expression was not shown, and the list of expressed genes included many drosophila 80S ribosomal subunit rRNAs (Anger et al., 2013), which might suggest contamination of the samples with somatic cells given that only the mitochondrial 55S ribosome is thought to be active in spermatozoa (Gur and Breitbart, 2006).

Following a 14-week exposure to HFD, expression of 23 miRNAs was altered in whole mouse whole testis, 11 of which were subsequently validated by qPCR (Fullston et al., 2013). Four of these also had altered expression in sperm, of which the expression of three was changed in the same direction as in whole testis. Interpretation of the miRNA expression did not include correction for multiple comparisons. 28 of 50 predicted target mRNAs in whole testis exhibited differential expression following exposure to HFD, with pathway analysis identifying enrichment for metabolic disease, cell death, production of ROS, DNA replication, NF-κB signalling, p53 signalling, recombination

and repair, lipid metabolism, spermatogenesis, and embryonic development (Fullston et al., 2013). Examination of the whole testis transcriptome means that mRNA from both somatic and germ cells is analysed. Comparison of the top 50 altered genes in the Fullston dataset and the data from the present study show a non-significant positive correlation (Figure 5.6). Differences between the two data-sets may have occurred as a result of the somatic cell component in the Fullston data. Gene expression might be expected to change in the somatic component following exposure to HFD. For example, HFD alters Leydig cell number (Li et al., 2013), and is reportedly associated with a loosening of the Sertoli cell tight junctions (Fan et al., 2015b).

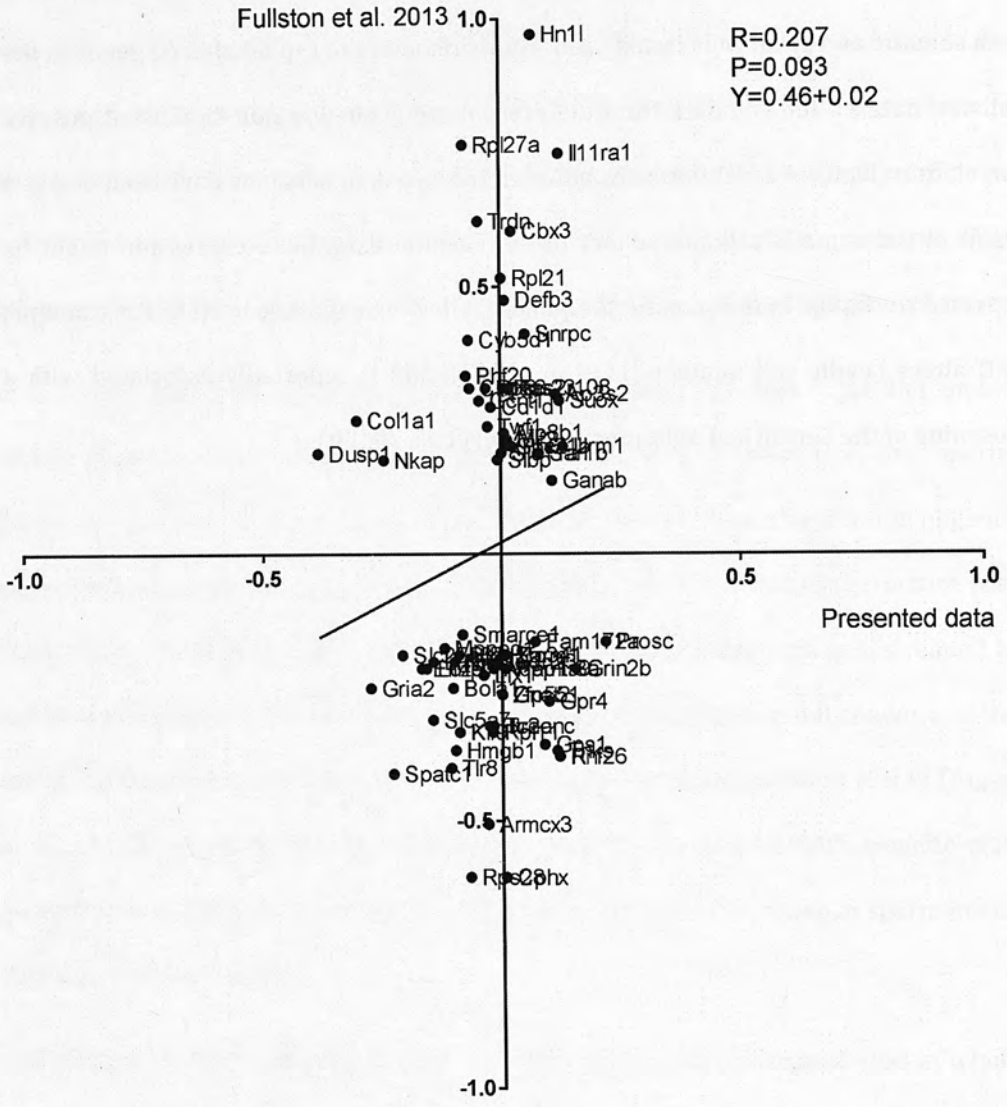

Figure 5.6 Comparison of Fullston et al. 2013 whole testis transcriptome changes following HFD exposure with the germ cell transcriptome from HFD-exposed rats in the present study. The top 50 altered genes from the micro array of whole testis tissue following 12 weeks HFD or CD in Fullston et al., 2013 are compared to the mRNA-seq data from the current study. Spearman correlation of the two data sets shows a non-significant positive correlation.

The present study, showing no change to the transcriptome in germ cells during spermatogenesis as a result of HFD exposure might imply that intergenerational effects occur as a result of down-stream changes to spermatozoa. During spermatozoal maturation in the epididymis, it has been suggested that methylation patterns on the DNA change (Ariel et al., 1994). Comparison of the miRNA profiles between testis, epididymal sperm and ejaculated sperm from boars showed some that miRNAs demonstrated large changes between the epididymis and the ejaculated sperm, whilst others showed high consistency. Interestingly miRNA-10b was the miRNA that showed the highest consistency in testis, epididymal sperm and ejaculated sperm (Luo et al., 2015). Thus, the transcriptional profile of spermatozoa changes during epididymal maturation, and might be perturbed by changes to the environment via HFD exposure.

No changes were found to the repeat or piRNA component of the germ cell transcriptome. Regulation of repeat elements involves DNA methylation and the compaction of heterochromatin (see section 1.3.1.1.3), processes that are dynamic in spermatogenesis. If the HFD had perturbed the epigenome during spermatogenesis, dysregulation of repeat elements might have been observed. However, there were no differences between the groups. Likewise, piRNAs are expressed during spermatogenesis in order to compensate for increased repeat element transcription (see 1.4.5.2.3) although again, no differences in expression were found following exposure to the HFD. It was not possible to examine lncRNA in the sequencing data as the library preparation enriched for poly-A tailed mRNA.

5.5 Conclusion

High fat diet did not alter the transcriptome of the germ cells in the presented rat model, and thus does not appear to account for the changes in phenotype observed in the offspring and grand-offspring. An alternative mechanism, which is either

downstream of testicular spermatogenesis or, which does not affect the transcriptome is therefore more likely to be responsible.

6 Final discussion

The aims of this thesis were to establish a rat model to test the hypothesis that parental exposure to HFD might perturb health in offspring and grand-offspring, to investigate potential mechanisms in the germ cells resulting in inter-generational effects and to investigate epigenetic regulators across different species during germ cell development.

In Chapter 4, a rat model of intergenerational inheritance of perturbed metabolic health in response to grandparental exposure to HFD was described: Rats whose maternal grandfathers had been exposed to HFD for 14 weeks were heavier, had more adipose tissue, exhibited an increased insulin response to glucose challenge and showed an increase in the LH to testosterone ratio. The transmission of effects as a result of change in grandparental environment most likely suggests a non-genetic mechanism.

Non-genetic inheritance encompasses several potential mechanisms (Bonduriansky and Day, 2013):

- Transgenerational epigenetic inheritance (DNA methylation or chromatin structure)
- Somatic inheritance- components of the parental soma alter development of the pre-implantation embryo such as glandular secretions
- Behavioural inheritance- for example influences of parents on offspring through effects on behaviour and learning
- Environmental inheritance- for example parental influences on the environment around offspring, for example supply of nutrition

It should also be considered that environmental exposures could impact upon the sequence of DNA resulting in a genetic transgenerational; inheritance.

Controlling for each of these, even in experimental studies is problematic, making robust conclusions as to the mechanisms resulting in transgenerational inheritance difficult. Strengths of the current study include the fact that a matched control diet was used, reducing the likelihood of altered micronutrient exposure, that control 'mates' were taken from the same cohort of animals, and were the same age, and that both sexes were exposed and examined. Furthermore, the findings were in agreement with similar studies in mice (Fullston et al., 2012, 2013). In order to examine if the germline transcriptome had been affected by HFD exposure, the use of the GCS-eGFP rat enabled pure populations of germ cells to be isolated for analysis. In contrast with other models in which the germline transcriptome has been interrogated following dietary interventions (Fullston et al., 2013; Öst et al., 2014), no significant perturbations were found. Key differences in the studies, and analyses, include the purity of the cells examined: for example Fullston *et al.* investigate whole testis, and then follow up findings in mature sperm, and Öst *et al.* find a high proportion of ribosomal RNAs in their RNA-seq data, suggesting somatic contamination. Furthermore, neither study corrects for multiple comparisons, increasing the risk of type I statistical error (Benjamini and Hochberg, 1995).

Several approaches could be taken to test the hypothesis that the HFD exposure had altered the germline epigenome in F0 males. No studies to date have examined the impact of HFD on the rat germ cell transcriptome, thus a targeted approach would have been difficult. MeDIP/WGBS or hmeDIP and sequencing would allow the genome wide assessment of DNA methylation and hydroxymethylation, likewise, ChIP-seq would allow the exploration of histone modifications (Greenleaf, 2015). Given that both methylation and histone modifications can regulate transcription, one might expect that changes to the epigenome would deregulate transcription. However, HFD exposure

did not alter the F0 male germ cell transcriptome, thus no data is presented to suggest perturbation of the germline epigenome by HFD.

Since the exposure did not result in changes to the transcriptome came as a surprise, the sensitivity of the technique was assessed, which confirmed adequate power to find changes in gene expression (Chapter 5). The findings, in support of the null hypothesis, suggest that altered germ cell transcription during spermatogenesis does not provide a cogent explanation for the observed intergenerational programming, although it does not rule out changes to the germ line epigenome; direct assessment of epigenetic changes in the germ cells would be obvious next experiments should this hypothesis warrant further investigation.

No mechanism for intergenerational inheritance was thus identified in the present study. Other potential mechanisms, which were not explored include epigenetic changes that do not alter germ cell transcription, or transcriptional, translational or epigenetic changes that occur during spermatozoal maturation. Furthermore, the study did not control for contents of seminal fluid, which can be affected by diet and can affect conception and fetal development (Binder et al., 2015; Bromfield et al., 2014; Crean et al., 2014). Nor did the study control for paternal and maternal behaviour, which may have changed as a result of exposure to HFD (Warneke et al., 2014), and, which could have affected interactions with offspring (Connor et al., 2012). With improved and more complex experimental design, for example using *in vitro* fertilisation and cross-fostering or surrogacy, potential confounding factors could be excluded and the relative influence of each mechanism could be assessed.

Transgenerational studies using rodents are attractive as they allow multiple generations to be investigated fairly rapidly, however, findings must be interpreted with caution, especially when extrapolating the meaning of results to human

populations. A justification for the use of a rodent model is given in Chapter 3: Conserved expression patterns of histone modifications, cytosine methylation and hydroxymethylation, and of the *de novo* DNA methyltransferases DNMT3A and DNMT3B are shown in rodent and primate testes during fetal and postnatal life. Conservation of expression of these proteins likely highlights a significant functional role for them in germ cell development. The embryonic lethality of *Dnmt3a* and *Dnmt3b* in knockout mice (Okano et al., 1999), and the mortality associated with ICF syndrome (Immunodeficiency, centromeric region instability and facial anomalies) (Weemaes et al., 2013), in which there is a mutation in DNMT3, makes assessment of their role in postnatal spermatogenesis difficult. However, knockout of the obligate co-factor *Dnmt3l* results in meiotic catastrophe (Bourc'his and Bestor, 2004), and patients with bilateral spermatogenic arrest have been found to have fewer DNMT3B positive preleptotene and pachytene spermatocytes (Adiga et al., 2011), suggesting essential roles. To date, the definitive investigations of spermatogenesis in ICF patients, or the generation of a germ cell specific *dnmt3a or dnmt3b* knockout have yet to be reported. In mouse studies, *in utero* exposure to under nutrition alters germline methylation, at specific loci (Radford et al., 2014) and HFD exposure reduced global methylation (Fullston et al., 2013). The impacts of diet on methylation in human spermatozoa has not been reported yet in the literature, however, paternal obesity has been associated with reduced methylation at DMRs for the imprinted genes MEST, PEG3 and NNAT in cord blood leukocytes of offspring (Soubry et al., 2015). The majority of studies where paternal environment has been perturbed find reduced methylation. Lower methylation is associated with a more open chromatin structure (Lehnertz et al., 2003; Saksouk et al., 2014), possibly suggesting a reduction in heterochromatin in response to the intervention

With respect to heterochromatin, the *Ezh2* knockout mouse displays early embryonic lethality (O'Carroll et al., 2001), making investigation of its role in germ cell development and reprogramming difficult. Germline specific knockout of *Suv39h1* and *2* exhibit germ cell developmental arrest during the spermatocyte stage, indicating the importance of H3K9 methylation for normal male meiosis (Peters et al., 2001). Human sperm retain around 5-10% of histones (Brykczynska et al., 2010; Hammoud et al., 2009), in contrast to around 1% in the mouse. A low folate diet reduces global levels of H3K4 and H3K9 methylation in epididymal sperm in mice (Lambrot et al., 2013) but there is no literature to date examining if histone retention in sperm is altered by environmental exposures in humans, which should be more straight forward given the abundance. The conserved nature of some histone modifications in germ cells in rodent and primate models (Chapter 3) suggests functional importance: likely as a means of enabling meiosis to proceed without the aberrant expression of repeat elements, to allow the restructuring of the chromatin and allow fertilisation to occur, and to enable the rapid reprogramming of cells following fertilisation.

6.1.1 Summary and suggestions for future study

The present studies find evidence in favour of non-genetic intergenerational inheritance of phenotype in a rat model of exposure to HFD, suggests that epigenetic alterations to the germline could be responsible given that regulators are present, but finds no evidence for epigenetic changes having altered the transcription of protein coding genes, miRNA, piRNA or repetitive elements as a result of exposure to HFD

Future studies should focus on answering three main questions

1. Does HFD alter the germline epigenome independently of the transcriptome?

   This could be answered using whole genome based screening for epigenetic changes (methylation, hydroxymethylation and histone modification) of FACS

sorted germ cells and purified mature spermatozoa following dietary intervention. The availability of purified ejaculated mature spermatozoa would be a useful refinement to the model, reducing the number of animals required, and allowing inspection of fully mature spermatozoa.

2. What role does behaviour and/or seminal fluid or the soma play in non-genetic inheritance?

   The best means of controlling for this would be use of *in vitro* fertilisation/ Intra cytoplasmic sperm injection with purified sperm (semen and soma free) to control for exposure to males.

3. Does diet affect sperm/semen and offspring and grand-offspring in human populations?

   If an epigenetic 'footprint' could be identified in animal sperm as a result of dietary exposure, and other confounding factors ruled out, the relevance of this could be investigated in humans; in the first instance, semen samples could be investigated to look for similar changes, and in the longer term, epidemiological studies might help to improve evidence for non-genetic inheritance, in particular looking at siblings born either side of parental weight-loss or weight gain might help to highlight the importance of parental diet/obesity on future generations.

6.2 What is the teleology of non-genetic inheritance?

The survival and evolution of a species relies upon an ability to adapt to changing conditions. Classical *neo Darwinism* suggests that a species evolves as a result of genetic mutations that result in a phenotypic advantage (Noble, 2015). One problem with this theory is that the frequency of potentially advantageous genetic mutations is low. Even

accounting for genetic drift, epistasis, directed mutation and genetic assimilation, genetics alone has difficulty explaining evolution (Laland et al., 2014; Noble, 2015; Skinner, 2015). Further, this model assumes that the variation within a species results in a shift in fitness if the environment were to change and thus the selection of a different set of individuals most suitable for survival should this occur. Thus the rate of evolution would be slow, and would lag behind somewhat more rapid changes in the environment (Olson-Manning et al., 2012). The inclusion of epigenetics into the model would allow far greater plasticity and a more rapid evolution.

Lamarck proposed in 1809 that:

'acquisitions or losses wrought by nature on individuals, through the influence of the environment in which their race has long been placed, and hence through the influence of the predominant use or disuse of an organ; all these are preserved by reproduction to the new individuals which arise, provided that the acquired modifications are common to both sexes, or at least to the individuals which produce the young' (Lamarck, translated 1914).

Although rejected by many 20th century geneticists, there is building evidence that the environment around our ancestors could influence phenotype, however, perhaps not in the direct way in which Lamarck envisaged. Thus for example, exposure to under nutrition might alter methylation patterns in offspring, which results in an altered phenotype (which may be better adapted for survival in the 'adverse' environment). Improved survival in this situation might apply a selection pressure to animals that have this adaptive mechanism in place, or whose genetic code allows the greatest epigenetic plasticity (Burggren, 2014; Noble, 2015; Skinner, 2015). The phenotypic findings of chapter 4 may support this *neo-Lamarckist* hypothesis.

Another factor to consider is the relative value a species places on reproductive success versus longevity. Telomeres are repetitive elements of DNA that cap the ends of chromosomes (see 1.3.1.1.3). Eisenberg's *thrifty telomere* hypothesis suggests that

telomere length serves to regulate somatic cell maintenance effort; a cell with longer telomeres requires more energy to undergo mitosis whereas shorter telomeres require less energy investment to maintain the cell. Reduced maintenance effort (and shortening of telomeres) might free up resources for growth and reproduction but at the cost of reduced longevity (Eisenberg, 2011). Thus telomere length could be a means of optimising longevity and reproductive success in offspring so as to best fit the environment into which they will be born, and natural selection of individuals with the most appropriate telomere length for the environment propagates an ideal balance between telomere length and environmental condition.

In humans, telomere length is associated with Diabetes mellitus (Type 1 and type 2)(Ma et al., 2013), obesity (García-Calzón et al., 2014; Nordfjäll et al., 2008) and cardiovascular disease (Hunt et al., 2015). Examination of telomere length in germ cells and soma in the three generations in the present study might help to identify if there is any evidence for this as being an associative factor with the adverse metabolic phenotype in the F2 animals. However, in the presented study, telomere length in the liver from F2 males was unaffected by founder diet (Appendix. 1).

Mechanisms allowing more plastic adaptation to the environment may infer an evolutionary benefit. For example, where the environment is lacking in nutrition, there may have been an advantage to adapting metabolism to improve storage and efficiency. Mankind is now experiencing novel environments with respect to over-nutrition, to levels not previously seen before (Cutler et al., 2003). The shift in environmental conditions for humans (in terms of diet and lifestyle) over the last 50 years has been rapid. If the resulting obesity epidemic has been partially programmed by the lifestyle of our ancestors, this might provide evidence for *neo-Lamarckian* inheritance.

Exposure to HFD can increase cortisol production, and could be interpreted biologically as stress (Mitra et al., 2010). It could thus be that exposure to 'stress' is what programmed the phenotypic changes seen in F2 males in the present study. The intergenerational response to stress (Gapp et al., 2014; Seong et al., 2011) and to both over- (Fullston et al., 2013; Ng et al., 2010; Williams et al., 2014) and under-nutrition (Carone et al., 2010; Correia-Branco et al., 2015; Erhuma et al., 2007) often comprise similar features of the metabolic syndrome and it may be that common mechanisms are involved. It is interesting to note, however, that in various rat models of exposure to different endocrine disrupting chemicals, which resulted in the same impaired reproductive phenotype and, in altered methylation levels at CpG deserts in sperm, the loci of changes was not consistent between the different exposures, perhaps suggesting an indirect mechanism (Skinner and Guerrero-Bosagna, 2014).

Intergenerational non-genetic inheritance may have evolved as a means of rapidly altering phenotype to cope with the environment, and to optimise energy usage for longevity or reproductive success, but most importantly maintenance of a species.

6.3 Altering maternal and paternal behaviour

The current NICE fertility guidelines advise that men and women should aim to have a BMI of <30 if they are having difficulty conceiving (NICE, 2013). However, many obese couples will conceive without medical intervention. British data suggest that 38% of women conceiving are overweight or obese (Heslehurst et al., 2010). 57% of the adult female English population have a BMI of >25(Moody, 2014), perhaps highlighting the reduced fertility (time to pregnancy) associated with overweight and obesity in women (Law et al., 2007; Nohr et al., 2009), an effect confounded when present in both partners (Ramlau-Hansen et al., 2007). Maternal obesity is associated with increased risk of infant (Johansson et al., 2014) and adult mortality (Reynolds et al., 2013). 75%

of 25-34 year old American women recognise obesity as a factor that might affect fertility (Lundsberg et al., 2014).

Improving BMI prior to pregnancy in both potential mothers and fathers may not only improve rates of successful pregnancy but also health in offspring, although it should be noted that no interventional study has shown direct improvement in the primary outcome of infant or adult mortality in humans. In mice, weight loss as a result of reversal of HFD to CD, or increased exercise improved outcomes in female offspring (McPherson et al., 2015; Wei et al., 2015). Despite the evidence that improving weight will likely benefit both mother and baby, to date, interventional trials have been poorly designed or have had little efficacy at improving weight (Birdsall et al., 2009; Fealy et al., 2014; Shirazian and Raghavan, 2009). However, there are some better powered studies underway (Fernandez et al., 2015) and there is some evidence that use of technology, for example text messaging (Soltani et al., 2015) and use of knowledge tools (McDonald et al., 2015), can make improvements. Few trials have been published looking at improving paternal BMI around conception, possibly as there is little evidence in humans relating paternal BMI to perinatal outcomes (Mutsaerts et al., 2012, 2014).

6.4 Summary

- DNMT3A and DNMT3B expression, and expression of the facultative heterochromatin marker H3K27me3 is conserved between rodents and primates during pre and postnatal spermatogenesis
- HFD consumption in females prior to conception and during pregnancy and weaning results in increased weight in males and females. Paternal consumption of HFD prior to conception results in increased weight in

daughters and increased weight, adiposity, insulin response to OGTT and LH to testosterone ratio in grandsons via the maternal line.

- HFD exposure does not alter the germ cell transcriptome
- Attention to the lifestyle of males and females around conception and during pregnancy may improve health outcomes in future generations of humans

Appendix 1: Telomere length in maternal grandsons is not affected by diet

Introduction

Telomere length declines with age. In humans and rodents, a more rapid rate of attrition of telomeres is associated with male sex (Coviello-McLaughlin and Prowse, 1997; Gardner et al., 2014), poor health, for example type I and type II diabetes (Ma et al., 2013), cardiovascular disease (Hunt et al., 2015) and obesity (García-Calzón et al., 2014; Nordfjäll et al., 2008). Furthermore, there is some evidence that telomere length can be inherited down the paternal line (Eisenberg et al., 2012; Ferlin et al., 2013; Hjelmborg et al., 2015; Prescott et al., 2012), although the strong correlation between maternal and paternal age mean it is possible that both contribute.

To investigate if telomere length had been affected by grandparental diet, somatic DNA from liver was extracted and telomere length assayed using the qPCR method of O'Callaghan and Fenech (O'Callaghan and Fenech, 2011) with Rplp0 as a reference single copy gene for which new primers were designed for the rat.

Methods

The caudate process of the liver was dissected at necropsy (age 17 weeks) and snap frozen on dry ice prior to storage at -80°C. DNA was extracted using the Qiagen DNeasy kit as per the manufacturers' instructions (see 2.1.2.1.1). DNA quality and quantity was assessed by spectrophotometry (see 2.4.2.1).

DNA was diluted to 5ng/µl in buffer AE. Reactions (run in triplicate) were set up as shown in Table I, a separate reaction for telomeres and Rplp0, a single copy gene used as a reference control were set up. Primers were as shown in Table II. Absolute quantification was determined by making 1:10 dilution standard curves starting at

15pg/µl using oligomeric standards, which were HPLC purified, for the PCR products as shown in Table III. Samples were run on the ABI 7900 HT thermocycler as per Table IV.

Reagent	µl for 10µl reaction
SYBR green (Agilent brilliant III superfast)	5
Primer F (2uM)	0.5
Primer R (2uM)	0.5
H2O	2
DNA	2

Table I Reactions for telomere assay

Primer	Sequence
Telomere F	CGG TTT GTT TGG GTT TGG GTT TGG GTT TGG GTT TGG GTT
Telomere R	GGC TTG CCT TAC CCT TAC CCT TAC CCT TAC CCT TAC CCT
Rplp0 F	GGA CCT CAC CGA GAT TAG GG
Rplp0 R	GCA CAG CTA CCT CCT CTC AT

Table II Primers for telomere assays

Standard	Sequence
Telomere	TTA GGG TTAG GG TTA GGG TTA GGG TTA GGG TTA GGG TTA GGG TTA GGG TTA GGG TTA GGG TTA GGG TTA GGG TTA GGG
Rplp0	GGA CCT CAC CGA GAT TAG GGA CAT GCT GCT GGC CAA TAA GGT AAG GGG CGG TAG GAC GGA TGA GAG GAG GTA GCT GTG C

Table III Standards for telomere assays

Temperature	Time (seconds)	
95°C	10 min	
95°C	15	X 40 cycles
60°C	60	
Melt curve		

Table IV PCR cycling for telomere assay

Results

Diet of the maternal grandfather had no effect on telomere length in the livers of grandsons.

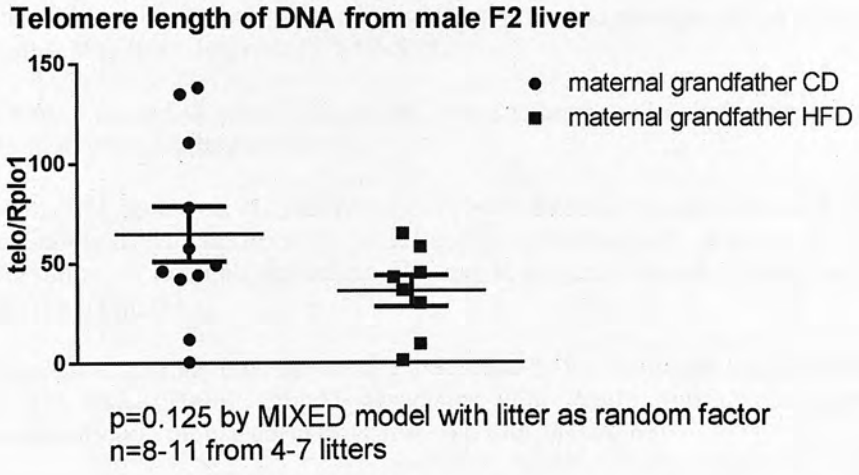

Figure 0.1 Telomere length in F2 liver Telomere length determined by qPCR was measured in the livers from F2 males from the control arm, or from the groups whose maternal grandfather had consumed the HFD. N= 8-11 from 4-7 litters, data are means ± SEM.

Discussion

Telomere length was not significantly affected by grand paternal diet. Either the intervention had no effect on telomere length, or the technique was insufficiently sensitive to identify a difference. A recent meta-analysis demonstrated that Southern blotting appeared to be a more sensitive technique than PCR at determining differences in telomere length in humans between males and females (Gardner et al., 2014). Also,

given that telomere length in somatic tissue declines rapidly following parturition (Eisenberg, 2011), an earlier time point might have been better at distinguishing between the two groups. This experiment however found no difference in telomere length in the adult male rats examined.

Appendix 2: References

Aapola, U., Shibuya, K., Scott, H.S., Ollila, J., Vihinen, M., Heino, M., Shintani, A., Kawasaki, K., Minoshima, S., Krohn, K., et al. (2000). Isolation and Initial Characterization of a Novel Zinc Finger Gene, DNMT3L, on 21q22.3, Related to the Cytosine-5-Methyltransferase 3 Gene Family. Genomics *65*, 293–298.

Abe, M., Tsai, S.Y., Jin, S.-G., Pfeifer, G.P., and Szabó, P.E. (2011). Sex-Specific Dynamics of Global Chromatin Changes in Fetal Mouse Germ Cells. PLoS ONE *6*, e23848.

Abrass, C.K., Hansen, K., Popov, V., and Denisenko, O. (2011). Alterations in chromatin are associated with increases in collagen III expression in aging nephropathy. Am. J. Physiol. Renal Physiol. *300*, F531–F539.

Adiga, S.K., Ehmcke, J., Schlatt, S., Kliesch, S., Westernströer, B., Luetjens, C.M., Wistuba, J., and Gromoll, J. (2011). Reduced expression of DNMT3B in the germ cells of patients with bilateral spermatogenic arrest does not lead to changes in the global methylation status. Mol. Hum. Reprod. *17*, 545–549.

Aiken, C.E., and Ozanne, S.E. (2014). Transgenerational developmental programming. Hum. Reprod. Update *20*, 63–75.

Allen, C.A., Banerjee, M., and Wu, F.C. (2000). Androgens and Coronary Artery Disease. In Endotext, L.J. De Groot, P. Beck-Peccoz, G. Chrousos, K. Dungan, A. Grossman, J.M. Hershman, C. Koch, R. McLachlan, M. New, R. Rebar, et al., eds. (South Dartmouth (MA): MDText.com, Inc.),.

Ancelin, K., Lange, U.C., Hajkova, P., Schneider, R., Bannister, A.J., Kouzarides, T., and Surani, M.A. (2006). Blimp1 associates with Prmt5 and directs histone arginine methylation in mouse germ cells. Nat. Cell Biol. *8*, 623–630.

Andersen, C.L., Jensen, J.L., and Ørntoft, T.F. (2004). Normalization of real-time quantitative reverse transcription-PCR data: a model-based variance estimation approach to identify genes suited for normalization, applied to bladder and colon cancer data sets. Cancer Res. *64*, 5245–5250.

Anderson, L.M., Riffle, L., Wilson, R., Travlos, G.S., Lubomirski, M.S., and Alvord, W.G. (2006). Preconceptional fasting of fathers alters serum glucose in offspring of mice. Nutrition *22*, 327–331.

Anderson, R., Copeland, T.K., Schöler, H., Heasman, J., and Wylie, C. (2000). The onset of germ cell migration in the mouse embryo. Mech. Dev. *91*, 61–68.

Andersson, A.-M., Jørgensen, N., Frydelund-Larsen, L., Rajpert-De Meyts, E., and Skakkebaek, N.E. (2004). Impaired Leydig cell function in infertile men: a study of 357 idiopathic infertile men and 318 proven fertile controls. J. Clin. Endocrinol. Metab. *89*, 3161–3167.

Anger, A.M., Armache, J.-P., Berninghausen, O., Habeck, M., Subklewe, M., Wilson, D.N., and Beckmann, R. (2013). Structures of the human and Drosophila 80S ribosome. Nature *497*, 80–85.

Anguera, M.C., Ma, W., Clift, D., Namekawa, S., Kelleher, R.J., and Lee, J.T. (2011). Tsx produces a long noncoding RNA and has general functions in the germline, stem cells, and brain. PLoS Genet. *7*, e1002248.

Antequera, F., and Bird, A. (1993). Number of CpG islands and genes in human and mouse. Proc. Natl. Acad. Sci. U. S. A. *90*, 11995–11999.

Anway, M.D., Cupp, A.S., Uzumcu, M., and Skinner, M.K. (2005). Epigenetic Transgenerational Actions of Endocrine Disruptors and Male Fertility. Science *308*, 1466–1469.

Anway, M.D., Memon, M.A., Uzumcu, M., and Skinner, M.K. (2006). Transgenerational Effect of the Endocrine Disruptor Vinclozolin on Male Spermatogenesis. J. Androl. *27*, 868–879.

Aravin, A.A., Sachidanandam, R., Bourc'his, D., Schaefer, C., Pezic, D., Toth, K.F., Bestor, T., and Hannon, G.J. (2008). A piRNA Pathway Primed by Individual Transposons Is Linked to De Novo DNA Methylation in Mice. Mol. Cell *31*, 785–799.

Argentaro, A., Yang, J.-C., Chapman, L., Kowalczyk, M.S., Gibbons, R.J., Higgs, D.R., Neuhaus, D., and Rhodes, D. (2007). Structural consequences of disease-causing mutations in the ATRX-DNMT3-DNMT3L (ADD) domain of the chromatin-associated protein ATRX. Proc. Natl. Acad. Sci. *104*, 11939–11944.

Ariel, M., Cedar, H., and McCarrey, J. (1994). Developmental changes in methylation of spermatogenesis-specific genes include reprogramming in the epididymis. Nat. Genet. *7*, 59–63.

Axtell, M.J. (2014). Butter: High-precision genomic alignment of small RNA-seq data. bioRxiv 007427.

Babiarz, J.E., Ruby, J.G., Wang, Y., Bartel, D.P., and Blelloch, R. (2008). Mouse ES cells express endogenous shRNAs, siRNAs, and other Microprocessor-independent, Dicer-dependent small RNAs. Genes Dev. *22*, 2773–2785.

Baillie, A.H. (1964). The histochemistry and ultrastructure of the gonocyte. J. Anat. *98*, 641–645.

Bannister, A.J., and Kouzarides, T. (2011). Regulation of chromatin by histone modifications. Cell Res. *21*, 381–395.

Bao, J., Zhang, Y., Schuster, A.S., Ortogero, N., Nilsson, E.E., Skinner, M.K., and Yan, W. (2014). Conditional inactivation of Miwi2 reveals that MIWI2 is only essential for prospermatogonial development in mice. Cell Death Differ. *21*, 783–796.

Basaria, S. (2014). Male hypogonadism. The Lancet *383*, 1250–1263.

Del Bas, J.M., Crescenti, A., Arola-Arnal, A., Oms-Oliu, G., Arola, L., and Caimari, A. (2015). Grape seed procyanidin supplementation to rats fed a high-fat diet during pregnancy and lactation increases the body fat content and modulates the inflammatory response and the adipose tissue metabolism of the male offspring in youth. Int. J. Obes. 2005 *39*, 7–15.

Bellisario, V., Berry, A., Capoccia, S., Raggi, C., Panetta, P., Branchi, I., Piccaro, G., Giorgio, M., Pelicci, P.G., and Cirulli, F. (2014). Gender-dependent resiliency to stressful and metabolic challenges following prenatal exposure to high-fat diet in the p66(Shc-/-) mouse. Front. Behav. Neurosci. *8*, 285.

Benatti, R.O., Melo, A.M., Borges, F.O., Ignacio-Souza, L.M., Simino, L. a. P., Milanski, M., Velloso, L.A., Torsoni, M.A., and Torsoni, A.S. (2014). Maternal high-fat diet consumption modulates hepatic lipid metabolism and microRNA-122 (miR-122) and microRNA-370 (miR-370) expression in offspring. Br. J. Nutr. *111*, 2112–2122.

Benjamini, Y., and Hochberg, Y. (1995). Controlling the False Discovery Rate: A Practical and Powerful Approach to Multiple Testing. J. R. Stat. Soc. Ser. B Methodol. *57*, 289–300.

Bergen, W.G., and Mersmann, H.J. (2005). Comparative Aspects of Lipid Metabolism: Impact on Contemporary Research and Use of Animal Models. J. Nutr. *135*, 2499–2502.

Bernstein, E., Caudy, A.A., Hammond, S.M., and Hannon, G.J. (2001). Role for a bidentate ribonuclease in the initiation step of RNA interference. Nature *409*, 363–366.

Bertani, S., Sauer, S., Bolotin, E., and Sauer, F. (2011). The non-coding RNA Mistral activates Hoxa6 and Hoxa7 expression and stem cell differentiation by recruiting Mll1 to chromatin. Mol. Cell *43*, 1040–1046.

Bestor, T. (1988). Structure of mammalian DNA methyltransferase as deduced from the inferred amino acid sequence and direct studies of the protein. Biochem. Soc. Trans. *16*, 944–947.

Biason-Lauber, A., Konrad, D., Navratil, F., and Schoenle, E.J. (2004). A WNT4 mutation associated with Müllerian-duct regression and virilization in a 46,XX woman. N. Engl. J. Med. *351*, 792–798.

Binder, N.K., Sheedy, J.R., Hannan, N.J., and Gardner, D.K. (2015). Male obesity is associated with changed spermatozoa Cox4i1 mRNA level and altered seminal vesicle fluid composition in a mouse model. Mol. Hum. Reprod.

Birdsall, K.M., Vyas, S., Khazaezadeh, N., and Oteng-Ntim, E. (2009). Maternal obesity: A review of interventions. Int. J. Clin. Pract. *63*, 494–507.

Bolger, A.M., Lohse, M., and Usadel, B. (2014). Trimmomatic: a flexible trimmer for Illumina sequence data. Bioinforma. Oxf. Engl. *30*, 2114–2120.

Bonasio, R., and Shiekhattar, R. (2014). Regulation of Transcription by Long Noncoding RNAs. Annu. Rev. Genet. *48*, 433–455.

Bonduriansky, R., and Day, T. (2013). Nongenetic inheritance and the evolution of costly female preference. J. Evol. Biol. *26*, 76–87.

Bošković, A., Bender, A., Gall, L., Ziegler-Birling, C., Beaujean, N., and Torres-Padilla, M.-E. (2012). Analysis of active chromatin modifications in early mammalian embryos reveals uncoupling of H2A.Z acetylation and H3K36 trimethylation from embryonic genome activation. Epigenetics *7*, 747–757.

Bostick, M., Kim, J.K., Estève, P.-O., Clark, A., Pradhan, S., and Jacobsen, S.E. (2007). UHRF1 plays a role in maintaining DNA methylation in mammalian cells. Science *317*, 1760–1764.

Bourc'his, D., and Bestor, T.H. (2004). Meiotic catastrophe and retrotransposon reactivation in male germ cells lacking Dnmt3L. Nature *431*, 96–99.

Bourc'his, D., Xu, G.-L., Lin, C.-S., Bollman, B., and Bestor, T.H. (2001). Dnmt3L and the Establishment of Maternal Genomic Imprints. Science *294*, 2536–2539.

Bowen, L., Taylor, A.E., Sullivan, R., Ebrahim, S., Kinra, S., Krishna, K.V.R., Kulkarni, B., Ben-Shlomo, Y., Ekelund, U., Wells, J.C., et al. (2015). Associations between diet, physical activity and body fat distribution: a cross sectional study in an Indian population. BMC Public Health *15*, 281.

Brennan, J., and Capel, B. (2004). One tissue, two fates: molecular genetic events that underlie testis versus ovary development. Nat. Rev. Genet. *5*, 509–521.

Brenseke, B., Bahamonde, J., Talanian, M., Kornfeind, E., Daly, J., Cobb, G., Zhang, J., Prater, M.R., Davis, G.C., and Good, D.J. (2015). Mitigating or exacerbating effects of maternal-fetal programming of female mice through the food choice environment. Endocrinology *156*, 182–192.

Bromfield, J.J., Schjenken, J.E., Chin, P.Y., Care, A.S., Jasper, M.J., and Robertson, S.A. (2014). Maternal tract factors contribute to paternal seminal fluid impact on metabolic phenotype in offspring. Proc. Natl. Acad. Sci. 201305609.

Brykczynska, U., Hisano, M., Erkek, S., Ramos, L., Oakeley, E.J., Roloff, T.C., Beisel, C., Schübeler, D., Stadler, M.B., and Peters, A.H.F.M. (2010). Repressive and active histone methylation mark distinct promoters in human and mouse spermatozoa. Nat. Struct. Mol. Biol. *17*, 679–687.

Buchold, G.M., Coarfa, C., Kim, J., Milosavljevic, A., Gunaratne, P.H., and Matzuk, M.M. (2010). Analysis of MicroRNA Expression in the Prepubertal Testis. PLoS ONE *5*, e15317.

Buchwald, U., Teupser, D., Kuehnel, F., Grohmann, J., Schmieder, N., Beindorff, N., Schlumbohm, C., Fuhrmann, H., and Einspanier, A. (2012). Prenatal stress programs lipid metabolism enhancing cardiovascular risk in the female F1, F2, and F3 generation in the primate model common marmoset (Callithrix jacchus). J. Med. Primatol. *41*, 231–240.

Burggren, W.W. (2014). Epigenetics as a source of variation in comparative animal physiology - or - Lamarck is lookin' pretty good these days. J. Exp. Biol. *217*, 682–689.

Burton, A., and Torres-Padilla, M.-E. (2014). Chromatin dynamics in the regulation of cell fate allocation during early embryogenesis. Nat. Rev. Mol. Cell Biol. *15*, 723–735.

Campolo, F., Gori, M., Favaro, R., Nicolis, S., Pellegrini, M., Botti, F., Rossi, P., Jannini, E.A., and Dolci, S. (2013). Essential role of Sox2 for the establishment and maintenance of the germ cell line. Stem Cells Dayt. Ohio *31*, 1408–1421.

Cannon, M.V., Buchner, D.A., Hester, J., Miller, H., Sehayek, E., Nadeau, J.H., and Serre, D. (2014). Maternal nutrition induces pervasive gene expression changes but no detectable DNA methylation differences in the liver of adult offspring. PloS One *9*, e90335.

Carmell, M.A., Girard, A., van de Kant, H.J.G., Bourc'his, D., Bestor, T.H., de Rooij, D.G., and Hannon, G.J. (2007). MIWI2 Is Essential for Spermatogenesis and Repression of Transposons in the Mouse Male Germline. Dev. Cell *12*, 503–514.

Carone, B.R., Fauquier, L., Habib, N., Shea, J.M., Hart, C.E., Li, R., Bock, C., Li, C., Gu, H., Zamore, P.D., et al. (2010). Paternally Induced Transgenerational Environmental Reprogramming of Metabolic Gene Expression in Mammals. Cell *143*, 1084–1096.

Carone, B.R., Hung, J.-H., Hainer, S.J., Chou, M.-T., Carone, D.M., Weng, Z., Fazzio, T.G., and Rando, O.J. (2014). High-Resolution Mapping of Chromatin Packaging in Mouse Embryonic Stem Cells and Sperm. Dev. Cell *30*, 11–22.

Cederroth, C.R., Auger, J., Zimmermann, C., Eustache, F., and Nef, S. (2010). Soy, phyto-oestrogens and male reproductive function: a review. Int. J. Androl. *33*, 304–316.

Cerase, A., Smeets, D., Tang, Y.A., Gdula, M., Kraus, F., Spivakov, M., Moindrot, B., Leleu, M., Tattermusch, A., Demmerle, J., et al. (2014). Spatial separation of Xist RNA and polycomb proteins revealed by superresolution microscopy. Proc. Natl. Acad. Sci. *111*, 2235–2240.

Chalmel, F., Lardenois, A., Evrard, B., Rolland, A.D., Sallou, O., Dumargne, M.-C., Coiffec, I., Collin, O., Primig, M., and Jégou, B. (2014). High-Resolution Profiling of Novel Transcribed Regions During Rat Spermatogenesis. Biol. Reprod. *91*, 5.

Chang, Y.-F., Lee-Chang, J.S., Imam, J.S., Buddavarapu, K.C., Subaran, S.S., Sinha-Hikim, A.P., Gorospe, M., and Rao, M.K. (2012). Interaction between microRNAs and actin-associated protein Arpc5 regulates translational suppression during male germ cell differentiation. Proc. Natl. Acad. Sci. *109*, 5750–5755.

Chassot, A.-A., Ranc, F., Gregoire, E.P., Roepers-Gajadien, H.L., Taketo, M.M., Camerino, G., de Rooij, D.G., Schedl, A., and Chaboissier, M.-C. (2008). Activation of beta-catenin signaling by Rspo1 controls differentiation of the mammalian ovary. Hum. Mol. Genet. *17*, 1264–1277.

Chen, L.-L., and Carmichael, G.G. (2009). Altered nuclear retention of mRNAs containing inverted repeats in human embryonic stem cells: Functional role of a nuclear noncoding RNA. Mol. Cell *35*, 467–478.

Chen, T., Ueda, Y., Xie, S., and Li, E. (2002a). A Novel Dnmt3a Isoform Produced from an Alternative Promoter Localizes to Euchromatin and Its Expression Correlates with Activede Novo Methylation. J. Biol. Chem. *277*, 38746–38754.

Chen, T., Ueda, Y., Xie, S., and Li, E. (2002b). A novel Dnmt3a isoform produced from an alternative promoter localizes to euchromatin and its expression correlates with active de novo methylation. J. Biol. Chem. *277*, 38746–38754.

Chen, X., McClusky, R., Chen, J., Beaven, S.W., Tontonoz, P., Arnold, A.P., and Reue, K. (2012). The number of x chromosomes causes sex differences in adiposity in mice. PLoS Genet. *8*, e1002709.

Chendrimada, T.P., Gregory, R.I., Kumaraswamy, E., Norman, J., Cooch, N., Nishikura, K., and Shiekhattar, R. (2005). TRBP recruits the Dicer complex to Ago2 for microRNA processing and gene silencing. Nature *436*, 740–744.

Cheong, Y., Sadek, K.H., Bruce, K.D., Macklon, N., and Cagampang, F.R. (2014). Diet-induced maternal obesity alters ovarian morphology and gene expression in the adult mouse offspring. Fertil. Steril. *102*, 899–907.

Cho, C., Willis, W.D., Goulding, E.H., Jung-Ha, H., Choi, Y.-C., Hecht, N.B., and Eddy, E.M. (2001). Haploinsufficiency of protamine-1 or -2 causes infertility in mice. Nat. Genet. *28*, 82–86.

Ciaramella, V., Chianese, R., Pariante, P., Fasano, S., Pierantoni, R., and Meccariello, R. (2015). Expression Analysis of *Gnrh1* and *Gnrhr1* in Spermatogenic Cells of Rat. Int. J. Endocrinol. *2015*, e982726.

Clermont, Y., and Perey, B. (1957). Quantitative study of the cell population of the seminiferous tubules in immature rats. Am. J. Anat. *100*, 241–267.

Connor, K.L., Vickers, M.H., Beltrand, J., Meaney, M.J., and Sloboda, D.M. (2012). Nature, nurture or nutrition? Impact of maternal nutrition on maternal care, offspring development and reproductive function. J. Physiol. *590*, 2167–2180.

Cordero, P., Gonzalez-Muniesa, P., Milagro, F.I., Campion, J., and Martinez, J.A. (2014). Perinatal maternal feeding with an energy dense diet and/or micronutrient mixture drives offspring fat distribution depending on the sex and growth stage. J. Anim. Physiol. Anim. Nutr.

Correia-Branco, A., Keating, E., and Martel, F. (2015). Maternal undernutrition and fetal developmental programming of obesity: the glucocorticoid connection. Reprod. Sci. Thousand Oaks Calif *22*, 138–145.

Cortellino, S., Xu, J., Sannai, M., Moore, R., Caretti, E., Cigliano, A., Le Coz, M., Devarajan, K., Wessels, A., Soprano, D., et al. (2011). Thymine DNA glycosylase is essential for active DNA demethylation by linked deamination-base excision repair. Cell *146*, 67–79.

Coviello-McLaughlin, G.M., and Prowse, K.R. (1997). Telomere length regulation during postnatal development and ageing in Mus spretus. Nucleic Acids Res. *25*, 3051–3058.

Crean, A.J., Kopps, A.M., and Bonduriansky, R. (2014). Revisiting telegony: offspring inherit an acquired characteristic of their mother's previous mate. Ecol. Lett. *17*, 1545–1552.

Crichton, J.H., Dunican, D.S., Maclennan, M., Meehan, R.R., and Adams, I.R. (2014). Defending the genome from the enemy within: mechanisms of retrotransposon suppression in the mouse germline. Cell. Mol. Life Sci. CMLS *71*, 1581–1605.

Croce, L.D., and Helin, K. (2013). Transcriptional regulation by Polycomb group proteins. Nat. Struct. Mol. Biol. *20*, 1147–1155.

Cronkhite, J.T., Norlander, C., Furth, J.K., Levan, G., Garbers, D.L., and Hammer, R.E. (2005). Male and female germline specific expression of an EGFP reporter gene in a unique strain of transgenic rats. Dev. Biol. *284*, 171–183.

Curley, J.P., Mashoodh, R., and Champagne, F.A. (2011). Epigenetics and the origins of paternal effects. Horm. Behav. *59*, 306–314.

Cutler, D., Glaeser, E., and Shapiro, J. (2003). Why have Americans become more obese? Natl. Bur. Econ. Res. *w9446*.

Daujat, S., Weiss, T., Mohn, F., Lange, U.C., Ziegler-Birling, C., Zeissler, U., Lappe, M., Schübeler, D., Torres-Padilla, M.-E., and Schneider, R. (2009). H3K64 trimethylation marks heterochromatin and is dynamically remodeled during developmental reprogramming. Nat. Struct. Mol. Biol. *16*, 777–781.

Davidovich, C., Zheng, L., Goodrich, K.J., and Cech, T.R. (2013). Promiscuous RNA binding by Polycomb repressive complex 2. Nat. Struct. Mol. Biol. *20*, 1250–1257.

Davidovich, C., Wang, X., Cifuentes-Rojas, C., Goodrich, K.J., Gooding, A.R., Lee, J.T., and Cech, T.R. (2015). Toward a Consensus on the Binding Specificity and Promiscuity of PRC2 for RNA. Mol. Cell *57*, 552–558.

Davis, T.L., Yang, G.J., McCarrey, J.R., and Bartolomei, M.S. (2000). The H19 methylation imprint is erased and re-established differentially on the parental alleles during male germ cell development. Hum. Mol. Genet. *9*, 2885–2894.

Dawlaty, M.M., Ganz, K., Powell, B.E., Hu, Y.-C., Markoulaki, S., Cheng, A.W., Gao, Q., Kim, J., Choi, S.-W., Page, D.C., et al. (2011). Tet1 is dispensable for maintaining pluripotency and its loss is compatible with embryonic and postnatal development. Cell Stem Cell *9*, 166–175.

Dawlaty, M.M., Breiling, A., Le, T., Raddatz, G., Barrasa, M.I., Cheng, A.W., Gao, Q., Powell, B.E., Li, Z., Xu, M., et al. (2013). Combined deficiency of Tet1 and Tet2 causes epigenetic abnormalities but is compatible with postnatal development. Dev. Cell *24*, 310–323.

Dearden, L., and Balthasar, N. (2014). Sexual dimorphism in offspring glucose-sensitive hypothalamic gene expression and physiological responses to maternal high-fat diet feeding. Endocrinology *155*, 2144–2154.

Deng, X., Berletch, J.B., Nguyen, D.K., and Disteche, C.M. (2014). X chromosome regulation: diverse patterns in development, tissues and disease. Nat. Rev. Genet. *15*, 367–378.

Denham, J., O'Brien, B.J., Harvey, J.T., and Charchar, F.J. (2015). Genome-wide sperm DNA methylation changes after 3 months of exercise training in humans. Epigenomics 1–15.

Denomme, M.M., White, C.R., Gillio-Meina, C., MacDonald, W.A., Deroo, B.J., Kidder, G.M., and Mann, M.R. (2012). Compromised fertility disrupts Peg1 but not Snrpn and Peg3 imprinted methylation acquisition in mouse oocytes. Epigenomics Epigenetics *3*, 129.

Desai, M., Jellyman, J.K., Han, G., Beall, M., Lane, R.H., and Ross, M.G. (2014). Maternal obesity and high-fat diet program offspring metabolic syndrome. Am. J. Obstet. Gynecol. *211*, 237.e1–e237.e13.

Desai, M., Jellyman, J.K., and Ross, M.G. (2015). Epigenomics, gestational programming and risk of metabolic syndrome. Int. J. Obes.

Dobin, A., Davis, C.A., Schlesinger, F., Drenkow, J., Zaleski, C., Jha, S., Batut, P., Chaisson, M., and Gingeras, T.R. (2013). STAR: ultrafast universal RNA-seq aligner. Bioinforma. Oxf. Engl. *29*, 15–21.

Doerfler, W. (1983). DNA Methylation and Cene Activity. Annu. Rev. Biochem. *52*, 93–124.

Dong, X., and Weng, Z. (2013). The correlation between histone modifications and gene expression. Epigenomics *5*, 113–116.

Drake, A.J., Walker, B.R., and Seckl, J.R. (2005). Intergenerational consequences of fetal programming by in utero exposure to glucocorticoids in rats. Am. J. Physiol. Regul. Integr. Comp. Physiol. *288*, R34–R38.

Drake, A.J., Liu, L., Kerrigan, D., Meehan, R.R., and Seckl, J.R. (2011). Multigenerational programming in the glucocorticoid programmed rat is associated with generation-specific and parent of origin effects. Epigenetics Off. J. DNA Methylation Soc. *6*, 1334–1343.

Drickamer, Gowaty, and Holmes (2000). Free female mate choice in house mice affects reproductive success and offspring viability and performance. Anim. Behav. *59*, 371–378.

Dunn, G.A., and Bale, T.L. (2009). Maternal High-Fat Diet Promotes Body Length Increases and Insulin Insensitivity in Second-Generation Mice. Endocrinology *150*, 4999–5009.

Dunn, G.A., and Bale, T.L. (2011). Maternal High-Fat Diet Effects on Third-Generation Female Body Size via the Paternal Lineage. Endocrinology *152*, 2228–2236.

Eickbush, T.H. (1997). Telomerase and retrotransposons: which came first? Science *277*, 911–912.

Eisenberg, D.T.A. (2011). An evolutionary review of human telomere biology: The thrifty telomere hypothesis and notes on potential adaptive paternal effects. Am. J. Hum. Biol. *23*, 149–167.

Eisenberg, D.T.A., Hayes, M.G., and Kuzawa, C.W. (2012). Delayed paternal age of reproduction in humans is associated with longer telomeres across two generations of descendants. Proc. Natl. Acad. Sci. *109*, 10251–10256.

Ekamper, P., van Poppel, F., Stein, A.D., Bijwaard, G.E., and Lumey, L.H. (2015). Prenatal famine exposure and adult mortality from cancer, cardiovascular disease, and other causes through age 63 years. Am. J. Epidemiol. *181*, 271–279.

Encinas, G., Zogbi, C., and Stumpp, T. (2012). Detection of Four Germ Cell Markers in Rats during Testis Morphogenesis: Differences and Similarities with Mice. Cells Tissues Organs *195*, 443–455.

Erhuma, A., Salter, A.M., Sculley, D.V., Langley-Evans, S.C., and Bennett, A. (2007). Prenatal exposure to a low protein diet programmes disordered regulation of lipid metabolism in the ageing rat. Am. J. Physiol. Endocrinol. Metab. *292*, E1702–E1714.

Eskandar, M., Al-Asmari, M., Babu Chaduvula, S., Al-Shahrani, M., Al-Sunaidi, M., Almushait, M., Donia, O., and Al-Fifi, S. (2012). Impact of Male Obesity on Semen Quality and Serum Sex Hormones. Adv. Urol. *2012*.

Fadloun, A., Gras, S.L., Jost, B., Ziegler-Birling, C., Takahashi, H., Gorab, E., Carninci, P., and Torres-Padilla, M.-E. (2013). Chromatin signatures and retrotransposon profiling in mouse embryos reveal regulation of LINE-1 by RNA. Nat. Struct. Mol. Biol. *20*, 332–338.

Fan, Y., Liu, Y., Xue, K., Gu, G., Fan, W., Xu, Y., and Ding, Z. (2015). Diet-Induced Obesity in Male C57BL/6 Mice Decreases Fertility as a Consequence of Disrupted Blood-Testis Barrier. PloS One *10*, e0120775.

Fealy, S., Hure, A., Browne, G., and Prince, C. (2014). Developing a clinical care pathway for obese pregnant women: A quality improvement project. Women Birth J. Aust. Coll. Midwives *27*, e67–e71.

Ferguson-Smith, A.C., Cattanach, B.M., Barton, S.C., Beechey, C.V., and Surani, M.A. (1991). Embryological and molecular investigations of parental imprinting on mouse chromosome 7. Publ. Online 20 June 1991 Doi101038351667a0 *351*, 667–670.

Ferlin, A., Rampazzo, E., Rocca, M.S., Keppel, S., Frigo, A.C., Rossi, A.D., and Foresta, C. (2013). In young men sperm telomere length is related to sperm number and parental age. Hum. Reprod. *28*, 3370–3376.

Fernandez, I.D., Groth, S.W., Reschke, J.E., Graham, M.L., Strawderman, M., and Olson, C.M. (2015). eMoms: Electronically-mediated weight interventions for pregnant and postpartum women. Study design and baseline characteristics. Contemp. Clin. Trials *43*, 63–74.

Frank, M., Albuisson, J., Ranque, B., Golmard, L., Mazzella, J.-M., Bal-Theoleyre, L., Fauret, A.-L., Mirault, T., Denarié, N., Mousseaux, E., et al. (2015). The type of variants at the COL3A1 gene associates with the phenotype and severity of vascular Ehlers-Danlos syndrome. Eur. J. Hum. Genet. EJHG.

Franklin, T.B., Russig, H., Weiss, I.C., Gräff, J., Linder, N., Michalon, A., Vizi, S., and Mansuy, I.M. (2010). Epigenetic transmission of the impact of early stress across generations. Biol. Psychiatry *68*, 408–415.

Fu, Q., and Wang, P.J. (2014). Mammalian piRNAs. Spermatogenesis *4*.

Fullston, T., Palmer, N.O., Owens, J.A., Mitchell, M., Bakos, H.W., and Lane, M. (2012). Diet-induced paternal obesity in the absence of diabetes diminishes the reproductive health of two subsequent generations of mice. Hum. Reprod. *27*, 1391–1400.

Fullston, T., Teague, E.M.C.O., Palmer, N.O., DeBlasio, M.J., Mitchell, M., Corbett, M., Print, C.G., Owens, J.A., and Lane, M. (2013). Paternal obesity initiates metabolic disturbances in two generations of mice with incomplete penetrance to the F2 generation and alters the transcriptional profile of testis and sperm microRNA content. FASEB J. *27*, 4226–42243.

Gaikwad, A.B., Gupta, J., and Tikoo, K. (2010). Epigenetic changes and alteration of Fbn1 and Col3A1 gene expression under hyperglycaemic and hyperinsulinaemic conditions. Biochem. J. *432*, 333–341.

Galbraith, S., Daniel, J.A., and Vissel, B. (2010). A Study of Clustered Data and Approaches to Its Analysis. J. Neurosci. *30*, 10601–10608.

Galetzka, D., Weis, E., Tralau, T., Seidmann, L., and Haaf, T. (2007). Sex-specific windows for high mRNA expression of DNA methyltransferases 1 and 3A and methyl-CpG-binding domain proteins 2 and 4 in human fetal gonads. Mol. Reprod. Dev. *74*, 233–241.

Gan, H., Wen, L., Liao, S., Lin, X., Ma, T., Liu, J., Song, C., Wang, M., He, C., Han, C., et al. (2013). Dynamics of 5-hydroxymethylcytosine during mouse spermatogenesis. Nat. Commun. *4*.

Gapp, K., Jawaid, A., Sarkies, P., Bohacek, J., Pelczar, P., Prados, J., Farinelli, L., Miska, E., and Mansuy, I.M. (2014). Implication of sperm RNAs in transgenerational inheritance of the effects of early trauma in mice. Nat. Neurosci.

García-Calzón, S., Moleres, A., Marcos, A., Campoy, C., Moreno, L.A., Azcona-Sanjulián, M.C., Martínez-González, M.A., Martínez, J.A., Zalba, G., Marti, A., et al. (2014). Telomere length as a biomarker for adiposity changes after a multidisciplinary intervention in overweight/obese adolescents: the EVASYON study. PloS One *9*, e89828.

Gardiner-Garden, M., and Frommer, M. (1987). CpG islands in vertebrate genomes. J. Mol. Biol. *196*, 261–282.

Gardner, M., Bann, D., Wiley, L., Cooper, R., Hardy, R., Nitsch, D., Martin-Ruiz, C., Shiels, P., Sayer, A.A., Barbieri, M., et al. (2014). Gender and telomere length: systematic review and meta-analysis. Exp. Gerontol. *51*, 15–27.

Gaucher, J., Boussouar, F., Montellier, E., Curtet, S., Buchou, T., Bertrand, S., Hery, P., Jounier, S., Depaux, A., Vitte, A.-L., et al. (2012). Bromodomain-dependent stage-specific male genome programming by Brdt. EMBO J. *31*, 3809–3820.

Di Giacomo, M., Comazzetto, S., Saini, H., De Fazio, S., Carrieri, C., Morgan, M., Vasiliauskaite, L., Benes, V., Enright, A.J., and O'Carroll, D. (2013). Multiple Epigenetic Mechanisms and the piRNA Pathway Enforce LINE1 Silencing during Adult Spermatogenesis. Mol. Cell *50*, 601–608.

Gillberg, L., and Ling, C. (2015). The potential use of DNA methylation biomarkers to identify risk and progression of type 2 diabetes. Genomic Endocrinol. *6*, 43.

Girard, A., Sachidanandam, R., Hannon, G.J., and Carmell, M.A. (2006). A germline-specific class of small RNAs binds mammalian Piwi proteins. Nature *442*, 199–202.

Goldberg, A.D., Allis, C.D., and Bernstein, E. (2007). Epigenetics: a landscape takes shape. Cell *128*, 635–638.

Goll, M.G., Kirpekar, F., Maggert, K.A., Yoder, J.A., Hsieh, C.-L., Zhang, X., Golic, K.G., Jacobsen, S.E., and Bestor, T.H. (2006). Methylation of tRNAAsp by the DNA Methyltransferase Homolog Dnmt2. Science *311*, 395–398.

Govin, J., Escoffier, E., Rousseaux, S., Kuhn, L., Ferro, M., Thévenon, J., Catena, R., Davidson, I., Garin, J., Khochbin, S., et al. (2007). Pericentric heterochromatin reprogramming by new histone variants during mouse spermiogenesis. J. Cell Biol. *176*, 283–294.

Greenleaf, W.J. (2015). Assaying the epigenome in limited numbers of cells. Methods *72*, 51–56.

Gregory, R.I., Yan, K., Amuthan, G., Chendrimada, T., Doratotaj, B., Cooch, N., and Shiekhattar, R. (2004). The Microprocessor complex mediates the genesis of microRNAs. Nature *432*, 235–240.

Grima, J., and Cheng, C.Y. (2000). Testin induction: the role of cyclic 3',5'-adenosine monophosphate/protein kinase A signaling in the regulation of basal and lonidamine-induced testin expression by rat sertoli cells. Biol. Reprod. *63*, 1648–1660.

Grimes Jr., S.R., and Henderson, N. (1983). Acetylation of histones during spermatogenesis in the rat. Arch. Biochem. Biophys. *221*, 108–116.

Gruenbaum, Y., Cedar, H., and Razin, A. (1982). Substrate and sequence specificity of a eukaryotic DNA methylase. Nature *295*, 620–622.

Gu, T.-P., Guo, F., Yang, H., Wu, H.-P., Xu, G.-F., Liu, W., Xie, Z.-G., Shi, L., He, X., Jin, S., et al. (2011). The role of Tet3 DNA dioxygenase in epigenetic reprogramming by oocytes. Nature *477*, 606–610.

Guenatri, M., Duffié, R., Iranzo, J., Fauque, P., and Bourc'his, D. (2013). Plasticity in Dnmt3L-dependent and -independent modes of de novo methylation in the developing mouse embryo. Dev. Camb. Engl. *140*, 562–572.

Guerrero-Bosagna, C., Settles, M., Lucker, B., and Skinner, M.K. (2010). Epigenetic Transgenerational Actions of Vinclozolin on Promoter Regions of the Sperm Epigenome. PLoS ONE *5*, e13100.

Guh, D.P., Zhang, W., Bansback, N., Amarsi, Z., Birmingham, C.L., and Anis, A.H. (2009). The incidence of co-morbidities related to obesity and overweight: a systematic review and meta-analysis. BMC Public Health *9*, 88.

Guibert, S., Forné, T., and Weber, M. (2012). Global profiling of DNA methylation erasure in mouse primordial germ cells. Genome Res. *22*, 633–641.

Guo, F., Li, X., Liang, D., Li, T., Zhu, P., Guo, H., Wu, X., Wen, L., Gu, T.-P., Hu, B., et al. (2014a). Active and passive demethylation of male and female pronuclear DNA in the Mammalian zygote. Cell Stem Cell *15*, 447–458.

Guo, H., Zhu, P., Wu, X., Li, X., Wen, L., and Tang, F. (2013). Single-cell methylome landscapes of mouse embryonic stem cells and early embryos analyzed using reduced representation bisulfite sequencing. Genome Res. *23*, 2126–2135.

Guo, H., Zhu, P., Yan, L., Li, R., Hu, B., Lian, Y., Yan, J., Ren, X., Lin, S., Li, J., et al. (2014b). The DNA methylation landscape of human early embryos. Nature *511*, 606–610.

Guo, J.U., Su, Y., Shin, J.H., Shin, J., Li, H., Xie, B., Zhong, C., Hu, S., Le, T., Fan, G., et al. (2014c). Distribution, recognition and regulation of non-CpG methylation in the adult mammalian brain. Nat. Neurosci. *17*, 215–222.

Gupta, B., and Hawkins, R.D. (2015). Epigenomics of autoimmune diseases. Immunol. Cell Biol. *93*, 271–276.

Gur, Y., and Breitbart, H. (2006). Mammalian sperm translate nuclear-encoded proteins by mitochondrial-type ribosomes. Genes Dev. *20*, 411–416.

Hackett, J.A., Sengupta, R., Zylicz, J.J., Murakami, K., Lee, C., Down, T.A., and Surani, M.A. (2013). Germline DNA Demethylation Dynamics and Imprint Erasure Through 5-Hydroxymethylcytosine. Science *339*, 448–452.

Hägg, S., Fall, T., Ploner, A., Mägi, R., Fischer, K., Draisma, H.H., Kals, M., de Vries, P.S., Dehghan, A., Willems, S.M., et al. (2015). Adiposity as a cause of cardiovascular disease: a Mendelian randomization study. Int. J. Epidemiol.

Hahn, M.A., Qiu, R., Wu, X., Li, A.X., Zhang, H., Wang, J., Jui, J., Jin, S.-G., Jiang, Y., Pfeifer, G.P., et al. (2013). Dynamics of 5-hydroxymethylcytosine and chromatin marks in Mammalian neurogenesis. Cell Rep. *3*, 291–300.

Hajkova, P., Erhardt, S., Lane, N., Haaf, T., El-Maarri, O., Reik, W., Walter, J., and Surani, M.A. (2002). Epigenetic reprogramming in mouse primordial germ cells. Mech. Dev. *117*, 15–23.

Hajkova, P., Ancelin, K., Waldmann, T., Lacoste, N., Lange, U.C., Cesari, F., Lee, C., Almouzni, G., Schneider, R., and Surani, M.A. (2008). Chromatin dynamics during epigenetic reprogramming in the mouse germ line. Nature *452*, 877–881.

Hajkova, P., Jeffries, S.J., Lee, C., Miller, N., Jackson, S.P., and Surani, M.A. (2010). Genome-Wide Reprogramming in the Mouse Germ Line Entails the Base Excision Repair Pathway. Science *329*, 78–82.

Håkonsen, L.B., Thulstrup, A.M., Aggerholm, A.S., Olsen, J., Bonde, J.P., Andersen, C.Y., Bungum, M., Ernst, E.H., Hansen, M.L., Ernst, E.H., et al. (2011). Does weight loss improve semen quality and reproductive hormones? results from a cohort of severely obese men. Reprod. Health *8*, 24.

Hammiche, F., Laven, J.S.E., Twigt, J.M., Boellaard, W.P.A., Steegers, E.A.P., and Steegers-Theunissen, R.P. (2012). Body mass index and central adiposity are associated with sperm quality in men of subfertile couples. Hum. Reprod. *27*, 2365–2372.

Hammoud, A.O., Gibson, M., Peterson, C.M., Meikle, A.W., and Carrell, D.T. (2008). Impact of male obesity on infertility: a critical review of the current literature. Fertil. Steril. *90*, 897–904.

Hammoud, S.S., Nix, D.A., Zhang, H., Purwar, J., Carrell, D.T., and Cairns, B.R. (2009). Distinctive chromatin in human sperm packages genes for embryo development. Nature *460*, 473–478.

Hasegawa, Y., Brockdorff, N., Kawano, S., Tsutui, K., Tsutui, K., and Nakagawa, S. (2010). The Matrix Protein hnRNP U Is Required for Chromosomal Localization of Xist RNA. Dev. Cell *19*, 469–476.

Hawkins, S.M., Buchold, G.M., and Matzuk, M.M. (2011). Minireview: The roles of small RNA pathways in reproductive medicine. Mol. Endocrinol. Baltim. Md *25*, 1257–1279.

Hayashi, K., Lopes, S.M.C. de S., and Surani, M.A. (2007). Germ Cell Specification in Mice. Science *316*, 394–396.

Hayashi, K., Chuva de Sousa Lopes, S.M., Kaneda, M., Tang, F., Hajkova, P., Lao, K., O'Carroll, D., Das, P.P., Tarakhovsky, A., Miska, E.A., et al. (2008). MicroRNA Biogenesis Is Required for Mouse Primordial Germ Cell Development and Spermatogenesis. PLoS ONE *3*, e1738.

Hazzouri, M., Pivot-Pajot, C., Faure, A.-K., Usson, Y., Pelletier, R., Sèle, B., Khochbin, S., and Rousseaux, S. (2000). Regulated hyperacetylation of core histones during mouse spermatogenesis: Involvement of histone-deacetylases. Eur. J. Cell Biol. *79*, 950–960.

He, Y.-F., Li, B.-Z., Li, Z., Liu, P., Wang, Y., Tang, Q., Ding, J., Jia, Y., Chen, Z., Li, L., et al. (2011). Tet-mediated formation of 5-carboxylcytosine and its excision by TDG in mammalian DNA. Science *333*, 1303–1307.

Heslehurst, N., Rankin, J., Wilkinson, J.R., and Summerbell, C.D. (2010). A nationally representative study of maternal obesity in England, UK: trends in incidence and demographic inequalities in 619 323 births, 1989-2007. Int. J. Obes. 2005 *34*, 420–428.

Himes, K.P., Young, A., Koppes, E., Stolz, D., Barak, Y., Sadovsky, Y., and Chaillet, J.R. (2015). Loss of inherited genomic imprints in mice leads to severe disruption in placental lipid metabolism. Placenta.

Hjelmborg, J.B., Dalgård, C., Mangino, M., Spector, T.D., Halekoh, U., Möller, S., Kimura, M., Horvath, K., Kark, J.D., Christensen, K., et al. (2015). Paternal age and telomere length in twins: the germ stem cell selection paradigm. Aging Cell.

Horgan, C.E., Roumimper, H., Tucker, R., and Lechner, B.E. (2014). Altered decorin and Smad expression in human fetal membranes in PPROM. Biol. Reprod. *91*, 105.

Hotchkiss, R.D. (1948). The quantitative separation of purines, pyrimidines, and nucleosides by paper chromatography. J. Biol. Chem. *175*, 315–332.

Howell, C.Y., Bestor, T.H., Ding, F., Latham, K.E., Mertineit, C., Trasler, J.M., and Chaillet, J.R. (2001). Genomic Imprinting Disrupted by a Maternal Effect Mutation in the Dnmt1 Gene. Cell *104*, 829–838.

Hu, J.-L., Zhou, B.O., Zhang, R.-R., Zhang, K.-L., Zhou, J.-Q., and Xu, G.-L. (2009). The N-terminus of histone H3 is required for de novo DNA methylation in chromatin. Proc. Natl. Acad. Sci. *106*, 22187–22192.

Huang, J., Zhang, H., Wang, X., Dobbs, K.B., Yao, J., Qin, G., Whitworth, K., Walters, E.M., Prather, R.S., and Zhao, J. (2015). Impairment of preimplantation porcine embryo development by histone demethylase KDM5B knockdown through disturbance of bivalent H3K4me3-H3K27me3 modifications. Biol. Reprod. *92*, 72.

Hunt, S.C., Kimura, M., Hopkins, P.N., Carr, J.J., Heiss, G., Province, M.A., and Aviv, A. (2015). Leukocyte Telomere Length and Coronary Artery Calcium. Am. J. Cardiol.

Huntriss, J., Hinkins, M., Oliver, B., Harris, S. e., Beazley, J. c., Rutherford, A. j., Gosden, R. g., Lanzendorf, S. e., and Picton, H. m. (2004). Expression of mRNAs for DNA methyltransferases and methyl-CpG-binding proteins in the human female germ line, preimplantation embryos, and embryonic stem cells. Mol. Reprod. Dev. *67*, 323–336.

Van den Hurk, R., and Zhao, J. (2005). Formation of mammalian oocytes and their growth, differentiation and maturation within ovarian follicles. Theriogenology *63*, 1717–1751.

Ikeda, R., Shiura, H., Numata, K., Sugimoto, M., Kondo, M., Mise, N., Suzuki, M., Greally, J.M., and Abe, K. (2013). Large, Male Germ Cell-Specific Hypomethylated DNA Domains With Unique Genomic and Epigenomic Features on the Mouse X Chromosome. DNA Res. *20*, 549–565.

Iqbal, K., Jin, S.-G., Pfeifer, G.P., and Szabó, P.E. (2011). Reprogramming of the paternal genome upon fertilization involves genome-wide oxidation of 5-methylcytosine. Proc. Natl. Acad. Sci. U. S. A. *108*, 3642–3647.

Ito, S., D'Alessio, A.C., Taranova, O.V., Hong, K., Sowers, L.C., and Zhang, Y. (2010). Role of Tet proteins in 5mC to 5hmC conversion, ES-cell self-renewal and inner cell mass specification. Nature *466*, 1129–1133.

Ito, S., Shen, L., Dai, Q., Wu, S.C., Collins, L.B., Swenberg, J.A., He, C., and Zhang, Y. (2011). Tet proteins can convert 5-methylcytosine to 5-formylcytosine and 5-carboxylcytosine. Science *333*, 1300–1303.

Jääskeläinen, A., Pussinen, J., Nuutinen, O., Schwab, U., Pirkola, J., Kolehmainen, M., Järvelin, M.-R., and Laitinen, J. (2011). Intergenerational transmission of overweight among Finnish adolescents and their parents: a 16-year follow-up study. Int. J. Obes. *35*, 1289–1294.

Jähner, D., Stuhlmann, H., Stewart, C.L., Harbers, K., Löhler, J., Simon, I., and Jaenisch, R. (1982). De novo methylation and expression of retroviral genomes during mouse embryogenesis. Nature *298*, 623–628.

Jenkins, T.G., Aston, K.I., Cairns, B.R., and Carrell, D.T. (2013). Paternal aging and associated intraindividual alterations of global sperm 5-methylcytosine and 5-hydroxymethylcytosine levels. Fertil. Steril.

Jensen, T.K., Andersson, A.-M., Jørgensen, N., Andersen, A.-G., Carlsen, E., Petersen, J. ørge. H., and Skakkebæk, N.E. (2004). Body mass index in relation to semen quality and reproductive hormonesamong 1,558 Danish men. Fertil. Steril. *82*, 863–870.

Jiang, L., Zhang, J., Wang, J.-J., Wang, L., Zhang, L., Li, G., Yang, X., Ma, X., Sun, X., Cai, J., et al. (2013). Sperm, but Not Oocyte, DNA Methylome Is Inherited by Zebrafish Early Embryos. Cell *153*, 773–784.

Jimenez-Chillaron, J.C., Isganaitis, E., Charalambous, M., Gesta, S., Pentinat-Pelegrin, T., Faucette, R.R., Otis, J.P., Chow, A., Diaz, R., Ferguson-Smith, A., et al. (2009). Intergenerational transmission of glucose intolerance and obesity by in utero undernutrition in mice. Diabetes *58*, 460–468.

Johansson, S., Villamor, E., Altman, M., Bonamy, A.-K.E., Granath, F., and Cnattingius, S. (2014). Maternal overweight and obesity in early pregnancy and risk of infant mortality: a population based cohort study in Sweden. BMJ *349*, g6572.

Johnson, T.B., and Coghill, R.D. (1925). RESEARCHES ON PYRIMIDINES. C111. THE DISCOVERY OF 5-METHYL-CYTOSINE IN TUBERCULINIC ACID, THE NUCLEIC ACID OF THE TUBERCLE BACILLUS1. J. Am. Chem. Soc. *47*, 2838–2844.

Jones, T.H., Arver, S., Behre, H.M., Buvat, J., Meuleman, E., Moncada, I., Morales, A.M., Volterrani, M., Yellowlees, A., Howell, J.D., et al. (2011). Testosterone replacement in hypogonadal men with type 2 diabetes and/or metabolic syndrome (the TIMES2 study). Diabetes Care *34*, 828–837.

Jurka, J., Kapitonov, V.V., Pavlicek, A., Klonowski, P., Kohany, O., and Walichiewicz, J. (2005). Repbase Update, a database of eukaryotic repetitive elements. Cytogenet. Genome Res. *110*, 462–467.

Kaati, G., Bygren, L.O., Pembrey, M., and Sjöström, M. (2007). Transgenerational response to nutrition, early life circumstances and longevity. Eur. J. Hum. Genet. *15*, 784–790.

Kageyama, S., Liu, H., Kaneko, N., Ooga, M., Nagata, M., and Aoki, F. (2007). Alterations in epigenetic modifications during oocyte growth in mice. Reproduction *133*, 85–94.

Kagiwada, S., Kurimoto, K., Hirota, T., Yamaji, M., and Saitou, M. (2013). Replication-coupled passive DNA demethylation for the erasure of genome imprints in mice. EMBO J. *32*, 340–353.

Kalish, J.M., Jiang, C., and Bartolomei, M.S. (2014). Epigenetics and imprinting in human disease. Int. J. Dev. Biol. *58*, 291–298.

Kaneko, S., Son, J., Shen, S.S., Reinberg, D., and Bonasio, R. (2013). PRC2 binds active promoters and contacts nascent RNAs in embryonic stem cells. Nat. Struct. Mol. Biol. *20*, 1258–1264.

Kappeler, L., Zizzari, P., Grouselle, D., Epelbaum, J., and Bluet-Pajot, M.T. (2004). Plasma and hypothalamic peptide-hormone levels regulating somatotroph function and energy balance in fed and fasted states: a comparative study in four strains of rats. J. Neuroendocrinol. *16*, 980–988.

Kasper, H., Thiel, H., and Ehl, M. (1973). Response of body weight to a low carbohydrate, high fat diet in normal and obese subjects. Am. J. Clin. Nutr. *26*, 197–204.

Kato, Y., Kaneda, M., Hata, K., Kumaki, K., Hisano, M., Kohara, Y., Okano, M., Li, E., Nozaki, M., and Sasaki, H. (2007). Role of the Dnmt3 family in de novo methylation of imprinted and repetitive sequences during male germ cell development in the mouse. Hum. Mol. Genet. *16*, 2272–2280.

Kazazian, H.H. (2004). Mobile Elements: Drivers of Genome Evolution. Science *303*, 1626–1632.

Keniry, A., Oxley, D., Monnier, P., Kyba, M., Dandolo, L., Smits, G., and Reik, W. (2012). The H19 lincRNA is a developmental reservoir of miR-675 that suppresses growth and Igf1r. Nat. Cell Biol. *14*, 659–665.

Kiani, J., Grandjean, V., Liebers, R., Tuorto, F., Ghanbarian, H., Lyko, F., Cuzin, F., and Rassoulzadegan, M. (2013). RNA-Mediated Epigenetic Heredity Requires the Cytosine Methyltransferase Dnmt2. PLoS Genet *9*, e1003498.

Kilcoyne, K.R., Smith, L.B., Atanassova, N., Macpherson, S., McKinnell, C., van den Driesche, S., Jobling, M.S., Chambers, T.J.G., De Gendt, K., Verhoeven, G., et al. (2014). Fetal programming of adult Leydig cell function by androgenic effects on stem/progenitor cells. Proc. Natl. Acad. Sci. U. S. A. *111*, E1924–E1932.

Kim, J.K. (2009). Hyperinsulinemic-euglycemic clamp to assess insulin sensitivity in vivo. Methods Mol. Biol. Clifton NJ *560*, 221–238.

King, V., Dakin, R.S., Liu, L., Hadoke, P.W.F., Walker, B.R., Seckl, J.R., Norman, J.E., and Drake, A.J. (2013). Maternal Obesity Has Little Effect on the Immediate Offspring but Impacts on the Next Generation. Endocrinology *154*, 2514–2524.

King, V., Norman, J.E., Seckl, J.R., and Drake, A.J. (2014). Post-weaning diet determines metabolic risk in mice exposed to overnutrition in early life. Reprod. Biol. Endocrinol. RBE *12*, 73.

Van der Klaauw, A., Keogh, J., Henning, E., Stephenson, C., Trowse, V.M., Fletcher, P., and Farooqi, S. (2015). Role of melanocortin signalling in the preference for dietary macronutrients in human beings. The Lancet *385*, S12.

Ko, M., Bandukwala, H.S., An, J., Lamperti, E.D., Thompson, E.C., Hastie, R., Tsangaratou, A., Rajewsky, K., Koralov, S.B., and Rao, A. (2011). Ten-Eleven-Translocation 2 (TET2) negatively regulates homeostasis and differentiation of hematopoietic stem cells in mice. Proc. Natl. Acad. Sci. *108*, 14566–14571.

Koh, K.P., Yabuuchi, A., Rao, S., Huang, Y., Cunniff, K., Nardone, J., Laiho, A., Tahiliani, M., Sommer, C.A., Mostoslavsky, G., et al. (2011). Tet1 and Tet2 regulate 5-

hydroxymethylcytosine production and cell lineage specification in mouse embryonic stem cells. Cell Stem Ceil *8*, 200–213.

Koopman, P., Gubbay, J., Vivian, N., Goodfellow, P., and Lovell-Badge, R. (1991). Male development of chromosomally female mice transgenic for Sry. Publ. Online 09 May 1991 Doi101038351117a0 *351*, 117–121.

Korhonen, H.M., Meikar, O., Yadav, R.P., Papaioannou, M.D., Romero, Y., Da Ros, M., Herrera, P.L., Toppari, J., Nef, S., and Kotaja, N. (2011). Dicer Is Required for Haploid Male Germ Cell Differentiation in Mice. PLoS ONE *6*, e24821.

Kotaja, N. (2014). MicroRNAs and spermatogenesis. Fertil. Steril. *101*, 1552–1562.

Kouzarides, T. (2007). Chromatin Modifications and Their Function. Cell *128*, 693–705.

Kozomara, A., and Griffiths-Jones, S. (2014). miRBase: annotating high confidence microRNAs using deep sequencing data. Nucleic Acids Res. *42*, D68–D73.

Kraus, P., Sivakamasundari, V., Lim, S.L., Xing, X., Lipovich, L., and Lufkin, T. (2013). Making sense of Dlx1 antisense RNA. Dev. Biol. *376*, 224–235.

Kriaucionis, S., and Heintz, N. (2009). The Nuclear DNA Base 5-Hydroxymethylcytosine Is Present in Purkinje Neurons and the Brain. Science *324*, 929–930.

Kristensen, D.G., Nielsen, J.E., Jørgensen, A., Skakkebæk, N.E., Meyts, E.R.-D., and Almstrup, K. (2013). Evidence that active demethylation mechanisms maintain the genome of carcinoma in situ cells hypomethylated in the adult testis. Br. J. Cancer.

Kuramochi-Miyagawa, S., Watanabe, T., Gotoh, K., Totoki, Y., Toyoda, A., Ikawa, M., Asada, N., Kojima, K., Yamaguchi, Y., Ijiri, T.W., et al. (2008). DNA methylation of retrotransposon genes is regulated by Piwi family members MILI and MIWI2 in murine fetal testes. Genes Dev. *22*, 908–917.

Lahn, B.T., Tang, Z.L., Zhou, J., Barndt, R.J., Parvinen, M., Allis, C.D., and Page, D.C. (2002). Previously uncharacterized histone acetyltransferases implicated in mammalian spermatogenesis. Proc. Natl. Acad. Sci. *99*, 8707–8712.

Laiho, A., Kotaja, N., Gyenesei, A., and Sironen, A. (2013). Transcriptome profiling of the murine testis during the first wave of spermatogenesis. PloS One *8*, e61558.

Laird, N.M., and Ware, J.H. (1982). Random-effects models for longitudinal data. Biometrics *38*, 963–974.

Laker, R.C., Lillard, T.S., Okutsu, M., Zhang, M., Hoehn, K.L., Connelly, J.J., and Yan, Z. (2014). Exercise prevents maternal high-fat diet-induced hypermethylation of the Pgc-1α gene and age-dependent metabolic dysfunction in the offspring. Diabetes *63*, 1605–1611.

Laland, K., Uller, T., Feldman, M., Sterelny, K., Müller, G.B., Moczek, A., Jablonka, E., Odling-Smee, J., Wray, G.A., Hoekstra, H.E., et al. (2014). Does evolutionary theory need a rethink? Nature *514*, 161–164.

Lamarck (1914). Zoological philosophy;: Lamarck, Jean Baptiste Pierre Antoine de Monet de,: Free Download & Streaming.

Lambrot, R., Xu, C., Saint-Phar, S., Chountalos, G., Cohen, T., Paquet, M., Suderman, M., Hallett, M., and Kimmins, S. (2013). Low paternal dietary folate alters the mouse sperm epigenome and is associated with negative pregnancy outcomes. Nat. Commun. *4*, 2889.

Latos, P.A., Pauler, F.M., Koerner, M.V., Şenergin, H.B., Hudson, Q.J., Stocsits, R.R., Allhoff, W., Stricker, S.H., Klement, R.M., Warczok, K.E., et al. (2012). Airn Transcriptional Overlap, But Not Its lncRNA Products, Induces Imprinted Igf2r Silencing. Science *338*, 1469–1472.

Law, D.C.G., Maclehose, R.F., and Longnecker, M.P. (2007). Obesity and time to pregnancy. Hum. Reprod. *22*, 414–420.

Lawson, K.A., Dunn, N.R., Roelen, B.A., Zeinstra, L.M., Davis, A.M., Wright, C.V., Korving, J.P., and Hogan, B.L. (1999). Bmp4 is required for the generation of primordial germ cells in the mouse embryo. Genes Dev. *13*, 424–436.

Lee, R.C., Feinbaum, R.L., and Ambros, V. (1993). The C. elegans heterochronic gene lin-4 encodes small RNAs with antisense complementarity to lin-14. Cell *75*, 843–854.

Lee, Y., Ahn, C., Han, J., Choi, H., Kim, J., Yim, J., Lee, J., Provost, P., Rådmark, O., Kim, S., et al. (2003). The nuclear RNase III Drosha initiates microRNA processing. Nature *425*, 415–419.

Lee, Y., Kim, M., Han, J., Yeom, K.-H., Lee, S., Baek, S.H., and Kim, V.N. (2004). MicroRNA genes are transcribed by RNA polymerase II. EMBO J. *23*, 4051–4060.

Lees-Murdock, D.J., De Felici, M., and Walsh, C.P. (2003). Methylation dynamics of repetitive DNA elements in the mouse germ cell lineage. Genomics *82*, 230–237.

Lees-Murdock, D.J., Lau, H.-T., Castrillon, D.H., De Felici, M., and Walsh, C.P. (2008). DNA methyltransferase loading, but not de novo methylation, is an oocyte-autonomous process stimulated by SCF signalling. Dev. Biol. *321*, 238–250.

Lehnertz, B., Ueda, Y., Derijck, A.A.H.A., Braunschweig, U., Perez-Burgos, L., Kubicek, S., Chen, T., Li, E., Jenuwein, T., and Peters, A.H.F.M. (2003). Suv39h-mediated histone H3 lysine 9 methylation directs DNA methylation to major satellite repeats at pericentric heterochromatin. Curr. Biol. CB *13*, 1192–1200.

Lei, H., Oh, S.P., Okano, M., Juttermann, R., Goss, K.A., Jaenisch, R., and Li, E. (1996). De novo DNA cytosine methyltransferase activities in mouse embryonic stem cells. Development *122*, 3195–3205.

Levine, A.S., and Morley, J.E. (1981). Stress-induced eating in rats. Am. J. Physiol. *241*, R72–R76.

Li, E., Beard, C., and Jaenisch, R. (1993). Role for DNA methylation in genomic imprinting. Publ. Online 25 Dec. 1993 Doi101038366362a0 *366*, 362–365.

Li, J., Chen, X., McClusky, R., Ruiz-Sundstrom, M., Itoh, Y., Umar, S., Arnold, A.P., and Eghbali, M. (2014). The number of X chromosomes influences protection from cardiac ischaemia/reperfusion injury in mice: one X is better than two. Cardiovasc. Res. *102*, 375–384.

Li, J.-H., Liu, S., Zheng, L.-L., Wu, J., Sun, W.-J., Wang, Z.-L., Zhou, H., Qu, L.-H., and Yang, J.-H. (2015a). Discovery of protein–lncRNA interactions by integrating large-scale CLIP-Seq and RNA-Seq datasets. Bioinforma. Comput. Biol. *2*, 88.

Li, J.-Y., Lees-Murdock, D.J., Xu, G.-L., and Walsh, C.P. (2004). Timing of establishment of paternal methylation imprints in the mouse. Genomics *84*, 952–960.

Li, S., Hansman, R., Newbold, R., Davis, B., McLachlan, J.A., and Barrett, J.C. (2003). Neonatal diethylstilbestrol exposure induces persistent elevation of c-fos expression and hypomethylation in its exon-4 in mouse uterus. Mol. Carcinog. *38*, 78–84.

Li, S.-Y., Liu, Y., Sigmon, V.K., McCort, A., and Ren, J. (2005a). High-fat diet enhances visceral advanced glycation end products, nuclear O-Glc-Nac modification, p38 mitogen-activated protein kinase activation and apoptosis. Diabetes Obes. Metab. *7*, 448–454.

Li, T., Yang, D., Li, J., Tang, Y., Yang, J., and Le, W. (2015b). Critical role of Tet3 in neural progenitor cell maintenance and terminal differentiation. Mol. Neurobiol. *51*, 142–154.

Li, Y., Putnam-Lawson, C.A., Knapp-Hoch, H., Friel, P.J., Mitchell, D., Hively, R., and Griswold, M.D. (2005b). Immunolocalization and regulation of cystatin 12 in mouse testis and epididymis. Biol. Reprod. *73*, 872–880.

Li, Y., Liu, L., Wang, B., Xiong, J., Li, Q., Wang, J., and Chen, D. (2013). Impairment of reproductive function in a male rat model of non-alcoholic fatty liver disease and beneficial effect of N-3 fatty acid supplementation. Toxicol. Lett.

Liao, Y., Smyth, G.K., and Shi, W. (2013). featureCounts: an efficient general-purpose program for assigning sequence reads to genomic features. Bioinformatics btt656.

Lister, R., Mukamel, E.A., Nery, J.R., Urich, M., Puddifoot, C.A., Johnson, N.D., Lucero, J., Huang, Y., Dwork, A.J., Schultz, M.D., et al. (2013). Global Epigenomic Reconfiguration During Mammalian Brain Development. Science *341*, 1237905.

Liu, D., Li, L., Fu, H., Li, S., and Li, J. (2012). Inactivation of Dicer1 has a severe cumulative impact on the formation of mature germ cells in mouse testes. Biochem. Biophys. Res. Commun. *422*, 114–120.

Liu, S., Brind'Amour, J., Karimi, M.M., Shirane, K., Bogutz, A., Lefebvre, L., Sasaki, H., Shinkai, Y., and Lorincz, M.C. (2014). Setdb1 is required for germline development and silencing of H3K9me3-marked endogenous retroviruses in primordial germ cells. Genes Dev. *28*, 2041–2055.

Livak, K.J., and Schmittgen, T.D. (2001). Analysis of Relative Gene Expression Data Using Real-Time Quantitative PCR and the 2−ΔΔCT Method. Methods *25*, 402–408.

Locke, A.E., Kahali, B., Berndt, S.I., Justice, A.E., Pers, T.H., Day, F.R., Powell, C., Vedantam, S., Buchkovich, M.L., Yang, J., et al. (2015). Genetic studies of body mass index yield new insights for obesity biology. Nature *518*, 197–206.

Lodde, V., Modina, S., Maddox-Hyttel, P., Franciosi, F., Lauria, A., and Luciano, A.M. (2008). Oocyte morphology and transcriptional silencing in relation to chromatin remodeling during the final phases of bovine oocyte growth. Mol. Reprod. Dev. *75*, 915–924.

Lorsbach, R.B., Moore, J., Mathew, S., Raimondi, S.C., Mukatira, S.T., and Downing, J.R. (2003). TET1, a member of a novel protein family, is fused to MLL in acute myeloid leukemia containing the t(10;11)(q22;q23). Leukemia *17*, 637–641.

Love, M.I., Huber, W., and Anders, S. (2014). Moderated estimation of fold change and dispersion for RNA-seq data with DESeq2. Genome Biol. *15*, 550.

Lovell-Badge, R., and Robertson, E. (1990). XY female mice resulting from a heritable mutation in the primary testis-determining gene, Tdy. Development *109*, 635–646.

Luciano, A.M., Franciosi, F., Dieci, C., and Lodde, V. (2014). Changes in large-scale chromatin structure and function during oogenesis: A journey in company with follicular cells. Anim. Reprod. Sci. *149*, 3–10.

Luk, A.C.-S., Chan, W.-Y., Rennert, O.M., and Lee, T.-L. (2014). Long noncoding RNAs in spermatogenesis: insights from recent high-throughput transcriptome studies. Reproduction *147*, R131–R141.

Lund, E., Güttinger, S., Calado, A., Dahlberg, J.E., and Kutay, U. (2004). Nuclear Export of MicroRNA Precursors. Science *303*, 95–98.

Lundsberg, L.S., Pal, L., Gariepy, A.M., Xu, X., Chu, M.C., and Illuzzi, J.L. (2014). Knowledge, attitudes, and practices regarding conception and fertility: a population-based survey among reproductive-age United States women. Fertil. Steril. *101*, 767–774.

Luo, Z., Liu, Y., Chen, L., Ellis, M., Li, M., Wang, J., Zhang, Y., Fu, P., Wang, K., Li, X., et al. (2015). microRNA profiling in three main stages during porcine spermatogenesis. J. Assist. Reprod. Genet. *32*, 451–460.

Lyon, M.F. (1961). Gene action in the X-chromosome of the mouse (Mus musculus L.). Nature *190*, 372–373.

Ma, P., and Schultz, R.M. (2013). Histone Deacetylase 2 (HDAC2) Regulates Chromosome Segregation and Kinetochore Function via H4K16 Deacetylation during Oocyte Maturation in Mouse. PLoS Genet *9*, e1003377.

Ma, D., Zhu, W., Hu, S., Yu, X., and Yang, Y. (2013). Association between oxidative stress and telomere length in Type 1 and Type 2 diabetic patients. J. Endocrinol. Invest. *36*, 1032–1037.

Ma, J., Prince, A.L., Bader, D., Hu, M., Ganu, R., Baquero, K., Blundell, P., Alan Harris, R., Frias, A.E., Grove, K.L., et al. (2014). High-fat maternal diet during pregnancy persistently alters the offspring microbiome in a primate model. Nat. Commun. *5*, 3889.

Ma, P., Pan, H., Montgomery, R.L., Olson, E.N., and Schultz, R.M. (2012). Compensatory functions of histone deacetylase 1 (HDAC1) and HDAC2 regulate transcription and apoptosis during mouse oocyte development. Proc. Natl. Acad. Sci. *109*, E481–E489.

Malfait, F., and De Paepe, A. (2005). Molecular genetics in classic Ehlers-Danlos syndrome. Am. J. Med. Genet. C Semin. Med. Genet. *139C*, 17–23.

Manku, G., and Culty, M. (2015). Mammalian gonocyte and spermatogonia differentiation: recent advances and remaining challenges. Reproduction *149*, R139–R157.

Marco, A., Kisliouk, T., Tabachnik, T., Meiri, N., and Weller, A. (2014). Overweight and CpG methylation of the Pomc promoter in offspring of high-fat-diet-fed dams are not "reprogrammed" by regular chow diet in rats. FASEB J. Off. Publ. Fed. Am. Soc. Exp. Biol.

Marczylo, E.L., Amoako, A.A., Konje, J.C., Gant, T.W., and Marczylo, T.H. (2012). Smoking induces differential miRNA expression in human spermatozoa: A potential transgenerational epigenetic concern? Epigenetics *7*, 432–439.

Marques, C.J., João Pinho, M., Carvalho, F., Bièche, I., Barros, A., and Sousa, M. (2011). DNA methylation imprinting marks and DNA methyltransferase expression in human spermatogenic cell stages. Epigenetics *6*, 1354–1361.

Martens, J.A., Laprade, L., and Winston, F. (2004). Intergenic transcription is required to repress the Saccharomyces cerevisiae SER3 gene. Nature *429*, 571–574.

Martianov, I., Brancorsini, S., Catena, R., Gansmuller, A., Kotaja, N., Parvinen, M., Sassone-Corsi, P., and Davidson, I. (2005). Polar nuclear localization of H1T2, a histone H1 variant, required for spermatid elongation and DNA condensation during spermiogenesis. Proc. Natl. Acad. Sci. U. S. A. *102*, 2808–2813.

Martin, S.A.L., Jameson, C.H., Allan, S.M., and Lawrence, C.B. (2014). Maternal high-fat diet worsens memory deficits in the triple-transgenic (3xTgAD) mouse model of Alzheimer's disease. PloS One *9*, e99226.

Martin-Rodriguez, E., Guillen-Grima, F., Martí, A., and Brugos-Larumbe, A. (2015). Comorbidity associated with obesity in a large population: The APNA study. Obes. Res. Clin. Pract.

Matzuk, M.M., McKeown, M.R., Filippakopoulos, P., Li, Q., Ma, L., Agno, J.E., Lemieux, M.E., Picaud, S., Yu, R.N., Qi, J., et al. (2012). Small-molecule inhibition of BRDT for male contraception. Cell *150*, 673–684.

McDonald, S.D., Park, C.K., Pullenayegum, E., Bracken, K., Sword, W., McDonald, H., Neupane, B., Taylor, V.H., Beyene, J., Mueller, V., et al. (2015). Knowledge translation tool to improve pregnant women's awareness of gestational weight gain goals and risks of gaining outside recommendations: a non-randomized intervention study. BMC Pregnancy Childbirth *15*, 105.

McElreavey, K., Vilain, E., Abbas, N., Herskowitz, I., and Fellous, M. (1993). A regulatory cascade hypothesis for mammalian sex determination: SRY represses a negative regulator of male development. Proc. Natl. Acad. Sci. U. S. A. *90*, 3368–3372.

McGraw, S., Oakes, C.C., Martel, J., Cirio, M.C., de Zeeuw, P., Mak, W., Plass, C., Bartolomei, M.S., Chaillet, J.R., and Trasler, J.M. (2013). Loss of DNMT1o disrupts imprinted X chromosome inactivation and accentuates placental defects in females. PLoS Genet. *9*, e1003873.

McGraw, S., Zhang, J.X., Farag, M., Chan, D., Caron, M., Konermann, C., Oakes, C.C., Mohan, K.N., Plass, C., Pastinen, T., et al. (2015). Transient DNMT1 suppression reveals hidden heritable marks in the genome. Nucleic Acids Res.

McKinnell, C., Mitchell, R.T., Morris, K., Anderson, R.A., Kelnar, C.J.H., Wallace, W.H., and Sharpe, R.M. (2013). Perinatal germ cell development and differentiation in the male marmoset (Callithrix jacchus): similarities with the human and differences from the rat. Hum. Reprod. Oxf. Engl. *28*, 886–896.

McPherson, S.M.G., and Longo, F.J. (1993). Nicking of Rat Spermatid and Spermatozoa DNA: Possible Involvement of DNA Topoisomerase II. Dev. Biol. *158*, 122–130.

McPherson, N.O., Fullston, T., Bakos, H.W., Setchell, B.P., and Lane, M. (2014). Obese father's metabolic state, adiposity, and reproductive capacity indicate son's reproductive health. Fertil. Steril.

McPherson, N.O., Owens, J.A., Fullston, T., and Lane, M. (2015). Preconception diet or exercise intervention in obese fathers normalizes sperm microRNA profile and metabolic syndrome in female offspring. Am. J. Physiol. - Endocrinol. Metab. *308*, E805–E821.

Meisel, A., Harms, C., Yildirim, F., Bösel, J., Kronenberg, G., Harms, U., Fink, K.B., and Endres, M. (2006). Inhibition of histone deacetylation protects wild-type but not gelsolin-deficient neurons from oxygen/glucose deprivation. J. Neurochem. *98*, 1019–1031.

Meistrich, M.L., Mohapatra, B., Shirley, C.R., and Zhao, M. (2003). Roles of transition nuclear proteins in spermiogenesis. Chromosoma *111*, 483–488.

Melo, A.M., Benatti, R.O., Ignacio-Souza, L.M., Okino, C., Torsoni, A.S., Milanski, M., Velloso, L.A., and Torsoni, M.A. (2014). Hypothalamic endoplasmic reticulum stress and insulin resistance in offspring of mice dams fed high-fat diet during pregnancy and lactation. Metabolism. *63*, 682–692.

Mendes-da-Silva, C., Lemes, S.F., Baliani, T. da S., Versutti, M.D., and Torsoni, M.A. (2015). Increased expression of Hes5 protein in Notch signaling pathway in the hippocampus of mice offspring of dams fed a high-fat diet during pregnancy and suckling. Int. J. Dev. Neurosci. *40*, 35–42.

Mertineit, C., Yoder, J.A., Taketo, T., Laird, D.W., Trasler, J.M., and Bestor, T.H. (1998). Sex-specific exons control DNA methyltransferase in mammalian germ cells. Development *125*, 889–897.

Messerschmidt, D.M., Knowles, B.B., and Solter, D. (2014). DNA methylation dynamics during epigenetic reprogramming in the germline and preimplantation embryos. Genes Dev. *28*, 812–828.

Mielnicki, L.M., Ying, A.M., Head, K.L., Asch, H.L., and Asch, B.B. (1999). Epigenetic regulation of gelsolin expression in human breast cancer cells. Exp. Cell Res. *249*, 161–176.

Miller, C.N., Kauffman, T.G., Cooney, P.T., Ramseur, K.R., and Brown, L.M. (2011). Comparison of DEXA and QMR for assessing fat and lean body mass in adult rats. Physiol. Behav. *103*, 117–121.

Miller, D., Brinkworth, M., and Iles, D. (2010). Paternal DNA packaging in spermatozoa: more than the sum of its parts? DNA, histones, protamines and epigenetics. Reproduction *139*, 287–301.

Mitchell, R.T., Cowan, G., Morris, K.D., Anderson, R.A., Fraser, H.M., Mckenzie, K.J., Wallace, W.H.B., Kelnar, C.J.H., Saunders, P.T.K., and Sharpe, R.M. (2008). Germ cell differentiation in the marmoset (Callithrix jacchus) during fetal and neonatal life closely parallels that in the human. Hum. Reprod. *23*, 2755–2765.

Mitra, A., Crump, E.M., Alvers, K.M., Robertson, K.L., and Rowland, N.E. (2010). Effect of high-fat diet on stress responsiveness in borderline hypertensive rats. Stress *14*, 42–52.

Mizuno, Y., Sotomaru, Y., Katsuzawa, Y., Kono, T., Meguro, M., Oshimura, M., Kawai, J., Tomaru, Y., Kiyosawa, H., Nikaido, I., et al. (2002). Asb4, Ata3, and Dcn are novel imprinted genes identified by high-throughput screening using RIKEN cDNA microarray. Biochem. Biophys. Res. Commun. *290*, 1499–1505.

Molaro, A., Falciatori, I., Hodges, E., Aravin, A.A., Marran, K., Rafii, S., McCombie, W.R., Smith, A.D., and Hannon, G.J. (2014). Two waves of de novo methylation during mouse germ cell development. Genes Dev. *28*, 1544–1549.

Monk, M., and McLaren, A. (1981). X-chromosome activity in foetal germ cells of the mouse. J. Embryol. Exp. Morphol. *63*, 75–84.

Monk, D., Arnaud, P., Apostolidou, S., Hills, F.A., Kelsey, G., Stanier, P., Feil, R., and Moore, G.E. (2006). Limited evolutionary conservation of imprinting in the human placenta. Proc. Natl. Acad. Sci. U. S. A. *103*, 6623–6628.

Moody, A. (2014). Adult anthropometric measures, overweight and obesity.

Moore, G.E., Ishida, M., Demetriou, C., Al-Olabi, L., Leon, L.J., Thomas, A.C., Abu-Amero, S., Frost, J.M., Stafford, J.L., Chaoqun, Y., et al. (2015). The role and interaction of imprinted genes in human fetal growth. Philos. Trans. R. Soc. Lond. B Biol. Sci. *370*, 20140074.

Moran-Crusio, K., Reavie, L., Shih, A., Abdel-Wahab, O., Ndiaye-Lobry, D., Lobry, C., Figueroa, M.E., Vasanthakumar, A., Patel, J., Zhao, X., et al. (2011). Tet2 loss leads to increased hematopoietic stem cell self-renewal and myeloid transformation. Cancer Cell *20*, 11–24.

Morgan, C.P., and Bale, T.L. (2011). Early prenatal stress epigenetically programs dysmasculinization in second-generation offspring via the paternal lineage. J. Neurosci. Off. J. Soc. Neurosci. *31*, 11748–11755.

Muñoz-López, M., and García-Pérez, J.L. (2010). DNA Transposons: Nature and Applications in Genomics. Curr. Genomics *11*, 115–128.

Murchison, E.P., Stein, P., Xuan, Z., Pan, H., Zhang, M.Q., Schultz, R.M., and Hannon, G.J. (2007). Critical roles for Dicer in the female germline. Genes Dev. *21*, 682–693.

Mutsaerts, M. a. Q., Groen, H., Huiting, H.G., Kuchenbecker, W.K.H., Sauer, P.J.J., Land, J.A., Stolk, R.P., and Hoek, A. (2012). The influence of maternal and paternal factors on time to pregnancy—a Dutch population-based birth-cohort study: the GECKO Drenthe study. Hum. Reprod. *27*, 583–593.

Mutsaerts, M. a. Q., Groen, H., Buiter-Van der Meer, A., Sijtsma, A., Sauer, P.J.J., Land, J.A., Mol, B.W., Corpeleijn, E., and Hoek, A. (2014). Effects of paternal and maternal lifestyle factors on pregnancy complications and perinatal outcome. A population-based birth-cohort study: the GECKO Drenthe cohort. Hum. Reprod. Oxf. Engl. *29*, 824–834.

Naifar, M., Rekik, N., Messedi, M., Chaabouni, K., Lahiani, A., Turki, M., Abid, M., Ayedi, F., and Jamoussi, K. (2015). Male hypogonadism and metabolic syndrome. Andrologia *47*, 579–586.

Nakamura, T., Arai, Y., Umehara, H., Masuhara, M., Kimura, T., Taniguchi, H., Sekimoto, T., Ikawa, M., Yoneda, Y., Okabe, M., et al. (2007). PGC7/Stella protects against DNA demethylation in early embryogenesis. Nat. Cell Biol. *9*, 64–71.

Nakamura, T., Liu, Y.-J., Nakashima, H., Umehara, H., Inoue, K., Matoba, S., Tachibana, M., Ogura, A., Shinkai, Y., and Nakano, T. (2012). PGC7 binds histone H3K9me2 to protect against conversion of 5mC to 5hmC in early embryos. Nature *486*, 415–419.

Napier, I.D., Simon, L., Perry, D., Cooke, P.S., Stocco, D.M., Sepehr, E., Doerge, D.R., Kemppainen, B.W., Morrison, E.E., and Akingbemi, B.T. (2014). Testicular development in male rats is sensitive to a soy-based diet in the neonatal period. Biol. Reprod. *90*, 40.

National Obesity Observatory (2010). The economic burden of obesity.

Newbold, R.R., Hanson, R.B., Jefferson, W.N., Bullock, B.C., Haseman, J., and McLachlan, J.A. (1998). Increased tumors but uncompromised fertility in the female descendants of mice exposed developmentally to diethylstilbestrol. Carcinogenesis *19*, 1655–1663.

Newbold, R.R., Padilla-Banks, E., and Jefferson, W.N. (2006). Adverse effects of the model environmental estrogen diethylstilbestrol are transmitted to subsequent generations. Endocrinology *147*, S11–S17.

Ng, S.-F., Lin, R.C.Y., Laybutt, D.R., Barres, R., Owens, J.A., and Morris, M.J. (2010). Chronic high-fat diet in fathers programs β-cell dysfunction in female rat offspring. Nature *467*, 963–966.

Ng, S.-Y., Bogu, G.K., Soh, B.S., and Stanton, L.W. (2013). The Long Noncoding RNA RMST Interacts with SOX2 to Regulate Neurogenesis. Mol. Cell *51*, 349–359.

NICE, C. (2013). Fertility | 1-Recommendations | Guidance and guidelines | NICE.

Nicol, B., and Yao, H.H.-C. (2014). Building an ovary: insights into establishment of somatic cell lineages in the mouse. Sex. Dev. Genet. Mol. Biol. Evol. Endocrinol. Embryol. Pathol. Sex Determ. Differ. *8*, 243–251.

Niles, K.M., Chan, D., La Salle, S., Oakes, C.C., and Trasler, J.M. (2011). Critical Period of Nonpromoter DNA Methylation Acquisition during Prenatal Male Germ Cell Development. PLoS ONE *6*, e24156.

Nilsson, C., Raun, K., Yan, F., Larsen, M.O., and Tang-Christensen, M. (2012). Laboratory animals as surrogate models of human obesity. Acta Pharmacol. Sin. *33*, 173–181.

Noble, D. (2015). Evolution beyond neo-Darwinism: a new conceptual framework. J. Exp. Biol. *218*, 7–13.

Nohr, E.A., Vaeth, M., Rasmussen, S., Ramlau-Hansen, C.H., and Olsen, J. (2009). Waiting time to pregnancy according to maternal birthweight and prepregnancy BMI. Hum. Reprod. *24*, 226–232.

Nordfjäll, K., Eliasson, M., Stegmayr, B., Melander, O., Nilsson, P., and Roos, G. (2008). Telomere length is associated with obesity parameters but with a gender difference. Obes. Silver Spring Md *16*, 2682–2689.

Northstone, K., Golding, J., Davey Smith, G., Miller, L.L., and Pembrey, M. (2014). Prepubertal start of father's smoking and increased body fat in his sons: further characterisation of paternal transgenerational responses. Eur. J. Hum. Genet. EJHG *22*, 1382–1386.

Novelli, E.L.B., Diniz, Y.S., Galhardi, C.M., Ebaid, G.M.X., Rodrigues, H.G., Mani, F., Fernandes, A. a. H., Cicogna, A.C., and Novelli Filho, J.L.V.B. (2007). Anthropometrical parameters and markers of obesity in rats. Lab. Anim. *41*, 111–119.

Oakes, C.C., La Salle, S., Smiraglia, D.J., Robaire, B., and Trasler, J.M. (2007). Developmental acquisition of genome-wide DNA methylation occurs prior to meiosis in male germ cells. Dev. Biol. *307*, 368–379.

Obata, Y., and Kono, T. (2002). Maternal Primary Imprinting Is Established at a Specific Time for Each Gene throughout Oocyte Growth. J. Biol. Chem. *277*, 5285–5289.

Oberdoerffer, P., and Sinclair, D.A. (2007). The role of nuclear architecture in genomic instability and ageing. Nat. Rev. Mol. Cell Biol. *8*, 692–702.

O'Callaghan, N.J., and Fenech, M. (2011). A quantitative PCR method for measuring absolute telomere length. Biol. Proced. Online *13*, 3.

O'Carroll, D., Erhardt, S., Pagani, M., Barton, S.C., Surani, M.A., and Jenuwein, T. (2001). The Polycomb-Group Gene Ezh2 Is Required for Early Mouse Development. Mol. Cell. Biol. *21*, 4330–4336.

O'Doherty, A.M., and McGettigan, P.A. (2014). Epigenetic processes in the male germline. Reprod. Fertil. Dev.

Ohhata, T., Senner, C.E., Hemberger, M., and Wutz, A. (2011). Lineage-specific function of the noncoding Tsix RNA for Xist repression and Xi reactivation in mice. Genes Dev. *25*, 1702–1715.

Ohinata, Y., Payer, B., O'Carroll, D., Ancelin, K., Ono, Y., Sano, M., Barton, S.C., Obukhanych, T., Nussenzweig, M., Tarakhovsky, A., et al. (2005). Blimp1 is a critical determinant of the germ cell lineage in mice. Nature *436*, 207–213.

Okano, M., Xie, S., and Li, E. (1998). Dnmt2 is not required for de novo and maintenance methylation of viral DNA in embryonic stem cells. Nucleic Acids Res. *26*, 2536–2540.

Okano, M., Bell, D.W., Haber, D.A., and Li, E. (1999). DNA Methyltransferases Dnmt3a and Dnmt3b Are Essential for De Novo Methylation and Mammalian Development. Cell *99*, 247–257.

Olson-Manning, C.F., Wagner, M.R., and Mitchell-Olds, T. (2012). Adaptive evolution: evaluating empirical support for theoretical predictions. Nat. Rev. Genet. *13*, 867–877.

Ono, R., Taki, T., Taketani, T., Taniwaki, M., Kobayashi, H., and Hayashi, Y. (2002). LCX, leukemia-associated protein with a CXXC domain, is fused to MLL in acute myeloid leukemia with trilineage dysplasia having t(10;11)(q22;q23). Cancer Res. *62*, 4075–4080.

Öst, A., Lempradl, A., Casas, E., Weigert, M., Tiko, T., Deniz, M., Pantano, L., Boenisch, U., Itskov, P.M., Stoeckius, M., et al. (2014). Paternal Diet Defines Offspring Chromatin State and Intergenerational Obesity. Cell *159*, 1352–1364.

Ozturk, S. (2015). Telomerase activity and telomere length in male germ cells. Biol. Reprod. *92*, 53.

Page, K.C., Jones, E.K., and Anday, E.K. (2014). Maternal and postweaning high-fat diets disturb hippocampal gene expression, learning, and memory function. Am. J. Physiol. Regul. Integr. Comp. Physiol. *306*, R527–R537.

Painter, R.C., Roseboom, T.J., and Bleker, O.P. (2005). Prenatal exposure to the Dutch famine and disease in later life: An overview. Reprod. Toxicol. *20*, 345–352.

Painter, R.C., de Rooij, S.R., Bossuyt, P.M., Simmers, T.A., Osmond, C., Barker, D.J., Bleker, O.P., and Roseboom, T.J. (2006). Early onset of coronary artery disease after prenatal exposure to the Dutch famine. Am. J. Clin. Nutr. *84*, 322–327; quiz 466–467.

Palmer, N.O., Fullston, T., Mitchell, M., Setchell, B.P., and Lane, M. (2011). SIRT6 in mouse spermatogenesis is modulated by diet-induced obesity. Reprod. Fertil. Dev. *23*, 929–939.

Palmer, N.O., Bakos, H.W., Fullston, T., and Lane, M. (2012). Impact of obesity on male fertility, sperm function and molecular composition. Spermatogenesis *2*, 253–263.

Panneerdoss, S., Chang, Y.-F., Buddavarapu, K.C., Chen, H.-I.H., Shetty, G., Wang, H., Chen, Y., Kumar, T.R., and Rao, M.K. (2012). Androgen-Responsive MicroRNAs in Mouse Sertoli Cells. PLoS ONE *7*, e41146.

Patro, B., Liber, A., Zalewski, B., Poston, L., Szajewska, H., and Koletzko, B. (2013). Maternal and Paternal Body Mass Index and Offspring Obesity: A Systematic Review. Ann. Nutr. Metab. *63*, 32–41.

Patten, M.M., Ross, L., Curley, J.P., Queller, D.C., Bonduriansky, R., and Wolf, J.B. (2014). The evolution of genomic imprinting: theories, predictions and empirical tests. Heredity *113*, 119–128.

Pecoraro, N., Reyes, F., Gomez, F., Bhargava, A., and Dallman, M.F. (2004). Chronic Stress Promotes Palatable Feeding, which Reduces Signs of Stress: Feedforward and Feedback Effects of Chronic Stress. Endocrinology *145*, 3754–3762.

Pembrey, M., Saffery, R., Bygren, L.O., Carstensen, J., Edvinsson, S., Faresjö, T., Franks, P., Gustafsson, J.-Å., Kaati, G., Lindahl, B.I.B., et al. (2014). Human transgenerational responses to early-life experience: potential impact on development, health and biomedical research. J. Med. Genet. jmedgenet – 2014–102577.

Pembrey, M.E., Bygren, L.O., Kaati, G., Edvinsson, S., Northstone, K., Sjöström, M., and Golding, J. (2006). Sex-specific, male-line transgenerational responses in humans. Eur. J. Hum. Genet. *14*, 159–166.

Penn, N.W., Suwalski, R., O'Riley, C., Bojanowski, K., and Yura, R. (1972). The presence of 5-hydroxymethylcytosine in animal deoxyribonucleic acid. Biochem. J. *126*, 781–790.

Peters, A.H.F.M., O'Carroll, D., Scherthan, H., Mechtler, K., Sauer, S., Schöfer, C., Weipoltshammer, K., Pagani, M., Lachner, M., Kohlmaier, A., et al. (2001). Loss of the Suv39h Histone Methyltransferases Impairs Mammalian Heterochromatin and Genome Stability. Cell *107*, 323–337.

Pfaffeneder, T., Hackner, B., Truß, M., Münzel, M., Müller, M., Deiml, C.A., Hagemeier, C., and Carell, T. (2011). The Discovery of 5-Formylcytosine in Embryonic Stem Cell DNA. Angew. Chem. Int. Ed. *50*, 7008–7012.

Phalke, S., Nickel, O., Walluscheck, D., Hortig, F., Onorati, M.C., and Reuter, G. (2009). Retrotransposon silencing and telomere integrity in somatic cells of Drosophila depends on the cytosine-5 methyltransferase DNMT2. Nat. Genet. *41*, 696–702.

Platt, K.M., Charnigo, R.J., and Pearson, K.J. (2014). Adult offspring of high-fat diet-fed dams can have normal glucose tolerance and body composition. J. Dev. Orig. Health Dis. *5*, 229–239.

Popp, C., Dean, W., Feng, S., Cokus, S.J., Andrews, S., Pellegrini, M., Jacobsen, S.E., and Reik, W. (2010). Genome-wide erasure of DNA methylation in mouse primordial germ cells is affected by AID deficiency. Nature *463*, 1101–1105.

Prescott, J., Du, M., Wong, J.Y.Y., Han, J., and Vivo, I.D. (2012). Paternal age at birth is associated with offspring leukocyte telomere length in the nurses' health study. Hum. Reprod. *27*, 3622–3631.

Puschendorf, M., Terranova, R., Boutsma, E., Mao, X., Isono, K., Brykczynska, U., Kolb, C., Otte, A.P., Koseki, H., Orkin, S.H., et al. (2008). PRC1 and Suv39h specify parental

asymmetry at constitutive heterochromatin in early mouse embryos. Nat. Genet. *40*, 411–420.

Radford, E.J., Ito, M., Shi, H., Corish, J.A., Yamazawa, K., Isganaitis, E., Seisenberger, S., Hore, T.A., Reik, W., Erkek, S., et al. (2014). In utero undernourishment perturbs the adult sperm methylome and intergenerational metabolism. Science *345*, 1255903.

Ramlau-Hansen, C.H., Thulstrup, A.M., Nohr, E.A., Bonde, J.P., Sørensen, T.I.A., and Olsen, J. (2007). Subfecundity in overweight and obese couples. Hum. Reprod. *22*, 1634–1637.

Rassoulzadegan, M., Grandjean, V., Gounon, P., Vincent, S., Gillot, I., and Cuzin, F. (2006). RNA-mediated non-mendelian inheritance of an epigenetic change in the mouse. Nature *441*, 469–474.

Rathke, C., Baarends, W.M., Awe, S., and Renkawitz-Pohl, R. (2014). Chromatin dynamics during spermiogenesis. Biochim. Biophys. Acta BBA - Gene Regul. Mech. *1839*, 155–168.

Ravelli, A.C., van Der Meulen, J.H., Osmond, C., Barker, D.J., and Bleker, O.P. (1999). Obesity at the age of 50 y in men and women exposed to famine prenatally. Am. J. Clin. Nutr. *70*, 811–816.

Redon, S., Reichenbach, P., and Lingner, J. (2010). The non-coding RNA TERRA is a natural ligand and direct inhibitor of human telomerase. Nucleic Acids Res. *38*, 5797–5806.

Reynolds, R.M., Allan, K.M., Raja, E.A., Bhattacharya, S., McNeill, G., Hannaford, P.C., Sarwar, N., Lee, A.J., Bhattacharya, S., and Norman, J.E. (2013). Maternal obesity during pregnancy and premature mortality from cardiovascular event in adult offspring: follow-up of 1 323 275 person years. BMJ *347*, f4539.

Richardson, B.E., and Lehmann, R. (2010). Mechanisms guiding primordial germ cell migration: strategies from different organisms. Nat. Rev. Mol. Cell Biol. *11*, 37–49.

Rodríguez-González, G.L., Vega, C.C., Boeck, L., Vázquez, M., Bautista, C.J., Reyes-Castro, L.A., Saldaña, O., Lovera, D., Nathanielsz, P.W., and Zambrano, E. (2014). Maternal obesity and overnutrition increase oxidative stress in male rat offspring reproductive system and decrease fertility. Int. J. Obes. 2005.

Roka, R., Michimi, A., and Macy, G. (2015). Associations Between Hypertension and Body Mass Index and Waist Circumference in U.S. Adults: A Comparative Analysis by Gender. High Blood Press. Cardiovasc. Prev. Off. J. Ital. Soc. Hypertens.

Romero, Y., Meikar, O., Papaioannou, M.D., Conne, B., Grey, C., Weier, M., Pralong, F., De Massy, B., Kaessmann, H., Vassalli, J.-D., et al. (2011). Dicer1 Depletion in Male Germ Cells Leads to Infertility Due to Cumulative Meiotic and Spermiogenic Defects. PLoS ONE *6*, e25241.

De Rooij, S.R., Painter, R.C., Phillips, D.I.W., Osmond, C., Michels, R.P.J., Godsland, I.F., Bossuyt, P.M.M., Bleker, O.P., and Roseboom, T.J. (2006). Impaired insulin secretion after prenatal exposure to the Dutch famine. Diabetes Care *29*, 1897–1901.

Rose, C.M., van den Driesche, S., Sharpe, R.M., Meehan, R.R., and Drake, A.J. (2014). Dynamic changes in DNA modification states during late gestation male germ line development in the rat. Epigenetics Chromatin *7*, 19.

Ruby, J.G., Jan, C.H., and Bartel, D.P. (2007). Intronic microRNA precursors that bypass Drosha processing. Nature *448*, 83–86.

Sachs, M., Onodera, C., Blaschke, K., Ebata, K.T., Song, J.S., and Ramalho-Santos, M. (2013). Bivalent chromatin marks developmental regulatory genes in the mouse embryonic germline in vivo. Cell Rep. *3*, 1777–1784.

Saitou, M., and Yamaji, M. (2012). Primordial Germ Cells in Mice. Cold Spring Harb. Perspect. Biol. *4*, a008375.

Sakai, Y., Suetake, I., Itoh, K., Mizugaki, M., Tajima, S., and Yamashina, S. (2001). Expression of DNA Methyltransferase (Dnmt1) in Testicular Germ Cells during Development of Mouse Embryo. Cell Struct. Funct. *26*, 685–691.

Sakai, Y., Suetake, I., Shinozaki, F., Yamashina, S., and Tajima, S. (2004). Co-expression of de novo DNA methyltransferases Dnmt3a2 and Dnmt3L in gonocytes of mouse embryos. Gene Expr. Patterns *5*, 231–237.

Saksouk, N., Barth, T.K., Ziegler-Birling, C., Olova, N., Nowak, A., Rey, E., Mateos-Langerak, J., Urbach, S., Reik, W., Torres-Padilla, M.-E., et al. (2014). Redundant Mechanisms to Form Silent Chromatin at Pericentromeric Regions Rely on BEND3 and DNA Methylation. Mol. Cell *56*, 580–594.

La Salle, S., and Trasler, J.M. (2006). Dynamic expression of DNMT3a and DNMT3b isoforms during male germ cell development in the mouse. Dev. Biol. *296*, 71–82.

La Salle, S., Mertineit, C., Taketo, T., Moens, P.B., Bestor, T.H., and Trasler, J.M. (2004). Windows for sex-specific methylation marked by DNA methyltransferase expression profiles in mouse germ cells. Dev. Biol. *268*, 403–415.

Sanders, T.R., Kim, D.W., Glendining, K.A., and Jasoni, C.L. (2014). Maternal obesity and IL-6 lead to aberrant developmental gene expression and deregulated neurite growth in the fetal arcuate nucleus. Endocrinology *155*, 2566–2577.

Santenard, A., Ziegler-Birling, C., Koch, M., Tora, L., Bannister, A.J., and Torres-Padilla, M.-E. (2010). Heterochromatin formation in the mouse embryo requires critical residues of the histone variant H3.3. Nat. Cell Biol. *12*, 853–862.

Santos, F., Peters, A.H., Otte, A.P., Reik, W., and Dean, W. (2005). Dynamic chromatin modifications characterise the first cell cycle in mouse embryos. Dev. Biol. *280*, 225–236.

Sarkar, A., Maji, R.K., Saha, S., and Ghosh, Z. (2014). piRNAQuest: searching the piRNAome for silencers. BMC Genomics *15*, 555.

Sasson, I.E., Vitins, A.P., Mainigi, M.A., Moley, K.H., and Simmons, R.A. (2015). Pre-gestational vs gestational exposure to maternal obesity differentially programs the offspring in mice. Diabetologia *58*, 615–624.

Sassone-Corsi, P. (2002). Unique Chromatin Remodeling and Transcriptional Regulation in Spermatogenesis. Science *296*, 2176–2178.

Schemmel, R., Mickelsen, O., and Motawi, K. (1972). Conversion of dietary to body energy in rats as affected by strain, sex and ration. J. Nutr. *102*, 1187–1197.

Schotta, G., Lachner, M., Sarma, K., Ebert, A., Sengupta, R., Reuter, G., Reinberg, D., and Jenuwein, T. (2004). A silencing pathway to induce H3-K9 and H4-K20 trimethylation at constitutive heterochromatin. Genes Dev. *18*, 1251–1262.

Schübeler, D. (2015). Function and information content of DNA methylation. Nature *517*, 321–326.

Schultz, D.C., Ayyanathan, K., Negorev, D., Maul, G.G., and Rauscher, F.J. (2002). SETDB1: a novel KAP-1-associated histone H3, lysine 9-specific methyltransferase that contributes to HP1-mediated silencing of euchromatic genes by KRAB zinc-finger proteins. Genes Dev. *16*, 919–932.

Schulz, R., Proudhon, C., Bestor, T.H., Woodfine, K., Lin, C.-S., Lin, S.-P., Prissette, M., Oakey, R.J., and Bourc'his, D. (2010). The Parental Non-Equivalence of Imprinting Control Regions during Mammalian Development and Evolution. PLoS Genet *6*, e1001214.

Seisenberger, S., Andrews, S., Krueger, F., Arand, J., Walter, J., Santos, F., Popp, C., Thienpont, B., Dean, W., and Reik, W. (2012). The Dynamics of Genome-wide DNA Methylation Reprogramming in Mouse Primordial Germ Cells. Mol. Cell *48*, 849–862.

Seki, Y., Hayashi, K., Itoh, K., Mizugaki, M., Saitou, M., and Matsui, Y. (2005). Extensive and orderly reprogramming of genome-wide chromatin modifications associated with specification and early development of germ cells in mice. Dev. Biol. *278*, 440–458.

Seki, Y., Yamaji, M., Yabuta, Y., Sano, M., Shigeta, M., Matsui, Y., Saga, Y., Tachibana, M., Shinkai, Y., and Saitou, M. (2007). Cellular dynamics associated with the genome-wide epigenetic reprogramming in migrating primordial germ cells in mice. Development *134*, 2627–2638.

Seong, K.-H., Li, D., Shimizu, H., Nakamura, R., and Ishii, S. (2011). Inheritance of stress-induced, ATF-2-dependent epigenetic change. Cell *145*, 1049–1061.

Sharpe, R.M., McKinnell, C., Kivlin, C., and Fisher, J.S. (2003). Proliferation and functional maturation of Sertoli cells, and their relevance to disorders of testis function in adulthood. Reproduction *125*, 769–784.

Shen, J., and Hung, M.-C. (2015). Signaling-Mediated Regulation of MicroRNA Processing. Cancer Res. *75*, 783–791.

Shirazian, T., and Raghavan, S. (2009). Obesity and pregnancy: Implications and management strategies for providers. Mt. Sinai J. Med. *76*, 539–545.

Shukla, S., and Meeran, S.M. (2014). Epigenetics of cancer stem cells: Pathways and therapeutics. Biochim. Biophys. Acta BBA - Gen. Subj. *1840*, 3494–3502.

Simpson, V.J., Johnson, T.E., and Hammen, R.F. (1986). Caenorhabditis elegans DNA does not contain 5-methylcytosine at any time during development or aging. Nucleic Acids Res. *14*, 6711–6719.

Singh, P., Li, A.X., Tran, D.A., Oates, N., Kang, E.-R., Wu, X., and Szabó, P.E. (2013). De Novo DNA Methylation in the Male Germ Line Occurs by Default but Is Excluded at Sites of H3K4 Methylation. Cell Rep.

Skinner, M.K. (2015). Environmental Epigenetics and a Unified Theory of the Molecular Aspects of Evolution: A Neo-Lamarckian Concept that Facilitates Neo-Darwinian Evolution. Genome Biol. Evol. *7*, 1296–1302.

Skinner, M.K., and Guerrero-Bosagna, C. (2014). Role of CpG deserts in the epigenetic transgenerational inheritance of differential DNA methylation regions. BMC Genomics *15*, 692.

Smallwood, S.A., Tomizawa, S., Krueger, F., Ruf, N., Carli, N., Segonds-Pichon, A., Sato, S., Hata, K., Andrews, S.R., and Kelsey, G. (2011). Dynamic CpG island methylation landscape in oocytes and preimplantation embryos. Nat. Genet. *43*, 811–814.

Smit, A.F., and Riggs, A.D. (1996). Tiggers and DNA transposon fossils in the human genome. Proc. Natl. Acad. Sci. U. S. A. *93*, 1443–1448.

Smit, A., and Hubley, R. (2001). Primate FORDPREFECT repetitive element - a consensus. Repbas Rep. *1*, 20.

Smith, Z.D., Chan, M.M., Humm, K.C., Karnik, R., Mekhoubad, S., Regev, A., Eggan, K., and Meissner, A. (2014). DNA methylation dynamics of the human preimplantation embryo. Nature *511*, 611–615.

Soltani, H., Duxbury, A.M.S., Arden, M.A., Dearden, A., Furness, P.J., and Garland, C. (2015). Maternal Obesity Management Using Mobile Technology: A Feasibility Study to Evaluate a Text Messaging Based Complex Intervention during Pregnancy. J. Obes. *2015*, 814830.

Song, R., Hennig, G.W., Wu, Q., Jose, C., Zheng, H., and Yan, W. (2011). Male germ cells express abundant endogenous siRNAs. Proc. Natl. Acad. Sci. *108*, 13159–13164.

Song, Y., Yu, Y., Wang, D., Chai, S., Liu, D., Xiao, X., and Huang, Y. (2015). Maternal high-fat diet feeding during pregnancy and lactation augments lung inflammation and remodeling in the offspring. Respir. Physiol. Neurobiol. *207*, 1–6.

Sorge, R.E., Martin, L.J., Isbester, K.A., Sotocinal, S.G., Rosen, S., Tuttle, A.H., Wieskopf, J.S., Acland, E.L., Dokova, A., Kadoura, B., et al. (2014). Olfactory exposure to males, including men, causes stress and related analgesia in rodents. Nat. Methods *11*, 629–632.

Soubry, A., Hoyo, C., Jirtle, R.L., and Murphy, S.K. (2014). A paternal environmental legacy: Evidence for epigenetic inheritance through the male germ line. BioEssays *36*, 359–371.

Soubry, A., Murphy, S.K., Wang, F., Huang, Z., Vidal, A.C., Fuemmeler, B.F., Kurtzberg, J., Murtha, A., Jirtle, R.L., Schildkraut, J.M., et al. (2015). Newborns of obese parents have altered DNA methylation patterns at imprinted genes. Int. J. Obes. 2005 *39*, 650–657.

Spiller, C.M., and Koopman, P. (2011). Cell cycle control of germ cell differentiation. Results Probl. Cell Differ. *53*, 269–308.

Spivakov, M., and Fisher, A.G. (2007). Epigenetic signatures of stem-cell identity. Nat. Rev. Genet. *8*, 263–271.

Stein, P., Rozhkov, N.V., Li, F., Cárdenas, F.L., Davydenk, O., Vandivier, L.E., Gregory, B.D., Hannon, G.J., and Schultz, R.M. (2015). Essential Role for Endogenous siRNAs during Meiosis in Mouse Oocytes. PLoS Genet *11*, e1005013.

Stein, R., Razin, A., and Cedar, H. (1982). In vitro methylation of the hamster adenine phosphoribosyltransferase gene inhibits its expression in mouse L cells. Proc. Natl. Acad. Sci. *79*, 3418–3422.

Stokes, V.J., Anderson, R.A., and George, J.T. (2015). How does obesity affect fertility in men - and what are the treatment options? Clin. Endocrinol. (Oxf.) *82*, 633–638.

Suh, N., Baehner, L., Moltzahn, F., Melton, C., Shenoy, A., Chen, J., and Blelloch, R. (2010). MicroRNA Function Is Globally Suppressed in Mouse Oocytes and Early Embryos. Curr. Biol. CB *20*, 271–277.

Symonds, M.E., Pearce, S., Bispham, J., Gardner, D.S., and Stephenson, T. (2004). Timing of nutrient restriction and programming of fetal adipose tissue development. Proc. Nutr. Soc. *63*, 397–403.

Tahiliani, M., Koh, K.P., Shen, Y., Pastor, W.A., Bandukwala, H., Brudno, Y., Agarwal, S., Iyer, L.M., Liu, D.R., Aravind, L., et al. (2009). Conversion of 5-Methylcytosine to 5-Hydroxymethylcytosine in Mammalian DNA by MLL Partner TET1. Science *324*, 930–935.

Tajar, A., Forti, G., O'Neill, T.W., Lee, D.M., Silman, A.J., Finn, J.D., Bartfai, G., Boonen, S., Casanueva, F.F., Giwercman, A., et al. (2010). Characteristics of secondary, primary, and compensated hypogonadism in aging men: evidence from the European Male Ageing Study. J. Clin. Endocrinol. Metab. *95*, 1810–1818.

Tam, P.P.L., and Snow, M.H.L. (1981). Proliferation and migration of primordial germ cells during compensatory growth in mouse embryos. J. Embryol. Exp. Morphol. *64*, 133–147.

Tanay, A., O'Donnell, A.H., Damelin, M., and Bestor, T.H. (2007). Hyperconserved CpG domains underlie Polycomb-binding sites. Proc. Natl. Acad. Sci. *104*, 5521–5526.

Tanna, M.S., Schwartzbard, A., Berger, J.S., Alukal, J., and Weintraub, H. (2015). The role of testosterone therapy in cardiovascular mortality: culprit or innocent bystander? Curr. Atheroscler. Rep. *17*, 490.

Le Thomas, A., Marinov, G.K., and Aravin, A.A. (2014). A Transgenerational Process Defines piRNA Biogenesis in Drosophila virilis. Cell Rep. *8*, 1617–1623.

Thorn, S.R., Baquero, K.C., Newsom, S.A., El Kasmi, K.C., Bergman, B.C., Shulman, G.I., Grove, K.L., and Friedman, J.E. (2014). Early life exposure to maternal insulin resistance has persistent effects on hepatic NAFLD in juvenile nonhuman primates. Diabetes *63*, 2702–2713.

Titus-Ernstoff, L., Troisi, R., Hatch, E.E., Palmer, J.R., Hyer, M., Kaufman, R., Adam, E., Noller, K., and Hoover, R.N. (2010). Birth defects in the sons and daughters of women who were exposed in utero to diethylstilbestrol (DES). Int. J. Androl. *33*, 377–384.

Tomizawa, S.-I., Nowacka-Woszuk, J., and Kelsey, G. (2012). DNA methylation establishment during oocyte growth: mechanisms and significance. Int. J. Dev. Biol. *56*, 867–875.

Tomizuka, K., Horikoshi, K., Kitada, R., Sugawara, Y., Iba, Y., Kojima, A., Yoshitome, A., Yamawaki, K., Amagai, M., Inoue, A., et al. (2008). R-spondin1 plays an essential role in ovarian development through positively regulating Wnt-4 signaling. Hum. Mol. Genet. *17*, 1278–1291.

Trautmann, E., Guerquin, M.-J., Duquenne, C., Lahaye, J.-B., Habert, R., and Livera, G. (2008). Retinoic acid prevents germ cell mitotic arrest in mouse fetal testes. Cell Cycle Georget. Tex *7*, 656–664.

Vardimon, L., Kressmann, A., Cedar, H., Maechler, M., and Doerfler, W. (1982). Expression of a cloned adenovirus gene is inhibited by in vitro methylation. Proc. Natl. Acad. Sci. *79*, 1073–1077.

Veenendaal, M.V.E., Painter, R.C., de Rooij, S.R., Bossuyt, P.M.M., van der Post, J.A.M., Gluckman, P.D., Hanson, M.A., and Roseboom, T.J. (2013). Transgenerational effects of prenatal exposure to the 1944-45 Dutch famine. BJOG Int. J. Obstet. Gynaecol. *120*, 548–553.

Veitia, R.A., Veyrunes, F., Bottani, S., and Birchler, J.A. (2015). X chromosome inactivation and active X upregulation in therian mammals: facts, questions, and hypotheses. J. Mol. Cell Biol. *7*, 2–11.

Vogt, M.C., Paeger, L., Hess, S., Steculorum, S.M., Awazawa, M., Hampel, B., Neupert, S., Nicholls, H.T., Mauer, J., Hausen, A.C., et al. (2014). Neonatal insulin action impairs hypothalamic neurocircuit formation in response to maternal high-fat feeding. Cell *156*, 495–509.

Wagner, J.R., Busche, S., Ge, B., Kwan, T., Pastinen, T., and Blanchette, M. (2014). The relationship between DNA methylation, genetic and expression inter-individual variation in untransformed human fibroblasts. Genome Biol. *15*, R37.

Wang, L., and Xu, C. (2015). Role of microRNAs in mammalian spermatogenesis and testicular germ cell tumors. Reproduction *149*, R127–R137.

Wang, H., Xue, Y., Wang, B., Zhao, J., Yan, X., Huang, Y., Du, M., and Zhu, M.-J. (2014a). Maternal obesity exacerbates insulitis and type 1 diabetes in non-obese diabetic mice. Reprod. Camb. Engl. *148*, 73–79.

Wang, L., Zhang, J., Duan, J., Gao, X., Zhu, W., Lu, X., Yang, L., Zhang, J., Li, G., Ci, W., et al. (2014b). Programming and Inheritance of Parental DNA Methylomes in Mammals. Cell *157*, 979–991.

Wang, Y.C., McPherson, K., Marsh, T., Gortmaker, S.L., and Brown, M. (2011). Health and economic burden of the projected obesity trends in the USA and the UK. Lancet *378*, 815–825.

Warneke, W., Klaus, S., Fink, H., Langley-Evans, S.C., and Voigt, J.-P. (2014). The impact of cafeteria diet feeding on physiology and anxiety-related behaviour in male and female Sprague–Dawley rats of different ages. Pharmacol. Biochem. Behav. *116*, 45–54.

Weemaes, C.M., Tol, M.J. van, Wang, J., Dam, M.M. van O., Eggermond, M.C. van, Thijssen, P.E., Aytekin, C., Brunetti-Pierri, N., Burg, M. van der, Davies, E.G., et al. (2013). Heterogeneous clinical presentation in ICF syndrome: correlation with underlying gene defects. Eur. J. Hum. Genet. *21*, 1219–1225.

Wei, Y., Yang, C.-R., Wei, Y.-P., Ge, Z.-J., Zhao, Z.-A., Zhang, B., Hou, Y., Schatten, H., and Sun, Q.-Y. (2015). Enriched environment-induced maternal weight loss reprograms metabolic gene expression in mouse offspring. J. Biol. Chem. *290*, 4604–4619.

Weissenberg, R., Bella, R., Yossefi, S., and Lewin, L.M. (1995). Changes during puberty in chromatin condensation, morphology and fertilizing ability of epididymal spermatozoa of the golden hamster. Andrologia *27*, 341–344.

Werken, C. van de, Heijden, G.W. van der, Eleveld, C., Teeuwssen, M., Albert, M., Baarends, W.M., Laven, J.S.E., Peters, A.H.F.M., and Baart, E.B. (2014). Paternal heterochromatin formation in human embryos is H3K9/HP1 directed and primed by sperm-derived histone modifications. Nat. Commun. *5*.

West, D.B., Boozer, C.N., Moody, D.L., and Atkinson, R.L. (1992). Dietary obesity in nine inbred mouse strains. Am. J. Physiol. *262*, R1025–R1032.

West, D.B., Waguespack, J., and McCollister, S. (1995). Dietary obesity in the mouse: interaction of strain with diet composition. Am. J. Physiol. *268*, R658–R665.

WHO (2010). WHO | WHO laboratory manual for the examination and processing of human semen.

WHO (2014). WHO | Obesity and overweight.

Wilczynska, A., and Bushell, M. (2015). The complexity of miRNA-mediated repression. Cell Death Differ. *22*, 22–33.

Williams, K., Christensen, J., Pedersen, M.T., Johansen, J.V., Cloos, P.A.C., Rappsilber, J., and Helin, K. (2011). TET1 and hydroxymethylcytosine in transcription and DNA methylation fidelity. Nature *473*, 343–348.

Williams, L., Seki, Y., Vuguin, P.M., and Charron, M.J. (2014). Animal models of in utero exposure to a high fat diet: A review. Biochim. Biophys. Acta BBA - Mol. Basis Dis.

Wossidlo, M., Nakamura, T., Lepikhov, K., Marques, C.J., Zakhartchenko, V., Boiani, M., Arand, J., Nakano, T., Reik, W., and Walter, J. (2011). 5-Hydroxymethylcytosine in the mammalian zygote is linked with epigenetic reprogramming. Nat. Commun. *2*, 241.

Wu, H., D'Alessio, A.C., Ito, S., Xia, K., Wang, Z., Cui, K., Zhao, K., Sun, Y.E., and Zhang, Y. (2011). Dual functions of Tet1 in transcriptional regulation in mouse embryonic stem cells. Nature *473*, 389–393.

Wu, Q., Song, R., Ortogero, N., Zheng, H., Evanoff, R., Small, C.L., Griswold, M.D., Namekawa, S.H., Royo, H., Turner, J.M., et al. (2012). The RNase III Enzyme DROSHA Is Essential for MicroRNA Production and Spermatogenesis. J. Biol. Chem. *287*, 25173–25190.

Xiao, X., Mruk, D.D., Wong, C.K.C., and Cheng, C.Y. (2014). Germ Cell Transport Across the Seminiferous Epithelium During Spermatogenesis. Physiology *29*, 286–298.

Yabuta, Y., Kurimoto, K., Ohinata, Y., Seki, Y., and Saitou, M. (2006). Gene Expression Dynamics During Germline Specification in Mice Identified by Quantitative Single-Cell Gene Expression Profiling. Biol. Reprod. *75*, 705–716.

Yamaguchi, S., Kimura, H., Tada, M., Nakatsuji, N., and Tada, T. (2005). Nanog expression in mouse germ cell development. Gene Expr. Patterns *5*, 639–646.

Yamaguchi, S., Hong, K., Liu, R., Shen, L., Inoue, A., Diep, D., Zhang, K., and Zhang, Y. (2012). Tet1 controls meiosis by regulating meiotic gene expression. Nature *492*, 443–447.

Yamaguchi, S., Shen, L., Liu, Y., Sendler, D., and Zhang, Y. (2013a). Role of Tet1 in erasure of genomic imprinting. Nature *504*, 460–464.

Yamaguchi, S., Hong, K., Liu, R., Inoue, A., Shen, L., Zhang, K., and Zhang, Y. (2013b). Dynamics of 5-methylcytosine and 5-hydroxymethylcytosine during germ cell reprogramming. Cell Res. *23*, 329–339.

Yamaji, M., Seki, Y., Kurimoto, K., Yabuta, Y., Yuasa, M., Shigeta, M., Yamanaka, K., Ohinata, Y., and Saitou, M. (2008). Critical function of Prdm14 for the establishment of the germ cell lineage in mice. Nat. Genet. *40*, 1016–1022.

Yeom, Y.I., Fuhrmann, G., Ovitt, C.E., Brehm, A., Ohbo, K., Gross, M., Hubner, K., and Scholer, H.R. (1996). Germline regulatory element of Oct-4 specific for the totipotent cycle of embryonal cells. Development *122*, 881–894.

Yin, H.L., and Stossel, T.P. (1979). Control of cytoplasmic actin gel-sol transformation by gelsolin, a calcium-dependent regulatory protein. Nature *281*, 583–586.

Yokomizo, H., Inoguchi, T., Sonoda, N., Sakaki, Y., Maeda, Y., Inoue, T., Hirata, E., Takei, R., Ikeda, N., Fujii, M., et al. (2014). Maternal high-fat diet induces insulin resistance and deterioration of pancreatic β-cell function in adult offspring with sex differences in mice. Am. J. Physiol. Endocrinol. Metab. *306*, E1163–E1175.

Yu, Z., Genest, P.-A., Riet, B. ter, Sweeney, K., DiPaolo, C., Kieft, R., Christodoulou, E., Perrakis, A., Simmons, J.M., Hausinger, R.P., et al. (2007). The protein that binds to DNA

base J in trypanosomatids has features of a thymidine hydroxylase. Nucleic Acids Res. *35*, 2107–2115.

Yuan, S., Ortogero, N., Wu, Q., Zheng, H., and Yan, W. (2014). Murine Follicular Development Requires Oocyte DICER, but Not DROSHA. Biol. Reprod. *91*, 39.

Zeng, J., Konopka, G., Hunt, B.G., Preuss, T.M., Geschwind, D., and Yi, S.V. (2012). Divergent Whole-Genome Methylation Maps of Human and Chimpanzee Brains Reveal Epigenetic Basis of Human Regulatory Evolution. Am. J. Hum. Genet. *91*, 455–465.

Zhang, J., Wang, Y., Liu, X., Jiang, S., Zhao, C., Shen, R., Guo, X., Ling, X., and Liu, C. (2015). Expression and Potential Role of microRNA-29b in Mouse Early Embryo Development. Cell. Physiol. Biochem. Int. J. Exp. Cell. Physiol. Biochem. Pharmacol. *35*, 1178–1187.

Zhang, L., Lu, H., Xin, D., Cheng, H., and Zhou, R. (2010). A novel ncRNA gene from mouse chromosome 5 trans-splices with Dmrt1 on chromosome 19. Biochem. Biophys. Res. Commun. *400*, 696–700.

Zhao, S., Gou, L.-T., Zhang, M., Zu, L.-D., Hua, M.-M., Hua, Y., Shi, H.-J., Li, Y., Li, J., Li, D., et al. (2013). piRNA-Triggered MIWI Ubiquitination and Removal by APC/C in Late Spermatogenesis. Dev. Cell *24*, 13–25.

Zimmermann, C., Romero, Y., Warnefors, M., Bilican, A., Borel, C., Smith, L.B., Kotaja, N., Kaessmann, H., and Nef, S. (2014). Germ Cell-Specific Targeting of DICER or DGCR8 Reveals a Novel Role for Endo-siRNAs in the Progression of Mammalian Spermatogenesis and Male Fertility. PLoS ONE *9*, e107023.